UNIVERSITÀ
DEGLI STUDI
FIRENZE

Ph.D. COURSE IN

SCIENCE FOR THE CONSERVATION OF CULTURAL HERITAGE

CYCLE XXVIII

Ph.D. COORDINATOR Prof. PIERO BAGLIONI

FILM FORMING PVA-BASED CLEANING SYSTEMS FOR THE REMOVAL OF CORROSION PRODUCTS FROM Cu-BASED ALLOYS

(Sistemi *film forming* a base di PVA per la rimozione di prodotti di corrosione da leghe base-Cu)

Disciplinary sector CHIM/02

Ph.D. Candidate
Dr. Erica Isabella Parisi

Tutor
Prof. Piero Baglioni

Coordinator
Prof. Piero Baglioni

Years 2012/2015

Abstract

Within restoration process of metallic artifacts, cleaning represents a great challenge for conservators. In fact this task requires a deep awareness on the intrinsic characteristics of the treated alloys and on the ongoing alteration processes. In the particular case of copper-based alloys, a suitable cleaning procedure should aim at the complete removal of the defacing and harmful corrosion products of Cu(II) (copper carbonates, sulphates, chlorides, etc.) and also at the preservation of the protective cuprite Cu(I) layer. Cleaning procedures of these materials are traditionally performed by mechanical (vibrating or abrasive tools, micro-peening with vegetal granulates, ultra-high-pressure water, laser) and/or chemical methods (complexing agents, bases, acids). Mechanical cleaning presents some limits related to scarce selectivity and invasiveness of this procedure, while the chemical action is generally affected by scarce control of the reactions involved.

An innovative polyvinyl alcohol-based film forming system was specifically devised for a controllable and selective cleaning of copper-based artifacts, with enhanced performances in terms of both applicability and efficacy. The main advantage consists in the simultaneous chemical and mechanical action, guaranteed respectively by the presence of a confined complexing agent and by the removal of the final film through a *peeling* action. Moreover, the physico-chemical properties (consistency, adhesiveness, transparency) can be adjusted by varying the additives content, to adapt to different substrates (non-horizontal, rough and irregular surfaces). The evolution of selected formulations with time, from a fluid initial polymeric solution to a final film, were investigated by gravimetric and rheological methods, while the mechanical properties of the final films, by thermoanalysis and FTIR spectroscopy.

Preliminary tests were executed firstly on artificially aged samples, then on real cases study.

INTRODUCTION 1

PART I – Fundamentals

CHAPTER 1
Metallic artifacts: copper-based alloys

1.1 Introduction 11

1.2 Copper-based alloys 13
1.2.1 Structure and composition 14
1.2.2 Methods for the production of metallic artifacts 23

1.3 The corrosion process 26
1.3.1 Corrosion and environment 30
1.3.1.1 Burial environment 32
1.3.1.2 Water environment 33
1.3.1.3 Outdoor environment 33
1.3.1.4 Indoor museum environment 35
1.3.2 Copper corrosion products 36
1.3.2.1 Copper oxides 36
1.3.2.2 Copper basic carbonates 38
1.3.2.3 Copper basic sulphates and sulphides 38
1.3.2.4 Copper nitrates and phosphates 39
1.3.3 Cooper chlorides and 'bronze disease' 40
1.3.4 Patina morphologies and investigation techniques 43
1.3.4.1 Patina morphologies 43
1.3.4.2 Optical microscopy (OM) 44
1.3.4.3 Scanning electron microscopy / microanalysis (SEM/EDS) 45
1.3.4.4 X-ray diffractometry (XRD) 47
1.3.4.5 FTIR spectroscopy 48

1.4 Traditional cleaning processes 49
1.4.1 Mechanical cleaning 51
1.4.2 Chemical cleaning 51
1.4.3 Protection and maintenance 54

1.5 Bibliography 57

CHAPTER 2
Gels and 'gel-like' systems for cleaning of Cultural Heritage artifacts

2.1 Introduction 59

2.2 Gels and 'gel-like' systems for cleaning 60
2.2.1 Definition and classification 62

2.3 Rheology of viscoelastic material 69
2.3.1 Viscosity 72
2.3.1.1 Rotational experiments, parallel-plate geometry 76
2.3.2 Linear viscoelasticity and its dynamic analysis 77

2.3.2.1 Dynamic methods, oscillatory test ... 79
2.4 Conventional gel systems in restoration practice ... 83
2.5 Innovative gels and polymeric dispersions ... 86
2.6 Bibliography ... 91

CHAPTER 3
Polyvinyl alcohol: a film forming polymer

3.1 Introduction ... 95
3.2 Polyvinyl alcohol (PVA): properties and structure ... 96
3.2.1 Thermodynamics of polymers in solution ... 99
3.2.2 Polymer crystallization ... 104
3.2.2.1 Crystallization mechanisms ... 104
3.2.2.2 Degree of crystallinity ... 108
3.2.2.3 Crystallinity of PVA ... 109
3.2.3 Transition temperatures ... 110
3.3 PVA-based hydrogels and 'peelable' formulations ... 112
3.4 Mechanism of film formation ... 114
3.5 Factors influencing the polymer solution and film properties ... 119
3.5.1 Polymer ... 119
3.5.2 Volatile fraction ... 120
3.5.3 Plasticizers ... 121
3.5.3.1 Characteristics, definitions and classification of plasticizers ... 121
3.5.3.2 Plasticizers theories and mathematical models ... 123
3.5.3.3 Compatibility ... 127
3.5.3.4 Plasticized PVA ... 128
3.6 Bibliography ... 129

CHAPTER 4
Transition metal ions complexation

4.1 Introduction ... 133
4.2 The complexation process ... 134
4.2.1 Complexation equilibria and stability constant ... 136
4.2.2 The influence of pH ... 139
4.3 Copper (II) complexing agents ... 140
4.3.1 EDTA ... 141
4.3.2 Rochelle salt ... 143
4.3.3 Glycine ... 144
4.3.4 Macrocycles ... 145
4.3.5 Polyamines ... 146
4.4 Bibliography ... 148

PART II - Experimental

CHAPTER 5
Preparation of the polymeric systems

5.1 Introduction....151

5.2 Design of film forming systems for cleaning of metallic substrates....153
5.2.1 Polymer....155
5.2.2 Additives....157
5.2.2.1 Ethanol....157
5.2.2.2 Plasticizers....158
5.2.3 Application tests on non-horizontal surfaces....162
5.2.4 Selected formulations....166

5.3 Preparation of the formulations....167
5.3.1 Materials....167
5.3.2 Preparation procedure....168

5.4 Complexing agents....169
5.4.1 Rochelle salt....169
5.4.2 EDTA....170
5.4.3 Glycine....171
5.4.4 Macrocycles....171
5.4.5 Polyethyleneamines....173

5.5 Bibliography....174

CHAPTER 6
Characterization of the polymeric systems

6.1 Introduction....177

6.2 Preparation of the polymeric systems and of the dry films....178.

6.3 Methods and instrumental conditions....180
6.3.1 Kinetics of film formation....181
6.3.1.1 Gravimetric measurements....181
6.3.1.2 Thermogravimetric analysis....182
6.3.1.3 Rheological measurements....182
6.3.2 Films characterization and evaluation of crystallinity degree....183
6.3.2.1 Thermoanalysis by DSC....183
6.3.2.2 ATR-FTIR spectroscopy....184

6.4 Results and discussion....185
6.4.1 Effect of the volatile fraction....185
6.4.2 Effect of the plasticizers....188
6.4.3 Effect of the complexing agent....195
6.4.4 The evolution of the viscoelastic behavior through time....198

6.5 Bibliography....203

CHAPTER 7
Applicative tests on artificially aged samples

7.1 Introduction 205

7.2 Artificially aged samples production 207
7.2.1 Production of the reference bronze alloys 207
7.2.2 Production of the artificial patina 208

7.3 Artificial samples characterization 211
7.3.1 Instrumental conditions 211
7.3.2 Characterization data sheets 212

7.4 Cleaning tests 222
7.4.1 Tests on chemically aged samples 222
7.4.1.1 Rochelle salt 222
7.4.1.2 EDTA 225
7.4.1.3 Glycine 228
7.4.1.4 Polyethyleneamines 228
7.4.2 Tests on buried samples 229
7.4.2.1 Rochelle salt 229
7.4.2.2 Glycine 231
7.4.2.3 EDTA 231
7.4.2.4 Macrocycles 232
7.4.2.5 Polyethyleneamines 233

7.5 Final remarks 235

7.6 Bibliography 236

CHAPTER 8
Applicative tests on real cases study

8.1 Introduction 237

8.2 The cases study of the 'Fontane dei Mostri Marini' by P. Tacca 238
8.2.1 The diagnostic project 239
8.2.2 Results and discussion 241
8.2.2.1 Instrumental conditions 244
8.2.3 Applicative cleaning tests 245

8.3 Applicative tests on gilded surfaces 251

8.4 Applicative tests on archaeological objects 253

8.5 Other applicative tests 259

8.6 Final remarks 262

8.7 Bibliography 262

CONCLUSIONS 263

AKNOWLEDGEMENTS 273

INTRODUCTION

Introduction

Cleaning is a restoration procedure that aims to bring the surface to a state that resembles as close to the original appearance of the work-of-art. Based on this concept the cleaning step represents a fundamental operation and the most delicate part of the restoration process. A correct cleaning operation requires to set-up specifically tailored treatments for each artifact, which is unique for definition, by taking into account its conservation condition and the stratigraphic composition of the *patina.*

In the specific case of metallic artifacts, cleaning still represents a great challenge for conservators. In fact this task requires a deep awareness on the intrinsic characteristics of the treated alloys and on the ongoing alteration processes, especially in case of outdoor monuments or buried artifacts. The alteration products of Cu-based alloys usually form thick and adherent concretions to thin and homogeneous *patina*. In particular, they are generally constituted by a multilayered structure comprising corrosion products of copper(I) and (II). Cu(II) oxides, carbonates and sulphates are esthetically defacing for the artifact, mainly because of their intense coloration and different solubility. The presence of the copper oxychlorides is generally considered as a symptom of the so-called 'bronze disease', a dangerous phenomenon induced by the exposure to air of the cuprous chloride nantokite (CuCl) that cyclically reacts with air moisture and oxygen, thus forming further oxychlorides and leading to a progressive deterioration of the artistic object. The inner layer, delimiting the artifacts interface, is usually constituted by Cu(I) oxide (cuprite), that represents a protective layer against further corrosion thanks to its passivating action. Thus, an adequate cleaning procedure should aim at the complete removal of the esthetically de-

facing and harmful corrosion products and also at the preservation of the protective cuprite layer.

Cleaning of metallic objects is traditionally performed by mechanical (vibrating or abrasive tools, micro-peening with vegetal granulates, ultra-high-pressure water, laser) and/or chemical methods (complexing agents, bases, acids), depending on the morphology and typology of the *patina* corrosion products to remove, trying to respect the principle of minimum intervention. Mechanical cleaning presents some limits related to scarce selectivity and invasiveness of this procedure, which can damage the protective cuprite layer, delete superficial information or trigger heating processes on the surface. Chemical treatment generally involves the use of reagents such as Rochelle salt, ethylenediaminetetraacetic acid disodium salt (EDTA), ammonia and ammonium salts, citric acid, alkaline glycerol, sodium hexametaphosphate and sodium carbonate solutions. The procedures commonly adopted for the application of these solutions, usually performed by means of compresses, brushing and immersion, presents important drawbacks related to: i) the scarce control of the cleaning process that can induce the attack of the cuprite layer, especially for low selective reagents; ii) the residues of these reagents left onto the metal surface, which can induce the uncontrolled progress of their chemical action; iii) the precipitation and redeposition of copper salts onto the surface. To avoid some of the above-mentioned drawbacks, reagents such as Rochelle salt and EDTA, thanks to their high selectivity, are generally preferred.

In the past decades, a wide range of thickeners and confining systems for different kinds of liquid phases (i.e. solvents, micellar solutions, microemulsions, aqueous solutions of chelating agents, etc.) were developed and tested. In particular Na_2EDTA solutions associated to thickeners, such as cellulose ethers, polyacrilic acids, agar, have been applied as cleaning tools for metal artifacts.

The development of an innovative system for the removal of corrosion products from a metal surface, which allows at the same time to retain the complexing agent solution, to control its spatial and chemical action and to perform a simultaneous chemical and mechanical action, is presented in this dissertation. In particular a new

polyvinyl alcohol-based film forming systems loaded with a chelating agent was specifically designed to be used for the selective surface cleaning of bronze artifacts. These film forming polymeric dispersions yield a cleaning system with enhanced performances in terms of both applicability and efficacy. In fact, this innovative approach permits to achieve: i) improved chemical control thanks to high selectivity of the selected complexing agent for Cu(II) ions; ii) simultaneous chemical and mechanical action (favored by the gentle peeling of the final film); iii) adjustability of the physico-mechanical properties (consistency, adhesiveness, transparency, etc.) to adapt to different substrates (non-horizontal, rough and irregular surfaces).

Preliminary tests were executed firstly on artificially aged samples, provided by ISMN-CNR of Rome, then on the real cases study: from outdoor exposed bronzes, as the 'Fontane dei Mostri Marini', to archaeological samples and non-metallic substrates (parchment, painted leather, gypsum).

This dissertation is divided in two parts: Fundamentals and Experimental.

In the Fundamentals part, the theoretical background is described based on an in-depth investigation of the relevant literature.

Chapter 1 reports a general overview of the physico-chemical and mechanical characteristics of copper alloys. The evolution of the manufacture technologies are then described, with a particular focus on the lost-wax castings, followed by an in-depth description of the main corrosion processes that can occur in function of the different environmental contexts. Each class of copper corrosion products is briefly described with a particular attention to copper oxychlorides and the related 'bronze disease' phenomenon. Finally, the traditional mechanical and chemical cleaning procedures are reported, along with the most common investigation techniques to analyze bronze alloys and their corrosion products.

Chapter 2 shows an overview of the gel or 'gel-like' systems available and used for restoration purposes, with particular attention focused on their definitions. A rheological approach is adopted to differentiate between 'real' gels and 'gel-like'

systems, with a brief description of the rheology technique. The most common cleaning systems for restoration purposes are presented along with the main drawbacks and limits related to their use. Finally, the innovative systems recently developed and proposed to overcome these problems are described.

Chapter 3 presents the polyvinyl alcohol characteristic features to justify its use for the development of this new cleaning system. In particular PVA behavior in solution, its ability to crystallize and its characteristic transition temperatures are briefly reported. Moreover, the influence of different additives (plasticizers, volatile fraction) over the polymer system properties is analyzed, as powerful elements to tune the system properties as desired.

In Chapter 4 some theoretical background over complexation chemistry is provided, in particular for Cu(II) complexing agents. Moreover, the stability constant is described, since it is a useful parameter for the choice of an effective sequestering agent, as though the right pH working conditions. An overview over different categories of chelating agents is provided, starting from the most used ones in the restoration filed, such as EDTA and Rochelle salt, up to macrocycles ligands (DOTA) and polyethyleneamines (TETA, TEPA, PEHA).

In the Experimental part, the research work is presented in four chapters, whereas the first two concern the preparation and the physico-chemical characterization of the developed gel systems, while the last two concern the evaluation of the application features accounting for cleaning tests on artificial samples and real cases study.

In Chapter 5, the development of the preparation method is detailed and the compounds used are explained. Several formulations were prepared by varying the relative amount and the typology of each component, in order to find the best equilibrium between them. Finally three different polymeric formulations were selected as the most suitable to be loaded with the complexing agent and to be used for applicative tests.

The Chapter 6 is dedicated to the preliminary physico-chemical characterization of selected polymeric systems. In particular two main aspects were studied over both,

complexing agent-loaded and not loaded systems: i) the kinetics of film formation, and ii) the evaluation of the formed films properties. The techniques used to obtain information over the evolution of the system with time, involved the use of gravimetry, thermogravimetry (both scanning and isothermal), and rheology (both dynamic and rotational experiments). On the other hand the evaluation of the mechanical properties and of the degree of crystallinity of the dried films was carried out through differential scanning calorimetry (DSC) and ATR-FTIR spectroscopy experiments.

In Chapter 7, several tests were performed over artificially aged Cu-based samples, in order to find the best combination between polymeric formulations and complexing agents, able to ensure a controlled and selective cleaning action. The procedure developed at ISMN-CNR laboratories to artificially reproduce typical ancient bronze alloys and archaeological *patina*, is described. The metallic samples were characterized in order to have a complete knowledge of the products to remove. Cleaning tests were then performed through a wide range of polymeric systems, loaded with different complexing agents, to select suitable and effective combinations applicable on real cases studies.

Conclusively, Chapter 8 reports the application features of the film forming systems in a relevant case study: the removal of copper corrosion products from the 'Fontane dei Mostri Marini' by P. Tacca. The diagnostic campaign previously carried out on the eastern fountain, allowed to better understand the conservative problems, identify the alteration products and study the metallurgical features of the alloy. The applicative tests were performed also on several archaeological objects and on non-metallic substrates, such as parchment, gypsum, and leather, thus demonstrating the extreme versatility of these cleaning systems.

PART I

Fundamentals

Chapter 1

Metallic Artifacts: copper-based alloys

1.1 Introduction

Metals have always played a preponderant role in the evolution of civilization and in the control of the surrounding environment. In fact one of the archaeological subdivision of the Prehistoric age is related to the predominant tool-making technologies: i) Stone Age (c. 2,500,000 - 5000 BC); ii) Copper Age (c. 4500 – 3500 BC); iii) Bronze Age (c. 3300 - 1200 BC); iv) Iron Age (c. 1200 - 500 BC).
The presence of a metal as a symbol for each Age, after Stone Age, suggests a simultaneous increasing in the level of civilization along with the progress of metals exploitation. The technological competences required for the ores extraction, smelting process and manufacturing became more and more specialized with time, thus entailing an improvement of the overall metallurgical craftsmanship [1–3]. Metals were used, by Prehistoric men, to build tools and weapons, thus playing an essential role in the advancement of agriculture, transport, arts and craft; they were fundamental for the Industrial Revolution, from steam to electricity, thus forging the path to today's modern society. In particular bronze alloy was widely used for the production of artistic objects, from ornaments and decorations to monumental statuary and coins. [4][1]

This chapter represents a general overview of the physico-chemical and mechanical characteristics of copper alloys, in order to understand why and how they were used for the production of artistic objects. In particular the microstructures of

[1] http://www.historyworld.net, consulted on October 2015

bronze alloys are reported in function of the most common ancient compositions and working methodologies. The evolution of the manufacture technologies are then reported, with a particular focus on the lost-wax castings, followed by an in-depth description of the main corrosion processes that can occur in function of the different environmental contexts (archaeological burial, underwater, outdoor, indoor). Each class of copper corrosion products is then briefly described (oxides, carbonates, sulphates, phosphates, nitrates, etc.) with a particular attention to the copper oxychlorides and the related 'bronze disease' phenomenon. Finally, the traditional cleaning procedures, for the removal of corrosion products (mechanical and chemical) are reported, along with the most common investigation techniques to analyze bronze alloys and their corrosion constituents (optical and electronic microscopy, X-ray diffraction, FTIR spectroscopy).

1.2 Copper-based alloys

The first evidences of the employment of metals (6000 BC) [1] are related to native gold, meteoritic iron and copper, both in its native and impure form and as malachite (a basic copper carbonate). The presence of these elements in nature was probably noted thanks to their striking colors and then used as they were.

The Chalcolithic period (Copper Age) corresponds to the real beginning of metallurgy, characterized by an anthropic modification of metals through hot/cold working and, later, through melting and casting.

The following technological step was the 'smelting' process, defined as "*a process by which a metal is obtained, either as the element or as a simple compound, from its ore by heating beyond the melting point, ordinarily in the presence of oxidizing agents, such as air, or reducing agents, such as coke*"[2]. Copper oxides and carbonates were initially subject to this process, in a low reducing environment and with a scarce slugs production.

[2] http://www.britannica.com/technology/smelting, consulted on October 2015

Arsenical copper was the first alloy intentionally produced, to enhance the mechanical properties of the sole copper, between Chalcolithic and the early Bronze Age. In particular the presence of arsenic didn't noticeably affect the mechanical properties of the alloy in the cast conditions (respect to those of pure copper), but it mainly improved the workability (hardening) and the castability (reduced melting temperature). The dangerous drawback of this alloy was the extreme toxicity of the arsenical vapors that necessarily led to its substitution with another alloying metal.

The transition from arsenic to tin in the Early Bronze Age was not painless, because the cassiterite (SnO_2, tin ore) deposits were scarcely available and located in detached veins in respect to those of copper. The necessity to stock this metal gave an essential contribution to the development of commercial trades and, consequently, also to cultural contacts and to evolution progresses. Furthermore tin conferred to copper additional strength, ease of castability and improved resistance to corrosion, avoiding the arsenic drawback of the toxic smokes.

In the Middle Bronze Age copper and its alloys became worked, exported, widespread and commercialized metals, thus improving trades, exploitation of mines (mainly copper sulphides ores) and massive industrial output with high slug production, until the development of iron metallurgy. Ancient metallurgists were able to produce high quantities of weapons, utensils and decorations for practical, functional, ritual, ornamental and economic reasons. In the Late Bronze Age, their ability to modify the structure of metals and of to create metallic objects, reached very high level of technological competence.[3] [1]

The principal microstructures and compositions of ancient bronze alloys are reported in the following paragraph.

1.2.1 Structure and composition

The microstructure of ancient metals [5] depends mainly on the manipulation methods, mainly constituted by casting or hot/cold working.

[3] http://www.copper.org/education/history/60centuries/, consulted on October 2015

- casting, when a mold is cooled in a cast, three types of microstructures can arise:
  - *dendritic* (Fig. 1.1 (a)), a typical segregation phenomenon of the great majority of ancient castings, caused by the presence of impurities or of different melting points of the costituents. Dendrites look like tiny fern-like growths randomly scattered throughout the metal, with shapes and sizes mainly influenced by the rate of cooling and by the alloy composition;
  - *equi-axial hexagonal* (Fig. 1.1 (b)), which can occur with particular conditions, as homogeneous castings relatively free of impurities and slow cooling. This corresponds to an ideal model of equilibrium at the lowest energy, where all the grains are of similar sizes, randomly oriented and roughly hexagonal in section;
  - *columnar growth*, associated to chill castings but rare to find in ancient metals. In this type of structure, long narrow crystals form by selective growth along an orientation towards the center of the mold
- cold/hot working, a combination of methods to change the shape of a metal/alloy by means of cyclical thermo-mechanical treatments. Different typologies of structures can result after these processes:
  - *flattened grains or distorted dendrites* (Fig. 1.1 (c)), following to cold hammering that causes a deformation of the previous structures, thanks to the presence of slip planes and dislocations in the crystal lattice. This treatment confers a progressive hardening to the structure until it becomes too brittle to be further worked;
  - *recrystallized and twinned grains*, found when the metal is annealed (in the range of 500-800 °C), in order to recover ductility and malleability. If the annealing process is carried out on a dendritic structure, an equi-axial hexagonal structure is obtained. If it follows a previously cold-mechanical worked structure, recrystallization occurs through a twin-

ning process, and parallel straight lines appear traversing the grains (Fig. 1.1 (d)). A further mechanical treatment causes a deformation visible as bent twins and strain lines on the grains (Fig.1.1 (e)).

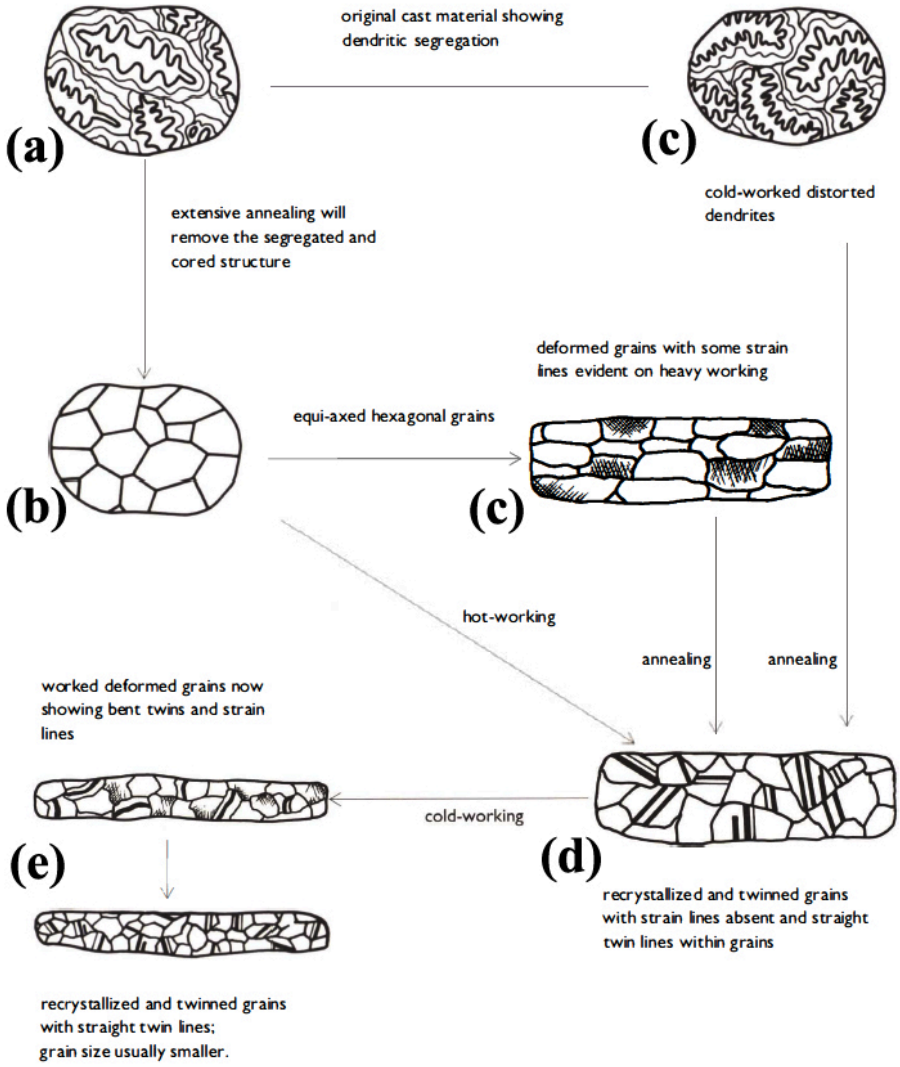

Figure 1.1 Schematic representation of the different microstructures that can arise after casting and hot/cold working. For detailed explanation see the text [5].

Another factor that can influence the microstructure of a metal is the presence of different phases, which can be predicted by using phase diagrams. When two metals are mixed together to form an alloy, there are three main possibilities depending on their relative solubility [5]:

- complete solubility, when a homogeneous alloy is obtained and a complete substitution between the constituent elements occur, thus resulting in a complete solid solution. Fig. 1.2 (a) shows an example of a phase diagram for the completely miscible gold-silver system, while in Fig. 1.2 (b) an enlargement of the copper-nickel diagram is showed. Following the cooling dotted line from *a* to *e*, the system evolves from a single liquid phase *a*, trough *b* where the solidification process starts, to *c* a two-phases region with some liquid in equilibrium with some solid and, after the end of solidification in *d*, finally a single homogeneous phase *e* is obtained with an equi-axial hexagonal structure.
- partial solubility of the components in each other; in this case the following structures can arise:
  - *eutectic*, an equilibrium point with a fixed composition and temperature (lower than the melting temperatures of any of the pure components) in which a liquid is in equilibrium with two solid phases. An example is showed in Fig. 1.2 (c) by the Pb/Sn eutectic point *i*, where the system evolves from a liquid phase *h* toward an eutectic structure of fine, intermixed matrix of alpha and beta phases. Another example of possible phases combinations is reported in Fig. 1.2 (d). The resulting cooled structures can show dendritic or equi-axial hexagonal forms, depending on the cooling rate, even if for archaeological materials the primary alpha phase was generally dendritic and cored. Then a further working and annealing treatment might remove dendritic segregation, although it could be very difficult. Therefore the final microstructure usually consisted elongated ribbons of one phase with possible traces of the previous structure;

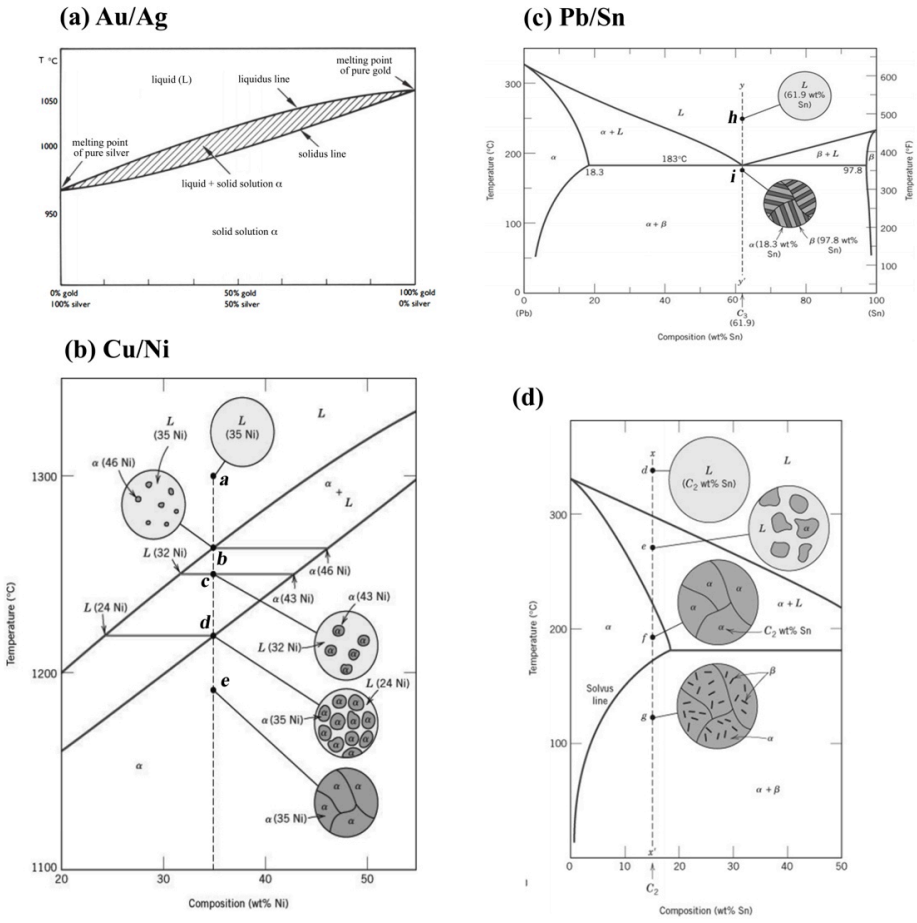

Figure 1.2 Examples of phase diagrams for different systems: (a) Au/Ag system, completely miscible; (b) detail of Cu/Ni system, completely miscible with typical phases formation during cooling; (c) Pb/Sn, eutectic system; (d) detail of the Pb/Sn eutectic system with typical phases formation during cooling [5].

- *eutectoid*, a very similar phase to the eutectic one that occurs when an already existing solid solution transforms into two distinct phases. Fig. 1.3 (b) shows an enlargement of the copper-tin diagram (tin bronze) until 40% w/w tin, which presents different phase transformations. Examples of eutectoid reactions are $\beta \leftrightarrow \alpha + \gamma$ and $\gamma \leftrightarrow \alpha + \delta$, as reported in Tab. 1.1. In particular the eutectoid $\alpha + \delta$ phase typically appears in the microstructure from a composition of 5-15 % w/w tin (and above), de-

pending on the cooling conditions of the alloy. The α phase is a copper-rich solid solution of tin in copper and δ an intermetallic compound of fixed composition, ($Cu_{31}Sn_8$). The microstructure of this blue δ phase is jagged shaped by grain boundary edges and often contains small islands of α phase dispersed trough it (see Fig. 1.4 (c)). For high content of tin in the alloy, a lot of these eutectoid phases are present in the matrix, thus making the bronze hard, brittle and difficult to work but also conferring increased strength and corrosion resistance [6];

- *peritectic*, a transformation that occurs when a liquid and a solid phase of fixed proportions react at a fixed temperature to yield a single solid phase, as showed by Fig 3(b). Examples of peritectic reactions are $\alpha + L \leftrightarrow \beta$ and $\beta + L \leftrightarrow \gamma$, as reported in Tab. 1.1, which structures are characterized by the incomplete transformation of a phase into the other one;
- *intermetallic* compounds of fixed composition occur when high affinity is present between the components. They are represented in the phase diagrams by a vertical line when stoichiometric (e.g. Fe_3C and Mg_2Ni), and by a Greek letter or a noun when ordered phases. An example is the above-mentioned δ phase ($Cu_{31}Sn_8$) of the bronze alloy, visible in Fig. 1.3 (b). These intermetallic ordered structures confer higher hardness and brittleness, thus making the working and annealing process more difficult.

In Fig. 1.3 (a) is reported the overall copper-tin system phase diagram, in the full equilibrium conditions, which is quite complicate and presents several of the above-mentioned structures, reported in Tab. 1.1.

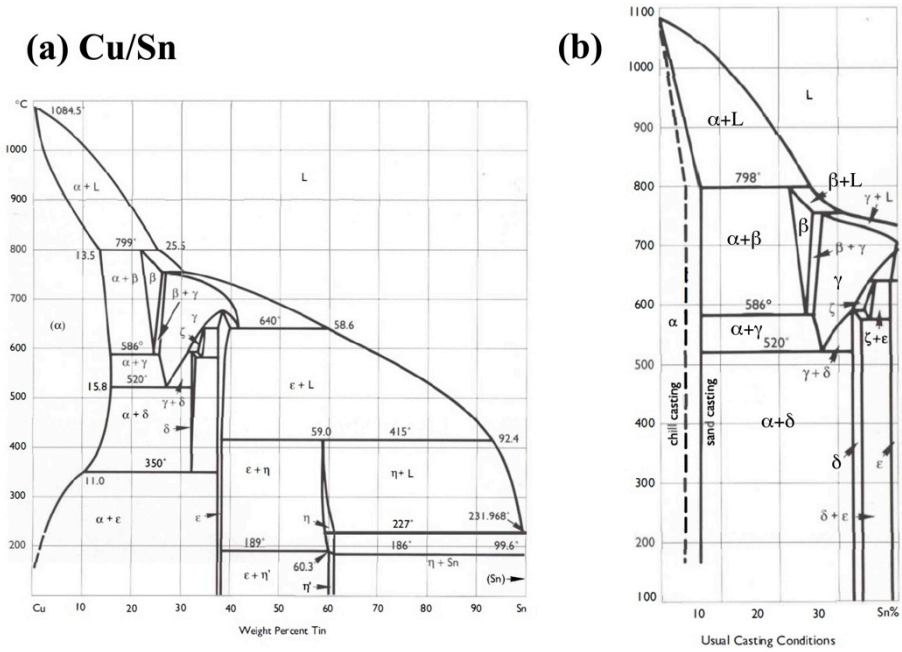

Figure 1.3 The Cu/Sn system reported as (a) the overall phase diagram in the full equilibrium conditions and as (b) an enlargement up to 40% w/w of tin. It is a good example of phase transitions, since it includes eutectic, eutectoid and peritectic reactions [5].

Reaction		Composition, at.% Sn		Temperature, °C	Reaction type
(Cu) + L ⇔ β	7.7	15.5	13.1	798	Peritectic
β + L ⇔ γ	15.8	19.1	16.5	755	Peritectic
ε ⇔ γ		25.0		676	Congruent
γ + ε ⇔ ζ	21.8	24.5	22.5	640	Peritectoid
γ ⇔ ε + L	27.9	25.9	43.1	640	Metatectic
γ + ζ ⇔ δ	19.8	20.9	20.3	590	Peritectoid
β ⇔ α + γ	14.9	9.1	15.4	586	Eutectoid
ζ ⇔ δ + ε	21.7	20.8	24.5	582	Eutectoid
γ ⇔ α + δ	16.5	9.1	20.4	520	Eutectoid
ε + L ⇔ η	24.9	86.7	43.5	415	Peritectic
δ ⇔ α + ε	20.5	6.2	24.5	350	Eutectoid
L ⇔ η + (βSn)	98.7	45.5	>99.9	227	Eutectic

Table 1.1 Temperature-invariant reactions in the Cu/Sn system [7].

Tin bronze alloys are usually divided depending on their tin content in low-tin (Sn ≤ 17 % w/w) and high-tin bronzes (Sn > 17 % w/w) [5,8].

For the low-tin bronzes, a tin content of about 15.8% w/w (at 520 °C) represents the limit for the formation of a monophasic solid solution *α* with copper (see Fig. 1.3 (a)) and face centered cubic crystals (FCC). For tin content higher

than 13.5% w/w, a peritectic reaction occurs at 799 °C to form the FCC β phase that undergoes a further transformation into the eutectoid $\alpha + \delta$ phase; the last eutectoidic transformation $\alpha + \varepsilon$ practically doesn't occur.

The equilibrium conditions requires extremely ideal conditions, such as very slow cooling, while casted tin bronzes, subject to a rapid cooling, usually present an extensive segregation in the form of cored dendrites, as showed in Fig. 1.4 (a) and (b). For very low tin content (2-5 % w/w) the formation of dendrites with a copper-rich center and tin-rich arms, without inter-dendritic δ phase, may be possible. However, the most common microstructure for ancient castings is represented by dendrites surrounded by a matrix of $\alpha + \delta$ eutectoid phase (see Fig. 1.4 (c)). The higher is the tin content the higher is the proportion of this brittle interdendritic eutectoid phase in the matrix.

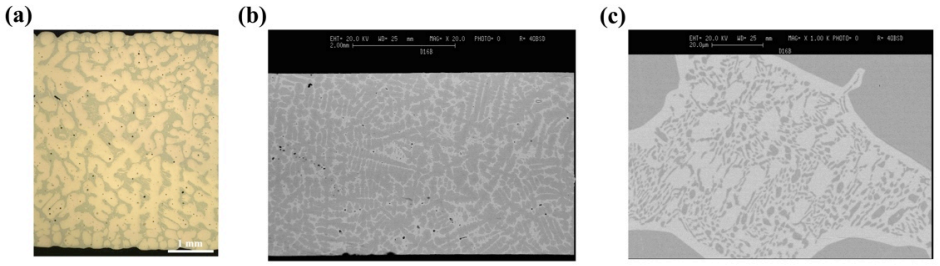

Figure 1.4 Typical microstructures of ancient castings: (a) metallographic image in bright field showing a dendritic growth; (b) backscattered electrons BSE-SEM image showing a dendritic microstructure; (c) BSE-SEM image of the $\alpha + \delta$ eutectoid phase.

An alloy with these microstructural characteristics and discontinuity zones may require an annealing and working treatment to recover its mechanical properties. The subsequent microstructure will show the presence of recrystallized grains (with annealing twins, strain lines, finer and/or flattened grains, as discussed before) of the α solid solution with the presence of inter-grain small islands of $\alpha + \delta$ eutectoid phase.

Ancient bronzes are generally characterized by a tin amount of 8-10% w/w, especially for the production of laminated artifacts, characterized by very good mechanical properties. An amount higher than 14% w/w was generally used for

castings; the resulting microstructures show an extensive presence of the infilled $\alpha + \delta$ phase that increases the hardness but dramatically causes the pinning of the slip planes, decreasing ductility. This kind of alloy is not cold-workable but an annealing treatment between 600 and 800°C would allow a further mechanical work, thanks to the presence of both α and β phase (see the phase diagram Fig. 1.3), readily workable at this temperature.

A tin content higher than 17% w/w was certainly intentional, because of its cost and difficulties of working, generally used for the production of objects with a particular function (e.g. bells or mirrors). Contents between 17-19 % w/w give as result an alloy very brittle and fragile because of the formation of the δ phase around the grain boundaries, thus decreasing the overall response to mechanical solicitations. Hot working can be performed again for content above 19% w/w, thanks to the presence of the β phase. In order to obtain a final $\alpha + \beta$ structure, thus avoiding the return to the $\alpha + \delta$ composition, the alloy can be subjected to a quenching treatment to retain β phase as a martensitic structure, to obtain increased hardness and lower fragility than the $\alpha + \delta$ phase, at room temperature. The tin content of mirrors, for example, could reach 35% w/w to obtain a silver-like surface appearance with a lower expensive material [9].

- complete immiscibility when no-solubility exists between the components of the alloy. An example is reported in Fig. 1.5 with the Cu-Pb phase diagram, where two distinct phases are formed, thus resulting in a final microstructure of copper grains containing lead globules. In casting of copper-rich alloys the formation of a dendritic structure hinders the formation of excessive lead segregation and high cooling rate causes its fine dispersion among the dendrites or grain boundaries. Some gravity segregation can occurs, thus causing an accumulation of lead in the bottom of the casting, even if a fine and random distribution is more common. The addition of lead in the bronze alloy was a very common practice especially in the Roman period because it lowers the melting point, increases the fluidity of the casting, eases the polishing process and is less expensive than tin; however

it entails detrimental effects and poor mechanical properties, thus reducing the workability, hardness and resistance of the objects [10–12]. Lead content could vary depending on the final function of the object (mirrors, castings), from artifact that had to be coined or subject to deformation processes (weapons, etc.) to artistic objects, such as statues or ornaments.

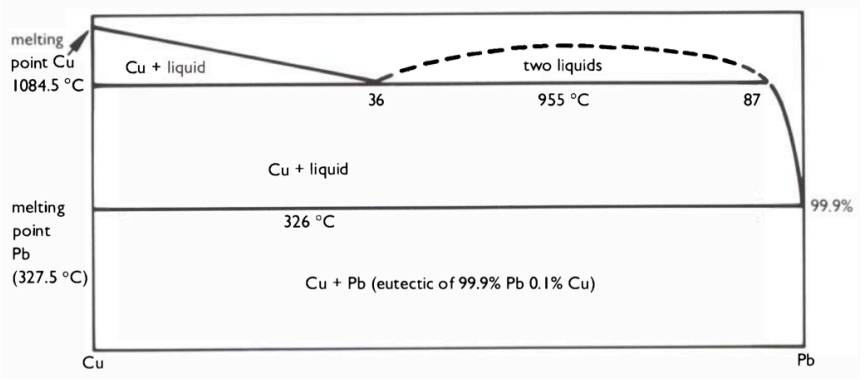

Figure 1.5 Phase diagram of the Cu-Pb system that presents complete immiscibility.

1.2.2 Methods for the production of metallic artifacts

The archaeological findings document that, at first, castings were performed in order to produce things of everyday usage, like utensils and weapons, then also for objects with a sole ornamental function. From the initial stone or terracotta mono- or bi-valves molds, where the melted bronze was casted and the molds used for in-series production, higher technological skills were obtained with the 'lost-wax casting with full model'. With this procedure the object was shaped in the wax model, then covered with a thin clay layer and finally with refractory terrain. After the firing of the model, wax is loss though opportunely fitted canals, thus creating an empty space, then filled up with the liquid alloy. After cooling the coating of clay was broken to reveal the bronze object, subject to a final finishing. The artifacts obtained with this method were unique because of the loss of the wax model and of the clay covering [8].

A further step toward the technological enhancement of this technique was the 'lost-wax casting with empty model', which allowed to obtain impressive and magnificent artifacts under artistic and technical point of view. Schematic representations of the *direct* and *indirect* methods are reported in Fig. 1.6 and Fig. 1.7 respectively. The 'direct method' required the realization of a clay nucleus with the approximate shape of the final objects (Fig. 1.6 (a)) then coated with a wax layer (Fig. 1.6 (c)), where the details were refined. A further thin coating of semi-liquid clay was added to perfectly reproduce the finest details and then invested with a ticker clay layer (Fig. 1.6 (j)). The external and the internal cover were fixed together with bronze or iron rivets (Fig. 1.6 (h)) and a series of channels were added to the wax model to allow the molten bronze to be poured in and gases to escape (Fig. 1.7 (g)). A first slow firing was performed in order to burn out the wax (hence the term 'lost wax') and then increased to higher temperatures to achieve the complete hardening of the coating (Fig. 1.7 (i)). The dried model was buried in a pit to avoid breaking due to the hydrostatic force of the melted bronze that was then poured into the void left by wax (Fig. 1.7 (j)). After cooling the clay mold was broken away and the residual rivets and canals removed from the metal surface (Fig. 1.7 (k)) that was finally cleaned, chased and polished to the desired degree of finish (Fig. 1.7 (l)). Although the direct lost-wax method was capable of casting models of great delicacy and complexity, it had two great disadvantages: i) if, for any reason, the casting failed, the wax model (the sculptor's entire work) was lost forever, since the model had been destroyed during the firing of the mold and ii) even if the casting was successful, only one bronze could be produced from the sculptor model.

Another lost-wax method is the 'indirect' one with the empty model, used also nowadays. The main difference is the preparation of the initial model, which consists, in this case, in a first clay model complete of every detail made by the artist (Fig. 1.7 (a)), from which a mold of gypsum is obtained (Fig. 1.7 (b)). This mold is constituted by different dowels that can be reused for further production of the same object. A coat of several layers of wax is applied on each mold with a brush or hot wax poured into them (Fig. 1.7 (c,d)) to obtain the same aspect of the initial model.

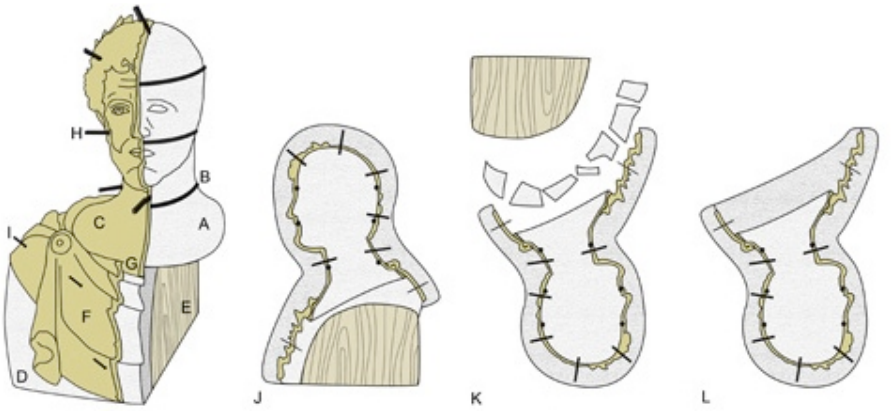

Figure 1.6 Schematic representation of the 'direct' lost wax method that allowed the production of a unique object (see the text for further details). [4]

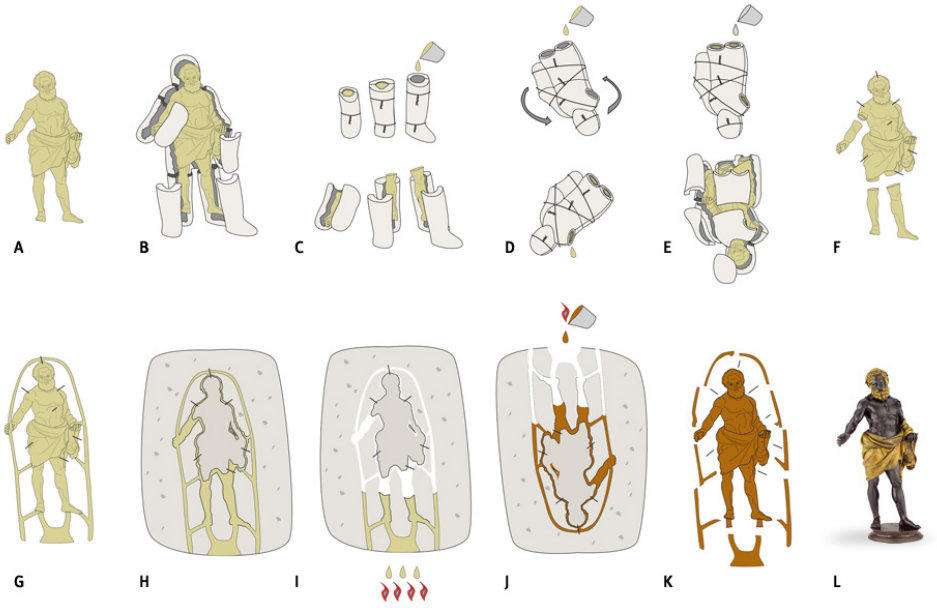

Figure 1.7 Schematic representation of the 'indirect' lost wax method that allows the in-series production of bronze objects (see the text for further details). [4]

[4] https://www.nga.gov/exhibitions/2011/antico/glossary.shtm, consulted on October 2015

The sheets of wax detached from the molds were then applied on a statue made of a refractory material, roughly shaped and reinforced with an internal trestle of wood or metal (Fig. 1.7 (e,f)). The joints between the wax sheets are then hidden and the resulting model further retouched and refined. The canals for the emission of the formed gases, the loss of the wax and the casting of the melt are placed (Fig. 1.7 (g)) and then covered with a refractory coating. From here on the process is the same of the direct method (firing and loss of wax, inserting of the melting, cooling and refining, Fig. 1.7 (h,i,j,k,l)). Indirect casting allowed the sculptor to produce numerous bronze replicas of a popular model. This early anticipation of mass production allowed the distribution of sculpture to a much larger audience than ever before.[4] [8]

1.3 The corrosion process

The 'corrosion phenomenon' consists in the gradual degradation of metals or metal alloys by chemical reactions with the environment. From a thermodynamic point of view, metals can be considered as an open system that continuously exchanges matter and energy with the surrounding environment with an overall decrease in their free energy ($\Delta G < 0$, where ΔG is the variation of the Gibbs free energy that is a measure of the thermodynamic driving force that makes a reaction occur). In fact, almost all the metals, except for the native ones, are naturally present in the form of oxides, carbonates, sulfates, sulfurs, silicates, etc. The metallurgical smelting process allows to convert these compounds into the metallic state, which is less stable than the natural starting compound [13,14].

The degradation process includes all the spontaneous reactions that, because of the above-mentioned exchanges, cause the partial or total alteration of the artifact in respect to its original conformation or chemical composition (e.g. corrosion phenomena). The task of the restoration is to intervene on the kinetic and/or on the thermodynamic of these processes in order to stop or to slow them down.

There are many ways to classify the corrosion process, in particular of copper and its alloys.

For example Robbiola [15] proposed in 1993 ion migration as unifying principle in the corrosion reaction, divided into corrosion under i) cationic and ii) anionic control. The first one is a slow process that tends to form *patina* through the diffusion of cations (copper or tin) toward the surface of the metal, e.g. cuprite layers, thus preserving the shape of the object. The second process is faster and it leads to the production of more destructive, thicker and less coherent corrosion layers, because of the easy transfer of anions (chlorides, sulphates) from the environment to the metal surface.

Another classification [16] considers the morphological changes caused by the growth of the corrosion layers, i) epitactic, ii) topotactic and iii) reconstructive. In epitactic transformation there is crystallography continuity between the first metallic layer and the structure of the corrosion products that assures the retention of shape and protective properties (e.g. cuprite layer). The topotactic events result from a solid-state transformation of a corrosion product into another with a potential different structure and morphology (e.g. from sulphide to sulphate). Reconstructive events may occur when a corrosion product is completely dissolved or chemically altered to form a new different product (e.g. deposition of metallic copper in place of cuprite).

The reactions involved in the corrosion process can be also divided into i) chemical and ii) electrochemical [16]. The main difference is related to the transfer of electric charges, only locally between atoms in chemical reactions, and through a conductor that connects an anodic and cathodic area in electrochemical reactions.

Chemical reactions directly occur between the metal and the surrounding environment with a dry or humid process [17]. The oxidation process of a metallic surface, trough the direct reaction with oxygen, is an example of a chemical gaseous reaction, as in the case of cuprite (Eq. 1.1)

$$2Cu + 1/2\, O_2 \rightarrow Cu_2O \qquad \text{(Eq. 1.1)}$$

This spontaneous reaction lead to the formation of a cuprous oxide layer, which presents good adhesion, insolubility, low reactivity and a crystal lattice structure similar to the metal (epitactic) thus allowing to obtain good protection from the cor-

rosion attack (passivation). The humid chemical reactions require the presence of moisture in the atmosphere, which may act as vehicle for dissolved atmospheric gaseous pollutants (e.g. solphurous anhydride or ozone). The acid attack induce oxy-reduction reactions with the formation of metallic cations which than react with available anionic species to precipitate as corrosion products.

However, most of the corrosive phenomena are of electrochemical nature and they occur in the presence of water or moisture and corrosive agents. This mechanism can be compared to a short circuit battery with an anode (the metallic part that oxidize) and a cathode (the metallic part that reduces, being protected) in the presence of an electrolyte (the aqueous solution). The electrons migrate (current flux), through the metal, from the anode towards the cathode, where they are consumed by species in contact with the metal that assume a negative charge. This process is governed by the potential difference between the anodic and the catodic area, reported for each metal in respect to the SHE (Standard Hydrogen Electron), which present a standard redox potential $E^0 = 0$. A common case of electrochemical corrosion occurs when two metal, with a different E^0, are in contact in presence of humidity, such as copper ($E^0_{Cu^{2+}/Cu}$ = + 0.34 V) and gold ($E^0_{Au^{+}/Au}$ = + 1.69 V) or copper and zinc ($E^0_{Zn^{2+}/Zn}$= - 0.76 V). The metal with lower potential represents the anode and it corrodes while the metal with higher potential is the cathode and it is protected [16,17].

A potential/pH (Eh/pH) diagram, can be very useful to predict the corrosion products that are thermodynamically favored to form in relation to the environmental pH; kinetics effects and reaction rate are not taken into account. These diagrams known as Pourbaix diagrams, combined with environmental information (concentration of different species, such as chlorine or sulphates ions) allow to identify the stability regions for each species formed. Some examples are reported in Fig. 1.8 from [16].

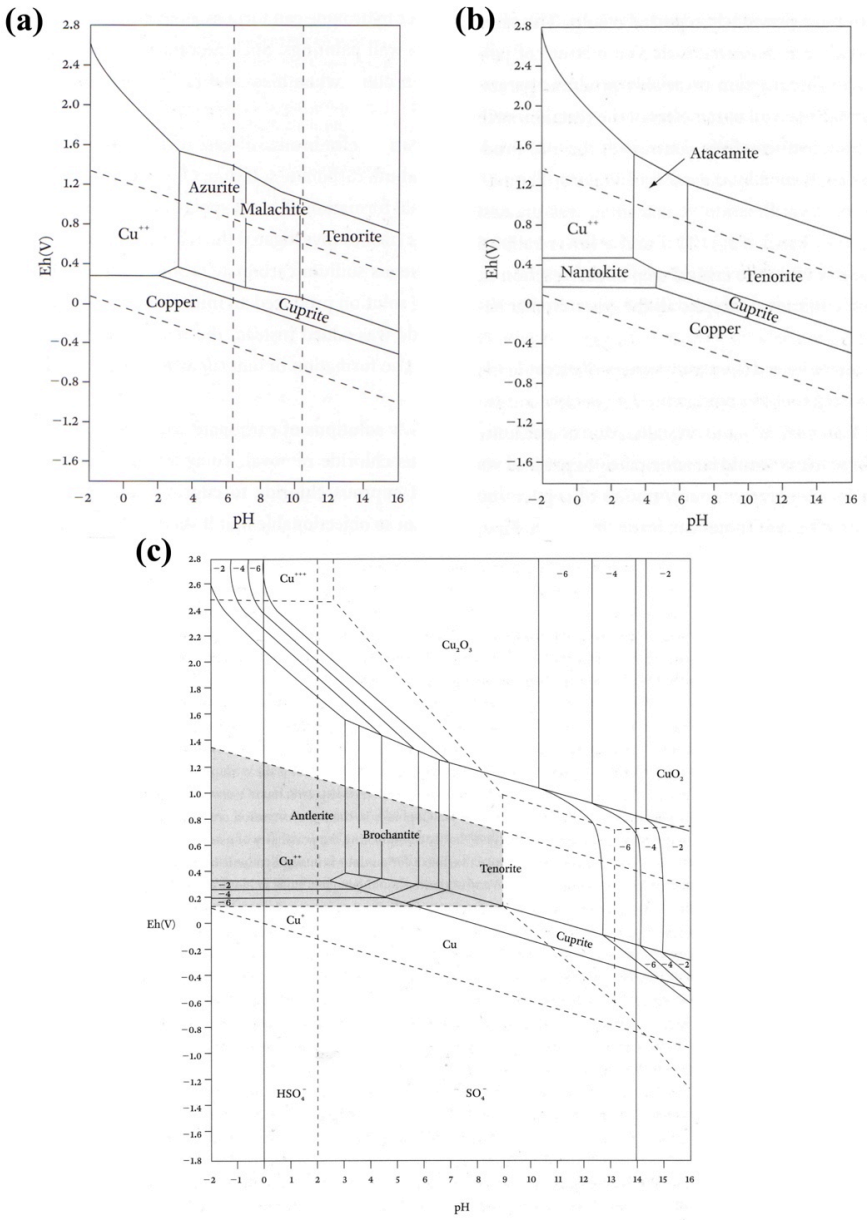

Figure 1.8 Some example of potential (Eh)/pH diagrams for different systems. (a) Cu-CO_3-H_2O at CO_2 concentration of 4400 ppm. (b) Cu-Cl-H_2O at Cl concentration of 3500 ppm. (c) Cu-SO_4-H_2O. The stability regions for each species are showed, although also a thermodynamic contribute is taken into account.

The corrosion process of a metallic artifact depends on several factors that are specifics of the material, such as chemical composition, structure and metallurgical features induced during the manufacturing process, and on external factors related to the environment, accidental events or inappropriate post-discovery conservation procedures. The alteration phenomena result in chemical, physical and structural modifications of the original artifacts.

Depending on the microstructures of the alloys (see section 1.2.1), the corrosion phenomena may presents different morphologies:

- inter-dendritic corrosion, which proceeds along the dendritic edges, due to their structural and chemical heterogeneities;
- inter-granular corrosion, which propagates along the grain boundaries, generally, without affecting the grain matrix. This phenomenon is probably induced by the presence at the grain boundaries of re-precipitated phases or segregated elements.

When the external conditions are particularly aggressive for the artifact, these phenomena may also be related to the dendrites and grains matrix, inducing a complete mineralization of the alloy. Inter-dendritic and inter-granular corrosion represents a real danger for the mechanical stability of the artifacts, since they seriously affect the bronze mechanical resistance.

1.3.1 Corrosion and environment

A detailed subdivision of the corrosion processes that can arise in different conservation environment for a metallic artifact is reported below [13,18]. Moreover Fig. 1.9 [5,6,7] shows some examples of bronze object placed in different environ-

[5] https://it.wikipedia.org/wiki/Satiro_danzante
[6] http://www.wikiart.org/en/benvenuto-cellini/perseus-with-the-head-of-medusa-1545
[7] http://cool.conservation-us.org/jaic/articles/jaic42-02-008.html
Consulted on November 2015

ments contexts (burial, water, outdoor, indoor) and the typical related alteration products.

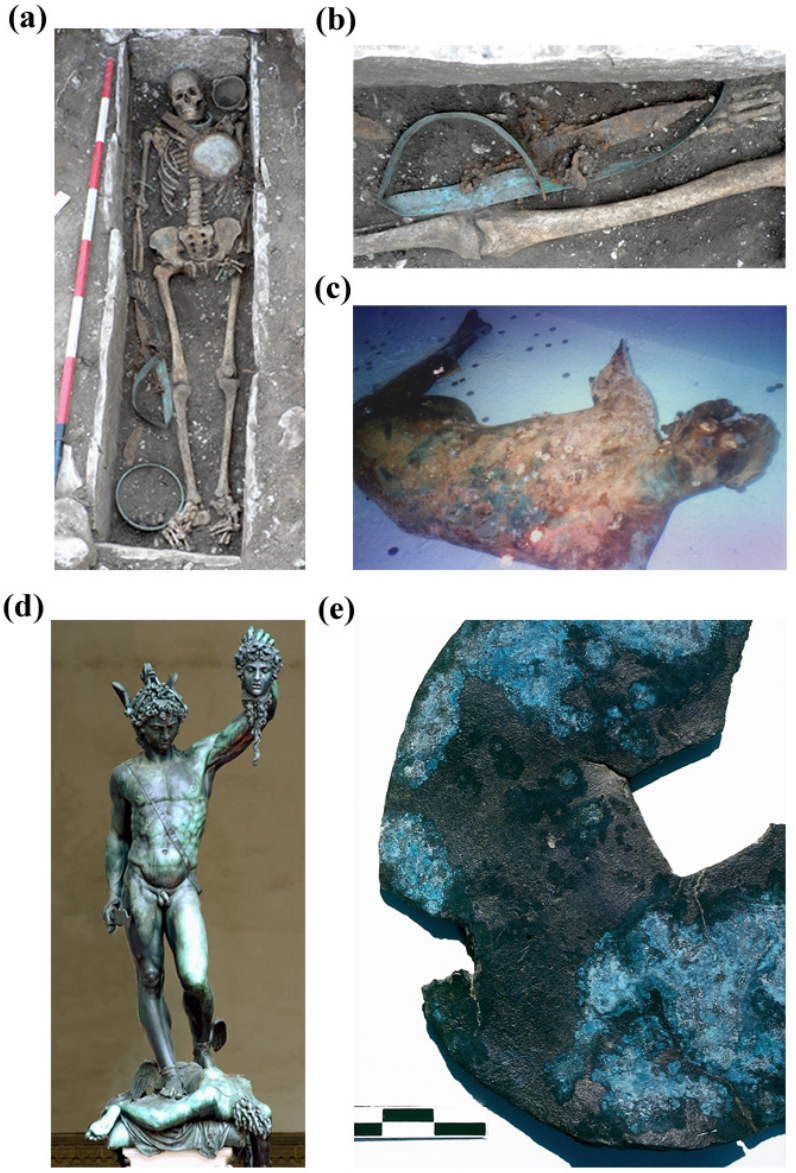

Figure 1.9 Bronze artifacts in different contexts. (a) Burial: grave goods from the archaeological site of Barrea (Abruzzo) belonging to a Samnite warrior; (b) detail of the bronze belt, covered with a green *patina* of corrosion products. (c) Water: the *Dancing Satir*, discovered in 1998 on the marine floor of the Sicilian channel, with an extended *patina* of corrosion

products. (d) Outdoor: *Perseo* by B. Cellini, placed under the *Loggia dei Lanzi* in Florence, is an example of a sculpture exposed to the environment effects. (e) Indoor: a sample coming from the Agora Collection of Athens, with bluish corrosion products (copper carbonate acetate) induced by incorrect conservation conditions.

1.3.1.1 Burial environment

- presence of water: the amount of moisture and water that is present in the subsoil environment is the predominant factor in determining the aggressiveness of the corrosive phenomena, because they favor the electrochemical conductivity and the formation of electrolytes, essential for the maintaining of the corrosion
- presence of oxygen: oxygen is an agent that controls the corrosion phenomena rate, which depends on both the amount of oxygen present in the soil and on the rate at which atmospheric oxygen can reach the surface of the metal; consequently the depth where the object is located influence the extent of the corrosion phenomenon
- electrical conductivity: the electrical conductivity of the soil affects the evolution of the corrosion; greater is this soil property, the more intense is the phenomenon
- chemical composition of the soil: the presence of soluble substances in the soil favors the electrical conductivity, and then the extent of the corrosion that tends to give rise to generalized or localized attacks, depending on the nature of the present anions. Furthermore, the presence of microorganisms in the soil (sulphur-reducing bacteria SRB) or the contact with human rests can greatly affect the aggressiveness of the soil
- pH of the soil: this value influences the formation and the stability of the corrosion products
- moisture retaining constituents are to be considered active for the corrosion development

1.3.1.2 Water environment

- presence of oxygen: the concentration of dissolved oxygen in the water, where the artifacts are immersed, has a considerable influence on the progress of the corrosion phenomena that occur on the surface of the artifacts. It has to be considered that the solubility of oxygen in water is affected by its temperature and conditions (stagnant or flowing water)
- presence of salts: the concentration and the type of salts dissolved in water affect the corrosion phenomena. Some anions, such as chlorides, tend to cause a rapid spread attack on metallic surfaces, due to their considerable ionic conductivity. Others, such as carbonates and bicarbonates, have a lower activity and tend to give localized corrosion phenomena
- temperature: high temperature induce the development of spread corrosion phenomena and the increasing in the corrosion rate, due to the oxygen solubility reduction by temperature increasing
- microorganisms: animal or vegetal microorganisms may locally vary the concentration of oxygen present in solution and cause corrosion by differential aeration, by being anchored onto the surface of the metal. They can also secrete substances, due to their metabolic activities, which are aggressive for the metal surfaces
- algae and aquatic animals can affect the corrosion phenomena, as well as some suspended solid substances

1.3.1.3 Outdoor environment

- presence of oxygen: the abundance of oxygen in an external context influences the oxidation process thus accelerating, even greatly, these reaction in respect to an anaerobic environment
- exposition to the atmospheric agents: ambient temperature, relative humidity, and pollution levels may activate or increase degradation processes. The amount, frequency, and duration of rain, wind, fog, mist, and freeze-thaw

events, complicated by wind and aerosol erosion effects that influence the time of wetness on a given surface, represent the main factors affecting the conservation of an exposed object. Water, in fact, gives the main contribution to the degradation processes, by transporting pollutants and particulate on the metallic surface. Besides water can solubilize some of the corrosion products, thus giving rise to aesthetical (striping) and compositional inhomogeneities on the metallic surface. The synergic action of these factors promotes electrochemical mechanism of corrosion, which can be very rapid, extensive and destructive for the object [19]

- exposition to the atmospheric pollutants: acid gases (CO_2, SO_2, SO_3, N_yO_x, Cl^-) vehiculated from water and the deposition of atmospheric particulate, formed by industrial activities or combustion reactions (combustion engines, domestic heating and energy production) are the main causes of the corrosion reactions in the external environment. The interaction between the principal alloying element (copper) and these pollutants leads to the formation of several corrosion products with different compositions and morphologies [15,18,19]:
  - *reactions with CO_2*: the natural equilibrium between the O_2/CO_2 production doesn't exists anymore since years, because of the anthropic effect. The excess of CO_2, which forms H_2CO_3 in aqueous solutions, leads to degradation reactions with carbonates and metallic substrates. In particular the interaction with copper leads to the formation of copper carbonate and hydroxycarbonates (Eq. 1.2), such as malachite ($CuCO_3 \cdot Cu(OH)_2$) and azurite ($2CuCO_3 \cdot Cu(OH)_2$)

$$2Cu + H_2O + O_2 + 2CO_2 \rightarrow 2CuCO_3 + H_2O \qquad \text{(Eq. 1.2)}$$

  - *reactions with sulphur compounds* (SO_2, SO_3, H_2SO_4): SO_2 produced from combustion of coal, wood or oil, oxidizes in the atmosphere to produce SO_3, which in presence of water reacts to form H_2SO_4. Basis or salts can buffer this acid, e.g. $CaCO_3$ thus forming gypsum ($CaSO_4 \cdot 2H_2O$) directly in the atmosphere. The formed gypsum precipi-

tates by dry or humid deposition over every object exposed to the atmosphere; the interaction between gypsum and the atmospheric particulate or heavy hydrocarbons leads to the formation of concretions very similar to black crusts of a carbonatic substrate. H_2SO_4, with HNO_3 and H_2CO_3, is a constituent of acid rains and it reacts with copper to form mainly two hydroxysulphates, antlerite (Eq. 1.3) and brochantite (Eq. 1.4)

$$6Cu + 2H_2SO_4 + 3O_2 + 2H_2O \rightarrow 2Cu_3(OH)_4SO_4 \quad \text{antlerite (Eq. 1.3)}$$

$$8Cu + 2H_2SO_4 + 4O_2 + 4H_2O \rightarrow 2Cu_4(OH)_{46}SO_4 \quad \text{brochantite (Eq. 1.4)}$$

- ❒ *reactions with nitrogen compounds* (N_yO_x): nitrogen oxides increasingly produced by industrial and civil combustions (parts per million ppm), can react with oxygen and water to form nitric and nitrous acid. These acids can be buffered in the atmosphere by basis or salts, or vehiculated by acid rains on the ground. The interaction with a copper-based alloy lead to the formation of nitrates (Eq. 1.5) and nitrites

$$4HNO_3 + 4Cu + O_2 \rightarrow 4Cu(NO_3)_2 + 2H_2O \quad \text{(Eq. 1.5)}$$

- ❒ *reactions with hydrochloric acid*: HCl can be produced (ppm) by industries or it can be natural (sea aerosol) and it causes a very common degradation phenomenon known as 'bronze disease' which will be treated in details in section 1.3.3.

- ❍ animal and vegetal organisms action that can entails mechanical stresses or the production of reactive substances
- ❍ photo-chemically or oxidizing reaction, induced by UV-radiations and ozone respectively, on organic substances (protectives, etc.).

1.3.1.4 Indoor museum environment

Indoor museum environment are not always completely safe for the conservation of an artistic object [20]. In fact thermo-hygrometric conditions are fundamental for attaining the suitable and the best conservation conditions. Also the presence of a

series of pollutants, such as gaseous NO_x, SO_2, H_2SO_3, acids, alcohols, aldehydes, ketones, etc. affects the conservative efficacy. Their sources can be structural or decorative materials, intrusion of outdoor pollutants, emanations from fabricated products (display cases, furnishings, storage materials, etc.), visitors (dust, fibers, skin particles, etc.) and staff activities (cleaning products); in special cases the artifacts themselves may emit significant and even dangerous amounts of polluting gases. The combined interaction of humidity, chemical reagents and particulate may trigger or worsen localized corrosive processes.

1.3.2 Copper corrosion products

Tab. 1.2 reports the overall corrosion products that can arise on the surface of a Cu-based artifact, related to the principal components of a bronze alloy (Cu, Sn and Pb), divided by chemical groups and identified by their colors. A detailed description of the principal corrosion product of sole copper is given in the following sections [15,16,18].

1.3.2.1 Copper oxides

- cuprite: this cuprous oxide has a fundamental importance in the protection of the metallic alloy. In fact it is the first layer to form when the metal is exposed to air, thus acting as a protective interface between the metal surface and the environment by slowing further corrosion processes [21]. For this reason a cleaning intervention should aim at preserving the cuprite layer to avoid the exposition of new metal surface. It usually forms epitactic layers (see section 1.3), maintaining the original shape of the surface; it has a cubic microstructure and dark-red to orange-red colors
- tenorite, this cupric oxide is a rare component of natural *patina*. Its formation, in fact, requires very specific conditions, such as heating processes in an oxidative environment. Although Pourbaix diagrams (see Fig. 1.8 (a)) suggest the presence of tenorite as a very stable species, its formation de-

pends more on kinetics than on thermodynamics. It has a monoclinic crystal system and gray to black colors

Corrosion compounds of copper-based (Cu, Sn, Pb) artifacts			
Copper	oxides	**cuprite**	**Cu_2O**
		tenorite	**CuO**
	carbonates	**malachite**	**$Cu_2(OH)_2CO_3$**
		azurite	**$Cu_3(OH)_2(CO_3)_2$**
	chlorides	**atacamite**	**$Cu_2(OH)_3Cl$**
		botallackite	**$Cu_2(OH)_3Cl \cdot H_2O$**
		clinoatacamite	**$Cu_2(OH)_3Cl$**
		nantokite	**CuCl**
	sulphides	**chalcocite**	**Cu_2S**
		covellite	**CuS**
		calcopirite	**$CuFeS_2$**
		digenite	**Cu_9S_5**
		roxbyte	**Cu_9S_5**
	sulphates	**antlerite**	**$Cu_4(SO)_4(OH)_4$**
		brochantite	**$Cu_4(SO)_4(OH)_6$**
		calcantite	**$CuSO_4 \cdot 5H_2O$**
	nitrates	**gherardtite**	**$Cu_2(NO)_3(OH)_3$**
	phosphates	**libethenite**	**$Cu_2(PO)_4(OH)$**
Tin	oxides	**cassiterite**	**SnO_2**
		romarchite	**SnO**
	hydroxides	**schoefliesite**	**$Mg[Sn(OH)_6]$**
Lead	oxides	**litharge**	**PbO**
		plattnerite	**PbO_2**
	carbonates	**cerussite**	**$PbCO_3$**
		hydrocerussite	**$Pb_3(CO_3)_2(OH)_2$**
	chlorides	**cotunnite**	**$PbCl_2$**
		phosgenite	**$Pb_3CO_3Cl_2$**
		pyromorphite	**$Pb_5(PO_4)_3Cl$**
		vanadinite	**$Pb_5(VO_4)_3Cl$**
	sulphides	**galena**	**PbS**
	sulphates	**anglesite**	**$PbSO_4$**
		leadhillite	**$Pb_4(SO_4)(CO_3)_2(OH)_2$**

Table 1.2 The table reports the main corrosion compounds that can occur on the surface of a copper-based alloy artefacts, whose formation depends on the properties of the material and on the surrounding environment; other uncommon products are also reported.

1.3.2.2 Copper basic carbonates

- malachite: this mineral represents a predominant component of the *patina* composition of long-buried objects, while it generally is a minor phase in outdoor exposed or sea buried artifacts; it can also occurs as a post excavation alteration products of other minerals. Malachite usually forms over the cuprite layer with a uniform growth, conferring the common green color to the *patina* seen on many bronze antiquities. It has a monoclinic crystal habitus, even if well-formed crystals are rare and different forms can occur for corrosion products. Acid substances can solubilize malachite by transforming it in other copper salts and, thus, creating an aesthetically inhomogeneous aspect of the *patina* (stripes, etc.)
- azzurrite: this basic copper carbonate is less common than malachite as a corrosion product. Both azurite and malachite formation occurs for the reaction between the copper of the alloy and CO_2 aqueous solutions (H_2CO_3) coming from soil water or condensed moisture, but azurite is less stable than malachite and it can be easily transformed into it by loosing CO_2 in presence of water. It rarely forms homogeneous *patina* and more commonly occurs as small crystals in association with malachite. It has a monoclinic crystal structure and a characteristic vitreous blue color (in fact it was mainly used as pigment).

1.3.2.3 Copper basic sulphates and sulphides

- brochantite: this basic copper sulphate is a very diffuse and stable component of the pale green *patina* present on the majority of artifacts exposed to polluted atmosphere in urban environments. Its crystal system is monoclinic and it presents a vitreous green color. It generally forms a uniform and resistant layer also on rainfall exposed areas even if acid water can produce its transformation into antlerite (longer exposition times) [15,18]

- antlerite: it is commonly associated to brochantite as predominant component of outdoor Cu-based *patina*. It has an orthorhombic crystalline lattice and vitreous green color. Its presence is increased in the last years as a pollutant indicator because it forms at lower pH (see Fig. 1.8 (c)). In fact the rainwater pH has become more and more acid since the half of the mid-twentieth century, thus entailing problem of dissolution of the stable *patina* [22]
- sulphides: they forms under anaerobic conditions in organic matter soils-rich and in presence of sulphur-reducing bacteria (SRS). They are common corrosion products for buried objects under soil or seawater sediments in reducing conditions, where the metabolic reduction of SRS bacteria produces the presence of sulphur ions, which react to form different kinds of minerals. The resulting dark colored *patina* are composed by chalcocite, covellite, digenite, etc. In atmospheric environment such corrosion products are less common because they are transformed in basic copper sulphates after their formation, but sometimes these products were found in museum environment because of the exposition to air containing H_2S.

1.3.2.4 Copper nitrates and phosphates

- nitrates: they are relatively rare as corrosion products mainly because of their high solubility in water, thus being immediately washed away by water as they form. Sometimes they can occur in archaeological contexts (mainly as gherardite, orthrombic crystal lattice, dark to emerald green color) or in case of artificial patination
- phosphates: they are not very common except for burial context where the metal object is in contact with bones (e.g. cremation or burial sites) or other phosphor sources. The most common phosphate as corrosion products is liberthinite (ortorombic crystal shape, olive green color).

1.3.3 Cooper chlorides and 'bronze disease'

- nantokite, a cuprous chloride that can occur as a gray or gray-green translucent waxy solid. It has a cubic crystal form, pale green color and low hardness (Tab. 1.3). It can remain dormant for long time, until the exposure to the air oxygen and moisture that can trigger the so-called 'bronze disease' phenomenon. The reactions involved entail the expansion of its volume or the transformation into copper oxychlorides. The location of cuprous chloride within the *patina* constituents can vary: in some cases it is adjacent to the metal surface, but in other examples it may overlie cuprite or be interposed between cuprite layers. An appropriate and stable RH is necessary for the correct storage of bronzes and values between 42-46% was found to be sufficient for the majority of bronze objects; at this humidity level cuprous chloride will not undergo chemical reaction, which already guarantees a margin of safety. More problematic objects may require lower levels. The relative stability and insolubility of cuprous chloride in unexposed pits may create problems during cleaning of ancient bronzes, since the exposure of such pits usually necessitates further stabilization measures or monitoring procedures
- atacamite: is the most common of the three basic copper chlorides polymorphs with an orthorhombic crystal system and vitreous green color. It is often found in association with its polymorphs and its presence suggest the presence of an active corrosion process (Tab. 1.3)
- clinoatacamite and paratacamite: there is a certain confusion surrounding these two copper oxychlorides and they often are confused. Paratacamite may contain zinc and it has a rhombohedral crystal form while the monoclinic system is referred to clinoatacamite and they both presents a pale green color (Tab. 1.3). They can occur together but paratacamite is less common, except for copper alloys containing appreciable amounts of zinc

- botallackite: is the least stable and common of the three isomers, with a monoclinic habitus and a pale bluish color (Tab. 1.3).

Mineral	Formula	Crystalline system	Color	Hardness (Mohs)
Nantokite	CuCl	Cubic	Light green/white	2.5
Atacamite	$Cu_2(OH)_3Cl$	Orthorhombic	Glassy green	3-3.5
Paratacamite	$Cu_{1.5}Zn_{0.5}(OH)_3Cl$	Rhombohedral	Light green	3
Clinoatacmite	$Cu_2(OH)_3Cl$	Monoclinic	Pale green	3
Botallackite	$Cu_2(OH)_3Cl$	Monoclinic	Light green/blue	3

Table 1.3 Chemical-physical characteristics of the copper chlorides related to the 'bronze disease' process.

The so-called 'bronze disease' [6,10,16,23–31] is a cyclic phenomenon, which leads to the progressive deterioration of ancient copper alloys (Fig. 1.10), mainly induced by the presence of nantokite. The main factors that can trigger this corrosion phenomenon are i) the humidity level of the environment (RH > 35%), ii) the presence of oxygen and aggressive agents (Cl^-, SO_2 and other polluting agents) in the atmosphere. From the conservation point of view, the most aggressive corrosion agent for Cu-based artifacts is chlorine (Cl^-), coming from the soil, water or atmosphere that generally forms cuprous chloride (nantokite) with copper at the interface between the external *patina* and the surviving metal. The exposure of the reactive cuprous chloride species to the atmospheric moisture and oxygen induces the development of the cyclic dissolution process of copper, known as 'bronze disease', very dangerous for the chemical-physical stability of the copper-based artifacts. When cuprous chloride is exposed to the atmosphere, it cyclically reacts with oxygen and water, thus giving rise to the formation of the greenish $2Cu_2(OH)_3Cl$ (atacamite and its polymorphs) that reacts with copper to form new cuprous chloride and water. In this way copper, chlorine, oxygen and water are converted into cuprite (Cu_2O) and atacamite in a cyclical and continuous process that can disfigure the archaeological object (see Eq. 1.6, 1.7, 1.8, 1.9). It is noteworthy, especially during a cleaning procedure, the protective role of the copper (II) compounds and of the cuprite layer that isolate the surface from the surrounding environment. In particular,

the presence of copper chlorides is potentially very dangerous for archaeological artifacts, because they often lie in a low-oxygen environment until they are excavated, then exposed to the air oxygen and moisture. Therefore, particular attention must be paid before and during the removal of surface encrustations and corrosion products layers, in order to avoid the exposure of the dormant copper chlorides and suitable conservation parameters (especially RH < 35%) should be kept.

$$Cu^0 = Cu^+ + e^- \quad \text{(Eq. 1.6)}$$

$$Cu^+ + Cl^- = CuCl \quad \text{(Eq. 1.7)}$$

$$4CuCl + 4H_2O + O_2 = 2Cu_2(OH)_3Cl + 2H^+ + 2Cl^- \quad \text{(Eq. 1.8)}$$

$$2Cu + 2HCl = 2CuCl + H_2 \quad \text{(Eq. 1.9)}$$

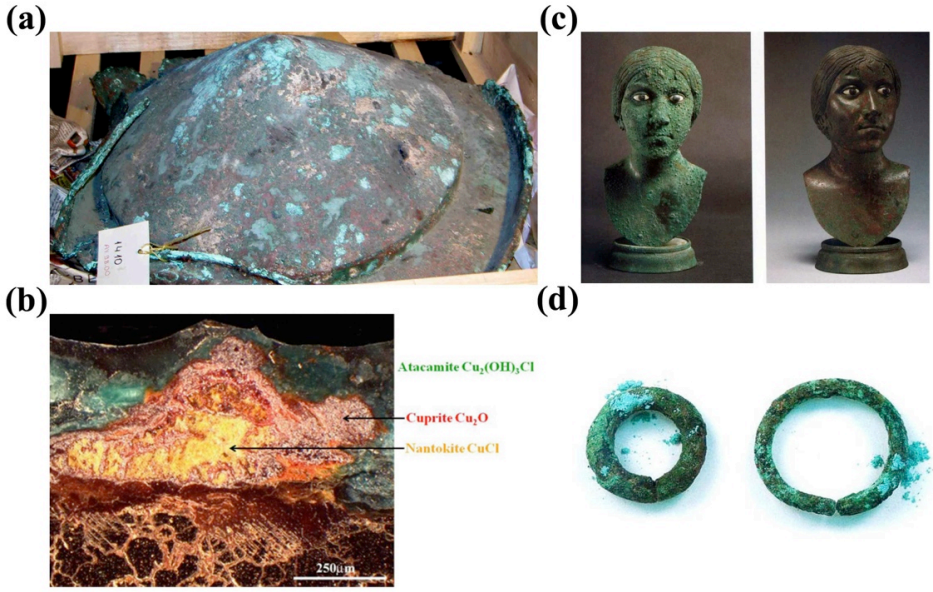

Figure 1.10 The morphology of the 'bronze disease' process over different metallic artifacts: (a) the surface of a shield from the Ayanis Fortress (Turkey) [28] and (b) the relative stratification of the corrosion products (dark-field metallographic image). (c) Two small bronze ornaments from the site of La Compañia, Ecuador, showing the light green, powdery eruptions typical of 'bronze disease' [16]. (d) Miniature Portrait bronze Bust of a Woman, Roman period. The bust before conservation (left) shows pustular corrosion with pitting created by the 'bronze disease'[16].

1.3.4 Patina morphologies and investigation techniques

1.3.4.1 Patina morphologies

Metallic artifacts are affected by corrosion phenomena that induce the formation of complex *patina* on their surface, characterized by different morphology and micro-chemical nature of the corrosion products, depending on the chemistry and metallurgical features of the artifacts and of the external conditions. Cu-based artifacts suffer from an intense dissolution of the alloy components that causes the formation of overlapping structures, whose chemistry and morphology, greatly, vary from the external surface to the metal interface (Fig. 1.11).

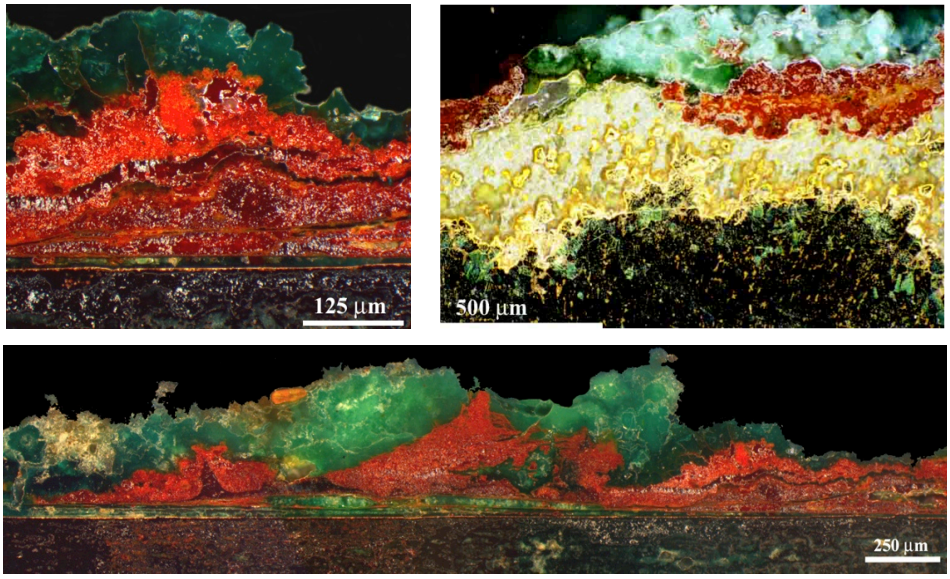

Figure 1.11 Some examples of stratified corrosion products on different archaeological artifacts [28,32]. The dark-field images of the metallographic microscope reveal a multi-layered structure, where cuprite (red) is generally placed at the interface between metal and Cu(II) corrosion products (green), unless the presence of nantokite (yellow-orange), symptom of an active corrosion process.

Therefore, from a cross section of a metal artifacts it is possible to observe the following areas (see Fig. 1.11):

- the inner area, characterized by the coexistence of the surviving metal and the corrosion compounds that preserve the original structure of the metal. The corrosion phenomena proceeds along the grain boundaries or dendrites, even to their complete destruction and the principal products are copper or tin oxides (cuprite, cassiterite, romarkite) and copper oxy-chlorides (atacamite and its polymorphs) finely mixed
- an intermediate area, highly stratified, composed by compact layers of cuprous chloride (nantokite), closer to the metal, cuprous oxide, tin oxide and copper oxy-chlorides. The presence of atacamite and its polymorphs (clinoatacamite and botallackite) has been frequently monitored and related to 'bronze disease'. This area, formed by the dissolution and the reaction of the alloying elements, can reach a considerable thickness
- the external area, with a variable thickness, is characterized by the presence of other compounds, strictly related with soil elements, such as P, S, Ca, Si, Fe, Al and Cl.

Different investigation techniques are commonly used to characterize the corrosion products and to study the alloy features by studying the surface and the section of the samples. In particular the combined use of optical and electronic microscopy, X-ray diffraction and FTIR spectroscopy, reported below in details, allow to obtain complete and reliable information.

1.3.4.2 Optical microscopy (OM)

Preliminary investigations by means of optical microscopy allow to obtain information on the superficial corrosion and alteration products of the alloy. The primary source of energy is the visible radiation and the reflected or transmitted radiation from the object allows to create the images. The optical microscopy is composed by a system of lenses (oculars and objectives) to magnify the images and a system to acquire them (CDD cameras). A particular type of optical microscopy is the stereomicroscopy in reflected light, very used in the field of cultural heritage, because it allows to obtain 3-D images, thanks to two different optical paths. This kind of sys-

tem allows to observe, with an effective and high spatial resolution, only sample with low variation along the *z* axis. This limit can be in part overcome with a MultiFocus system, which allow to automatically acquire images at different focal positions, then merged together to enhance the vision also of rough surfaces, with an extended focal depth.

Metallographic microscopy is commonly used for the observation of metallic sectioned samples, opportunely prepared by embedding in epoxy resin and polishing to to a very high luster and eventually chemically etched to observe microstructural details. The observation of the reflected light can be carried out both in bright and dark field to obtain different information. In fact the bright field illumination allow to observe the microstructure of the sample and to identify the different phases (e.g. $\alpha + \delta$ eutectoid or sulphides inclusions) that have a natural color reflectivity difference from the bulk of the metal. Dark field illumination generates improved image contrast and a self-luminous effect that offers increased resolution and visibility over bright field. It's very useful to identify multi-layered species of corrosion products thanks to their typical colors, e.g. copper oxides light up vividly red, basic copper chlorides appears with various shades of green and nantokite from yellow to orange-red (see Fig. 1.11).

1.3.4.3 Scanning electron microscopy / microanalysis (SEM/EDS)

Scanning electron microscopy allows to obtain images of the samples at very high resolution and magnification in comparison to the conventional optical microscopy. The electron gun produces an electron beam that is accelerated and focused by applying a potential difference. The beam passes through a system of electromagnetic lenses that manage the beam reducing the size up to the order of nm. When the primary electrons, accelerated along a column, affect the material, the electron-matter interaction produces backscattered electrons (BSE), secondary electrons (SE), Auger electrons and X-rays.

Secondary electrons are obtained by inelastic scattering phenomena between the electron beam and the material (valence electrons of the material). Their energy is

lower than the energy value of the primary electron beam and the backscattered electrons (< 50 eV). They lose part of their energy on their way to the surface, being involved in more inelastic process and, therefore, only those closest to the surface of the material can actually escape from it and provide useful information. SE come from the outer regions of the material (10-50 nm) giving maximum resolution topography (edges are bright, recesses are dark). The number of SE depends on different parameters and factors, mainly the atomic number Z of the sample and the energy of the incident beam.

Backscattered electrons are generated by the elastic scattering interactions between the electrons of the primary beam and the atoms of the material, whose energy is therefore close to that of the incident beam (> 50 eV). BSE come from a depth of the order of about 0.5-1 μm, therefore, they are not characterized by high topographical resolution. The BSE signal provides information on the local chemical composition of the material according to the backscatter coefficient

$$\eta = n_{BS}/n_B \qquad \text{(Eq. 1.10)}$$

where n_B is the number of incident electrons on the sample and n_{BS} is the number of backscattered electrons. By increasing atomic number, the number of BSE increases, so the morphology of the surface can be related to its local chemical composition.

The produced electrons are revealed by two different detectors able to discriminate BSE and SE signals. The composition of the two information i) signal from the detector and ii) the local coordinates of the primary beam allows to reconstruct a 3-D image. In fact each XY coordinates explored by the primary electron beam is associated to a z-value, directly connected with the amplitude of the signal revealed by the detector used and a black and white image is finally visible on the screen.

The scanning is performed by means of two pairs of electromagnetic coils placed internally to the objective lens, which move the electron beam on Cartesian coordinates X and Y of the sample surface via the signal electric sent.

Combining the scanning electron microscope with a microanalysis system, which analyzes the characteristic X-rays emitted from the sample (EDS and WDS system)

gives the possibility to obtain qualitative and quantitative chemical information. The EDS principle is based on the analysis of the X-ray fluorescence phenomenon that occurs when the sample is irradiated by an electron beam. The incident beam may excite an electron in an inner shell, ejecting it from the shell while creating an electron hole where the electron was. An electron from an outer, higher-energy shell then fills the hole, and the difference in energy between the higher-energy shell and the lower energy shell may be released in the form of an X-ray. The number and energy of the X-rays emitted from a specimen can be measured by an energy-dispersive spectrometer. As the energies of the X-rays are characteristic of the difference in energy between the two shells and of the atomic structure of the emitting element, EDS allows the elemental composition of the specimen to be measured.

1.3.4.4 X-ray diffractometry (XRD)

X-ray diffraction (XRD) allows to obtain compositional information on the crystalline phases that constitute the different alteration *patina*.

XRD is based on constructive interference of monochromatic X-rays and a crystalline sample. These X-rays are generated by a cathode ray tube, filtered to produce monochromatic radiation, collimated to concentrate, and directed toward the sample. The interaction of the incident rays with the sample produces constructive interference (and a diffracted ray) when conditions satisfy Bragg's Law (Eq. 1.11)

$$2dsin\theta = n\lambda \qquad \text{(Eq. 1.11)}$$

The determination of the typology and lattice structure is possible if the d parameter (spacing between diffracting planes) is obtained, knowing the wavelength (λ) of the incidental X-rays beam and its incident angle (θ). This law relates the wavelength of electromagnetic radiation to the diffraction angle and the lattice spacing in a crystalline sample. The diffracted X-rays are then detected, processed and counted. By scanning the sample through a range of 2θ angles, all the possible diffraction directions of the lattice should be attained due to the random orientation of the powdered material. Conversion of the diffraction peaks to d-spacings allows the identification

of the mineral because each mineral has a set of unique spacings between the crystalline planes. Typically, this is achieved by comparison of *d*-spacings with standard reference patterns.

For the above-mentioned feature, this technique is useful only for the characterization of crystalline materials, while for amorphous phases, with a non-defined or ordered structures, no information are obtainable.

1.3.4.5 FTIR spectroscopy

Fourier transform infrared spectroscopy (FTIR) is a reliable and powerful analytical tool based on the vibrations of the atoms of a molecule. An infrared spectrum is commonly obtained by comparing IR radiation returned by (micro-FTIR, ATR-FTIR) or transmitted (KBr) through a sample and determining what fraction of the incident radiation is absorbed at a particular energy. Covalent bonding vibrational frequencies, such as asymmetric stretching and deformation stretching are determined by correlation to the wavelengths in the IR Spectrum.

FTIR spectroscopy represents a very useful technique in diagnostic analysis of cultural heritage because it allows to analyze almost every kind of samples (solid, liquid, crystalline and amorphous, organic and inorganic).

In particular the classic method used is that of KBr pellets in transmission mode, characterized by high energy throughput and a resulting high sensibility, for qualitative and quantitative analysis of powder or liquid samples. Very small amounts of sample are required but sample preparation can be not well reproducible.

Micro-FTIR is a more recent technique that improved the potential of vibrational spectroscopy in the field of diagnostic and conservation of art works thanks to the coupling of a FTIR spectrometer with an optical microscope. At any interface between two materials, an incident radiation is split into reflected and transmitted beams in different proportions according to the refractive index ratio of the two materials in question. Based on this principle, in parallel to transmission measurements, reflection techniques have been widely developed due to the non-destructivity of this type of analysis towards the sample. In fact, reflection meas-

urements can also be directly performed on the surface of an object without any sampling and thus have been easily applied on a large variety of materials. If the object is small enough, it can be placed directly on the microscope stage.

The attenuated total reflection (ATR-FTIR) method operates by measuring the changes that occur in a totally internally reflected infrared beam when the beam comes into contact with a sample. An infrared beam is directed onto an optically dense crystal (diamond, germanium, etc.) with a high refractive index at a certain angle. This internal reflectance creates an evanescent wave that extends beyond the surface of the crystal into the sample (0.5 - 5 μm) held in contact with the crystal. Consequently, there must be good contact between the sample and the crystal surface. In regions of the infrared spectrum where the sample absorbs energy, the evanescent wave will be attenuated or altered. The attenuated energy from each evanescent wave passed back to the IR beam, which then exits the opposite end of the crystal and is passed to the detector in the IR spectrometer. The system then generates an infrared spectrum. This versatile and non-destructive technique allow to analyze very well thin polymeric films thanks to the very strict contact with the crystal and to the high difference of the refractive index between the two materials.

1.4 Traditional cleaning processes

Cleaning is a restoration procedure that aims to bring the surface to a state that resembles as close to the original appearance of the work-of-art. Based on this concept the cleaning step represents a fundamental operation and the most delicate part of the restoration process. A correct cleaning operation requires to set-up specifically tailored treatments for each artifact, which is unique for definition, by taking into account its conservation condition and the stratigraphic composition of the *patina* [33,34].

Diagnostic analyses of the artifact and of its conservation environment, along with historical-artistic researches, should precede the cleaning intervention in order to individuate the most suitable, effective and less aggressive cleaning methodology to use. Furthermore, the desired level at which the cleaning action should be

stopped has to be defined, based on the definition of *patina*, its historical value and/or the protective role that it may have. A careful evaluation has also to be carried out between the occurrence of a natural *patina,* spontaneously formed onto ancient works of art as the result of the transformation of the original matter and of an artificial *patina*, intentionally created by the artist to obtain a particular aesthetical effect, so an alteration that is part of the original aspect of the piece of art [34].

Besides, the term *patina* and the related historical-artistic implications, has been object of debates for centuries between those who sustained its drastic, integral removal to re-establish the original aspect with bright and vivid colors/surfaces and those who, on the other hand, defended its authenticity [33,35,36].

Nowadays, as concern the Italian concept of restoration, is generally accepted that each cleaning methodology must be differentiate according to the material and to its conservative conditions, and that the *patina* has not to be completely removed, by performing a selective, gradual and controllable cleaning action. In this way also the age and the historical information of the object are respected [37].

Within restoration process of metallic artifacts, cleaning still represents a great challenge for conservators. In fact this task requires a deep awareness on the intrinsic characteristics of the treated alloys and on the ongoing alteration processes, especially in case of outdoor monuments or buried artifacts. The alteration products of Cu-based alloys usually form thick and adherent concretions to thin and homogeneous *patina* (see 1.3.4.1 section). An adequate cleaning procedure should aim at the complete removal of the esthetically defacing and harmful corrosion products and also at the preservation of the protective cuprite layer. Cleaning is traditionally performed by mechanical and/or chemical methods, depending on the morphology and typology of the *patina* corrosion products to remove, trying to respect the principle of minimum intervention. Often, more than one method is used in combination, depending on each case, in order to find the best treatment and a specific approach for the different surfaces considered, depending on the core (typology of corrosion), its surface treatment (gilding, original or artificial *patina*), its alteration (corrosion products) and age (harder encrustations).

1.4.1 Mechanical cleaning

Mechanical cleaning is usually performed by means of vibrating or abrasive tools, micro-peening with vegetal granulates, ultra-high-pressure water, laser [38].

Some example of the most commonly used mechanical methods are: i) vibrating tools, particularly recommended for lime or calcareous crusts; ii) rotating tools, generally used as finishing tools to make the superficial colors uniform; iii) soft blasting with vegetable flakes [39], with different size and hardness, used to remove incoherent deposits and incrustations mainly of calcium carbonates and sulphates; iv) laser cleaning, performed under specific conditions, *i.e.* surface wetting by water before the cleaning process starts.

Mechanical cleaning presents some limits related to scarce selectivity and invasiveness of this procedure, which can damage the protective cuprite layer or delete superficial information on the surface [16,40]. Laser ablation seems a very promising techniques and it's commonly used in association with other cleaning methods, as in the case of the 'Porta del Paradiso', the east door of the Baptistery of Florence, where optimized QS-Nd:YAG laser ablation was used on the gilded surfaces (see Fig. 1.13) [41,42]. However some risks of surface overheating and damage (discoloring/darkening of the surface) can occur if laser is not properly used (correct wavelength ore fluency).

1.4.2 Chemical cleaning

Chemical treatment generally involves the use of reagents such as Rochelle salt, ethylenediaminetetraacetic acid disodium salt (Na_2EDTA), ammonia and ammonium salts, citric acid, alkaline glycerol, sodium hexametaphosphate and sodium carbonate solutions.

The procedures commonly adopted for the application of these solutions, usually performed by means of compresses, brushing and immersion, presents important drawbacks related to i) the scarce control of the cleaning process that can induce the attack of the cuprite layer, especially for low selective reagents (as citric acid and

sodium hexametaphosphate); ii) the residues of these reagents left onto the metal surface, which can induce the uncontrolled progress of their chemical action; iii) the precipitation and redeposition of copper salts onto the surface.

To avoid some of the above-mentioned drawbacks, reagents such as Rochelle salt and EDTA, thanks to their high selectivity, are generally preferred [16]. The use of such chelating agents as cleaning tools allows, in fact, to solubilize the corrosion coatings on metal objects almost without any structural risk. The chelator, in fact, acts against the metallic ions of the patina but it stops when it reaches the healthy core of the metal where only metal atoms are present and no more ions (the speed of extraction of the chelating agent on the atoms is so low that it can be considered nothing). The correct choice of a selective complexing agent for Cu^{2+} ions also allows to maintain the protective cuprite layer intact.

In particular, Na_2EDTA (3-12% w/w aqueous solution) is the most common complexing agent used for the chemical cleaning of metal artifacts. In fact, it presents i) high stability of the EDTA-M^{n+} hexadentate complexes (for Cu^{2+} $\log K_f$ = 18.8, at 20-25°C and 0.1M ionic strength, [43]) ii) high selectivity in removing only the surface layer composed by the alteration products; for example, in the case of bronzes, Na_2EDTA is very efficient in removing only cupric salts Cu(II), negligibly affecting the Cu(I) protective cuprite layer; iii) adjustable efficacy by varying the pH value.

The sodium tartrate (Rochelle salt) has a milder effect in respect to EDTA, because it is a bidentate ligand and its stability constant is lower than EDTA (for Cu^{2+} $\log K_f$ = 3.3, at 20-25°C and 0.1M ionic strength [43]). For this reason it provides better control in the cleaning of bronzes, by complexing corrosion products, but retaining the cuprite layer, on which it acts weakly. The bland action ensured by this complexing agent makes it suitable, in particular, for the cleaning of gilded bronzes, when it is necessary to preserve the original gold leaf and simultaneously remove the surface deposits of copper salts, as for the cleaning of 'Porta del Paradiso' by L. Ghiberti (Fig. 1.12 and 1.13) [44]. Thanks to its mid action Rochelle salt aqueous solution are used with concentration up to 35% w/w (or 15% w/w with increased

pH with 5-10 w/w NaOH) with application times from 30 min to several hours, by immersion, brushing or compress.

A combined approach between mechanical and chemical methods usually allow to obtain the best cleaning performances, by balancing out the limits of one technique with the other, as for the combination of laser and chemical cleaning with complexing agent for the 'Porta del Paradiso' (Fig. 1.13).

Moreover, in the past decades, a wide range of thickeners and confining systems for different kinds of liquid phases (*i.e.* solvents, micellar solutions, microemulsions, solutions of chelating agents, etc.) were developed and tested. These innovative confining systems were mainly devised for easel and mural painting, paper, etc., but not for the specific case of metal cleaning. In fact there is a serious lack of literature concerning the application of confining systems for cleaning procedures on metal artifacts. Na_2EDTA solutions, commonly used as chelating agent, are generally associated to thickeners, such as cellulose ethers [45], polyacrilic acids and agar, but very few data about their efficacy or applicability are available.

Figure 1.12 Left: panel from the *Porta del Paradiso* depicting "Scenes from the life of Joseph'. Right: cleaning tests with chemical agents (resin, EDTA disodium salt and Rochelle salt) [44].

Figure 1.13 Left: panel from the *Porta del Paradiso* depicting 'Noah's histories'. Right: cleaning tests with laser ablation (mechanical cleaning) followed by light sodium potassium tartrate poultice application (chemical cleaning) [41].

1.4.3 Protection and maintenance

A complete conservation treatment aims, not only to re-establish the best esthetical and conservative condition for the object, but also to maintain this state as long as possible. For this reason a barrier between the cleaned metal surface and the environment has to be created, in order to protect the object from further corrosion phenomena [13]. These protective materials were often developed for industrial application, but their use as anti-corrosion systems for cultural heritage should respect some criteria:

- efficacy in every storage conditions of the artifact (outdoor, indoor, controlled or uncontrolled environmental conditions)
- treatment efficacy both in presence or absence of corrosion products on the surface
- final visual appearance of the treated object surface which should not be altered
- reversibility of the protective system, *i.e.* easy removal of the protective system, to allow future treatments on the object
- non-toxicity of the chemical substance responsible for the inhibition properties
- low price of the protection system.

Because of their weak influence on the modification of the surface appearance, lacquers (varnishes), waxes and corrosion inhibitors are the most common protection systems used in the context of restoration works.

As concerns varnishes, the most used as protective coatings are, for example, cellulose nitrate (weak performances, for indoor conservation), acrylic polymers (Paraloid B72, Incralac, for outdoor coatings) and vinylic polymers (Rhodopas M and Pioloform, for archaeological artifacts). The very limited visual changes observed after their application and the theoretical reversibility of these products, allow their use on a wide range of metallic surfaces. Nevertheless, these mechanical barriers represent only a passive and temporary protection and, in some cases, local corrosion phenomena can arise at the metal/coating interface due to weak adhesion between the polymer and the substrate. In addition, the removal of the polymer coatings often demands complex procedures using organic solvents because of oxidative aging processes.

Because wax-based protective coatings, both natural and synthetic, respect the requirements of transparency and reversibility, they were intensively used in the past decades, especially for the protection of outdoor sculptures. But the ageing of natural waxes in contact with moisture is known to produce some organic acids that can interact with the metal. For this reason, the application of synthetic waxes is nowadays rather recommended. Many types or combinations of synthetic microcrystalline or polyethylene waxes are used for the protection of both outdoor monuments and indoor metal artifacts. These coatings, which were developed for industrial applications, have not been refined specifically for the protection of metallic cultural heritage artifacts. Therefore, several studies have been devoted to the measurement of the efficiency of commercial waxes on different metals of metallic artifacts, *i.e.* different waxes compositions (microcrystalline and polyethylene wax), multilayered systems (waxes-Incralac), new formulations (Ormocers), etc. Nevertheless, these coatings systems have only limited long-term stability and require considerable maintenance to provide good protection properties for long duration, and regular application of waxes must be done two or three times per year.

The use of corrosion inhibitors to form insoluble compounds at the metal surface, which can provide better corrosion resistance, attracted a large amounts of interests. The application of inhibitor compounds allows the formation of a thin passive layer which can retard the anodic and/or cathodic reactions responsible for corrosion. The most widely used inhibitor compound is benzotriazole (BTA) in the case of copper alloys for protection purposes, thanks to its ability to form Cu(I) and Cu(II) complexes[46]. The effectiveness of BTA has clearly been proved for clean copper surfaces, but its efficacy for corroded copper alloys is still controversial, especially for artifacts containing chlorinate phases. Besides, BTA is considered as suspect carcinogenic, so research efforts are now directed to find a substitute, e.g. 2-aminopyrimidine (AP), 2-amino-5-mercapto-1,3,4-thiadiazole (AMT), 5,6-dimethyl -benzimidazole (DB), 2-mercaptopyrimidine (MP), 2-mercaptobenzimidazole (MBI), 2-mercaptobenzothiazole (MBT) and 2-mercaptobenzothiazole (MBO). These compounds reduce the toxic risk related to the use of BTA and they are also able to prevent the conversion of nantokite into oxychlorides species. Considering the performance and various requirements, like change in the visual appearance, MBT seems to be the most promising substitute for the preventive treatment of copper-based artifacts [13].

Innovative methods and materials for the inhibition of the corrosion process are currently under study. As an example, the deposition of diamond-like carbon coatings, was proposed as safe and innovative materials for the long-term conservation of archaeological bronzes, in order to ensure the chemical-physical stability of the ancient artifacts against the dangerous post-burial corrosion phenomena, during a PhD project between the Polytechnic of Turin and the ISMN-CNR of Rome [47].

However, further researches are needed in this field, by the development of new environmentally friendly systems that could be easily applied without expensive restoration works. In the meanwhile the only way to avoid expensive and frequent restoration interventions consists of regular maintenance, in order to keep as long as possible the results obtained with an extraordinary intervention by means of an ordinary and less expensive one.

1.5 Bibliography

[1] TYLECOTE, R.F. *A History of Metallurgy.* Maney Publishing, London, **1992**.

[2] AITCHINSON, L. *A History of Metals.* McDonald & Evans Ltd, London, **1960**.

[3] HOFMAN, H.O. *Metallurgy of copper.* McGrow-Hill Book Company, New York, **1914**.

[4] WINSTON REVIE, R., ED. *Uhlig's corrosion handbook.* ECS, Wiley, Hoboken, **2011**.

[5] SCOTT, D.A. *Metallography and Microstructure of Ancient and Historic Metals.* The Getty Conservation Institute, Malibu, **1991**.

[6] RICCUCCI, C., INGO, G.M., PARISI, E.I., ET AL. *Micro-chemical and metallurgical study of Samnite bronze belts from ancient Abruzzo (central Italy, VIII-IV BC).* Applied Physics A: Materials Science and Processing *113*, (**2013**), 959–970.

[7] SAUNDERS, N. AND MIODOWNIK, A. *The Cu-Sn (Copper-Tin) System.* Bulletin of Alloy Phase Diagrams *11*, 3 (**1990**), 278–287.

[8] LEONI, M. *Elementi di metallurgia applicata al restauro delle opere d'arte.* OpusLibri, Firenze, **1984**.

[9] INGO, G.M., PLESCIA, P., ANGELINI, E., RICCUCCI, C., AND DE CARO, T. *Bronze roman mirrors: the secret of brightness.* Applied Physics A: Materials Science and Processing *83*, (**2006**), 611–615.

[10] INGO, G.M., ANGELINI, E., DE CARO, T., AND BULTRINI, G. *Combined use of surface and micro-analytical techniques for the study of ancient coins.* Applied Physics A *79*, 2 (**2004**), 171–176.

[11] INGO, G.M., ANGELINI, E., DE CARO, T., BULTRINI, G., AND CALLIARI, I. *Combined use of GDOES, SEM + EDS, XRD and OM for the microchemical study of the corrosion products on archaeological bronzes.* Applied Physics A *79*, 2 (**2004**), 199–203.

[12] INGO, G.M., DE CARO, T., RICCUCCI, C., AND KHOSROFF, S. *Uncommon corrosion phenomena of archaeological bronze alloys.* Applied Physics A *83*, 4 (**2006**), 581–588.

[13] DILLMANN, P. ET AL., ED. *Corrosion of Metallic Heritage Artefacts.* Woodhead Publishing Limited, Cambridge, **2007**.

[14] STAMBOLOV, T. *The corrosion and conservation of metallic antiquities and works of art.* Central Research Laboratory for Objects of Art and Science, Amsterdam, **1985**.

[15] ROBBIOLA, L., FIAUD, C., AND PENNEC, S. *New model of outdoor bronze corrosion and its implications for conservation.* ICOM Committee for Conservation 10th triennial meeting: Washington, DC, 22-27 August 1993: preprints, (**1993**), 796–802.

[16] SCOTT, D.A. *Copper and bronze in art.* The Getty Conservation Institute, Malibu, **2002**.

[17] CAMPANELLA, L. ET AL. *Chimica per l'arte.* Zanichelli, Bologna, **2007**.

[18] LALLI, C. *L'impatto ambientale sulle opere d'arte esposte all'aperto: cause e problemi di degrado.* In *Monumenti in bronzo all'aperto. Esperienze a confronto.* Nardini Editore, Firenze, **2004**, 63–74.

[19] LETARDI, P. ET AL., ED. *Monumenti in bronzo all'aperto.* Nardini Editore, Genova, **2004**.

[20] KNELL, S., ED. *Care of Collections.* Routledge, London, New York, **2015**.

[21] LUCEY, V.F. *Developments Leading to the Present Understanding of the Mechanism of Pitting Corrosion of Copper.* British Corrosion Journal *7*, 1 (**1972**), 36–41.

[22] LINS, A. AND POWER, T. *The corrosion of bronze monuments in polluted urban sites.* In D. et al. Scott, ed., *Ancient & Historic metals*. The Getty Conservation Institute, **1991**, 119–151.

[23] SCOTT, D.A. *Bronze disease: a review of some chemical problems and the role of relative humidity.* JAIC *29*, (**1990**), 193–206.

[24] INGO, G.M., DE CARO, T., RICCUCCI, C., ET AL. *Large scale investigation of chemical composition, structure and corrosion mechanism of bronze archeological artefacts from Mediterranean basin.* Applied Physics A *83*, 4 (**2006**), 513–520.

[25] INGO, G.M., ANGELINI, E., BULTRINI, G., DE CARO, T., PANDOLFI, L., AND MEZZI, A. *Contribution of surface analytical techniques for the microchemical study of archaeological artefacts.* Surface and Interface Analysis *34*, 1 (**2002**), 328–336.

[26] MCNEIL, M.B. AND LITTLE, B.J. *The Use of Mineralogical Data in Interpretation of Long-Term Microbiological Corrosion Processes: Sulfiding Reactions.* Journal of the American Institute for Conservation *38*, 2 (**1999**), 186–199.

[27] MEEKS, N.D. *Tin-rich surfaces on bronze. Some experimental and archaeological considerations.* Archaeometry *28*, 2 (**1986**), 133–162.

[28] FARALDI, F. ET AL. *Micro-chemical and micro-structural investigation of archaeological bronze weapons from the Ayanis fortress (lake Van, Eastern Anatolia, Turkey).* Applied Physics A: Materials Science and Processing *113*, (**2013**), 911–921.

[29] INGO, G.M., ÇILINGIROĞLU, A., FARALDI, F., ET AL. *The bronze shields found at the Ayanis fortress (Van region, Turkey): manufacturing techniques and corrosion phenomena.* Applied Physics A *100*, 3 (**2010**), 793–800.

[30] INGO, G.M., RICCUCCI, C., FARALDI, F., CASALETTO, M.P., AND GUIDA, G. *Micro-chemical and micro-structural investigation of the corrosion products on "The Dancing Satyr" (Mazara del Vallo, Sicily, Italy).* Applied Physics A *100*, 3 (**2010**), 785–792.

[31] CASALETTO, M.P., INGO, G.M., ALBINI, M., ET AL. *An integrated analytical characterization of corrosion products on ornamental objects from the necropolis of Colle Badetta-Tortoreto (Teramo, Italy).* Applied Physics A *100*, 3 (**2010**), 801–808.

[32] INGO, G.M. AND PARISI, E.I. ET AL. *Gold coated copper artifacts from the Royal Tombs of Sipán (Huaca Rajada, Perù): manufacturing techniques and corrosion phenomena.* Applied Physics A *113*, 4 (**2013**), 877–887.

[33] BRANDI, C. *Teoria del restauro.* Einaudi, Torino, **1977**.

[34] MERCALLI, M. *Storia del concetto di patina. Riflessioni teoriche intorno al restauro dei manufatti in bronzo.* In P. Letardi, ed., *Monumenti in bronzo all'aperto. Esperienze a confronto.* Nardini Editore, **2004**, 49–52.

[35] CONTI, A. *Manuale di restauro.* Einaudi Editore, **2001**.

[36] BALDINUCCI, F. *Vocabolario toscano dell'Arte del disegno.* **1681**.

[37] CIATTI, M. *Appunti per un manuale di storia e teoria del restauro. Dispense per gli studenti.* **2009**.

[38] DEGRIGNY, C. *Survey of European experiences on cleaning procedures.* In P. Letardi, ed., *Monumenti in bronzo all'aperto. Esperienze a confronto.* Nardini Editore, **2004**, 101–108.

[39] MORIGI, G. *La pulitura a micropeening con granulati vegetali.* In P. Letardi, ed., *Monumenti in bronzo all'aperto. Esperienze a confronto.* Nardini Editore, **2004**, 95–98.

[40] SIANO, S., AGRESTI, J., CACCIARI, I., ET AL. *Laser cleaning in conservation of stone, metal, and painted artifacts: state of the art and new insights on the use of the Nd:YAG lasers.* Applied Physics A *106*, 2 (**2011**), 419–446.

[41] MATTEINI, M., LALLI, C., TOSINI, I., GIUSTI, A., AND SIANO, S. *Laser and chemical cleaning tests for the conservation of the Porta del Paradiso by Lorenzo Ghiberti.* Journal of Cultural Heritage *4*, (**2003**), 147–151.

[42] FERRETTI, M. AND SIANO, S. *The gilded bronze panels of the Porta del Paradiso by Lorenzo Ghiberti: non-destructive analyses using X-ray fluorescence.* Applied Physics A *90*, 1 (**2007**), 97–100.

[43] RICHARDSON, H.W., ED. *Handbook of Copper Compounds and Applications.* Marcel Dekker, Inc, **1997**.

[44] FIORENTINO, P., MARABELLI, M., MATTEINI, M., AND MOLES, A. *The condition of the 'Door of Paradise' by L. Ghiberti. Tests and proposals for cleaning.* Studies in Conservation *27*, (**1982**), 145–153.

[45] MARABELLI, M. *The Monument of Marcus Aurelius: facts and comments.* In D. Scott, ed., *Ancient & Historic Metals.* The Getty Conservation Institute, Malibu, **1993**, 1–20.

[46] MEZZI, A., ANGELINI, E., DE CARO, T., ET AL. *Investigation of the benzotriazole inhibition mechanism of bronze disease.* Surface and Interface Analysis *44*, 8 (**2012**), 968–971.

[47] FARALDI, F. *Environmentally friendly plasma treatments for surface nano-functionalisation and protection of metals.* **2014**.

Chapter 2
Gels and 'gel-like' systems for cleaning of Cultural Heritage artifacts

2.1 Introduction

Gels and 'gel-like' materials have received considerable attention in the past decades and they are widely present in various fields of everyday life. The ongoing research is continuously developing new gel materials for a wide range of applications, with tailored features for each purpose. The possibility of having versatile gels, with performing properties for application purposes, makes them potential materials for cleaning applications in the field of Cultural Heritage conservation.
In fact, cleaning with gels or 'gel-like' materials has been receiving increasing attention since the last decades, because the development of confining systems should help to overcome some well-known problems related to cleaning procedures of Cultural Heritage artifacts. As already mentioned in section 1.4, the cleaning process represents one of the most delicate and potentially dangerous procedures, aimed to the removal of undesired layers from an artifact surface. Moreover, since each work-of-art is unique and a universally valid cleaning procedure does not exist, every intervention must be carefully adapted and tailored to the considered case study. These systems should allow a better control over the cleaning action, although they can presents some disadvantages, such as a difficult and not complete removal of the residues.

The aim of this chapter is to show an overview of the gel or 'gel-like' systems available and used for restoration purposes. Particular attention will be focused on the understanding of what can be called a gel or not, fundamental to define and classify the commonly used confining systems and to place the polymeric systems

developed in this thesis among them. In particular a rheological approach will be adopted to differentiate between 'real' gels and 'gel-like' systems, with a brief description of the rheology technique. The most common cleaning systems for restoration purposes will be presented along with the main drawbacks and limits related to their use. Finally, the innovative systems recently developed and proposed to overcome these problems will be described.

2.2 Gels and 'gel-like' systems for cleaning

Since the 1980's to the present days, a wide range of technologically advanced cleaning systems for work of art surfaces have been developed and tested. In particular the use of gels and 'gel-like' systems has encountered a great diffusion, thanks to the possibility of confining inside them different kinds of fluids (*i.e.* solvents, micellar solutions, microemulsions, solutions of chelating agents, etc.) and to enhance both the gradualness and the spatial control of the cleaning action [1]. In fact, the confinement of cleaning systems within a gel network that releases them gradually onto the treated substrates, permits to address the task of removing undesired layers without affecting the materials of the artifact either chemically or physically [2].

The main goal for the development of these new cleaning tools was the resolution of some typical problems related to the removal of unwanted layers (grime, varnishes, adhesives, etc.) from porous thin stratified substrates (e.g. easel paintings). In fact the use of pure organic solvents, in common restoration practices, entails several drawbacks, such as: i) uncontrolled penetration in the artifact porous structure, ii) poor selectivity and iii) scarce environmental safety and high toxicity. The confinement of solvents into gel or 'gel-like' formulations (e.g. thickening agents), is a nowadays common practice, because it permits to attain enhanced control over the cleaning action and to minimize the above-mentioned drawbacks thanks to: i) increased viscosity that drastically lowers the extent and the rate of penetration into the porous substrate and that also reduces the solubilization rate; ii) drastic decrease of the evaporation rate, with a strong reduction of toxicity issues; iii) confinement

of both, organic solvents and aqueous methods (*i.e.* enzymes, chelating agents, microemulsions, etc.) and applicability on a great variety of supports (easel paintings, wall paintings, glass, metals, paper, etc.).

In particular the main characteristics required for a gel system to be efficiently used over almost every materials that can be subject to a restoration process, may be summarized as follows:

- high retention features, necessary to grant low diffusivity rates of the cleaning system within the artifacts matrix, thus permitting a controlled cleaning action in addition to a reduction of volatility of the fluid and a resulting decrease of toxicity;
- easy and residues-free removal, usually achieved by enhancing the mechanical properties. In fact the stronger are the cohesive forces between the gel network, the better are the mechanical features of the system and the less are the adhesive forces, which cause residues left onto the treated surfaces;
- good adhesion properties, necessary to grant a homogeneous interaction and thus a uniform cleaning action especially onto irregular and rough surfaces. For this reason a compromise between the previous requirement and this one might be achieved;
- versatility and adaptability to different cleaning issues (removal of various classes of detrimental materials), materials to be treated (painted layers, papers, metals, etc.) and surfaces (rough, irregular, non-horizontal, etc.) that might be found;
- chemical inertness towards the original materials composing the artifact.

It is improbable that a single gel formulation can meet these features all together: the most appropriate choice for each case study will be chosen case-by-case depending on the specific needs and on the characteristics of the artifact.

The polymeric system presented in this dissertation tried to compromise between the necessity of a good contact and interaction with the artifact surface (thanks to a certain initial fluidity) and the absence of final residues (thanks to the characteristics of the final film) in order to achieve an effective but controllable cleaning action, as extensively discussed elsewhere.

2.2.1 Definition and classification

Despite the conspicuous literature available and the huge number of publications a universal recognized definition of 'gel' is still lacking. Many definitions have been proposed since the early phrase of J. Lloyd in 1926: "*the colloidal condition, the 'gel', is one which is easier to recognize than to define*" [3]. Different points of views have been taken into account to achieve a unique and thorough definition of gel, such as the macroscopic phenomenological behavior, the microscopic structure or the mechanical properties, as summarized in Tab. 2.1. However, owing to the numerous fields of application and to the variability of the characteristics of gel systems, definitions and classification criteria greatly depend on the reference theoretical background (*i.e.* chemical, physical, biological, engineering, etc.) and on the constitutive properties of the described systems (e.g. source of the gelator, network structure, type of bonds, etc.). Besides, since the evaluation of measurable parameters strictly depends both on the patience of the observer and on the instrumental limits, it can be concluded that, as philosophically stated by Nijenhuis [4]: "*a gel is a gel, as long as one cannot prove that it is not a gel*".

In order to give a clear understanding of what it has to be considered a 'gel' in this work, the mechanical definition of gel condition was adopted, according to Almdal et al. [5], the firsts to give a precise definition based on experimental data from rheological measurable parameters (a brief description of rheological methods will be provided in section 2.3). In particular: i) a gel consists of two or more components, one of which is a liquid, present in substantial quantity and ii) it must show a flat mechanical spectrum in oscillatory shear measurements, *i.e.* the storage modulus (*G'*) exhibits a pronounced plateau extending to times of the order of se-

conds and the loss modulus (*G''*) is considerably smaller than *G'* over a wide range of frequencies (as showed in Fig. 2.1 (c)).

Author/s	Year	Proposed gel definition
Lloyd, D.J [3]	1926	- Built up from two components: one is a liquid at the temperature under consideration, and the other is a solid; - can maintain its form under the stress of its own weight; - shows the phenomenon of strain, under any mechanical stress.
Bungenberg de Jong, H. G. [6]	1949	- colloidal system of solid character; - the colloidal particles constitute a coherent structure, being interpenetrated usually by a liquid system consisting in kinetic units smaller than colloidal particles.
Hermans, P. H. [7]	1949	- coherent colloid disperse systems of at least two components; - exhibits mechanical properties characteristic of a solid; - both the dispersed component and the dispersion medium extend themselves continuously throughout the whole system.
Flory, P. J. [8]	1974	- solid-like behavior; - when deformed, its response is that of an elastic body; - the modulus of elasticity is low.
Ferry, J. D. [9]	1980	- a substantially diluted system, which exhibits no steady state flow.
Burchard, W. & Ross-Murphy, S. B. [10]	1990	- possess a plateau in the real part of the complex modulus extending over an appreciable window of frequencies; - they are viscoelastic solids.
Almdal, K. et al. [5]	1993	- soft, solid or liquid-like material of two or more components, one of which is a liquid, present in substantial quantity; - solid-like gels are characterized by the absence of an equilibrium modulus, by a storage modulus, G'(ω), which exhibits a pronounced plateau extending to times at least of the order of seconds, and by a loss modulus, G''(ω), which is considerably smaller than the storage modulus in the plateau region; - materials with moduli of the order of 108 Pa are far too rigid to be called gel.
Nishinari, K. [11]	2009	- intermediate state between a liquid-like rheological behavior and a solid-like rheological behavior; - consists of a dispersed phase (polymers or colloids) and a dispersing medium (water or other solvents), and can be very close to a liquid or to a solid; - liquid-like properties are due to the fact that the major constituent is water or other solvents; - solid-like behavior is due to the network, which prevents the system from flowing, and characterized by a finite elastic modulus.

Table 2.1 Summary of the most cited proposed gel definitions.

In the particular case of polymer solutions, the classification proposed by Ross-Murphy is adopted [11,12], where four type of rheological behavior are described,

by considering the dependence of the storage *G'* and loss *G''* shear moduli with the frequency (range of 10^{-3}-10^{2} rad/s):

- strong gel behavior (an elastic gel or a true gel), *i.e. G'* is far larger than *G''* and both moduli are independent on frequency (Fig. 2.1 (c, d));
- structured liquids behavior, *i.e. G'* is slightly larger than *G''* and both moduli are only scarcely dependent on frequency;
- entangled polymer solution behavior, *i.e. G'* is smaller than *G''* at lower frequencies but both moduli increase with increasing frequency and show a crossover, then *G'* becomes larger than *G''* at higher frequencies (Fig. 2.1 (b));
- a non-entangled polymer solution behavior, *i.e. G'* is far smaller than *G''* at all the frequencies and both moduli are strongly dependent on the frequency; at very low frequencies the relations $G' \sim \omega^2$ and $G'' \sim \omega$ are known for polymer solutions (Fig. 2.1 (a)).

The polymeric cleaning systems described in this work are characterized by an evolution of the rheological behavior with time, from a simple polymeric solution, through the formation of an entangled network, towards a final system ascribable to a solid, as extensively described in Chapter 6.

For what concerns the classification of polymer networks and gels, a structural subdivision is adopted here, by taking into account the nature of the interactions responsible for the formation of the 3-D network [13,14]:

- chemical gels, composed by cross-linked polymer networks that are built by covalent bonds (Fig. 2.2 (a)). The permanent nature of these bonds (from 200 up to 650 kJ mol^{-1}) is responsible for the thermoset nature of these materials: only over a critical temperature the bonds can be irreversibly broken. Their behavior is similar to solids; in fact chemical gels are able to load high amounts of liquid without undergoing polymer solubilization. Due to their cohesive force, chemical gels can be easily removed from

any surface, without breaking or leaving residues, which is a very important characteristic for the cleaning of Cultural Heritage artifacts (e.g. p(HEMA)/PVP gels described in section 2.4);

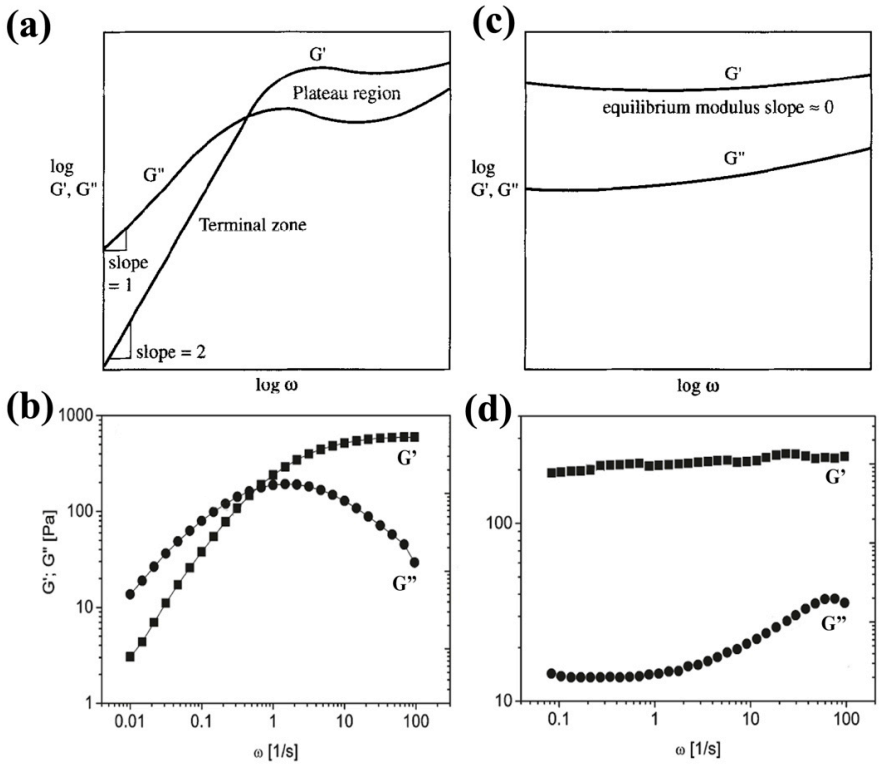

Figure 2.1 Shear moduli *G'* and *G"* reported in function of the angular frequency (ω) for: (c) and (d) a strong gel behavior, where the storage modulus *G'* is always higher than the loss modulus *G"*; (a) and (b) a typical behavior of an entangled polymer solution is showed, where a cross-over occurs between the two moduli and, at high frequencies, *G'* becomes higher than *G"* [13,15].

- entangled networks, formed by the simple topological interaction of polymer chains rather than by crosslinking (Fig. 2.2 (a)). IUPAC defines chain entanglements as "*interlocking of polymer chains in a polymer material forming a transient or permanent network junction over the time-scale of the measurement*". Entanglements constitute the major structural feature in

polymer solutions because polymer chains cannot cross each other, but they can mutually interpenetrate, thus becoming entangled. In this way the individual chains motions become constrained, and it is impossible to move freely as a whole in all directions, thus affecting the dynamical properties. Further and thorough details on entangled polymer dynamics and viscoelastic properties can be found in the complete monographs by Ferry [9], and Doi and Edwards [16]. Highly viscous polymeric dispersions (HVPD) represent an example of systems that fills within this category (see section 2.4 and Chapter 3 for more details). These systems allow to obtain a compromise between good mechanical properties, typical feature of chemical gels, and the advantages in terms of applicability of the following systems;

- physical gels, polymeric systems gelled by the presence of non-covalent interactions between chains, such as hydrophobic, electrostatic, Van der Waals forces or the rather stronger hydrogen bonds (Fig. 2.2 (c)). Due to the weak nature of this kind of bonds, less energy is necessary to break them (around 1-120 kJ mol^{-1}) in respect to the covalent ones, but they can also be easily reformed in certain conditions. For this reason, physical gels are named as thermo-reversible: by increasing the temperature over a given threshold, the single molecules are dispersed again in the solvent bulk phase and a 'sol' is obtained; by cooling back to the original temperature a sol-gel transition occurs and the system turns back into the gelled form. Common examples of natural source of physical gels are the ones based on polysaccharides and proteins. Moreover, physical gels can be molded and may grant a perfect adhesion to the surface, which are good characteristics for the cleaning of artifacts although residues problems can arise (cellulose ethers, polyacrylic acids and polysaccharides-based gels).

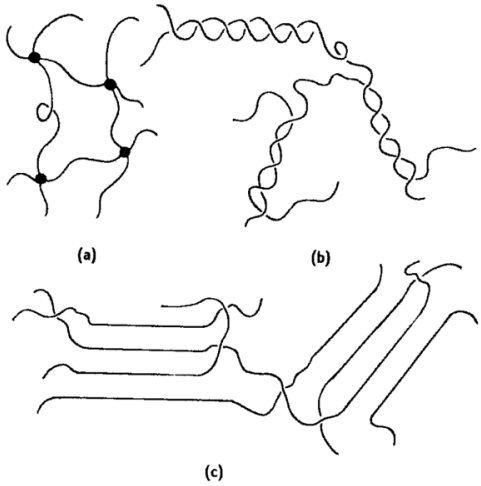

Figure 2.2 Example of polymer structures for: (a) chemical gels with cross-linking points, (b) entangled networks with topological interactions between the polymer chains and (c) physical gel with crystalline junctions [17].

The nature of the interaction within a polymer network directly influences the applicability properties of these cleaning systems, such as mechanical stability, adhesiveness and consistency. In fact, as mentioned in the introduction, the most appropriate gel or ‘gel-like’ system must be carefully selected for each cultural heritage artifacts. Each confining system presents both advantages and disadvantages: the strong cohesive forces in chemical gels permit to ensure that no gel residues remain on the treated surface, but they can be too rigid and not able to uniformly interact with irregular surfaces; on the other hand, physical gels have the advantage of being mechanically adjustable, thus ensuring a perfect and homogeneous interaction with the treated substrate, but residues can be left onto the treated substrate. An intermediate system is represented by entangled polymer networks, possibly enhanced by the presence of additional interactions (e.g. borax, further H-bonds). The resulting system shows the applicability properties of a physical gel, without residues problems, thanks to the prevalence of cohesive forces over the adhesive ones.

A second criterion that can be used for the classification of gels is based on the fluid that can be retained by the network (‘gelator’) and its hydrophobic/hydrophilic

features. In fact, if the gelator consists in a hydrophobic polymer, the network will equilibrate with a non-polar solvent, forming a so-called organogel. On the other hand, a hydrophilic network will swell in presence of a hydrophilic solvent, like water (hydrogel). If the fluid is not a liquid but a gas, as for instance air, the gel is called aerogel. Finally, xerogels are solid systems obtained after drying a swollen gel (these last systems cannot be actually considered true gels, according to Almdal et al. definition [5], because only one phase is present). The affinity of the network for different solvents is of paramount importance for application purposes: if for example a hydrophilic gel is immersed in a hydrophobic solvent, the network will shrink in order to minimize the contact with the solvent, thus making the system completely unusable. Both organogels and hydrogels are widely used for the cleaning of works of art, as reported in section 2.4 and 2.5.

2.3 Rheology of viscoelastic material

As previously described, the macroscopic recognition of a gel state can be somewhat ambiguous and, among the various classifications proposed, the mechanical study through rheological parameters, appears to be the best way to follow the changes in gel or 'gel-like' viscoelastic materials behavior [5].

The term 'viscoelastic' is used to describe a behavior that falls between the classical extremes of Hookean elastic response (typical of solids), and Newtonian viscous behavior (typical of liquids). In particular a 'solid' material "*does not continuously change its shape when subjected to a given stress, i.e. for a given stress there is a fixed final deformation, which may or may not be reached instantaneously on application of the stress*"; a 'liquid' is a material that "*continuously changes its shape (i.e. it flows) when subjected to a given stress, irrespective of how small that stress may be*" [18].

The term 'rheology' is referred to the science of material flow behavior and deformation of matter, under the effect of an applied force. When a material is subject to outside forces (examples given in Fig. 2.3) it yields a stress/strain response. In

order to explain this phenomenon, the simple example of a shear stress on a cube is schematized in Fig. 2.4.

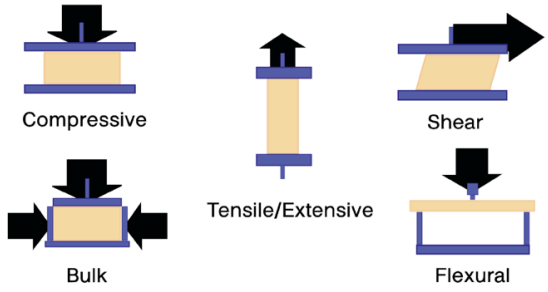

Figure 2.3 Examples of deformation modes. Geometric arrangements or methods of applying stress are shown [19].

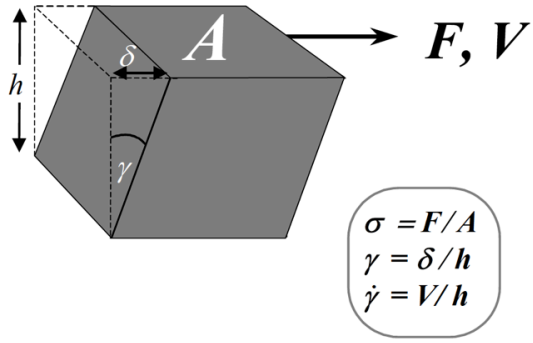

Figure 2.4 Definition diagram for shear flow, representing the shear stress and the shear strain on a cube sample [18].

The force F is applied to the upper plane of the cube (with an area A) while the base is hold firmly (parallel-plate geometry). The resulting deformation shows a displacement with an angle γ. The relation between the applied force and the deformation is due to the physical properties of the material. The deformation is called *shear strain* (γ), which is independent from the size of the material (dimensionless unit):

$$\gamma = \frac{\delta}{h} \quad \text{(Eq. 2.1)}$$

The applied force is better explained by the *shear stress* (σ) which is the force divided by the upper area of the cube, expressed in Pa or $N \cdot m^{-2}$:

$$\sigma = \frac{F}{A} \quad \text{(Eq. 2.2)}$$

that is proportional to the velocity gradient, the *shear rate* ($\dot{\gamma}$), expressed in s^{-1}:

$$\dot{\gamma} = \frac{V}{h} \quad \text{(Eq. 2.3)}$$

The *shear modulus* (G) is now obtained, expressed in Pa [20]:

$$G = \frac{\sigma}{\gamma} \quad \text{(Eq. 2.4)}$$

To distinguish between the liquid-like and solid-like character of a gel, the viscoelasticity features of the system should be addressed. With imposing a constant strain, the size of the stress is determined by the shear modulus (see Eq. 2.4). Considering that the molecules that were forced to a higher energy state, rearrange in the material to return to the initial energy state, some of the stored energy is dissipated by viscous flow and some stress is reduced. The *relaxation time* (τ) is the time required for viscous flow to occur, when the material is subject to strain, determined by the balance of elastic and viscous processes [20,21]:

$$\tau = \frac{\eta}{G} \quad \text{(Eq. 2.5)}$$

where η is the *viscosity* of the material. The ratio of the relaxation time to the *experimental observation time* (t), is defined by the *Deborah number* (De):

$$De = \frac{\tau}{t} \quad \text{(Eq. 2.6)}$$

where De reflects the tendency of the material to appear either more viscous or more elastic. It is based on the premise that given enough time even a solid-like material will flow, such as mountains (Deborah, Judges 5.5: "*The mountains flowed down at the presence of the Lord, even yon Sinai at the presence of the Lord, the God of Israel*.") or cats (Fig. 2.5).

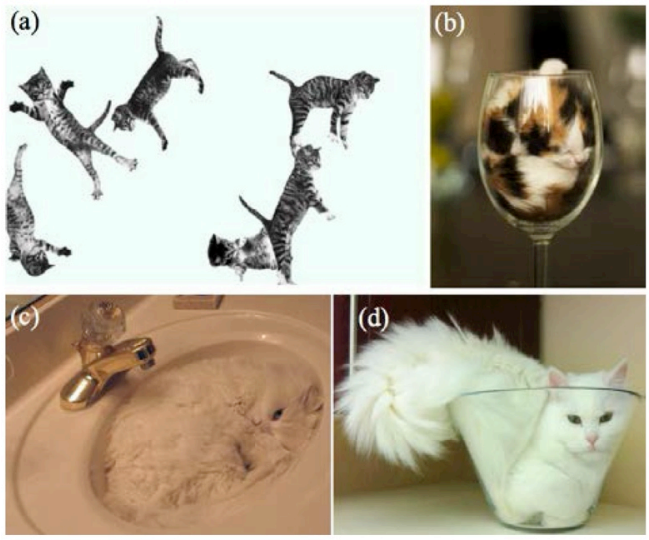

Figure 2.5 Different feline states can be observed: (a) a solid-like cat, which can rotate and bounce for short observation times (De >> 1); (b, c, d) at longer time scales, a cat flows filling different containers, with a liquid-like behavior (De << 1) [22].

Therefore, the classification of the gels behavior can be:

$De \gg 1$,	$De \sim 1$	and	$De \ll 1$
solid-like	viscoelastic		liquid-like

If observational times are rather small (in the order of seconds) and if $t \approx \tau$ the material displays both elastic and viscous characteristic and it is named as 'viscoelastic'.

2.3.1 Viscosity

'Viscosity' η is defined as "*the resistance of fluids to external mechanical stresses*" and it is written as the ratio of shear stress to shear rate:

$$\eta = \frac{\sigma}{\dot{\gamma}} \qquad \text{(Eq. 2.7)}$$

The viscosity of real materials can be significantly affected by different variables, as shear rate, temperature, pressure and time of shearing. In particular the shear rate dependence can show a Newtonian viscosity behavior when: i) the only stress gen-

erated in simple shear flow is the shear stress σ, the two normal stress differences being zero; ii) the shear viscosity does not vary with shear rate; iii) the viscosity is constant with respect to the time of shearing and the stress (see Fig. 2.6). A fluid showing any deviation from the above behaviors is non-Newtonian, with η values as a function of shear rate, while it is constant for Newtonian fluids. [18,23].

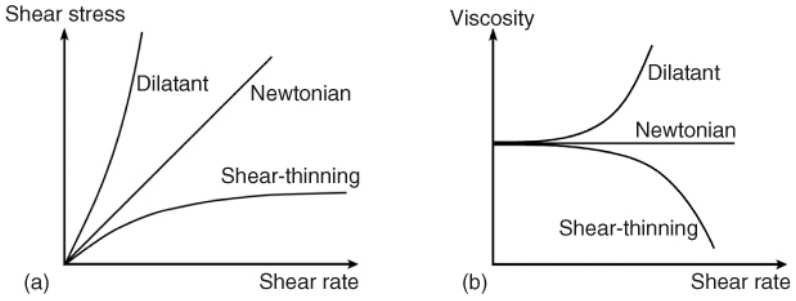

Figure 2.6 Flow curves in function of shear rate, showing Newtonian behavior, where shear stress is proportional to shear rate (a) and viscosity is constant (b). Any deviations from these behaviors are typical of non-Newtonian fluids.

However it has to be mentioned that if the shear rate is high-enough, all liquids become non-Newtonian, as showed in Fig. 2.7.

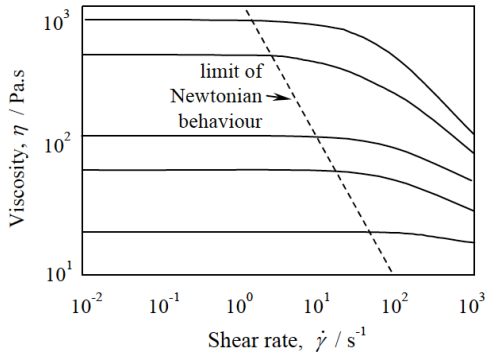

Figure 2.7 Viscosity curves versus shear rate, showing a non-Newtonian behavior after a certain limit of shear rate, for some silicone oils [18].

In the vast majority of cases, such as for dispersions, emulsions and polymer solutions, viscosity generally decrease with increasing shear rate, giving rise to what is called 'shear-thinning' behavior, while increasing viscosity with shear rate entails a

'shear-thickening' behavior. For shear-thinning materials, the general shape of the curve representing the variation of viscosity with shear rate is shown in Fig. 2.8. Moreover it can be observed that, in the limit of very low shear rates (or stresses) of the flow curves, the viscosity shows constant values, the so-called 'zero-shear viscosity' (η_0), whilst in the limit of high shear rates (or stresses) the viscosity shows another plateau, at a lower level (with value η_∞). These two extremes are known as the lower and upper Newtonian regions, respectively, separated by a power-law behavior, where viscosity values decrease with shear rates (or stresses) entering a straight-line region on the logarithmic plot (Fig 2.8).

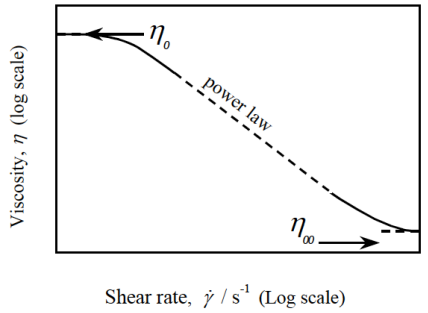

Figure 2.8 An example of a shear thinning material, with a decrease of viscosity in function of shear rate. The lower η_0 and upper η_∞ Newtonian regions are also indicated [18].

For the mathematical description of the flow curves some well-known models are usually employed, for different parts of the curves as showed in Fig. 2.9.

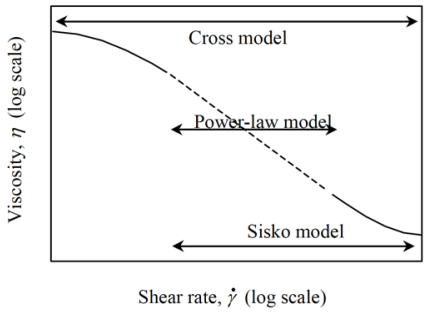

Figure 2.9 Schematic representation of the different mathematical models generally used and of the ranges of the curve they cover [18].

One equations that predict the shape of the general flow curve is that of the Cross model (1965):

$$\frac{\eta-\eta_\infty}{\eta_0-\eta_\infty} = \frac{1}{(1+(K\dot{\gamma})^m)} \quad \text{(Eq. 2.8)}$$

where K has the dimensions of time, and m is dimensionless. When this model is used to describe non-Newtonian liquids, the degree of shear thinning is dictated by the value of m: when m tends to zero it describes more Newtonian liquids, while the most shear-thinning liquids have a value of m tending to unity.

A popular alternative to the Cross model is the model due to Carreau (1972):

$$\frac{\eta-\eta_\infty}{\eta_0-\eta_\infty} = \frac{1}{(1+(K_1\dot{\gamma})^2)^{m_1/2}} \quad \text{(Eq. 2.9)}$$

the same of Cross's at very low and high shear rates, but slightly different at $K\dot{\gamma} \sim 1$.

By making certain approximations of the Cross model, other and popular models can be obtained. For example, for $\eta << \eta_0$ and $\eta >> \eta_\infty$ and with a simple change of the variables K and m, the Cross model reduces to the well-known 'power-law' model:

$$\eta = K_2\dot{\gamma}^{n-1} \quad \text{(Eq. 2.10)}$$

where K_2 is called the *consistency* and n the *power-law index*.

By simply adding a Newtonian contribution to the power-law description of the viscosity, the Sisko model is obtained:

$$\eta = \eta_\infty + K_2\dot{\gamma}^{n-1} \quad \text{(Eq. 2.11)}$$

very good at describing the flow behavior of most emulsions and suspensions in the practical everyday shear rate range.

If n is set equal to zero and with a simple redefinition of the parameters in the Sisko model, we obtain the Bingham model:

$$\sigma = \sigma_y + \eta_p \dot{\gamma} \qquad \text{(Eq. 2.12)}$$

which describes the shear stress/shear rate behavior of many shear-thinning materials at low shear rates, but only over a one-decade range (approximately) of shear rate [18,23].

2.3.1.1 Rotational experiments, parallel-plate geometry

The measure of viscosity entails the application of a force or a velocity to the sample, through different geometry arrangements (tubes, cone-plate, parallel-plate, etc.), and the measurement of the relative response. Then the conversion of the applied force F to a shear stress σ, and of the velocity V to a shear rate $\dot{\gamma}$ can be done by using geometric constants to obtain the viscosity η values [18].

Rotational experiments are widely used to investigate the flow behavior of liquids, dispersions, gels, etc. of every day usage. With most of the rheometers there is a rotational motion to achieve simple shearing flow over a fixed element; the obtained response in measured by the same member driving the rotation [23].

In simple geometries the shear rate, hence the shear stress, are the same everywhere in the sample, as for the cone-and-plate and narrow-gap concentric cylinder geometries. In other geometries, either the shear rate or the shear stress varies in a known manner independently of the rheology of the test liquid, but the basic experimental data can be converted into unambiguous viscosity/shear-rate data by the use of appropriate mathematical equations, as for the parallel-plate geometry or wide-gap concentric cylinders.

In particular, for parallel-plate geometry, the upper plate is usually rotated and the couple C is like-wise measured on the upper plate. The shear rate varies from zero at the center to $a\Omega/h$ at the edge of the plates, where a is the plate radius, h the gap and Ω the rotation rate in rad/s (Fig. 2.10). By assuming that the viscosity/shear rate curve obeys to a power-law relationship, the shear rate at the edge is given by:

$$\dot{\gamma}_a = \frac{a\Omega}{h} \qquad \text{(Eq. 2.13)}$$

and the viscosity (evaluated at the edge shear rate $\dot{\gamma}_a$) is given by:

$$\eta = \frac{3Ch}{2\pi a^4 \Omega(1+\frac{1dlogC}{3dlog\Omega})} \quad \text{(Eq. 2.14)}$$

where *C* is the couple on one of the plates. For a power-law models *dlogC/dlogΩ* is simply *n*, *i.e*. the power-low index.

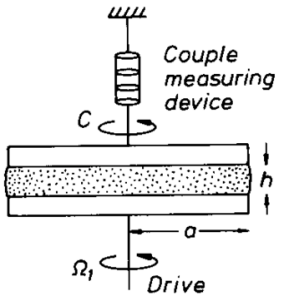

Figure 2.10 Cross-section of the torsional parallel-plate viscometer, where C, h, a and Ω are illustrated [23].

2.3.2 Linear viscoelasticity and its dynamic analysis

In the linear viscoelasticity [18,23,24] region each applied stress yields a proportional strain, that is, a straight line is observed if the force applied is plotted in function of the deformation. Over a critical limit, the force applied causes irreversible modifications on the material that may eventually break with further increasing stress. The phenomenological rheological behavior of materials in the linear viscoelasticity region can be represented by combinations of Hookean springs and Newtonian dashpots. A Hookean spring obeys Hooke's law: the stress is linearly related to the displacement. An ideal Hookean solid has therefore an infinite elasticity, which is represented by *G*, accounting for the spring response (see Eq. 2.4). The dashpot is represented by a filled cup of Newtonian fluid and a piston over the fluid. Therefore, the constant of proportionality is the shear viscosity expressed in Eq. 2.7.

Viscoelastic materials are represented by the combination of these two models and they can be visualized in series or in parallel. In the 'Maxwell model', the spring and the dashpot are placed in series, while they are represented by the 'Kelvin-Voigt model' when placed in parallel (see Fig. 2.11). The constitutive equations

are derived from the Eq. 2.3 and 2.7. When a stress is applied on the parallel elements of a 'Kelvin model' both the elements will respond. Then a linear addition of the stresses gives the equation:

$$\sigma = G\gamma + \eta\dot{\gamma} \qquad \text{(Eq. 2.15)}$$

which is one of the simplest models of viscoelasticity.

For the 'Maxwell model' (in series) the linear addition interests the strain, thus obtaining:

$$\dot{\gamma} = \frac{\dot{\sigma}}{G} + \frac{\sigma}{\eta} \qquad \text{(Eq. 2.16)}$$

The Maxwell and Kelvin-Voigt models may be expanded to give either multiple Maxwell models, which are usually combined in parallel, or else multiple Kelvin-Voigt models, which are usually combined in series. They can also be combined, as for the 'Burgers model', made by a Maxwell and a Kelvin-Voigt model in series, to better simulate the real trend of the stress/strain relations with more complicated mechanical models (Fig. 2.11).

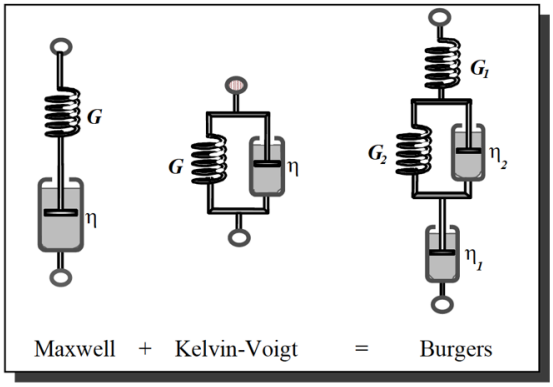

Figure 2.11 The combination of springs and dashpots (in series or parallel) for the Maxwell, Kelvin-Voigt and Burgers models [18].

Two different types of methods are available to determine linear viscoelastic behavior: i) a static one, which involves the imposition of a step change in stress (or strain) and the observation of the subsequent development of the strain (or stress)

with time (not reported here) and ii) a dynamic one, which involve the application of an oscillatory strain.

2.3.2.1 Dynamic methods, oscillatory test

Dynamic mechanical analysis (DMA) is based on the application of an oscillating force to a sample and the observation of the material response to that force. When a material is loaded with a constant force and a sinusoidal oscillating stress or strain is applied, it will deform sinusoidally, thus offering detailed information on material characteristics, if this test is carried out within the linear viscoelastic region. The sinusoidal oscillating strain can be expressed by:

$$\gamma(t) = \gamma_0 sin\omega t \qquad \text{(Eq. 2.17)}$$

where γ is the strain at time t, γ_0 is the strain amplitude and ω is the oscillation or angular frequency. The strain rate, $\dot{\gamma}(t)$, becomes:

$$d\gamma/dt = \dot{\gamma}(t) = \omega\gamma_0 cos\omega t \qquad \text{(Eq. 2.18)}$$

The applied strain generates a sinusoidal strain or stress output with a certain amount of solid-like response, which is in phase with the input, and a corresponding amount of liquid-like response which is 90° out of phase with the input (see Fig. 2.12), which sum express the generated total stress (σ_0):

$$\sigma_0 = \mathrm{G}'\,\gamma_0 \sin(\omega t) + \mathrm{G}''\,\gamma_0 \cos(\omega t) \qquad \text{(Eq. 2.19)}$$

In a viscoelastic material, the generated stress shows a difference between the applied strain, showed by a phase lag of δ radians (Fig. 2.12). Therefore, the viscoelastic stress response, $\sigma(t)$, of the materials to the applied strain over time in the linear viscoelastic region is:

$$\sigma(t) = \sigma_0 \sin(\omega t + \delta) \qquad \text{(Eq. 2.20)}$$

By combining the Eq. 2.19 and Eq. 2.20 it is possible to obtain:

$$G' = \left[\frac{\sigma_0}{\gamma_0}\right] cos\delta \quad \text{(Eq. 2.21)}$$

$$G'' = \left[\frac{\sigma_0}{\gamma_0}\right] sin\delta \quad \text{(Eq. 2.22)}$$

where *G'*(Pa) is the *storage modulus* associated with the elastic response of the material, and *G''*(Pa) is the *loss modulus*, associated to the energy loss in internal motion. Therefore, for an ideal elastic solid, *G''*, is zero, while for an ideal liquid, the elastic component, *G,'* is zero. The vector sum of these two moduli provides the *complex shear modulus*:

$$G^* = G' + iG'' = \sqrt{G'^2 + G''^2} \quad \text{(Eq. 2.23)}$$

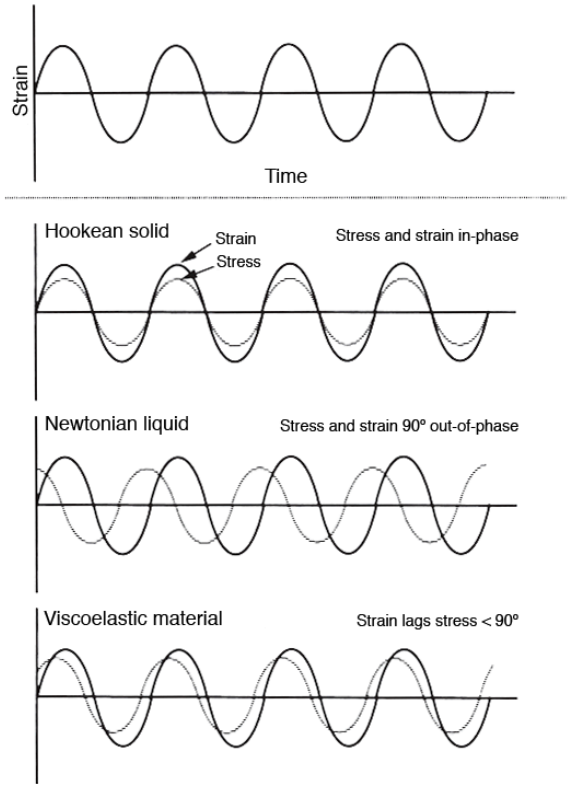

Figure 2.12 Stress and strain responses of an ideal solid, an ideal liquid and a viscoelastic [25].

If $G' >> G''$ the material behaves more like a solid, *i.e.* the deformations are essentially elastic or recoverable. If $G'' >> G'$ then the energy used to deform the material is dissipated by the viscosity of the system, so the material behaves more like a liquid. The viscoelastic moduli, determined over a range of frequencies, can indicate different transition zone, which correspond to relaxation processes dependent on the material structure. Fig. 2.13 shows the general overall response of a real structured liquid, with a:

- viscous/terminal region, characterized by predominant G' values and viscous (flow) behavior prevails. This region is present for all material, also solids, but the frequency where this is seen is often so low that most instruments cannot detect this part of the curve. At low-enough frequencies, G'' is linear with increasing frequency and G' is quadratic
- transition-to-flow region, where a transition from a predominant viscous behavior, $G'' > G'$ towards an elastic one, $G' > G''$ occurs with increasing frequencies. The point where the two moduli cross-over is given by the inverse of the relaxation time τ and characterized by a specific frequency ω_c and modulus G_c
- rubbery/plateau region, where elastic behavior dominates and G'' is always lower than G'. This region is characterized by a flat plateau, even if there is always a slight increase of G'
- leathery/transition region, where, due to high-frequency relaxation and dissipation mechanisms, the value of G'' again rises, faster than G' and another cross-over point can be defined
- glassy region, at the highest frequencies, where G'' again predominates and continues to rise faster than G'.

The typical range of frequencies available for most rheometers (10^{-2} to 10^{2} rad/s), allows usually to observe only two of the regions described above, depending mainly on the longest relaxation time, τ_{max}, of the material being tested.

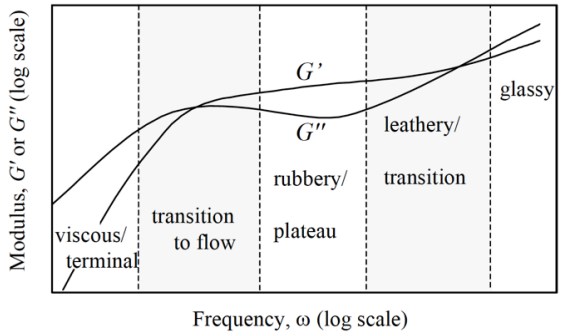

Figure 2.13 The various regions in the viscoelastic spectrum of non-Newtonian liquids [18].

The tangent of the phase angle (δ), also called *damping factor*, can define how efficiently the material loses energy to molecular rearrangements and internal friction. In other words, it is the ratio of the energy dissipated to that stored per cycle of deformation, therefore:

$$tan\delta = G''/G' \qquad \text{(Eq. 2.24)}$$

In addition, the *complex viscosity*, η^*, can be calculated as:

$$\eta^* = \frac{\sqrt{G\prime\,(\omega^2)+G\prime\prime\,(\omega^2)}}{\omega} \qquad \text{(Eq. 2.25)}$$

Since there is an extensive literature on this subject, viscoelastic parameters are usually expressed in various ways. The parameters used in this thesis are summarized in Tab. 2.2.

Parameter	Symbol	Parameter	Symbol
Shear strain	γ	Complex viscosity	η*
Shear stress	σ	Zero shear viscosity	η_0
Shear rate	$\dot{\gamma}$	Storage modulus	G'
Shear modulus	G	Loss modulus	G''
Shear viscosity	η	Complex modulus	G*
Dynamic viscosity	η'	Damping factor	tanδ

Table 2.2 Summary of the viscoelastic parameters described and used in this thesis.

2.4 Conventional gel systems in restoration practice

As mentioned in section 2.2 different cleaning systems were devised in order to attain better control over the cleaning action, through the use of thickeners and gellants, mainly constituted by water-soluble polymers. Restorers commonly refer to the overall typologies of confining systems with the term 'gel' because of their macroscopic appearance, although only some of them fulfill the requisites of a true gel, provided in section 2.2.1.

The use of thickeners or gellants allows to reduce some of the drawbacks related to the use of cleaning mechanical methods (e.g. friction with a soaked cotton swab) and free solvent (toxicity, scarce selectivity and control). Some products, commonly used in restoration procedures, are:

- cellulose ethers (e.g. Klucel®, an hydroxypropyl cellulose; Tylose®, an hydroxyethyl cellulose), a class of materials widely used to thicken water and polar solvents (e.g. alcohols), which can form physical gels. The preparation procedure consists in dispersing the polymer into the liquid phase by stirring at room temperature or under heating, then letting equilibrate for at least one day. The obtained jam-like system can be applied on the surface to be cleaned, as showed in Fig. 2.14, with a consistence able to fill and follow also rough surfaces. But the prevalence of adhesive forces over cohesive ones causes residues to remain on the treated surfaces. The subsequent removal often implies the use of invasive or aggressive methods (e.g. mechanical) for the original substrate, thus nullifying the advantages of using a confining system [26]. Moreover, the retention features of those systems are usually unsatisfactory, and high solvent evaporation rates can lead to the formation of dry films of solid material on the treated surface;

Figure 2.14 Application and removal of a Klucel® formulation [1].

- polyacrylic acid (e.g. Carbopol®, Pemulens®), a synthetic polymer introduced in the late 1980's along with the development of 'solvent gels' by R. Wolbers [27]. 'Solvent gels' formulations, *i.e.* solvents in their thickened state, are one of the most used retentive cleaning tools, based on the combination of two materials: i) the gellant (*i.e.* polyacrilic acid), characterized by the presence of many carboxylic groups and ii) a non-ionic surfactant (Ethomeen C12 or C15) with weak basic properties. The preparation of solvent gels is made by dispersing polyacrilic acid (~ 1% w/w) into the solvent or solvent mixture, then adding the surfactant (10-15 % w/w) under stirring. The further addition of water in small amounts (~ 5% w/w) produces a drastic increase in viscosity, leading to a physical gel formation. Gelation of the system occurs consequently to the partial neutralization of the acidic functions of polyacrilic acid that produces negatively charged carboxylate groups that repel each other through electrostatic interactions. This effect results in a significant extension of the chains, otherwise in

folded conformation, thus forming a gelled network. The most important drawback concerning the safe use of solvent gels is related to the residues that might remain on the works of art after cleaning, as for cellulose ethers. Thus, a following treatment is always necessary, usually carried out through organic solvent blends. Furthermore, after mechanical removal and solubilization of the solvent gel system, non-volatile residues of surfactant may remain on artifacts surface. Several studies have been carried out to investigate on the residue question; for example Stulik [28] et al. Burnstock et al. [29] demonstrate that some polyacrylic acid residues can remain after the application of the relative gels;

- polysaccarides (e.g. agar, gellan gum), materials recently proposed as residual-free and biodegradable materials [30,31]. Polysaccaride gellants can be applied on the surfaces to be cleaned either as a highly viscous solution or as so-called 'rigid gels' (see Fig. 2.15). Their use as 'rigid gels' permits to perform cleaning treatments leaving almost no residues, as reported in literature [32]. The procedure for obtaining the gels starting form polysaccharide polymers is very similar for the two considered materials: the gellant is added to water (concentrations usually range from 1 to 4% w/w) and heated up to 80°C, which leads to random coil conformation of the macromolecules of the gellant. Rearrangement of the molecules upon cooling results in formation of a thermo-reversible highly porous gel structure.
  - *Agar* is extracted from cell walls of red seaweed (mainly *Gelidium* and *Gracilara*) and is composed by agarose (linear polysaccaride) and agaropectin (mixture of smaller molecules). Agar gels can be used with chelating agents, enzymes or surfactants at different pH values [32]; recently they have been also used loaded with nanostructured cleaning fluids (microemulsions) for the removal of hydrophobic materials from porous surfaces [33].
  - *Gellan gum*, also branded as Phytagel® and Kelcogel®, is a water-soluble polysaccharide produced by the bacterium *Pseudomonas*

elodea; its repeating unit is a tetrasaccharide consisting of (1-4)-β-D-glucose, (1-4)-β-D-glucuronic acid, (1-4)-β-D-glucose and (1-4)-α-L-rhamnose. Gellan gum hydrogels used for the cleaning of artifacts present compact, visco-elastic, non-adhesive and homogeneous structures, stable at different pH values.

Agar and gellan gum gels seem the safest confining agents among the above-mentioned systems. They are also able to retain small amounts of polar solvents, enzymes, etc. and they can also be used for gentle surface cleaning or controlled humidification over water-sensitive artifacts (e.g. paper). However, in some cases, their water retention features can be not sufficient, as for instance when leaching or loss of components (water-soluble colors or inks) might take place due to excessive wetting [34].

2.5 Innovative gels and polymeric dispersions

A solution to the gel residue, mentioned in the previous section, has been pursued by formulating completely innovative gel systems with specific key features, such as improved mechanical properties (to ensure ease of handling and a completely residue-free treatment) and high retentiveness (to permit a highly controlled cleaning process even on sensitive substrates). Some of these systems can also be adapted for the cleaning of metal substrates, although they were not specific designed for them.

In this context, colloid and soft matter science has produced a significant contribution, designing a large array of advanced gels and 'gel-like' systems. Some examples, mainly developed in CSGI research group, are reported:

- stimuli-responsive gels, *i.e.* gels that can be easily and rapidly removed owing to their responsiveness to either a chemical, physical or mechanical 'switch'. As an example, polyamine (*i.e.* polyallilamine, PAA, or polyethylenime, PEI) based rehoreversible gels, are able switch from a solution into a gel system, through a simple chemical action [35,36]. In fact PAA solution converts into a gallant, by bubbling CO_2 through it, thanks to the

formation of polyallylammonium carbamate ($PAACO_2$) characterized by strong inter-chain interactions. The as formed gel is directly applicable onto a painted surface. After cleaning action rheoreversible gels can be removed by a simply in situ addition of a small amount of a weak aqueous solution (0.05M) of acetic acid (see Fig. 2.15 (a)). Decarboxylation reaction promoted by the acetic acid solution reverts the gel back to a liquid, which can be soaked up with a cotton swab. Gelled systems of PAA in 1-pentanol were used for the removal of aged varnish from a gilded 19th century frame [37], while PEI based gels proved to be effective on painted surfaces and gilded wood artifacts [37–39].

Gels responsiveness to external stimuli was further investigated by synthesis of networks able to respond to an external magnetic field. With this purpose, magnetic nanoparticles were functionalized and associated with acrylamide-based gels [40,41]. Acrylamide hydrogels act as confining agents for water or aqueous solutions (e.g. microemulsions), which can be released on the surface in a controlled way. Thanks to magnetic properties, the removal of the gel can be carried out by completely avoiding any direct handling of the gels, by means of a permanent magnet. This feature might be particularly suited in case of artistic surfaces that are extremely sensitive to mechanical stress (Fig. 2.15 (b));

- chemical hydrogels, permit a safe and effective cleaning providing, at the same time, completely residue-free results. Semiinterpenetrating networks (semi-IPN) were obtained by embedding poly(vinylpirrolidone) (PVP) within a poly(2-hydroxyethylmethacrylate) (p(HEMA)) network [34,42]. Blending p(HEMA) and PVP permits to take advantage of the best features of both polymers, *i.e.* the good mechanical strength provided by p(HEMA) and the high hydrophilicity characteristic of PVP. Moreover hydrogels characteristics, as for instance water retention properties, can be tuned by varying compositional ratios. Hydrogels are transparent and can be prepared in the shape of elastic foils that can be easily manipulated and re-

moved from surface after cleaning (see Fig. 2.15 (c)), without leaving residues (as assessed through FT-IR analysis. Gels can be loaded (by immersion) with water or water-based nanostructured fluids (*i.e.* microemulsions) for the removal of both, hydrophilic surface grime [34] or hydrophobic materials [42]. Although gels were originally designed for water-based systems, they are also able to load some polar solvents (e.g. glycols, alcohols, ethanolamine, etc.);

- 'gel-like' systems, such as polyvinyl alcohol (PVA, or partially hydrolyzed polyvinyl acetate, PVAc) based systems [15,43,44]. These systems cannot be strictly defined as gels, because of their rheological behavior, therefore they are referred to as Highly Viscous Polymeric Dispersions (HVPD), with a network structure characterized by the presence of entanglements, hydrogen bonds and borax-induced cross-linking. HVPDs were obtained by adding borax to a PVA aqueous solution. The gel-like network is due to the well-known ability of borate ions to cross-links PVA polymer chains. The nature of cross-links depends on several factors as pH, temperature, concentration of the reagents and chemical composition of the system [45,46]. The principal characteristic of these viscoelastic systems, used as cleaning tools, concerns their removal through a simple peeling action and the absence of residues left onto the treated surface (see Fig. 2.15 (d)). In fact, if compared to traditional cellulose or polyacrylic acid-based hydrogles, PVA- and PVAc-borax HVPDs behave in a more elastic way to the mechanical action (peeling) typically involved during removal. This rheological feature permits a safe removal without leaving detectable residues, as assessed by FT-IR measurements. HVPDs are able to load different solvents including ethanol, 1-pentanol, 2-butanol, 1- and 2-propanol, acetone, cyclohexanone, N-methyl-pyrrolidinone and propylene carbonate. The use of partially hydrolyzed PVAc further extends the range of solvents that can be loaded, and allows the preparation of HVPDs with increased quantities of organic solvent [47]. As an example, PVA-borax-acetone sys-

tems were used for the removal of highly degraded and darkened layers of natural resins from the 'Coronation of the Virgin with Saints', an egg tempera on wood panel by Neri di Bicci [44].

- physical hydrogels, such as blended PVA-based hydrogels are innovative systems that permit both, homogenous adhesion, thanks to their mechanical adaptability, and an easy and complete removal thanks to strong cohesion forces. Hydrogel synthesis is performed through cast-drying (Fig. 2.15 (e)) or repeated freezing and thawing (Fig. 2.15 (f)) of neat or blended (PEG, PVP) PVA aqueous solutions. Gelification process involves the formation of micro-crystalline regions that act as tie-points, contributing to formation of the three-dimensional network. In respect to the already existing gel systems, the development of these new hydrogels was addressed principally for the improvement of the mechanical adaptability of the hydrogel accounting for irregular or molded surfaces. In fact, the presented PVA-based hydrogels are characterized by pronounced elastic properties that permit the systems to be stressed and adapted to different surfaces and supports without loosing their mechanical integrity. Moreover, the possibility of tuning hydrogels properties through blending process of PVA with further polymers (PVP, PEG) was also investigated. These very promising cleaning systems, which permit to unify the advantages of a chemical system (strong cohesive forces, absence of residues), with those of a physical system (adaptability to irregular surfaces) were developer within a PhD in the CSGI group [48].

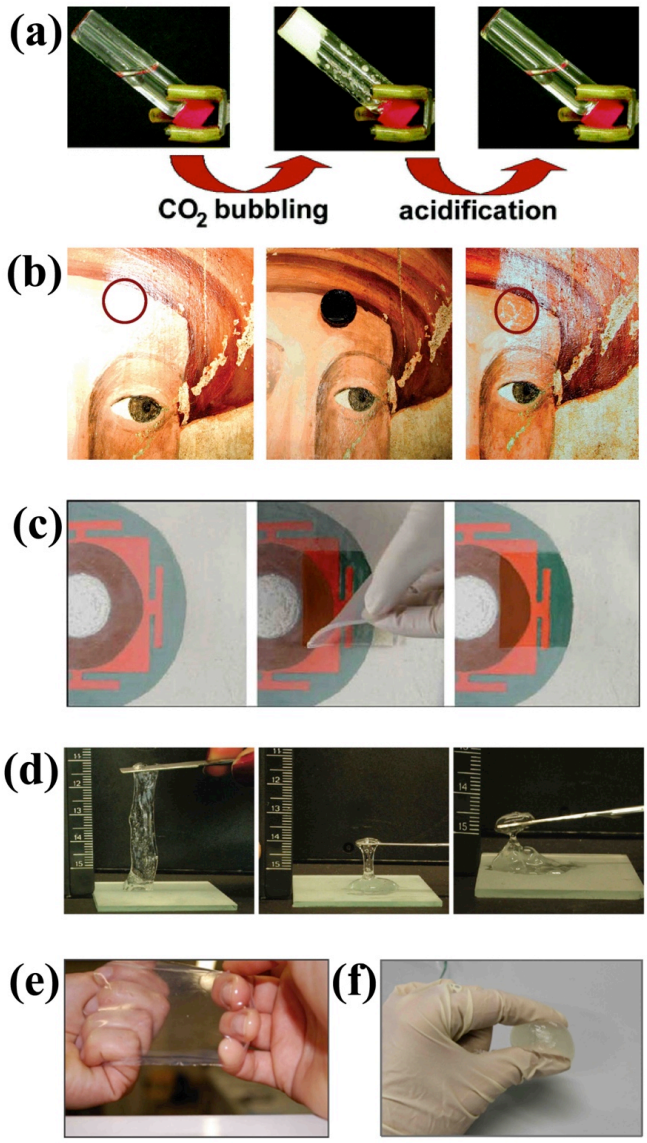

Figure 2.15 An overview of the innovative confining agents developed within the CGSI group: (a) rheoreversible PAA-based gel, able to switch from a solution to a gel through a chemical action; (b) acrylamide-based hydrogel loaded with magnetic nanoparticles, removable without any interaction with the surface; (c) semi-IPN p(HEMA)/PVP chemical hydrogels, with excellent mechanical and retentive properties; (d) PVA-borax HVPD (left, center) elastic properties compared with those of a traditional polyacrylic acid gel; (e) elastic properties PVA/PVP film obtained through the cast-drying method; (f) adhesion properties of a PVA/PVA hydrogel obtained by freeze-thaw method.

2.6 Bibliography

[1] BAGLIONI, P., CHELAZZI, D., AND GIORGI, R. *Nanotechnologies in the Conservation of Cultural Heritage. A compendium of materials and techniques*. Springer, Dordrecht, **2015**.

[2] BAGLIONI, P., CHELAZZI, D., AND O'BRIEN, P., EDS. *Nanoscience for the Conservation of Works of Art.* Royal Society of Chemistry, Cambridge, **2013**.

[3] LLOYD, D.J. *The problem of gel structure.* In J. Alexander, ed., *Colloid Chemistry. Theoretical and Applied*. The Chemical Catalogue Company, New York, **1926**, 767–782.

[4] NIJENHUIS, K. T. *Thermoreversible Networks. Viscoelastic properties and structure of gels*. Advances in Polymer Science *130*, (**1997**).

[5] ALMDAL, K., DYRE, J., HVIDT, S., AND KRAMER, O. *Towards a phenomenological definition of the term 'gel.'* Polymer Gels and Networks *1*, 1 (**1993**), 5–17.

[6] BUNGENBERG DE JONG, H.G. *A survey of the study objects in this volume.* In *Colloid science*. Elsevier Publishing Company, Amsterdam, **1949**, 1–18.

[7] HERMANS, P.H. *Gels.* In *Colloid science*. Elsevier Publishing Company, Amsterdam, **1949**, 483–651.

[8] FLORY, P.J. *Introductory lecture.* Faraday Discussions of the Chemical Society *57*, (**1974**), 7–18.

[9] FERRY, J.D. *Viscoelastic properties of polymers*. John Wiley &Sons, Inc., **1980**.

[10] BURCHARD, W. AND ROSS-MURPHY, S.B. *Introduction: physical gels from synthetic and biological macromolecules.* In W. Burchard and S.B. Ross-Murphy, eds., *Physical Networks: Polymers and Gels*. Elsevier Applied Science, London, **1990**, 1–14.

[11] NISHINARI, K. *Some thoughts on the definition of a gel.* Colloid and Polymer Science *136*, (**2009**), 87–94.

[12] CLARK, A.H. AND ROSS-MURPHY, S.B. *Biopolymers.* Journal of Polymer Science Part C: Polymer Letters *26*, 6 (**1987**), 207.

[13] KAVANAGH, G.M. AND ROSS-MURPHY, S.B. *Rheological characterization of polymer gels.* Prog. Polym. Sci. *23*, 97 (**1998**), 533–562.

[14] FRATINI, E. AND CARRETTI, E. *Cleaning IV: Gels and Polymeric Dispersions.* In P. Baglioni, D. Chelazzi and P. O'Brien, eds., *Nanoscience for the Conservation of Works of Art*. Royal Society of Chemistry, Cambridge, **2013**, 259–279.

[15] CARRETTI, E., GRASSI, S., COSSALTER, M., BAGLIONI, P., AND DEI, L. *Poly(vinyl alcohol)-borate hydro/cosolvent gels: viscoelastic properties,*

solubilizing power, and application to Art Conservation. Langmuir *25*, 15 (**2009**), 8656–8662.

[16] DOI, M. AND EDWARDS, S.F. *The theory of polymer dynamics.* Clarendon Press, Oxford, **1986**.

[17] SPERLING, L.H. *Introduction to Physical Polymer Science.* John Wiley & Sons Inc, Hoboken, **2006**.

[18] BARNES, H.A. *A handbook of elementary rheology.* University of Wales. Insitute of non-Newtonian fluid, Aberystwyth, **2000**.

[19] MENARD, K.P. *Dynamic Mechanical Analysis. A Practical Introduction.* CRC Press, Boca Raton, **1999**.

[20] GOODWIN, J. AND HUGHES, R. *Rheology for Chemists.* The Royal Society of Chemistry, **2008**.

[21] HUGHES, R. *Practical Rheology.* In *Colloid Science*. Blackwell Publishing Ltd., **2009**, 201–227.

[22] FARDIN, M.A. *On the rheology of cats.* Rheology Bullettin *83*, 2 (**2014**), 16–18.

[23] BARNES, H.A., HUTTON, J.F., AND K. WALTERS, F.R.S. *An Introduction to Rheology.* **1993**.

[24] MARK, J.E., NGAI, K., AND GRAESSLEY, W. *Physical Properties of Polymers.* Cambridge University Press, Cambridge, **2004**.

[25] RAO, M.A. *Measurement of Flow and Viscoelastic Properties.* In *Rheology of Fluid, Semisolid, and Solid Foods*. Springer US, Boston, **2014**, 63–160.

[26] CASOLI, A., DI DIEGO, Z., AND ISCA, C. *Cleaning painted surfaces: evaluation of leaching phenomenon induced by solvents applied for the removal of gel residues.* Environmental Science and Pollution Research *21*, 23 (**2014**), 13252–13263.

[27] WOLBERS, R., STERMAN, N., AND STAVROUDIS, C. *Notes for the Workshop on New Methods in the Cleaning of Paintings.* The Getty Conservation Institute, Malibu, **1998**.

[28] STULIK, D. *Solvent Gels for the cleaning of works of art: the residue question.* Getty Publications, Malibu, **2004**.

[29] BURNSTOCK, A. AND KIESLICH, T. *A study of the clearance of solvent gels used for varnish removal from paintings. 11th triennial meeting, Edinburgh, Scotland, 1-6 September, 1996: preprints (ICOM Committee for Conservation)*, James & James (**1996**), 253–262.

[30] CAMPANI, E., CASOLI, A., CREMONESI, P., SACCANI, I., AND SIGNORINI, E. *L'uso di agarosio e agar per la preparazione di "gel rigidi."* In *Quaderni del*

Cesmar 7. Il Prato Editore, Padova, **2007**.

[31] IANNUCCELLI, S. AND SOTGIU, S. *Wet treatments of works of art on paper with rigid gellan gels. 29*, (**2010**), 25–39.

[32] GULOTTA, D., SAVIELLO, D., GHERARDI, F., ET AL. *Setup of a sustainable indoor cleaning methodology for the sculpted stone surfaces of the Duomo of Milan.* Heritage Science, (**2014**), 1–13.

[33] GOREL, F. *Assessment of agar gel loaded with micro-emulsion for the cleaning of porous surfaces.* In *Conservation, exposition, Restauration d'Objets d'Art*. CeROArt, **2010**.

[34] DOMINGUES, J.A.L., BONELLI, N., GIORGI, R., FRATINI, E., GOREL, F., AND BAGLIONI, P. *Innovative Hydrogels Based on Semi-Interpenetrating p(HEMA)/PVP Networks for the Cleaning of Water-Sensitive Cultural Heritage Artifacts.* Langmuir *29*, (**2013**), 2746–2755.

[35] CARRETTI, E., DEI, L., MACHERELLI, A., AND WEISS, R.G. *Rheoreversible Polymeric Organogels: The Art of Science for Art Conservation.* Langmuir *20*, 20 (**2004**), 8414–8418.

[36] CARRETTI, E., DEI, L., BAGLIONI, P., AND WEISS, R.G. *Synthesis and Characterization of Gels from Polyallylamine and Carbon Dioxide as Gellant.* Journal of the American Chemical Society *125*, 17 (**2003**), 5121–5129.

[37] CARRETTI, E., DEI, L., AND WEISS, R.G. *Soft matter and art conservation. Rheoreversible gels and beyond.* Soft Matter *1*, 1 (**2005**), 17–22.

[38] CARRETTI, E., BONINI, M., DEI, L., ET AL. *New Frontiers in Materials Science for Art Conservation : Responsive Gels and Beyond. 43*, 6 (**2010**), 751–760.

[39] CARRETTI, E., DEI, L., WEISS, R.G., AND BAGLIONI, P. *A new class of gels for the conservation of painted surfaces.* Journal of Cultural Heritage *9*, 4 (**2008**), 386–393.

[40] BONINI, M., LENZ, S., FALLETTA, E., ET AL. *Acrylamide-Based Magnetic Nanosponges: A New Smart Nanocomposite Material.* Langmuir *24*, 21 (**2008**), 12644–12650.

[41] BONINI, M., LENZ, S., GIORGI, R., AND BAGLIONI, P. *Nanomagnetic Sponges for the Cleaning of Works of Art.* Langmuir *23*, 17 (**2007**), 8681–8685.

[42] DOMINGUES, J., BONELLI, N., GIORGI, R., AND BAGLIONI, P. *Chemical semi-IPN hydrogels for the removal of adhesives from canvas paintings.* Applied Physics A *114*, 3 (**2014**), 705–710.

[43] E., C. *Physicochemical characterization of partially hydrolized poly(vinyl acetate)-borate aqueous dispersions.* Soft Matter, (**2014**).

[44] CARRETTI, E., NATALI, I., MATARRESE, C., ET AL. *A new family of high*

viscosity polymeric dispersions for cleaning easel paintings. Journal of Cultural Heritage *11*, 4 (**2010**), 373–380.

[45] WU, W.L., SHIBAYAMA, M., ROY, S., ET AL. *Physical gels of aqueous poly(vinyl alcohol) solutions: a small-angle neutron-scattering study*. Macromolecules *23*, 8 (**1990**), 2245–2251.

[46] KEITA, G., RICARD, A., AUDEBERT, R., PEZRON, E., AND LEIBLER, L. *The poly(vinyl alcohol)-borate system: influence of polyelectrolyte effects on phase diagrams*. Polymer *36*, 1 (**1995**), 49–54.

[47] ANGELOVA, L.V., TERECH, P., NATALI, I., DEI, L., CARRETTI, E., AND WEISS, R. G. *Cosolvent gel-like materials from partially hydrolized poly(vinyl acetate)s and borax*. Langmuir *27*, 18 (**2011**), 11671–11682.

[48] BONELLI, N. *Cleaning works of art: tuning hydrogels properties by blending PVA-based systems*. University of Florence - CSGI, **2014**.

Chapter 3

Polyvinyl alcohol: a film forming polymer

3.1 Introduction

Polyvinyl alcohol (PVA) is one of the most important commercial water-soluble polymer, widely used in the field of cosmetics, packaging, pharmaceutics, biomedicine, adhesives, textiles industries thanks to its desirable characteristics and ease of processing. In fact, PVA presents excellent chemical stability, high biocompatibility, low toxicity, low cost and peculiar film-forming properties. In particular, partially hydrolyzed PVA, thanks to the presence of both ordered (crystalline) and amorphous domains, presents at the same time high water solubility and the ability to form films characterized by good mechanical properties.

As already discussed in Chapter 2 (section 2.5), innovative PVA-based cleaning systems have already been used as confining systems for the cleaning of Cultural Heritage artifacts, with good performances in terms of cleaning efficacy, applicability, easy and safe removal without residues. In particular PVA-borax polymeric dispersions (HVPD) were extensively studied and tested on real and artificial sample, while PVA/PVP and PVA/PEG blended systems showed very promising performances for applicative uses as new cleaning tools.

This chapter will present an overview on polyvinyl alcohol characteristic features to justify its use for the development of a new cleaning system, specifically tailor-made for metallic artifacts. In particular the PVA behavior in solution, its ability to crystallize and its characteristic transition temperatures will be briefly reported. In particular, the ability to form films is of paramount importance as the peculiar prop-

erty of the system presented within this work. Moreover, the influence of different additives (plasticizers, volatile fraction) over the polymer system properties will be analyzed, as powerful elements to tune the system properties as desired.

3.2 Polyvinyl alcohol (PVA): properties and structure

PVA is a vinyl polymer with a simple chemical structure, characterized by pendant hydroxyl groups (Fig. 3.1). The vinyl alcohol monomer does not exist in a stable form, because it rearranges in its tautomer, acetaldehyde. For this reason PVA is not polymerized directly from a monomer, but obtained from the hydrolysis of the polyvinyl acetate (PVAc) in alcohol solution. Since the hydrolysis reaction is not complete, the resulting product is always a copolymer of PVA and PVAc with a certain 'hydrolysis degree' (HD, usually expressed as molecular %). Different PVA grades are commercially available as *fully hydrolyzed* (HD ≈ 95-99%) or *partially hydrolyzed* (HD ≈ 85-92%) products, thus entailing different resulting properties. In fact the content of hydroxyl/acetate groups in the polymer has a great influence on the overall chemical properties, in particular over solubility and crystallinity [1].

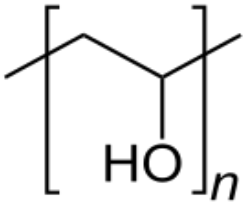

Figure 3.1 Chemical structure of polyvinyl alcohol.

PVA is soluble in highly polar or hydrophilic solvents (e.g. DMSO, glycols, etc.), although water is the best solvent. Water solubility is mainly influenced by: i) degree of hydrolysis (HD), ii) degree of polymerization (DP) and iii) temperature. The presence of a high number of hydroxyl groups in fully hydrolyzed PVA determines the formation of several inter- and intra-molecular hydrogen bonds, thus impedes the overall solubility (see Fig. 3.2 (a)). On the other hand, the presence of residual hydrophobic acetate groups, instead, weakens inter- and intra-molecular hydrogen

bonds, thus favoring the dissolution process, even at room temperature (see Fig. 3.2 (b)). Due to the existence of this strong hydrogen bonding network, it can be difficult to achieve molecularly dispersed PVA solutions, especially for PVA of large molecular weight. In such cases, stirring and/or heating could help the dissolution process [2].

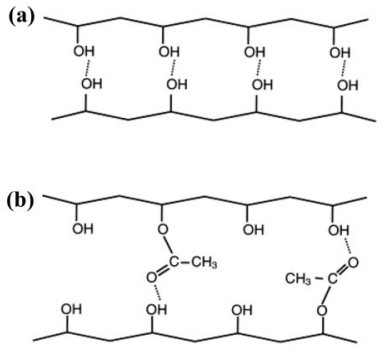

Figure 3.2 Hydrogen bonding in (a) fully hydrolysed PVA, where many hydroxyls groups are available, and for (b) partially hydrolysed PVA, where the residual acetate groups act as spacers thus reducing the established hydrogen bonding.

The combined effect of temperature, DP and HD is showed in Fig. 3.3. At low degree of polymerization and hydrolysis, complete solubility can be achieved even at low temperatures (Fig. 3.3 (b)). As the degrees of hydrolysis and polymerization increase, higher temperature (80 to 90 °C) may be required to obtain complete solubility (Fig. 3.3 (c, d)). At very high DP and low HD, the polymer starts to gel at room temperature and the solubility decreases rapidly (Fig. 3.3 (a)).

As mentioned before, in fact, the hydroxyl groups on neighboring chains of a low-hydrolysis degree PVA, are prevented from getting close enough to form inter-chain hydrogen bonds, due to the bulky size and hydrophobic character of the remaining acetate groups in the molecules. The solubility of partially hydrolyzed PVA is thus high at room temperature while fully hydrolyzed PVA is essentially insoluble in water at the same situation. By increasing temperature, the mobility of water molecules disrupts inter- and intra-chains hydrogen bonds, while enhancing

the water polymer ones. As a result, the solubility of also highly hydrolyzed PVA dramatically increases as showed in Fig. 3.3 (c, d). For low hydrolysis degree, instead, the hydrophobic nature of the acetate groups, causes the decrease of solubility as the temperature increases (Fig. 3.3 (a)).

In Tab. 3.1 are summarized the principal differences between the fully and the partially hydrolyzed PVA.

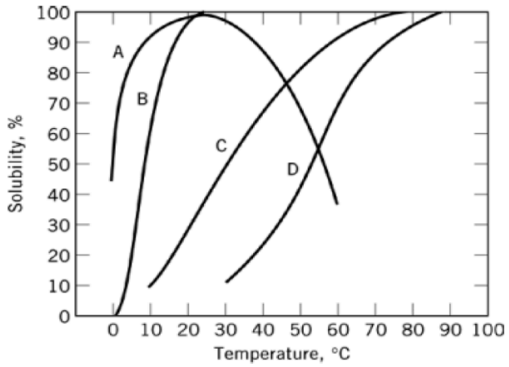

Figure 3.3 Solubility of PVA in water as a function of temperature for (a) 78–81% hydrolyzed PVA, DP = 2000–2100; (b) 87–89 % hydrolyzed PVA, DP = 500–600; (c) 98–99 % hydrolyzed, DP = 500–600; (d) 98–99 % hydrolyzed, DP = 1700–1800 [2].

Parameter	Fully hydrolyzed	Partially hydrolyzed
Water solubility	Moderately soluble	Very soluble
Degree of crystallinity	40-50%	20-40%
Film mechanical properties	Hard and brittle	Soft and flexible
Glass transition temperature	85 °C	58 °C
Melting temperature	220-240 °C	160-170 °C

Table 3.1 Summary of the main differences between fully-hydrolyzed and partially-hydrolyzed polyvinyl alcohol [3].

3.2.1 Thermodynamics of polymers in solution

The theoretical basis to understand the thermodynamics of polymer behavior in solution was developed independently by Flory and Huggins around the mid-

twentieth century [4,5]. The Flory-Huggins theory is based on a simplified model and some assumptions, but it still remains very useful for the theoretical prediction of experimental data.

The theory leads to a modification of the classical expression of the free energy of mixing ΔG_{mix}, by taking into account the different properties of a polymeric solution, where polymer solute molecules are much larger than the solvent ones. Moreover the introduction of 'the Flory-Huggins parameter' (χ) allows a quantitative prediction of a solvent goodness for a given polymer.

Since the Flory-Huggins theory is based on a statistical approach, it has to be introduced the three-dimensional lattice model, where the entire volume is divided into N_0 cells, which can be occupied randomly by solvent or by polymer segments (Fig. 3.4). Each polymer segment is assumed to have the same size of a solvent molecule, thus being interchangeable within the lattice positions.

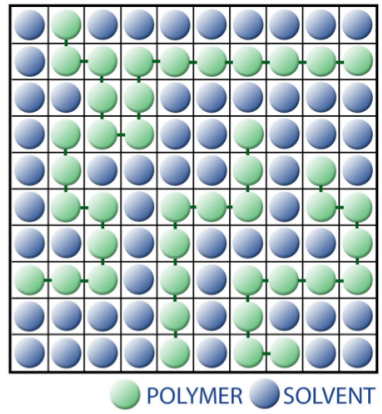

Figure 3.4 Schematic representation of the lattice model for a polymer-solvent binary system.

Considering a monodispersed polymer, the number of segments χ, contained in a polymer chain, is given by the ratio between the molar volumes of the polymer, V_p, and the solvent, V_s:

$$\chi = \frac{V_p}{V_s} \quad \text{(Eq. 3.1)}$$

The relation between the number of cells N_0 and the number of solvent and solute molecules, respectively N_s and N_p, occupying a single lattice position is:

$$N_0 = N_s + \chi N_p \quad \text{(Eq. 3.2)}$$

The thermodynamic criteria of solubility are based on the free energy of mixing equation, which predict the mutual solubility of two substances if, at least, ΔG_{mix} is negative:

$$\Delta G_{mix} = \Delta H_{mix} + T\Delta S_{mix} \quad \text{(Eq. 3.3)}$$

where ΔH_{mix} and ΔS_{mix} are the enthalpy and the entropy of mixing, respectively.
To compute the entropy of mixing, we recall that, according to Boltzmann, entropy depends on the possible configuration of a system:

$$S = k \ln \Omega \quad \text{(Eq. 3.4)}$$

where Ω is the number of possible arrangements and k the Boltzmann constant. In our specific case, Ω corresponds to the possible configurations that can arise by placing randomly polymer chains into the lattice and subsequently filling the voids with solvent molecules.

Statistical computation, not discussed herein, permits to evaluate Ω for a polymer solution. In respect to small molecule solutions, Ω values are greatly limited in the number of possible configurations, due to the dimensions and the covalent bonds between polymer segments. Thus the expression of entropy of mixing obtained through the Flory-Huggins theory is:

$$\Delta S_{mix} = -k \left[N_s \ln \chi \frac{N_s}{N_s + \chi N_p} + N_p \ln \frac{\chi N_p}{N_s + \chi N_p} \right] \quad \text{(Eq. 3.5)}$$

Since χ is related to the molar volumes (see Eq. 3.1), the expression can be changed on a molar basis (*i.e.* $k = R/N_a$):

$$\Delta S_{mix} = -R\left[n_s ln\phi_s + n_p ln\phi_p\right] \quad \text{(Eq. 3.6)}$$

where n_s and n_p are the number of moles of each component and ϕ_s and ϕ_p are the volume fractions, respectively, of solvent and polymer, generally defined as:

$$\phi_i = \frac{n_i V_i}{\Sigma_i n_i V_i} \quad \text{(Eq. 3.7)}$$

The expression described in (Eq. 3.6) is very similar to the classical expression of the entropy of mixing for small-molecule solvent-solute systems, but the great innovation introduced by the Flory-Huggins theory is that volume fractions are here considered rather than molar fractions. However for small molecule solutes, the mole fractions and the volume fractions are essentially the same, thus making Eq. 3.6 a more general expression for the entropy of mixing.

To compute the free energy of mixing for the solvent-polymer system, also the enthalpic term needs to be derived. The energy variation related to dissolution can be associated to the fact that solvent-solvent and solute-solute interactions are replaced by solvent-solute interactions. If W_{ss} is energy related to solvent-solvent interactions and W_{pp} the energy related to polymer-polymer interactions, the energy associated to dissolution, *i.e.* to formation of a new interaction solvent-polymer W_{sp}, will be:

$$\Delta W = W_{sp} + \frac{1}{2}(W_{ss} + W_{pp}) \quad \text{(Eq. 3.8)}$$

Obviously covalent bonds between chain segments are not included in W_{pp}; only interactions between neighboring molecules are here taken into account. The total enthalpy of mixing will depend on the number of solvent-polymer interactions (*i.e. sp* contacts). The formation probability of a new solvent-polymer contact will depend in our lattice model on the coordination number Z (that is the number of possible adjacent sites to a position in the lattice), and on the contact probability with sites occupied by a solvent molecule. Considering that χN_p is the total number of polymer segments, $\chi N_p Z$ is the total number of sites near a polymer segment. Since the probability that any of these sites is occupied by a solvent molecule, is approximately equal to solvent volume fraction ϕ_s, the total number of contacts will be:

$$\chi N_p Z \phi_s = N_s Z \phi_p \quad \text{(Eq. 3.9)}$$

while the enthalpy of mixing will be equal to energy change (Eq. 3.8) multiplied by the number of interactions (Eq. 3.9):

$$\Delta H_{mix} = \mathrm{Z} \Delta W_{sp} N_s \phi_p \quad \text{(Eq. 3.10)}$$

The χ parameter is introduced to give a measure of the energetic change, in RT units, that occurs when a mole of solvent molecules is removed from pure solvent ($\phi_p = 0$) and is immersed in a non-infinite amount of polymer $\phi_p = 1$, and defined as:

$$\chi = \frac{Z \Delta W}{RT} \quad \text{(Eq. 3.11)}$$

This dimensionless parameter is material-specific, and it generally has positive values. By introducing the χ parameter, the expression of the enthalpy of mixing becomes:

$$\Delta H_{mix} = RT \chi n_s \phi_p \quad \text{(Eq. 3.12)}$$

According to (Eq. 3.12), if χ is generally positive, the dissolution of a polymer in a solvent is generally an endothermic process.

By introducing the expressions for ΔS_{mix} and ΔH_{mix} in Eq. 3.3, the free energy of mixing for a polymer-solvent system is obtained:

$$\Delta G_{mix} = RT\left[\chi n_s \phi_p + n_s \ln \phi_s + n_p \ln \phi_p\right] \quad \text{(Eq. 3.13)}$$

It is now clear that the dissolution of a polymer will occur depending on concentration and on sign and magnitude of χ; χ is inversely related to temperature, so increasing T will thermodynamically favor dissolution.

The value assumed by the χ parameter is a measure of the polymer-solvent interactions, as well as for the polymer-polymer interactions, thus it can predict the goodness of a solvent for a given polymer. In general, the smaller the value of χ the greater the rates of free energy decreasing during dissolution:

- $\chi < 0$, negative values may indicate strong polar attractions between polymer and solvent;
- $\chi < 0.5$, the selected solvent acts as a good solvent for the given polymer;

- χ = 0.5, the so-called 'theta-condition'; polymer chains act as ideal chains, that is, they are not affected by wide range interactions with other polymer chains because they are compensated by the effect of the solvent; such a solvent is called 'theta-solvent' and the temperature at which this condition is achieved is the 'theta-temperature';
- $\chi > 0.5$, the selected solvent is a poor solvent and polymer will not dissolve.

3.2.2 Polymer crystallization

3.2.2.1 Crystallization mechanisms

Crystallization of polymers is a process associated with the partial alignment of their molecular chains. These chains fold together and form ordered regions called 'lamellae', which compose larger spheroidal structures named 'spherulites'.

When considering small molecules, the traditional classification into three physical states (gas, liquid, solid) is generally sufficient to explain most of their physicochemical behaviors. For long-chain molecules, such as polymers, characterized by strong inter-molecular forces and entangled chains, the typical states are the amorphous and the crystalline one. The amorphous phase can be assimilated to the liquid state, characterized by molecular disorder and chain statistical conformation called 'random coil'; the crystalline phase is more similar to a solid state, with a tridimensional order over at least a portion of the chain (Fig. 3.5). Moreover, the amorphous state is characterized by elastic moduli of about five orders of magnitude higher in respect to the rigid and inelastic crystalline state [6].

The essential requirement for crystallinity in polymers is some sort of stereoregularity, with significant isotactic or syndiotactic zones. However ordered polymers are seldom completely crystalline but they generally consist of a combination between crystalline and amorphous regions (Fig. 3.6). In fact the stereoregular components of a macromolecules usually represent only a proportion of the overall material and irregularities may occur in the form of chain branching, copolymerization, etc. Non-crystalline polymers, instead, are those which include high levels of irreg-

ularity within their structure, *i.e.* atactic polymers [7]. An exception to this statement is represented by PVA (see section 3.2.2.4).

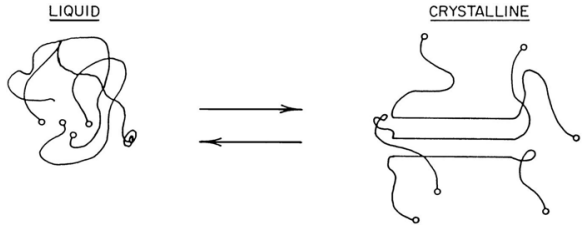

Figure 3.5 Schematic illustration of conformational differences between chain molecules in the liquid (amorphous) and crystalline states. Straight lines represent an ordered conformation. [6]

Semi-crystalline polymers are characterized by intermediate properties between the crystalline and the amorphous state: in fact they combine the strength conferred by the crystallites with the ductility due to the amorphous regions. The crystalline platelets are thus responsible for polymers strength, enhanced by the secondary bonding facilitated by closely packed and parallel chains, but also for their brittleness. For this reason the control over the balance between the two regions can be very useful in order to obtain desired ad specific properties.

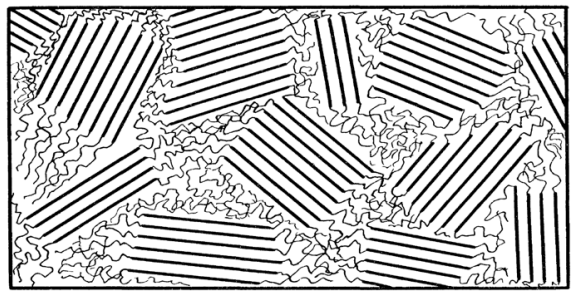

Figure 3.6 Morphology of a semi-crystalline polymer, with amorphous and crystalline zones [8]

For what concern the crystallization mechanism, different theories and models have been proposed since the first observation of a crystalline behavior in the early

1920's [9]. The presence of regions of crystallinity was first explained by the 'fringed micelle model', introduced by Herman et al. to explain the structure of gelatin, then expanded by Flory [8,10]. The fringed micelle model is based on the idea that parts of the polymer segments (either in solution or in the melt) align themselves together to form bundled crystalline regions. These bundles can then grow in the direction of chain axis by adjoining chain segments into the crystalline region or by lateral accretion of chain segments from other molecules. The growth of these structures however is impeded by the presence of entanglements and strained regions, which then constitute the amorphous phase. The 'fringes' are the regions of the chains traveling from the crystalline region to the surrounding amorphous regions. The crystalline regions than serve as physical crosslinks (see Fig. 3.6). This model has been historically very important since it permitted to explain a great number of experimental findings and of polymers physical properties, however it is now considered an oversimplification and replaced by the 'lamellar' and 'spherulites' models (not discussed here in detail).

The main innovation introduced by the 'lamellar model' is the recognition of the fi brous-lamellar nature of the polymer crystallites [11], where a lamellar crystal is the fundamental structural form by which polymers most generally crystallize. The polymer chains fold back and forth along layers, with lamellar thickness determinate by the length of the folds [12]. Besides, this model allows to explain the experimental observation of large crystalline superstructures characterized by spherical symmetry. These spherical aggregates, called 'spherulites', can be easily recognizable by their typical appearance when observed in polarized microscope between crossed polarizers (see Fig. 3.7), showing a characteristic Maltese cross.

These kinds of structures are the product of the crystalline lamellae aggregation, growing radially from a primary central nucleus, as shown in Fig. 3.8. While the lamellar structures present in spherulites are similar to those present in polymer single crystals, the folding of chains in spherulites is less organized. Further, the structures that exist between these lamellar structures are generally occupied by amorphous structures, as showed in Fig. 3.8. The same molecule may in fact have seg-

ments being part of a crystallite or others passing through the amorphous regions, thus acting as tie molecules, by providing inter-crystalline links that are responsible for the characteristic good toughness found in semi-crystalline polymers [9]. Spherulitic structure is considered to be the universal mode of crystallization [12,13] since it was observed in a great variety of crystallizable polymers, even though, more recent studies [14,15] have shown that spherulitic structures are not always found, and that different supramolecular structures exist.

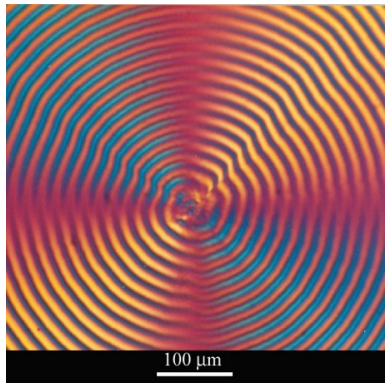

Figure 3.7 Transmitted cross-polarised light micrograph of a spherulite, displaying banding and a Maltese cross pattern [1]

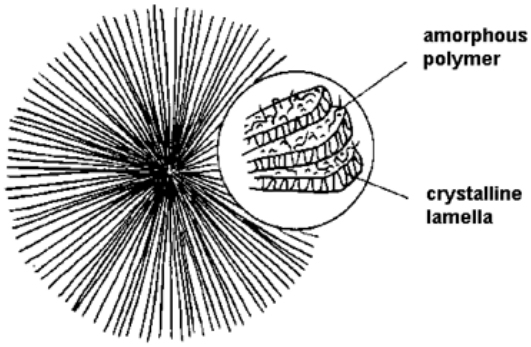

Figure 3.8 Schematic representation of a 'spherulite', with a radial orientation of the 'lamella', interspersed within the amorphous phase [1]

[1] http://www.doitpoms.ac.uk/tlplib/polymers/spherulites.php consulted on November 2015

Polymers can crystallize upon i) cooling from the melt, ii) mechanical stretching or iii) solvent evaporation. In particular the crystallization process from a solution upon the evaporation of a solvent mainly depends on the degree of dilution. In dilute solutions molecular chains have no connection with each other and exist as a separate polymer coils in the solution. Increase in concentration, which can occur for example via solvent evaporation, induces the interaction between molecular chains, thus increasing the possibility of crystallization. Generally, linear polymers form a variety of single crystals when they are crystallized from very dilute solutions upon cooling. For increasing polymer concentration a precipitate of lamellar aggregates will be observed, while further concentration leads up to more complex structures (twins, spirals, dendritic multilayer structures, etc.). At the highest concentrations, or when polymers crystallize from the melt, spherulites are the most common structure [9].

3.2.2.2 Degree of crystallinity

The amount of crystallinity in the polymer sample has a direct relationship with the materials mechanical behavior. Also a large number of optical, physical, thermal and chemical properties depend primarily on this parameter.

The *degree of crystallinity* (*DC%*) is defined as "the fractional amount of crystallinity in the polymer sample", which typically ranges between 10% and 80% (expressed here as mass fraction) [16]. One assumption of this definition entails that the polymer sample is made by a mixture of perfect crystalline and totally disordered areas. This two-phase model is assumed to show identical properties for both the crystalline and amorphous phase in their ideal state, without interface interactions [17].

The level of crystallinity, at a given temperature, is strongly dependent on the molecular weight (high *DC* for low M_w) and on the structural regularity of the chain. The large range of crystallinity degree that can be obtained for homopolymers depends mainly on topological factors, such as chain entanglements that restraint on

the process of crystallization. The level of crystallinity can be further reduced by the random introduction of non-crystallizing structural units into the chain, such as plasticizers [6].

There are several experimental techniques available to determine the degree of crystallinity; the most used are i) density measurement, ii) differential scanning calorimetry (DSC), iii) X-ray diffraction (XRD), iv) infrared spectroscopy (FTIR) and v) nuclear magnetic resonance (NMR). The measured value depends on the method used, which is therefore quoted together with the degree of crystallinity. It is worth to note, that even the degree of crystallinity is demonstrated to be a quantitative concept, some disagreement among the results obtained by the different techniques is frequently observed, especially at low degrees of crystallinity [16].

Further details on the experimental methods used to determine this parameter will be given in the experimental section (see Chapter 6).

3.2.2.3 Crystallinity of PVA

The PVA ability to crystalize is unusual (see section 3.2.2.1), because it is essentially an atactic linear polymer, *i.e.* the pendant hydroxyl groups are randomly positioned along the chain. This is generally accompanied by an inability to form crystallites domains, as for polyvinyl acetate, whereas the small dimensions of the PVA hydroxyl groups, allows polymer crystallization regardless stereoregularity [1].

Fuji extensively studied crystallizability of PVA in relation to its stereoregularity [18], finding that the sole atactic polymer is readily crystallizable, while the more stereoregular isotactic form is the least crystallizable. In fact, as stated by Bunn [19], the lateral hydroxyl groups on PVA chains represent no steric hindrance, since they are small enough to be interchangeable with hydrogen atoms within the crystalline lattice. Moreover, the isotactic structure promotes more inter-molecular hydrogen bondings, while the atactic form promotes intra-molecular ones, thus favoring chains orientation and crystallites formation. Another characteristic affecting PVA crystallizability is the hydrolysis degree. In fact, the presence of residual ace-

tate groups weakens intra- and inter-molecular hydrogen bondings, resulting in more difficult crystallites formation [3].

On a molecular level, PVA crystallites are made of ad double-layered structure, held together by hydrogen bridges, while Van der Waals forces operate between the two layers. These folded structures lead to small ordered regions (crystallites), scattered in a disordered, amorphous polymer matrix. PVA can crystallize as single crystals or as lamellar or spherulitic aggregates and its crystalline structure belong to the monoclinic system with a unit cell consisting of two monomeric units. Lamellar thickness was estimated around 100-150 Å.

Peppas et al. investigated through a profuse work started in the early 70's, the mechanism of PVA hydrogel formation that involves the sole physical crosslinking due to crystallites formation through different methods [20]. In particular he reports the unusual characteristic of PVA to form crystallites upon repeated cycles of freezing and thawing of PVA solutions ('freeze-thaw' method). Other methods to induce crystallization were since then explored (irradiation, 'cast-drying', etc.) and briefly described along with common PVA hydrogels in section 3.3.

3.2.3 Transition temperatures

Typical thermal transitions interest the two different regions of a semi-crystalline polymer under heating, *i.e.* the 'glass transition temperature' for the amorphous phase and the 'melt temperature' for the crystalline one.

The *glass transition temperature* (T_g), one of the most important parameters for understanding the mechanical properties of a polymer (strength, hardness, brittleness, elongation, etc.), is defined as "the temperature at which the amorphous phase of the polymer is converted between rubbery and glassy states" [6]. This phenomenon is observed in linear amorphous polymers, and it occurs at a fairly well defined temperature, when the bulk material ceases to be brittle and glassy and becomes less rigid and more rubbery. Many physical properties are profoundly dependent from the glass transition temperature, including coefficient of thermal expansion,

heat capacity, refractive index, mechanical damping, and electrical properties. Each one can thus be used to monitor the point at which this transition occurs. Unfortunately, as for the determination of the degree of crystallinity, the T_g values obtained from these various techniques can vary widely.

Heating the polymer up to its glass transition point and beyond, the molecular rotation around single bonds suddenly becomes significantly easier. Different factors can affect the ease of molecular rotation, hence influence the actual value that the glass transition temperature takes. Some examples are i) the presence of pendant groups or rigid structures to the polymer backbone, ii) cross-linking or hydrogen bonds between polymer chains, iii) high molar mass, making more difficult polymer movements, iv) effect of plasticizers (see section 3.5.3).

A number of methods exist for determining T_g, for example i) dilatometry, ii) dynamic mechanical thermal analysis (DMTA), iii) dielectric thermal analysis (DETA), iv) differential scanning calorimetry (DSC). Further details on the experimental methods used to determine this parameter will be given in the experimental section (Chapter 6).

For what concerns the *crystalline melting temperature* (T_m), it is defined as "the transition from a crystalline or semi-crystalline phase to an amorphous phase, a viscous liquid" [7]. Unlike conventional organic substances, crystalline polymers do not show a well-defined melting point, because they are effectively mixtures of different molar masses, with different melting temperatures. The range of melting temperature of homopolymers is thus influenced by the i) molar mass (lower T_m for low relative molar mass than high relative molar mass species) and ii) by the crystallites size, since smaller and less perfect crystallites melt before larger ones, as the temperature is raised. Other factors which influence the value of the range of temperature over which melting takes place are iii) the presence of co-monomers in the polymer and iv) the presence of solvent or plasticizer in the polymer.

Since glass transition is a second-order transition, it differs from the usual first-order phase changes of substances, such as melting or boiling, characterized by distinct changes in volume, optical properties and by a related latent heat [7]. Fig. 3.9.

shows the differences between the melting temperature, characteristic of a crystalline polymer, and of the glass transition temperature, typical of amorphous polymers. As the majority of polymers have crystalline and amorphous regions, usually by heating such a semi-crystalline polymer, both these transitions can be observed, first passing through the second-order transition at T_g (always lower than T_m), and then through a first-order transition as the crystallites undergo a true phase change on melting.

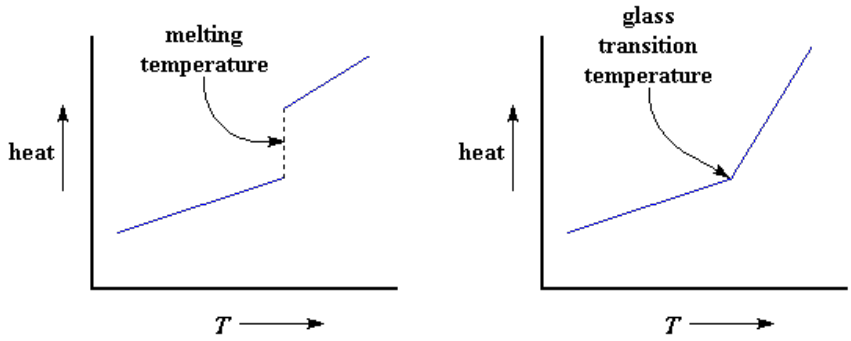

Figure 3.9 Temperature transitions differences between a first-order transition (melting) and a second-order one (glass transition), for completely crystalline and amorphous polymer, respectively.

A relationship between these two transitions can be evaluated by the empirical rule of Eq. 314, but with some restrictions and only for certain polymers:

$$T_g = 0.66 \pm 0.44 T_m \qquad \text{(Eq. 3.14)}$$

with T expressed in Kelvin [7].

3.3 PVA-based hydrogels and 'peelable' formulations

A brief overview over the most common PVA-based hydrogel and of their principal application fields will be provided here.

PVA is able to form hydrogels either by chemical or physical cross-links. Chemically cross-linked PVA networks can be obtained through the use of di-functional cross-linking agents, such as glutaraldehyde, acetaldehyde, formaldehyde, etc. In

acid environment (e.g. sulfuric acid, acetic acid) or methanol, acetal bridges form between hydroxyl groups, thus resulting in a tridimensional network. However, for applications in the biomedical field, undesirable toxic residues of crosslinking agents must be avoided. Thus, other chemical crosslinking methods, such as electron beam or γ-irradiation of concentrated PVA solutions, have been developed [21,22].

The properties of partially crystalline PVA hydrogels, first chemically cross-linked through electron beam irradiation and afterwards subject to a process of dehydration and annealing, were firstly examined by Peppas and Merrill [23]. In addition to the chemical cross-links produced through irradiation of the aqueous PVA solution, the resulting materials contained also crystallites. These additional cross-links, produced by the heat treatment, permit to enhance the hydrogels mechanical properties by redistributing external stresses along the crystallites.

As mentioned in section 3.2.2.3 Peppas widely investigated the mechanism of PVA hydrogel formation by the sole physical crosslinking, through to crystallites formation [20]. One explored method allowed to obtain hydrogel by a cyclical 'freeze-thaw' process, exhibiting higher mechanical strength, high degree of swelling in water and a rubbery and elastic nature, in respect to hydrogels obtained through conventional crosslinking methods. Moreover, these new materials, exhibit low toxicity, they contain no impurities and their water content matches that of tissue, thus making them very suitable for biomedical applications.

Further investigated methods to introduce physical crosslinks through crystallites formation in PVA hydrogels are crystallization through aging [24] and by means of slow-drying rate dehydration in isothermal conditions after chemical crosslinking with electron beam irradiation [25].

More recently, a method to obtain physically cross-linked PVA hydrogels, without addition of further chemicals or irradiation is reported [26,27]. In these studies, PVA-water solutions are casted and dried at room temperature: after dehydration gels swell, but do not solubilize in water at room temperature.

For what concern the field of cultural heritage, PVA-based hydrogels and polymer dispersions, have already been used or are under testing as described in Chapter 2, section 2.5, such as blended PVA system (PVA/PVP, PVA/PEG) or PVA/borax dispersions. The absence of toxic elements, the biocompatibility, easy of processing and the intermediate features between chemical and physical gel, make these systems suitable for a wide range of specific cleaning problems.

The emulsifying, binding, thickening, adhesive and film-forming properties of PVA were extensively used in the cosmetic field. In particular, for what concerns the so-called 'peelable' systems, PVA-based formulations able to be removed in one peace, without breaking, were extensively explored in the cosmetic field for the removal of skin impurities [28–31]. But the sole aqueous PVA solution does not fulfill all the requirement of cosmetic products, such as applicability, rapid evaporation, suitable mechanical properties for an easy removal, etc. Thus, often modification of the polymeric solution, e.g. with plasticizers or volatile solvents, are considered.

The cosmetic masks formulations inspired the idea of a similar system for the cleaning of Cultural Heritage artifacts. The principle of applying something fluid on the surface, waiting for its drying and then removing it with an easy peeling action, was transferred from skin cleaning to very different substrates. Also the composition of these products, mainly made by PVA and other additives, was taken as guidelines for the setup of the synthesis process and for devising suitable systems for completely different purposes.

3.4 Mechanism of film formation

The PVA ability of film formation through the evaporation of a liquid phase from an aqueous solution is well known from literature [32–35]. PVA is a good film-forming polymer and it found applications in different industrial sectors, for example, as high oxygen barrier film, membranes, packaging material and polarizing film [32]. In fact, PVA films, from the fully hydrolyzed polymer, often with the ad-

dition of plasticizers (see section 3.5.3) are transparent, tough, tear and puncture resistant, with good gas barrier properties and solvent and oil resistance; if partially hydrolyzed PVA is used, films presents higher levels of hygroscopy and solubility to water vapor. The property of water resistance can be further enhanced by cross-linking or by heat treatment to promote crystallization, thus reducing hygroscopy and water permeability.

The changes that affect polymer microstructure and properties during solvent evaporation, from a polymeric solution toward the formation of a dry film, will be here briefly described.

As stated by Mallapragada et al. [36–39], which extensively studied this process, the isothermal drying of PVA semi-crystalline polymer involves an overall increase, over time, in polymer:

- chains vicinity, as the solvent is progressively removed, polymer concentration increases and chains approach each other;
- degree of crystallinity, as a consequence of the previous point, chains vicinity promote the formation of crystallites domains;
- glass transition temperature, which can entail a glassy-rubbery transition.

During the evaporation process, the formation of two distinct regions occurs, as shown in Fig. 3.10. A glassy region forms at the polymer-air interface, where the solvent evaporation proceeds faster and the progressive chains immobility hinders the formation of further crystallites domains. The solvent evaporation rate decreases because of this glassy barrier formation, but additional crystallites domains can still form in the underlying rubbery region, thanks to residual polymer mobility and entanglement. The glassy-rubbery interface moves inward as the drying process proceeds until an entirely glassy system, containing local crystalline domains, is obtained and a film is formed. A summary of the differences between the two regions is given in Tab. 3.2

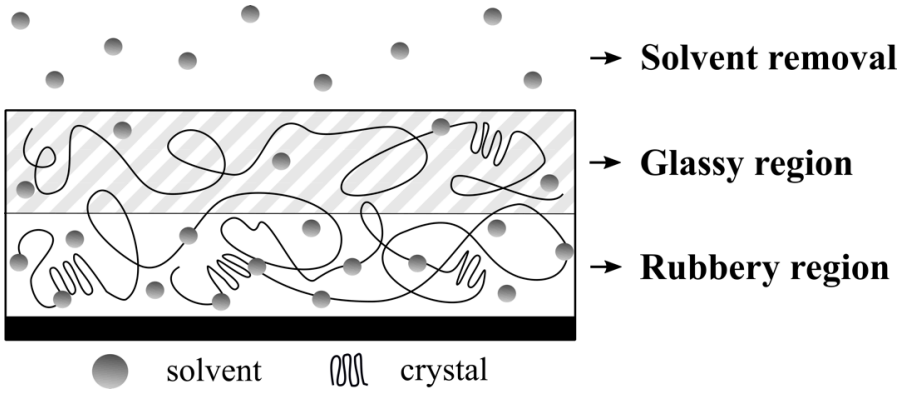

Figure 3.10 Schematic representation of the glassy and rubbery regions forming during drying.

Event	Glassy region	Rubbery region
Solvent removal	Fast	Slow
Entanglements formation	No	Yes
Polymer chains mobility	No	Yes
Crystallinity formation	No	Yes

Table 3.2 Summary of the main differences between the two regions occurring during solvent evaporation from a PVA solution towards the formation of a film.

The mathematical model, proposed by Ngui and Mallaprgada in 1998 [39], was developed to predict the isothermal drying kinetics of semi-crystalline polymers, by taking into account the:

- crystallization kinetics
- changes of the degree of crystallinity
- rubber-glassy transition
- skin formation

The existing mathematical models for amorphous polymers were not adequate to the description of the drying process, because they didn't consider that the increase of the degree of crystallinity in semi-crystalline polymers significantly changes the drying rates during solvent removal.

A schematic representation of polymer film during drying is reported in Fig. 3.11, where:

- ❒ at $x = 0$ no solvent loss occur because the interface polymers-substrate is considered impermeable, while at $x = L$ the solvent is removed from the film;
- ❒ the polymer in the region $0 < x < R$ is in the rubbery state, whereas in the region $R < x < L$ the polymer is in the glassy state;
- ❒ initially L coincides with R since the entire polymer film is in the rubbery state

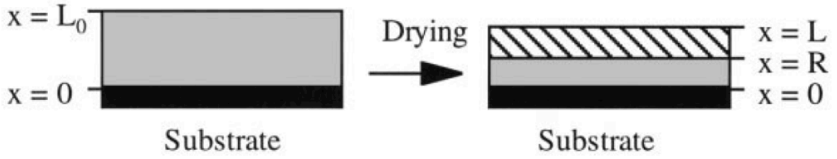

Figure 3.11 Schematic representation of the drying of a semi-crystalline polymer [37].

This model can be applied by taking into account some assumptions:

- ❒ isothermal drying kinetics;
- ❒ one-dimensional transport;
- ❒ immediate escape of the solvent as soon as it reaches polymer-air interface;
- ❒ uniform initial size distribution of the crystals.

Crystallization kinetics considers a system of three components, *i.e.* i) solvent, ii) the amorphous and iii) crystalline part of the polymer, identified by the respective suffix *1*, *2a* and *2c*. The rate of changes of the components during drying is expressed in terms of volume fractions (v), which sum is equal to unity:

$$v_1 + v_{2a} + v_{2c} = 1 \qquad \text{(Eq. 3.15)}$$

The expression for the rate of change for the amorphous portion in the rubbery region $0 < x < R$ is given by:

$$\frac{\partial v_{2a}}{\partial t} = \frac{\partial}{\partial x}\left(D\,\frac{\partial v_{2a}}{\partial x}\right) - k_1 v_1 \qquad \text{(Eq. 3.16)}$$

with a generalized Fickian diffusion term and another term for the decrease of the amorphous phase due to the crystalline phase formation during the chain folding process. *The diffusion coefficient* (*D*) depends on solvent volume fraction, crystallinity, tortuosity and temperature; the *chain folding rate* (k_1) was calculate based on the theory of Lauritzen and Hoffman for crystallization kinetics (note reported here, see ref [37]) and it is proportional to the solvent volume fraction and to the rate of change of crystalline volume fraction.

The movement of the glassy-rubbery interface can be predicted by using the expression proposed by Astarita and Joshi:

$$\frac{\partial R}{\partial t} = -k_2\left(v_{1|x=R} - v_{1t}\right)^n \qquad \text{(Eq. 3.17)}$$

where v_{1t} is the volume fraction corresponding to the threshold activity for deswelling, while k_2 and n are fitting parameters of the kinetic model; these parameters can be determined by sorption experiments.

Since the degree of crystallinity remains constant in the glassy region $R < x < L$, only one equation is required to predict the volume fractions of solvent, both amorphous and crystalline regions during drying. The rate of change of amorphous volume fraction in the glassy state is calculate from the following equation:

$$\frac{\partial v_{2a}}{\partial t} = \frac{\partial}{\partial x}\left(D\,\frac{\partial v_{2a}}{\partial x}\right) \qquad \text{(Eq. 3.18)}$$

without the term related to the crystalline portion. In fact in the glassy region chains do not have enough flexibility to fold and the crystallinity is assumed to remain constant.

Additional models were developed from Mallapragada et al. to describe also a ternary system [36] and to consider more variable for the above-exposed model.

3.5 Factors influencing the polymer solution and film properties

The formation of a film starting from a PVA polymeric solution has to take into account different factors that can influence the i) drying time, ii) applicability and iii) film-forming performances. The principal components of the system (water and polymer) confer specific basic properties, which can be further modified by the addition of other substances (plasticizers, solvents) [40], as reported below.

3.5.1 Polymer

As reported in section 3.2 several commercial PVAs are available with different hydrolysis degrees (from 75% up to >99%) and molecular weight. The choice of the appropriate PVA is of paramount importance, because it affects i) water solubility, ii) applicability and iii) film-forming performances.

In fact, low hydrolysis degree (HD) and low molecular weights (M_w) mean higher water solubility, thus reducing the time needed for the preparation of the polymeric solution. But too low HD and M_w imply also poorer mechanical properties of the resulting PVA films. Moreover, fully hydrolyzed PVA often requires very long times to be solubilized with a resulting final film hard and brittle, not suitable for example, for an easy peeling action.

The viscosity of the polymeric solution is the main applicability-related characteristic of the formulation. It is mainly influenced by the PVA molecular weight, which is a measure of the degree of polymerization *DP*. Three ranges of M_w are generally commercially available: i) ~200,000 for high viscosity, ii) ~130,000 for medium viscosity and iii) ~30,000 for low viscosity (viscosity is given as the value in *cps* of a 4% w/w concentrated water polymeric solution at 20 °C). Moreover low molecular weights PVA require higher amount of polymer powder to be solubilized, at equal w/w% overall concentration.

PVA concentration, instead, is one of the most important factors influencing the film-forming performances. In fact it represent the main component of the final film, when the solvent is loss, with mechanical properties directly related to the

chosen polymer. Low concentrations would confer poor mechanical properties to the final film and a liquid initial consistency, while too high concentration can confer good mechanical properties but it would be too difficult to solubilize.

A compromise between the *HD*, the M_w and the polymer concentration allows to obtain the solubilization of the polymer in reasonable times, thanks to intermediate *HD* and M_w, while by adjusting the concentration and M_w values it can be compensate the loss of mechanical properties (i.e. tensile strength, tear resistance, elongation and flexibility, etc.).

In the experimental section the formulations compositions chosen for the development of the cleaning system will be described in detail, by taking into account all these factors.

3.5.2 Volatile fraction

The volatile or liquid fraction content mainly affects the drying time and, indirectly, the time of film formation.

Depending on the final purpose of the system, the evaporation rate can be adjusted to meet the formulation requirements. For example a facial cosmetic masks product must dry in few minutes with very high evaporation rates. This parameter mainly depend on the overall water content of the polymeric solution and, obviously, on external factors, such as temperature and relative humidity. So, the reduction of the overall liquid/volatile fraction content would increase the evaporation rate. Moreover it is a common practice the addition of a solvent with high vapor pressure (e.g. alcohols) in order to enhance the evaporation rate, thus reducing the time for film formation.

Furthermore, the ethanol acts upon water as a structuring agent, by disrupting its intrinsic anomalies an by incrementing the hydrogen-bonds formation probability, thus reinforcing the overall 3-D network structure, as reported in ref. [41]. The structuring process of a binary water/ethanol mixture is extensively described in ref. [42] and here briefly reported. As showed in Fig. 3.12, stable hydration shells forms

around ethanol molecules at low concentrations; by increasing the alcohol mole fraction insufficient water molecules remain to form stable hydration shells. Above the x_1 concentration value hydration structures become less stable and inter-molecular interactions between water and alcohol become predominant, with the preference of water to aggregate around the –OH groups of ethanol, thus favoring the formation of an extended H-bonds network. At the composition of x_2 the highest degree of structuring is achieved to finally reach x_3 where the solution dynamics of water and ethanol becomes independent from each other.

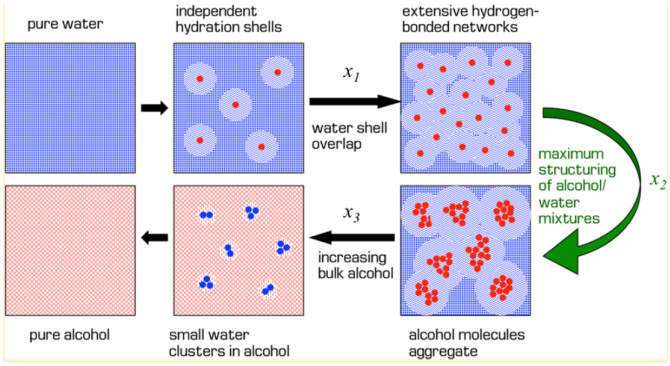

Figure 3.12 Schematic representation of the structuring process of a binary water/ethanol mixture, from [42]

3.5.3 Plasticizers

3.5.3.1 Characteristics, definitions and classification of plasticizers

The addition of plasticizers is one of the most common ways to modify the polymer properties. A summary of their main properties, definitions and classification is provided in Tab. 3.3, from ref. [43].

Plasticizers expectations
- decrease of the glass transition temperature of the polymer;
- increased flexibility, influenced by the changes in polymer structure;
- increased elongation and decreased tensile strength;
- decrease in ductility and improvement of impact resistance;
- improvement of low temperature properties;
- viscosity control;
- modification of rheological properties;
- effect on chemical reactivity;
- decrease of the temperature of dissolution;
- effect on processability by lowering the melting temperature;
- modification of interaction with water depending on their hydrophobic or hydrophilic nature;
- improvement of optical clarity by homogenizing system components;
- reduction of crystallinity, even if it can increase because of polymer chains mobility;
- increased compatibility between additives, polymer with additives, and polymers in blends;
- increase in gas permeability.
Plasticizers definitions
- an additive that reduces intermolecular forces in polymers making them more flexible;
- a low molecular weight material added to polymeric materials such as paints, plastics or adhesives to improve their flexibility;
- high-boiling compatible liquid that lowers T_g and flexibilizes the polymer;
- plasticizer interacts with the polymer chains on the molecular level as to increase chain mobility;
- a material incorporated into a plastic to increase its workability, flexibility or dispensability. The addition of a plasticizer may lower the melt viscosity, elastic modulus, and T_g;
- specialty plasticizers impart characteristic properties such as flame retarding, low temperature flexibility, or resistance to weather conditions;
- polymeric plasticizer has high molecular weight (usually M_n higher than 5,000), low vapor pressure and low diffusion rate.
Plasticizers classification
- chemical classification in three main families: phthalate esters, trimellitate esters, and adipate esters;
- internal plasticization, produced through copolymerization by including flexible monomers (soft segments) regularly or irregularly incorporated between inflexible monomers (hard segments) of a polymer chain; external plasticization, achieved through incorporation of a plasticizing agent into a polymer, through mixing and/or heating, which interact only physically with the elastomer, without chemical reactions;
- primary plasticizers, used as either the sole or the major plasticizer, with the effect of being compatible (enters the crystalline regions) with some solvating nature (enters the amorphous regions); secondary plasticizers, generally used as diluent for primary plasticizer to improve some performances (e.g. flame resistance) or to reduce cost, without penetrating the original polymer system.

Figure 3.13 Plasticizer polymer response based on 'lubricity theory'.

A plasticizer is a substance that can be incorporated into a polymer to increase its flexibility, workability or distensibility. It is characterized by a relative molar mass well below those of polymers to be plasticized and it usually is a liquid substance, non-volatile, non-mobile, inert, inexpensive, nontoxic, and compatible with the system to be plasticized. The addition of a plasticizer lends higher homogeneity to the material that results softer, more flexible and easier to process in respect to the sole polymer; moreover it reduces the melt viscosity, lowers the temperature of glass transition and the elastic modulus of a polymer.

3.5.3.2 Plasticizers theories and mathematical models

The effect of plasticizers has been explained by the i) lubricity theory, ii) gel theory and iii) free-volume theory [43]:

- the lubricity theory states that the plasticizer acts as an internal lubricant and permits the polymers molecules to slip over each another, by reducing the intermolecular frictions. As a polymer is flexed, the molecules glide back and forth with the plasticizer providing the gliding planes, as showed in Fig. 3.12. This theory assumes the polymer macromolecules have, at the most, very weak bonds away from their cross-linked sites

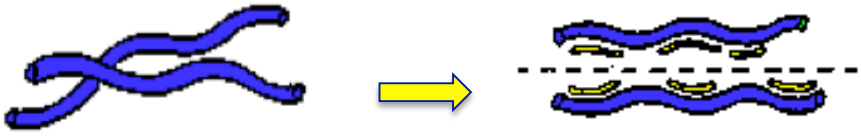

Table 3.3 Summary of the main characteristics, definitions and classification of plasticizers.

- the gel theory, which is applicable to amorphous polymers, considers the polymers formed by a tridimensional honeycomb structure maintained by loose attachments between the polymer molecules along their chains. This theory assumes that a polymer has many intermolecular attractions that are weakened by the presence of a plasticizer. The rigidity in polymers is primarily due to the resistance of their tridimensional structures, given by gel points of weak

attachments at intervals along the polymer chains, as showed in Fig. 3.13, rather than to the internal frictions, as the lubricity theory states. These points of gel are close together, thus, permitting little movement. Gel sites might be the result of van der Waals forces, hydrogen bonding, or crystalline structure. The plasticizer function is to reduce the number of these points of attachments, letting the polymer to be deformed without breaking. In spite of lubricating the glide planes, the plasticizer reduces the rigidity of polymers thereby reducing the aggregation of the polymer molecules, thus allowing them to move more freely

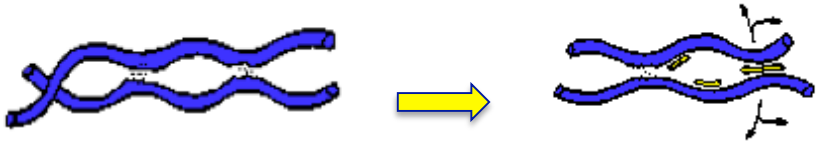

Figure 3.14 Gel theory of plasticizers.

- in the free-volume theory, postulated by Fox and Flory [44], it is assumed that the addition of a plasticizer increases the free volume of a polymer and that the glass transition happen at that physical state where all materials exhibit the same 'fractional free volume'. The 'free volume' is defined as the difference between the observed volume at absolute zero and the volume measured at a selected temperature. Addition of plasticizer into the polymer mass implies not only addition of molecules with T_g lower than that of the polymer itself, but the relatively small plasticizer molecules add a great free volume to the system, thus clarifying the lowering of the glass transition temperature. Consequently it can be stated that the plasticizers with lower T_g are more efficient in reducing the T_g of the plasticized system. Moreover, for the same molecular weight, a branched plasticizer is more efficient than the linear one, since there is more free volume associated in the branched plasticizer. In respect to the molecular weight of the plasticizer, increasing the molecular size of the plasticizer increases the free volume introduced into polymer, thus the

plasticizer efficiency. Nevertheless, on a weight basis, the total free volume increment could be greater for small molecular weight plasticizers. As pointed out by Sears and Darby [45], the Free-Volume theory explains successfully (at least qualitatively) the diminution of the T_g in plasticized polymers, but it presents some limits that they tried to overcome. Their theory considers polymer according to the fringed micelle theory, already exposed in section 3.2.2.1 (Fig. 3.14). The amorphous regions of a polymer, where short chains, abnormal branching, impurities or irregularities don't allow the formation of crystallites, have associated more free volume and so tend to be more flexible. Plasticizer molecules situate themselves around the polymer chains, preferentially in the amorphous areas, thus introducing more free volume and so, more flexibility and ease of movement to macromolecules. When a small quantity of plasticizer is added, many polymers tend to increase the number and size of their crystallites since with the small increase of the free volume a new redistribution of the configurations is allowed. For non-crystalline polymers, an increase in order has also been observed. This results in a more rigid resin with higher tensile strength and modulus, which is known as 'antiplasticization'. When larger quantities of plasticizer are added to the polymer, the crystallinity may increase, but the amorphous areas are swollen, resulting in a softer material. In this case the polymer becomes more flexible, has better elongation, higher impact resistance, but lower tensile strength and modulus. When even more plasticizer is added the crystallites could be dissolved and a gel is obtained.

All theories together give an approximate picture of fundamental principles of plasticization and they explain satisfactorily most aspects of behavior of plasticized polymers, even if none is able to explain plasticization by itself.

The mathematical models available are mainly based on the Free-Volume Theory and they try to correlate the T_g of the plasticized system with the polymer and the plasticizer T_g. The extent to which a plasticizer reduces the glass transition tempera-

ture of polymer is used as a measure of plasticizer efficiency. The earliest models to appear were developed by Kanig [46], Wood [47]and Gordon and Taylor [48]. These models were based on quite simple expressions such as that of Fox, derived from that of Gordon and Taylor:

$$\frac{1}{T_g} = \frac{w_1}{T_{g1}} + \frac{w_2}{T_{g2}} \qquad \text{(Eq. 3.19)}$$

where T_g, T_{g1} and T_{g2} are the glass transition temperatures of the mixture, the polymer and the plasticizer respectively, while w_1 and w_2 are the weight fraction of the polymer and of the plasticizer. This model assumes that the free volume of a liquid can be added

to that of the polymer to obtain the free volume of a mixture, and that the free volume of all the substances at their transition temperature are equal.

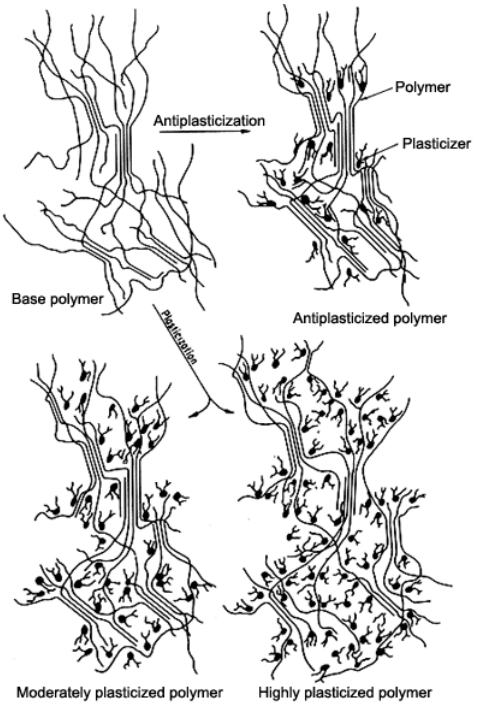

Figure 3.15 Plasticization concept according to Sears and Darby [45].

The Kelly and Bueche [49] expression introduced other parameter, like the thermal expansion coefficient:

$$T_g = \frac{4.8 \times 10^{-4} c T_{g1} + \alpha_1 (1-c) T_{g2}}{4.8 \times 10^{-4} c + \alpha_1 (1-c)} \qquad \text{(Eq. 3.20)}$$

where c is the volume fraction of the polymer and α_l is the thermal expansion coefficient of a liquid.

These equations are rather simple and present some limits, as they don't take into account the polymer/plasticizer interactions or the influence of the molecular structure. Di Marzio and Gibbs [50] proposed a theory that took into account the intramolecular polymer/plasticizer interactions, but not the inter-molecular ones.

Recently Mauritz and Storey [51] proposed a free volume based theory that predicts plasticizer diffusion coefficients and requires a minimum input of experimental parameters. Briefly, these authors take into account the redistribution of the free volume required to incorporate the plasticizer molecules into the polymer mass. Above T_g the polymer molecular structure is dynamic and local conformations transitions could serve to create sufficient large free volume for plasticizer molecule to penetrate. The probability of the formation of an adjacent hole to permit the plasticizer translation is also considered. An entropic factor relating to the liberation of a translational degree of freedom for the plasticizer molecule is added to the model. The model also includes the possibility of diffusion of large molecules of any shape. Finally, the authors consider polymer-plasticizer interactions as well as the effect of the temperature on penetrant conformation.

3.5.3.3 Compatibility

Compatibility is the ability of a plasticizer to form a homogenous system with the polymer. The rule "like dissolves like" was the earliest compatibility concept, then completed by the 'cohesion energy' and the 'solubility parameter' for which more specific literature is available. Plasticizers with solubility parameters and type of bonding similar to those of the polymer are more apt to be compatible than when the solubility parameters are different. To be compatible a plasticizers should re-

semble as close as possible the structure and the inter-molecular forces of the polymer they plasticize. As it is difficult to find plasticizers with high inter-molecular forces comparable to those of a strongly crystalline polymer, plasticization is generally more effective for amorphous or semi-crystalline (where the crystalline phase is not predominant) polymers.

A numerical way to measure the polymer/ plasticizer compatibility, by their solvency bejhavior, is through the *solubility parameter* (δ), suggested by Hildebrand [52] and defined as "*the square root of the cohesive energy density*":

$$\delta = \sqrt{\frac{\Delta E}{V}} = \sqrt{\frac{\Delta H_v - RT}{V}} \qquad \text{(Eq. 3.21)}$$

which is the molar energy of vaporization per unit molar volume. The conventional unit is the *Hildebrand (H), $(cal/c^3)^{1/2}$*. Similar values of this parameter assure compatibility, resulting in solvation, miscibility or swelling. In particular the presence of plasticizers help the flexibility of polymers, by allowing segmental mobility, without dissolving them. Through experience, it is found that the solubility parameter differences between the plasticizer and polymer should be less than 1.8 *H* for to have compatibility between them [43].

3.5.3.4 Plasticized PVA

By taking into account the above-mentioned compatibility requirement and also the permanence capacity of a plasticizer into the polymer matrix, polyvinyl alcohol most used plasticizers belong to the polyols family. In fact they possess –OH groups, which can form hydrogen bonds with –OH of PVA. By decreasing the inter- and –intra-molecular H-bonds between the PVA chains, the plasticizers are able to effectively reduce the structural regularity [53]. Moreover polyols are characterized by low molecular weight and, thus, able to enter within the PVA molecular chains and to migrate all around. Therefore, the use of a mix of plasticizers with different molecular weight, allows an easier penetration of other plasticizers with higher molecular weights.

Some examples of polyols used to plasticize PVA found in literature are reported in Tab. 3.4 [43].

Plasticizer	Application
polyethylene glycol	- pharmaceutical tablets - coating composition - hydrogels
ethylene glycols and propylene glycol	- removable coatings - adhesive gel - hydrogels
glycerin	- high performance compounds - adhesive gels - pharmaceutical tablets - coating compositions - water soluble films - hydrogels - biodegradable - composite articles
dipropylene glycol	- strippable coating

Table 3.4 Frequently used plasticizers for PVA and their applications. For references see [43].

3.6 Bibliography

[1] OGUR, E. *Polyvinyl Alcohol: Materials, Processing and Applications.* Rapra Review Report, **2005**.

[2] MARTEN, F.L. *Vinyl Alcohol Polymers.* In Kirk-Othmer, ed., *Encyclopedia of Chemical Technology*. John Wiley & Sons, Inc., **2000**.

[3] HASSAN, C.M. AND PEPPAS, N.A. *Structure and applications of poly(vinyl alcohol) hydrogels produced by conventional crosslinking or by freezing/thawing methods.* Advances in Polymer Science *153*, (**2000**), 37–65.

[4] FLORY, P.J. *Thermodynamics of High Polymer Solutions.* The Journal of Chemical Physics *10*, 1 (**1942**).

[5] HUGGINS, M.L. *Some properties of solutions of long-chain compounds.* The Journal of Physical Chemistry *46*, 1 (**1942**), 151–158.

[6] MARK, J.E., NGAI, K., AND GRAESSLEY, W. *Physical Properties of Polymers.*

Cambridge University Press, Cambridge, **2004**.

[7] NICHOLSON, J.W. *The chemistry of polymers.* Royal Society of Chemistry Publishing, Cambridge, **2006**.

[8] FLORY, P.J. *Principles of Polymer Chemistry: Paul J. Flory.* Cornell University Press, New York, **1953**.

[9] CARRAHER, C.E. *Seymour/Carraher's Polymer Chemistry, Sixth Edition.* CRC Press, **2003**.

[10] HERMAN, K., GERNGROSS, O., AND ABITZ, W. *X-ray studies of the structure of gelatin micelles.* Journal of Physical chemistry B *10*, (**1930**), 371–394.

[11] HEARLE, J.W.S. *The fine structure of fibers and crystalline polymers. I. Fringed fibril structure.* Journal of Applied Polymer Science *7*, 4 (**1963**), 1175–1192.

[12] KELLER, A. *Polymer single crystals.* Polymer *3*, (**1962**), 393–421.

[13] HILL, R., ED. *Fibers from synthetic polymers.* Elsevier Publishing Company, Amsterdam, **1953**.

[14] MAXFIELD, J. AND MANDELKERN, L. *Crystallinity, Supermolecular Structure, and Thermodynamic Properties of Linear Polyethylene Fractions.* Macromolecules *10*, 5 (**1977**), 1141–1153.

[15] MANDELKERN, L., GLOTIN, M., AND BENSON, R.A. *Supermolecular structure and thermodynamic properties of linear and branched polyethylenes under rapid crystallization conditions.* Macromolecules *14*, 1 (**1981**), 22–34.

[16] IUPAC. *Definitions of Terms Relating to Crystalline Polymers.* **1988**.

[17] MANDELKERN, L. *Crystallization of polymers. Kinetics and mechanisms.* Cambridge University Press, Cambridge, **2004**.

[18] FUJII, K. *Stereochemistry of poly(vinyl alcohol).* Journal of Polymer Science: Macromolecular Reviews *5*, 1 (**1971**), 431–540.

[19] BUNN, C.W. *Crystal structure of Polyvinyl Alcohol.* Nature *161*, (**1948**), 929–930.

[20] PEPPAS, N.A. *Turbidimetric studies of aqueous poly(vinyl alcohol) solutions.* Die Makromolekulare Chemie *176*, 11 (**1975**), 3433–3440.

[21] DANNO, A. *Gel Formation of Aqueous Solution of Polyvinyl Alcohol Irradiated by Gamma Rays from Cobalt-60.* Journal of the Physical Society of Japan *13*, 7 (**1958**), 722–727.

[22] PEPPAS, N.A. AND MERRILL, E.W. *Differential scanning calorimetry of crystallized PVA hydrogels.* Journal of Applied Polymer Science *20*, (**1976**), 1457–

1465.

[23] PEPPAS, N.A. AND MERRILL, E.W. *Development of semicrystalline poly(vinyl alcohol) hydrogels for biomedical applications.* Journal of Biomedical Materials Research *11*, 3 (**1977**), 423–434.

[24] SONE, Y., HIRABAYASHI, K., AND SAKURADA, I. *Variation in the degree of swelling in water and hot water resistance of gel by aging.* Kobunshi Kagaku Chem High Polym *10*, (**1953**), 1–7.

[25] PEPPAS, N.A. *Crystallization of polyvinyl alcohol-water films by slow dehydration.* European Polymer Journal *12*, 8 (**1976**), 495–498.

[26] PEPPAS, N.A. AND TENNENHOUSE, D. *Semicrystalline poly (vinyl alcohol) films and their blends with poly (acrylic acid) and poly (ethylene glycol) for drug delivery applications. 14*, 4 (**2004**), 291–297.

[27] OTSUKA, E. AND SUZUKI, A. *A simple method to obtain a swollen PVA gel crosslinked by hydrogen bonds.* Journal of Applied Polymer Science *114*, 1 (**2009**), 10–16.

[28] SPERANDIO, J. AND WARD, J.B. *Cosmetic Application of PVA.* Journal of the Society of Cosmetic Chemists *15*, (**1964**), 327–335.

[29] KADAJJI, V.G. AND BETAGERI, G. V. *Water Soluble Polymers for Pharmaceutical Applications.* Polymers *3*, 4 (**2011**), 1972–2009.

[30] GANGADHARAN, B. AND HAYWARD, M. *Skin cleanser. EP 0 609 2*, **1994**.

[31] CRIMI, R. AND COZZI, R. *Vynil mask with peel-off effect for topical use containing high concentrations of retinoic acid. US2013/001*, **2013**.

[32] GHOSHAL, S., DENNER, P., STAPF, S., AND MATTEA, C. *Study of the formation of poly(vinyl alcohol) films.* Macromolecules *45*, (**2012**), 1913–1923.

[33] FELTON, L. A. *Mechanisms of polymeric film formation.* International Journal of Pharmaceutics *457*, 2 (**2013**), 423–427.

[34] BANKER, G.S. *Film coating. Theory and practice.* Journal of Pharmaceutical Science *55*, 1 (**1996**).

[35] FINCH, C.A. *Chemistry and technology of water-soluble polymers.* Springer Science + Business Media, **1985**.

[36] WONG, S., ALTINKAYA, S.A., AND MALLAPRAGADA, S.K. *Understanding the effect of skin formation on the removal of solvents from semicrystalline polymers.* Journal of Polymer Science Part B: Polymer Physics *43*, (**2005**), 3191–3204.

[37] NGUI, M.O. AND MALLAPRAGADA, S.K. *Quantitative analysis of crystallization and skin formation during isothermal solvent removal from semicrystalline polymers. 40*, (**1999**), 5393–5400.

[38] NGUI, M.O. AND MALLAPRAGADA, S.K. *Mechanistic investigation of drying regimes during solvent removal from poly(vinyl alcohol) films.* Journal of Applied Polymer Science *72*, 14 (**1999**), 1913–1920.

[39] NGUI, M.O. AND MALLAPRAGADA, S.K. *Understanding isothermal semicrystalline polymer drying: mathematical models and experimental characterization.* Journal of Polymer Science *36*, (**1998**), 2771–2780.

[40] O'REILLY BERINGHS, A., ROSA, J.M., STULZER, H.K., AND BUDAL, R.M. *Green clay and aloe vera peel-off facial masks: response surface methodology applied to the formulation design.* AAPS PharmSciTech *14*, 1 (**2013**), 445–455.

[41] LAMANNA, R. AND CANNISTRARO, S. *Effect of ethanol addition upon the structure and the cooperativity of the water H bond network.* Chemical Physics *213*, 1–3 (**1996**), 95–110.

[42] LI, R., D'AGOSTINO, C., MCGREGOR, J., MANTLE, M.D., ZEITLER, J.A., AND GLADDEN, L.F. *Mesoscopic structuring and dynamics of alcohol/water solutions probed by terahertz time-domain spectroscopy and pulsed field gradient nuclear magnetic resonance.* Journal of Physical Chemistry B *118*, 34 (**2014**), 10156–10166.

[43] WYPYCH, G., ED. *Handbook of plasticizers.* William Andrew Publishing, Toronto, New York, **2004**.

[44] FOX, T.G. AND FLORY, P.J. *Second-order transition temperatures and related properties of polystyrene.* Journal of Applied Physics *21*, 6 (**1950**).

[45] SEARS, J.K. AND DARBY, J.R. *The technology of plasticizers.* Journal of Polymer Science: Polymer Letters Edition *20*, 8 (**1982**), 459.

[46] UEBERRETER, K. AND KANIG, G. *Die Kettenlängenabhängigkeit des Wolumens, deS Ausdehnungs-Koeffizienten und der Einfriertemperatur von fraktionierten Polystyrolen.* Naturforsch *6a*, (**1951**), 551.

[47] WOOD, L.A. *Glass transition temperatures of copolymers.* Journal of Polymer Science *28*, 117 (**1958**), 319–330.

[48] GORDON, M. AND TAYLOR, J.S. *Ideal copolymers and the second-order transitions of synthetic rubbers. i. non-crystalline copolymers.* Journal of Applied Chemistry *2*, 9 (**1952**), 493–500.

[49] KELLEY, F.N. AND BUECHE, F. *Viscosity and glass temperature relations for polymer-diluent systems.* Journal of Polymer Science *50*, 154 (**1961**), 549–556.

[50] DI MARZIO, E.A. AND GIBBS, J.H. *Molecular interpretation of glass temperature depression by plasticizers.* Journal of Polymer Science Part A: General Papers *1*, 4 (**1963**), 1417–1428.

[51] MAURITZ, K.A. AND STOREY, R.F. *A general free volume based theory for the*

diffusion of large molecules in amorphous polymers above Tg. 2. Molecular shape dependence. Macromolecules *23*, 7 (**1990**), 2033–2038.

[52] HILDEBRAND, J.H. AND SCOTT, R.L. *The solubility of nonelectrolytes.* Reinhold Pub. Corp., New York, **1950**.

[53] WU, W., TIAN, H., AND XIANG, A. *Influence of Polyol Plasticizers on the Properties of Polyvinyl Alcohol Films Fabricated by Melt Processing.* Journal of Polymers and the Environment *20*, 1 (**2012**), 63–69.

Chapter 4

Transition metal ions complexation

4.1 Introduction

In chemistry, a coordination complex or metal complex consists of a central atom or ion, which is usually metallic and is called the coordination center, and a surrounding array of bound molecules or ions, known as ligands or complexing agents. Many metal-containing compounds, especially those of transition metals, are coordination complexes. Chelation describes a particular way that ions and molecules bind metal ions, involving the formation of two or more separate coordinate bonds between a polydentate (multiple bonded) ligand and a single central atom. Chelation is useful in applications such as providing nutritional supplements, in chelation therapy to remove toxic metals from the body, as contrast agents in MRI scanning, in manufacturing using homogeneous catalysts, and in fertilizers.

In the field of Cultural Heritage, chelating agents are frequently used for the removal of salts (efflorescences, corrosion and oxidation layers) from carbonatic or metallic substrates, as mentioned in Chapter 1 (section 1.4.2). Their mechanism of chemical action involves the dissociation of the molecule through the complexation a selected ion (*i.e.* Cu(II)).

In this chapter some theoretical background over complexation chemistry will be provided, in particular for Cu(II) complexing agents. Moreover, the stability constant will be described, since it is a useful parameter for the choice of an effective sequestering agent, as though the right pH working conditions. An overview over different categories of chelating agents will be also provided, starting from the most

used ones in the restoration filed, such as EDTA and Rochelle salt, up to macrocycles ligands (DOTA) and polyethyleneamines (TETA, TEPA, PEHA).

4.2 The complexation process

A coordination complex consists of a donor species with, at least, a pair of electrons available for a covalent coordination bond with an acceptor ion or atom. The donor species is also called 'ligand' and it behaves like a Lewis base, while the acceptor, a Lewis acid, is usually a positive ion. In particular, the ability of accept electron pairs from molecules or ions, is a typical feature of transition metals (Cu, Fe, Zn, etc.). The complex formed, between the donor and the acceptor, can be i) positive (e.g. Cu(II) and ammine, $Cu(NH_3)_4^{2+}$), ii) neutral (e.g. Cu(II) and glycine, $Cu(NH_2CH_2COO)_2$) or iii) negative (e.g. Cu(II) and chloride ion, $CuCl_4^{2-}$), depending on the nature of the ligand. The maximum number of covalent bonds that a cation tends to form with an electron donor is called 'coordination number'. A ligand with a single donor group is termed as 'monodentante' (e.g. H_2O and NH_3), whereas when two groups are available as 'bidentate'(e.g. ethylendiamine) and so on with the tri-, tetra-, penta-, hexadentate (e.g. EDTA), etc. [1].

A 'chelate' is a particular kind of coordination compound, formed "*when a metal ion coordinates with two or more non-adjacent donor groups of a single ligand to form a five- or six-membered heterocyclic ring*" [1]. The 'chelate effect' asserts that complexes of bidentate or polydentate ligands are more stable in respect to those of monodentate ligands with similar force (or similar donor atoms). It was originally explained by Schwarzenbach [2], who hypnotized that once the first donor atom had attached itself to the metal ion, the other donors can move only in a restricted volume. In this way the entropy of the subsequent donor atoms is greatly reduced in respect to the same for unidentate ligands. A similar but simpler approach to the chelate effect was proposed by Adamson [3], for which a complete literature is available [4].

The result of the chelate effect is that multidentate ligands, such as the polyamines in Fig. 4.1, form thermodynamically more stable complexes than analogous complexes containing unidentate ligands, as showed by the increasing value of the formation constat (see next section for its significance).

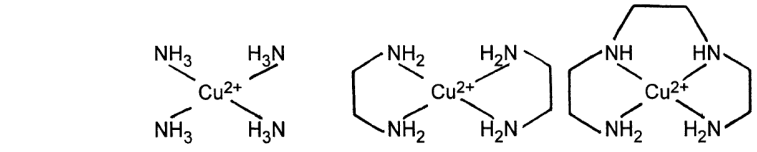

ligand:	ammonia	ethylenediamine	triethylenetetramine.
Denticity:	1	2	4
	$\log \beta_4 = 13.0$	$\log \beta_2 = 19.6$	$\log K_1 = 20.1$

Figure 4.1 Formation constants of complexes of copper(II) with nitrogen donor ligands of differing denticity [4].

Another important type of complex is formed between metal ions and cyclic organic compounds, known as 'macrocycles'. These molecules contain rings of nine or more atoms, such as crown ethers (Fig. 4.2), and include at least three heteroatoms as potential donors, usually oxygen, nitrogen or sulfur. The 'macrocyclic effect' is a specific case of the 'chelate effect', asserting that complexes of macrocyclic ligands are more stable in respect to those of linear polydentate ligands with similar force (or similar donor atoms). The same is for multicycle macrocycles, or cryptand (Fig. 4.2), where the 'cryptand effect' is even stronger.

The donor atoms of a macrocycle are arranged in more fixed positions, thus entailing a lower entropic effect of the macrocyclic binding energy as compared to monodentate, bidentate ligands or their open-chain analogues, with the same number of donor atoms. Some macrocyclic compounds form three-dimensional cavities that can just accommodate appropriately sized metal ions, such as cryptands. Selectivity occurs to a large extent because of the size and shape of the cycle or cavity in relation to that of the metal ion, although also the nature of the heteroatoms, their

electron densities, the compatibility of the donor atoms with the metal ion, and several other factors also play important roles.

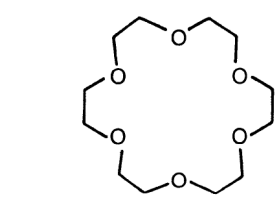

Crown ether

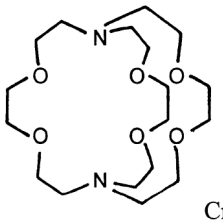

Cryptand

Figure 4.2 Examples of crown ether and cryptand molecules [4].

4.2.1 Complexation equilibria and stability constant

The formation of a complex (*ML*) in solution involves the reaction between a metal ion (*M*) and a ligand (*L*), omitting the charges for simplicity:

$$M + L \rightleftharpoons ML \qquad \beta_1 = \frac{[ML]}{[M][L]} = k_1 \qquad \text{(Eq. 4.1)}$$

which often is the result of stepwise reactions, each one associated to a stepwise equilibrium constant (*k*), which products constitute the overall 'formation' or 'stability constant' (β) [1]:

$$M + 2L \rightleftharpoons ML_2 \qquad \beta_2 = \frac{[ML_2]}{[M][L]^2} = k_1 k_2 \qquad \text{(Eq. 4.2)}$$

$$M + 3L \rightleftharpoons ML_3 \qquad \beta_3 = \frac{[ML_3]}{[M][L]^3} = k_1 k_2 k_3 \qquad \text{(Eq. 4.3)}$$

$$M + \mathrm{n}L \rightleftharpoons ML_\mathrm{n} \qquad \beta_\mathrm{n} = \frac{[ML_\mathrm{n}]}{[M][L]^\mathrm{n}} = k_1 k_2 \ldots k_\mathrm{n} \qquad \text{(Eq. 4.4)}$$

The values associated to the formation constant, generally expressed as logarithmic value *Log* β, represents an index of the relative species concentration at equilibrium in a determinate medium, at controlled conditions (ionic strength, temperature). Therefore high value of this constant indicates a strong tendency to the formation of the metal-ligand chelate, thus *Log* β can be used to predict the selectivity of the chelation reaction when more than one metal is present.

The chelate effect can be pictured by comparing the stability constant of a chelating ligand with a monodentate one, with a similar donor power. For example, considering the equilibria in aqueous solution between copper(II)/ethylenediamine (*en*) and methylamine (*me*):

$$Cu^{2+} + en \rightleftharpoons [Cu(en)]^{2+} \quad \text{(Eq. 4.5)}$$

$$Cu^{2+} + 2me \rightleftharpoons [Cu(me)_2]^{2+} \quad \text{(Eq. 4.6)}$$

Ethylenediamine (Fig. 4.3) is a bidentate ligand and it forms a five-membered chelate complex with the copper ion, while two molecules of the monodentate methylamine (Fig. 4.3) assure similar enthalpy of formation of Cu-N bonds in the two reactions. Under conditions of equal copper concentrations and when then concentration of methylamine is twice the concentration of ethylenediamine, the concentration of the complex Eq. 4.5 will be greater than the concentration of the complex Eq. 4.6. The effect increases with the number of chelate rings so the concentration of the EDTA complex, which has six chelate rings, is much higher than a corresponding complex with two monodentate nitrogen donor ligands and four monodentate carboxylate ligands. Thus, the phenomenon of the chelate effect is empirically explained. The thermodynamic approach to explaining the chelate effect considers the equilibrium constant for the reaction: the larger the equilibrium constant, the higher the concentration of the complex. In fact $K_\beta en >> K_\beta me$, because of entropic and steric effect, solvation changes and ring formation.

The chelate effect increases as the number of chelate rings increases, where the number of chelate rings is one less than the number of donor atoms in the ligand. For example the complex $[Ni(dien)_2)]^{2+}$ is more stable than the complex $[Ni(en)_3)]^{2+}$; both complexes are octahedral with six nitrogen atoms around the nickel ion, but *dien* (diethylenetriamine, Fig. 4.3) is a tridentate ligand while *en* is bidentate. EDTA (ethylenediaminetetracetic acid) has six donor atoms so it forms very strong complexes with five chelate rings. 5-membered and 6-membered chelate rings give the most stable complexes; 4-membered rings are subject to internal strain because of the small inter-bond angle is the ring; the chelate effect is also re-

duced with 7- and 8- membered rings, because the larger rings are less rigid, so less entropy is lost in forming them.

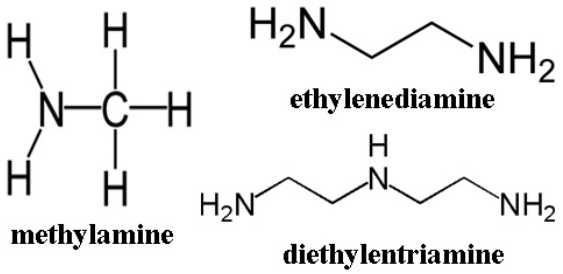

Figure 4.3 Amines with different chelating effects.

The macrocyclic effect can be interpreted as both an enthalpic and an entropic effect [5]. An empirical explanation concerns, for example, the higher stability contants of the complex of copper(II) with the macrocyclic ligand cyclam (1,4,8,11-tetra-azacyclotetradecane) in comparison to the stability of the complex with the corresponding open-chain amine. An important difference between macrocyclic ligands and open-chain (chelating) ligands is that they have selectivity for metal ions, based on the size of the cavity into which the metal ion is inserted when a complex is formed. For example, the crown ether 18-crown-6 forms much stronger complexes with the potassium ion, K^+ than with the smaller sodium ion, Na^+ [6].

4.2.2 The influence of pH

The stability constant is not the only parameter to consider that affects the complexing ability. Other factors to consider are, for example, the steric effect, the concentration of the protonated species and the pH. In particular, the pH of the medium influences the ionization rate of the functional groups of the chelator and, consequently, its charge and affinity towards the different cations. In fact for each complexing agent a characteristic distribution diagram can be defined (as reported in Fig. 4.4 for EDTA).

A species distribution diagram is a powerful tool for the assessment of the concentrations of the species present as a function of pH, where the curves represent the areas of prevalence of the various species differently protonated as a function of the pH. Therefore, the complexation reaction can be enhanced by the choice of the right working pH, trying to avoid at the same time the risk of hydroxides precipitation.

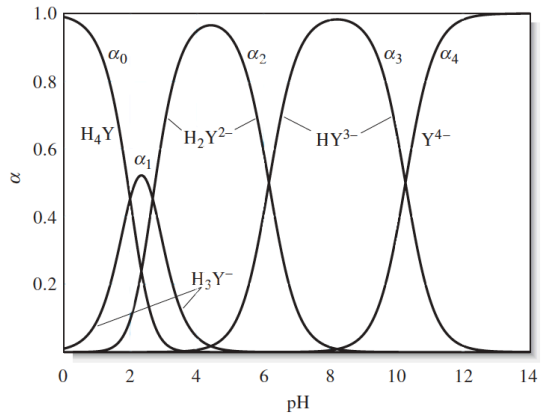

Figure 4.4 Distribution diagram in function of pH for EDTA [1].

The parameter α, reported in the distribution diagrams, represents the fraction of each species present and, for a generic ligand, it is defined as the concentration of the considered fraction (L) over the total concentration of the species (c_L):

$$\alpha_L = \frac{[L]}{c_L} \qquad \text{(Eq. 4.7)}$$

Thus the stability constant can be written, by taking into account the influence of a fixed pH value over the species present, as the 'conditional stability constant' for a generic ligand as:

$$K'_\beta = \alpha_L K_\beta \qquad \text{(Eq. 4.8)}$$

Knowing the formation constants between the ligand and the different metal cations allow the choice of the most suitable and selective complexing agents. The pH is a

further element useful for the evaluation of the best working conditions to enhance the complexing reaction towards a specific metal.

4.3 Copper (II) complexing agents

As already reported in Chapter 1 (section 1.3.2), the most common corrosion products to remove from a copper-based artifact is that of Cu(II), such as copper carbonates, sulphates, chlorides, etc. A selection between the different typologies of complexing agents for Cu(II) must be carefully done, in order to effectively remove the undesired products but respecting at the same time the protective cuprite layer of Cu(I).

A brief overview of some complexing agents, belonging to different categories, commonly used for Cu(II) are listed below.

4.3.1 EDTA

Ethylenediaminetetraacetic acid (EDTA) is a compound that forms strong 1:1 hexadentate complexes with most metal ions and finds a wide use in quantitative analysis (titrations). EDTA it's a tetraprotic acid containing four carboxylic groups (-COOH), which can be neutralized with a base, for example with sodium hydroxide (NaOH), forming water-soluble salts (mono-, bi-, tri- or tetra-sodium EDTA). Disodium salt of EDTA is also frequently used in the field of restoration, as the tetrasodic is less soluble in water and more harmful.

EDTA is a remarkable reagent, not only because it is able to forms chelates with all cations, but also because most of these chelates are very stable. This great stability undoubtedly results from the several complexing sites within the molecule that give rise to a cage-like structure in which the cation is effectively surrounded and isolated from solvent molecules. The structural formula of EDTA and of a generic metal/EDTA complex is shown in Fig. 4.4.

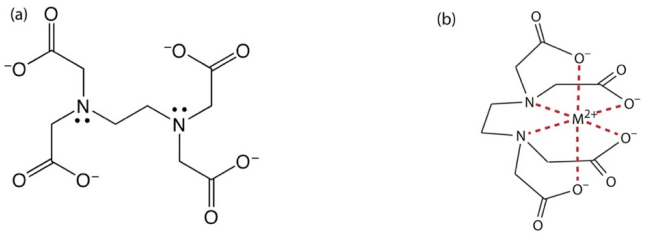

Figure 4.5 (a) Structural formula of EDTA and (b) a generic EDTA/metal complex structure.

The formation constants of EDTA toward various metal species (logK_β = 18.8 for Cu^{2+}), reported in Tab. 4.1 [7,8], are referred to the Y^{4-} species, *i.e.* the fully deprotonated form:

$$M^{n+} + Y^{4-} \rightleftharpoons MY^{(n-4)+} \qquad K_\beta = \frac{[MY^{(n-4)+}]}{[M^{n+}][Y^{4-}]} \qquad \text{(Eq. 4.9)}$$

Ion	log K_β	Ion	log K_β	Ion	log K_β
Li^+	2.95	V^{3+}	25.9[a]	Tl^{3+}	35.3
Na^+	1.86	Cr^{3+}	23.4[a]	Bi^{3+}	27.8[a]
K^+	0.8	Mn^{3+}	25.2	Ce^{3+}	15.93
Be^{2+}	9.7	Fe^{3+}	25.1	Pr^{3+}	16.30
Mg^{2+}	8.79	Co^{3+}	41.4	Nd^{3+}	16.51
Ca^{2+}	10.65	Zr^{4+}	29.3	Pm^{3+}	16.9
Sr^{2+}	8.72	Hf^{4+}	29.5	Sm^{3+}	17.06
Ba^{2+}	7.88	VO^{2+}	18.7	Eu^{3+}	17.25
Ra^{2+}	7.4	VO_2^+	15.5	Gd^{3+}	17.35
Sc^{3+}	23.1[a]	Ag^+	7.20	Tb^{3+}	17.87
Y^{3+}	18.08	Tl^+	6.41	Dy^{3+}	18.30
La^{3+}	15.36	Pd^{2+}	25.6[a]	Ho^{3+}	18.56
V^{2+}	12.7[a]	Zn^{2+}	16.5	Er^{3+}	18.89
Cr^{2+}	13.6[a]	Cd^{2+}	16.5	Tm^{3+}	19.32
Mn^{2+}	13.89	Hg^{2+}	21.5	Yb^{3+}	19.49
Fe^{2+}	14.30	Sn^{2+}	18.3[b]	Lu^{3+}	19.74
Co^{2+}	16.45	Pb^{2+}	18.0	Th^{4+}	23.2
Ni^{2+}	18.4	Al^{3+}	16.4	U^{4+}	25.7
Cu^{2+}	18.78	Ga^{3+}	21.7		
Ti^{3+}	21.3	In^{3+}	24.9		

Table 4.1 Formation constants for metal/EDTA complexes. Values in table apply at 25 °C and ionic strength 0.1 M unless otherwise indicated. a) 20 °C, ionic strength 0.1 M b) 20 °C, ionic strength 1 M [9].

The complexation efficiency of EDTA is strongly affected by the pH, as the most reactive is the fully deprotonated form Y^{4-}. Therefore in strongly basic solution, the hydrogens are removed by reaction with hydroxide ion. In more acidic solutions, metal ions must be able to displace the hydrogens if a complex is to be formed. Since metal ions differ significantly in their ability to displace the hydrogens, the solution acidity can be used to 'regulate' the reactivity of EDTA toward metal ions. Thus the choice of the best pH working interval is of paramount importance to control the strength and stability of the EDTA complexes. This information can be obtained from the distribution diagram of α in function of the pH as reported in Fig. 4.3. The parameter α can be calculate for all the different species that EDTA forms in solution, in particular for Y^{4-} as:

$$\alpha_4 = \frac{Y^{4-}}{c_T} \qquad \text{(Eq. 4.10)}$$

where c_T is the total molar concentration of uncomplexed EDTA:

$$c_T = [Y^{4-}] + [HY^{3-}] + [H_2Y^{2-}] + [H_3Y^{3-}] + [H_4Y] \qquad \text{(Eq. 4.11)}$$

In Tab. 4.2 the values of α_4 for EDTA at 20 ºC and ionic strength of 0.1 M are reported. Therefore the conditional formation constant can be calculated for the selected pH.

pH	$\alpha_{Y^{4-}}$
0	1.3×10^{-23}
1	1.4×10^{-18}
2	2.6×10^{-14}
3	2.1×10^{-11}
4	3.0×10^{-9}
5	2.9×10^{-7}
6	1.8×10^{-5}
7	3.8×10^{-4}
8	4.2×10^{-3}
9	0.041
10	0.30
11	0.81
12	0.98
13	1.00
14	1.00

Table 4.2 Values of $\alpha_{Y^{4-}}$ for EDTA at 20 °C and 0.1M [9].

4.3.2 Rochelle salt

The potassium sodium tartrate is a double salt known also as Rochelle salt, commonly used in restoration practice as complexing agent for Cu(II), with the structural formula showed in Fig. 4.6. Since it is a bidentate ligand, it presents a lower formation constant ($\log K_\beta = 3.3$ for Cu^{2+} [10]) in respect to EDTA, even if the complex is formed by two molecules chelating the cation with an overall $\log K_\beta = 5.7$ [10]. In fact it exerts a weaker and milder action towards Cu(II), thus providing better control over the removal of undesired products and respecting the cuprite layer. The bland action ensured by this complexing agent makes it suitable, in particular, for the cleaning of gilded bronzes, when it is necessary to preserve the original gold leaf, simultaneously removing the surface deposits of copper salts, as already mentioned in Chapter 1 (section 1.4) for the Ghiberti's 'Porta del Paradiso' [11–13]. Thanks to its weak action and to its great solubility in water, it can be used at high concentrations, up to 35-40% w/w (or at lower concentration at higher pH).

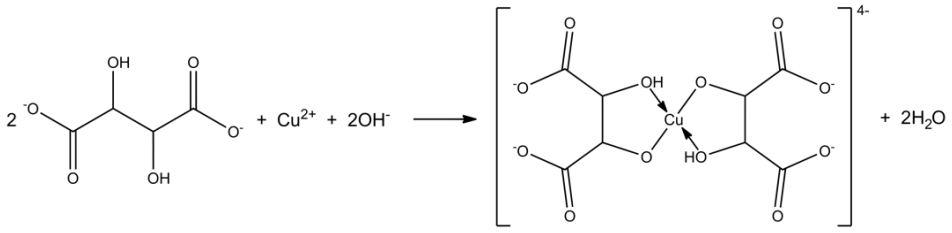

Figure 4.6 Structural formula of the Rochelle salt and its bidentate complex with copper.

4.3.3 Glycine

Glycine is a the simplest amino acid and, when dissolved in water, it undergoes an internal acid/base reaction to produce a zwitterion, *i.e.* a species that has both a positive and a negative charge as showed in Fig. 4.7. Therefore there are two atoms capable of donating a pair of electrons (the N of the amine group and an O of the carboxylic acid group), thus simultaneously forming two bonds with Cu(II) cation (bidentate ligand). The glycine/copper(II) exists both in the *cis* (donor atoms on the

same side of the copper) and *trans* (donor atoms on opposite sides) form, as showed in Fig. 4.8 (a), where the amino acid acts as a chelating ligand and results in the formation of a deep blue colored $Cu(gly)_2$ complex (Fig. 4.8 (b)), with a stability constant $\log K_\beta = 15.2$ [8].

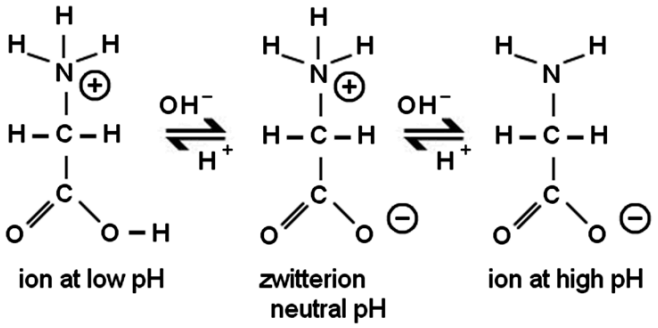

Figure 4.7 Zwitterionic form of glycine compared with its ionic form.

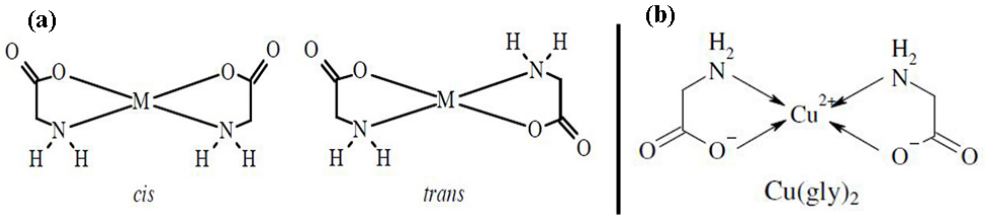

Figure 4.8 Structural formula of the glycinate complexes isomers with a generic metallic cationis reported in (a), while the *cis*-Bis(glycinato)copper(II) complex is showed in (b).

There are no evidences in literature concerning the use of glycine as complexing agent for the chemical removal of corrosion products from copper-based artifacts.

4.3.4 Macrocycles

Macrocyclic chelators can form very stable complexes with transition metals, with high formation constant for Cu(II) ions. Thanks to the macrocyclic effect, reported in section 4.2, the formed complex are very strong and stable.

Macrocyclic ligands have traditionally been divided into two classes, those with oxygen donors, such as the crown ethers and cryptands, and the nitrogen donor macrocycles [4]. In particular, the nitrogen donor macrocycles form very stable complexes with transition and post-transition metal ions. Examples of cyclic polyamines, able to form strong complexes with Cu(II), are the Cyclen (1,4,7,10-tetraazacyclododecane, logK_β = 23.3 [4]) with the structure reported in Fig. 4.9 and its very similar derivative DOTA with pendant donor group (1,4,7,10-tetraazacyclododecane-1,4,7,10-tetraacetic acid, logK_β = 22.7 [4]). The selectivity of the Cyclen toward Cu(II) is mainly due to the size of the metal ion, suitable for the macrocyclic cavity of the ligand while its ionic radium is little smaller for the DOTA cavity.

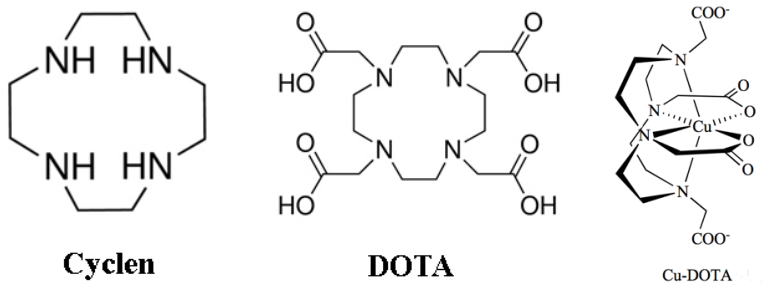

Figure 4.9 Structure of the macrocycle Cyclam and of its derivative DOTA with pendant donor groups. The Cu(II)-DOTA complex is also showed.

4.3.5 Polyamines

A polyamine is an organic compound having two or more primary amino groups - NH_2 as cations which can act as donors towards metal ions. In particular, polyethyleneamines refer to a series of polyamines in which the molecule is made up of primary, secondary or tertiary amino groups connected through ethylene groups, thus forming linear, cyclic or branched structures. These molecules are widely used as chelators in the medicine field, as triethylenetetramine (TETA) to treat the Wilson disease by complexing Cu(II) [14]. Some structural formulas of linear polyethyleneamines are reported in Fig. 4.10, TETA (logK_β = 20.1), tetraethylenepentamine

(TEPA, logK_β = 22.8) and pentaethylenehexamine (PEHA, logK_β = 26.2), with increasing number of ethylene and amino groups.

Copper(II) ions tend to form more stable complexes with nitrogen than with oxygen, thus polyethyleneamines can form very stable chelates. For example TETA has four nitrogen groups, thus fitting the square-planar geometry in which Cu(II) is most stable (Fig. 4.11); therefore, it binds Cu(II) very tightly. As the chain length and the number of amino groups increase also the stability of the resulting complex increase, because of the higher number of potential bonds. However steric effects may hinder the stability of more than six-membered chelate rings, because they cannot be joined together about a square planar or octahedral metal ion without causing a high level of steric strain [4].

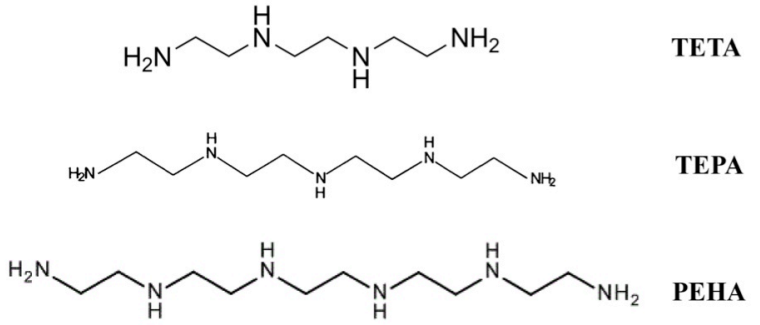

Figure 4.10 Structural formula of some linear polyethyleneamines with progressive number of amino and ethylene groups, triethylenetetramine TETA), tetraethylenepentamine (TEPA) and pentaethylenehexamine (PEHA).

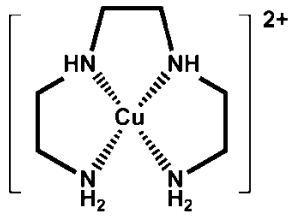

Figure 4.11 Cu(II)-TETA tetradentate complex.

A summary of the stability constants for the complexing agents mentioned in this chapter and belonging to different chemical categories, is reported in Tab. 4.3.

Ligand	Reaction	Log$K\beta$
EDTA	$Cu^{2+} + L^{4-} = CuL^{2-}$	18.8 [8]
Rochelle salt	$Cu^{2+} + L^{2-} = CuL$	3.3 [10]
	$Cu^{2+} + 2L^{2-} = CuL_2^{2-}$	5.7 [10]
Glycine	$Cu^{2+} + L^{-} = CuL^{+}$	8.1 [8]
	$Cu^{2+} + 2L^{-} = CuL_2$	15.0 [8]
DOTA	ML/M·L	22.2 [8]
TETA	ML/M·L	20.1 [15]
TEPA	ML/M·L	22.8 [15]
PEHA	ML/M·L	26.2 [16]

Table 4.3 Summary of the stability constants, at 0.1M e 25 °C, of the chelating agents mentioned in this chapter.

4.4 Bibliography

[1] SKOOG, W. *Fundamentals of Analytical Chemistry.* F.J. Holler, S.R. Crouch, **2013**.

[2] SCHWARZENBACH, G. *Der Chelateffekt.* Helvetica Chimica Acta *35*, 7 (**1952**), 2344–2359.

[3] ADAMSON, A.W. *A Proposed Approach to the Chelate Effect.* Journal of the American Chemical Society *76*, 6 (**1954**), 1578–1579.

[4] MARTELL, A.E. AND HANCOCK, R.D. *Metal complexes in aqueous solutions.* Springer Science + Business Media, **1996**.

[5] LINDOY, L.F., ED. *The chemistry of macrocyclic ligand complexes.* Cambridge University Press, Cambridge, **1989**.

[6] PEDERSEN, C.J. *Cyclic polyethers and their complexes with metal salts.* Journal of the American Chemical Society *89*, 26 (**1967**), 7017–7036.

[7] MARTELL, A.E. AND SMITH, R.M. *Critical stability constants. First supplement.* Springer Science + Business Media, New York, **1977**.

[8] MARTELL, A.E. AND SMITH, R.M. *Critical stability constants. Second supplement.* Springer Science + Business Media, New York, **1989**.

[9] HARRIS, D.C. *Quantitative Chemical Analysis.* W.H. Freeman and Company, China Lake, **2007**.

[10] SILLÉN, L.G. AND MARTELL, A.E. *Stability constants of metal-ion complexes. Special Publications n. 17 and 25.* .

[11] FIORENTINO, P., MARABELLI, M., MATTEINI, M., AND MOLES, A. *The condition of the 'Door of Paradise' by L. Ghiberti. Tests and proposals for cleaning.* Studies in Conservation *27*, (**1982**), 145–153.

[12] FERRETTI, M. AND SIANO, S. *The gilded bronze panels of the Porta del Paradiso by Lorenzo Ghiberti: non-destructive analyses using X-ray fluorescence.* Applied Physics A *90*, 1 (**2007**), 97–100.

[13] MATTEINI, M., LALLI, C., TOSINI, I., GIUSTI, A., AND SIANO, S. *Laser and chemical cleaning tests for the conservation of the Porta del Paradiso by Lorenzo Ghiberti.* Journal of Cultural Heritage *4*, (**2003**), 147–151.

[14] LU, J. *Triethylenetetramine pharmacology and its clinical applications.* Molecular cancer therapeutics *9*, 9 (**2010**), 2458–2467.

[15] SMITH, R.M. AND MARTELL, A.E. *Critical stability constant. Amines Vol.2.* Springer Science + Business Media, **1976**.

[16] MARTELL, A.E. AND CALVIN, M. *Chemistry of the Metal Chelate Compounds.* Soil Science *74*, 5 (**1952**).

PART II

Experimental

Chapter 5

Preparation of the polymeric systems

5.1 Introduction

The topic about the cleaning methods traditionally used for metal artifacts has already been treated in Chapter 1 (section 1.4). Basically both mechanical and chemical methods present advantages and drawbacks, so they are often used in combination (e.g. laser ablation and chemical cleaning with chelating agents).

During this PhD project a system able to perform both a chemical and a mechanical action, specifically tailored for the cleaning of Cu-based artifacts, has been developed. In particular the 'peeling' of a polymeric film from the surface assures a certain mechanical action, while the presence of a chelating agent specific for Cu(II), carries out the chemical action.

The development of such a system required primarily the selection of a suitable film forming polymer (PVA), then of opportune additives able to modify the polymeric dispersion depending on the desired final properties (high volatile molecules and plasticizers). Thus different formulations were prepared to find the best composition that fulfills the desired requirements in terms of applicability and mechanical properties.

The design of this innovative confining system was completed by the selection of suitable complexing agents to load into the polymer matrix. They had to be specific for Cu(II), the main species of the corrosion products related to Cu-based artifacts, and able to entrap these cupric ions as effectively as possible, thus removing them from the surface. The research of such chelating agents started from commonly

used products in the restoration field (e.g. EDTA and Rochelle salt), and was then carried on with the selection of more effective complexing agents, belonging to the class of macrocycles or polyethyleneamines, by using as selective criterion their stability constant with Cu(II).

Several formulations were prepared by varying the relative amount and the typology of each component, in order to find the best equilibrium between them. Finally three different polymeric formulations were selected as the most suitable to be loaded with the complexing agent and to be used for applicative tests.

5.2 Design of film forming systems for cleaning of metallic substrates

The design of a new polymeric system with suitable properties for the cleaning of metal surfaces has started by taking into account the general characteristics required for a confining system, reported in Chapter 2 (section 2.2).

The leading idea has been inspired by cosmetic facial masks for the removal of skin impurities by a 'peeling' action [1–9]. These exfoliator products assure a scrub action that cleanses the pores and removes dead cells from skin, thanks to the stripping of the polymeric film from the surface. The presence of both adhesive and cohesive forces assures, on one hand the removal of the impurities from skin, on the other the removal of the final film without breakages. The principle of applying something with a fluid initial consistency on the surface, waiting for its dehydratation, to finally remove the formed film in only one piece, has been opportunely modified to fit different requirements and application purposes.

A system able to modify its consistency from initial fluidity towards the formation of an elastic film easily removable from the surface, seemed forthwith having good applicative potentialities for cleaning purposes. In fact the initial fluidity assures to perfectly follow any surface morphology, as typical for corroded metallic surfaces while the formation of a film, after dehydration, further assist the cleaning action by exerting a certain mechanical action. The addition of a complexing agent, selective for Cu^{2+} ions, into the polymeric confining system carries out the chemical

action of cleaning by sequestering and entrapping metal ions coming from the corrosion layers. Such a complete cleaning system is thus able to perform both a mechanical and chemical action, representing a good alternative tool for cleaning purposes.

In particular the main requirements considered during the design process of the formulations have been:

- need to apply the system on both horizontal and non-horizontal surfaces;
- modulation of the liquid phase evaporation rate in order to find a compromise between the time required for the chelating reaction with the surface and the time of film formation (not more than four hours for a single application);
- easy and residues-free removal of the final film in a single step, by means of a peeling action;
- effective and controllable cleaning action thanks to the selected ligand.

The final system, designed by following the above-mentioned requirements, consists of a viscous transparent dispersion that can be easily taken and applied with a spatula, a hard brush or a syringe (without the needle) on the surface to be treated, as schematized in Fig. 5.1 (b). The stratigraphic morphology of a common corrosion *patina* is showed in Fig. 5.1 (a): the cuprite layer must be kept during the cleaning procedure, as protective layer from further corrosion phenomena, while the defacing green layers of copper(II) carbonate, sulphates, chlorides has to be removed.

The applied system is able to perfectly follow the roughness and irregularities of the corroded surface thanks to its fluidity, but at the same time spatial control can be attained, by modulating the viscoelastic properties: in this way the applied system maintain its position without flowing in the confining zones, thus permitting a spatially defined action. After complete evaporation of the volatile fraction, a transparent film is formed, which can be easily removed by tweezers through a gentle peeling-off action (Fig. 5.1 (c)). Moreover the specificity of the chosen complexing agents in removing only the selected ions (*i.e.* Cu^{2+}) allows to maintain intact the

cuprite layer (Cu^{+}). The time required by the film to form depends on the composition and thickness of the applied formulation, as well as on the environmental parameters (T, RH%), but it generally takes from one to four hours.

The main advantages related to the use of these polymeric dispersions loaded with a complexing agent, presented in this thesis work, concern enhanced performances in terms of both applicability and efficacy. To summarize, this innovative approach permits to achieve:

- improved chemical control, thanks to the high selectivity of the chelating agent for Cu^{2+} ions and to the gradual action of the cleaning process;
- simultaneous chemical and mechanical action, favored by the presence of a complexing agent and by the gentle peeling of the final film;
- adjustability of the physico-mechanical properties (consistency, adhesiveness, transparency, etc.) to adapt to different substrates (non-horizontal, rough and irregular surfaces);
- vehiculation of more effective complexing agents (macrocycles, polyethyleneamines).

5.2.1 Polymer

Polyvinyl alcohol (PVA) has very good film forming properties, as extensively reported in Chapter 3. For this reason it is widely used in cosmetic industry for peelable masks for skin cleansing. PVA was considered the most sutable film forming base polymer for the development of these systems. However, the ample commercial availability of several products, characterized by different degrees of hydrolysis and molecular weights, required an accurate selection of the most suitable characteristics of the polymer to attain the final desired properties.

On one hand, good water solubility in reasonable times was required, on the other hand, good mechanical properties to avoid breaking of the film or residues left onto the surface were essential for the final peeling action. Different products were used

to prepare formulations able to satisfy the above-mentioned requisites, as reported in Tab. 5.1.

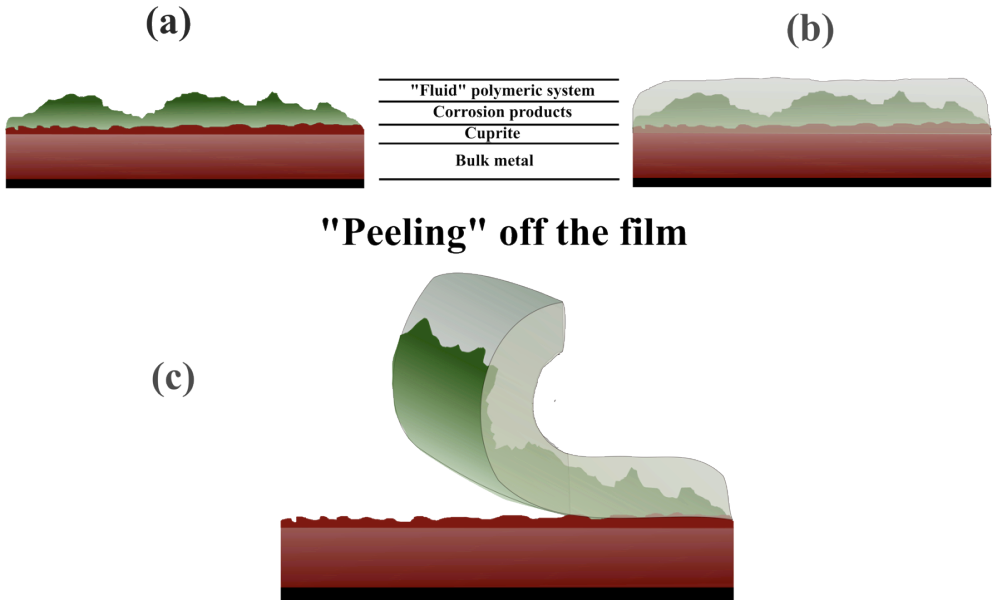

Figure 5.1 Schematic representation of the application and removal of the film forming systems: (a) typical stratigraphic morphology of a corroded copper-based alloy, showing the red layer of cuprite at the metal-corrosion products interface; (b) application of the polymeric dispersion with a fluid consistency able to follow the irregularities of the surface; (c) removal of the film after the evaporation of the volatile content along with the undesired corrosion products, thanks both to the peeling mechanical action and to the chemical action of the chelating agent.

Degree of hydrolysis higher than 87-89%, *i.e.* the fully hydrolyzed form, require very long times for the solubilization process; decreasing the molecular weight favors solubilization but too high concentrations of polymer are necessary to obtain films with the desired properties. At the same time, lower degrees of hydrolysis (80%) allow solubilization also at room temperature, but the low M_w implies the use of a considerable amount of polymer, in respect to the water content. The best results, in terms of solubility of the polymer and mechanical properties of the final film, were obtained by using a partially hydrolyzed polymer (89-89% HD) with intermediate molecular weight (85,000-124,000). In fact partially hydrolyzed polyvi-

nyl alcohol can be solubilized also at room temperature (or more easily at 90 °C), while the lower mechanical properties in respect to the fully hydrolyzed PVA, can be balanced out by the high molecular weight. As highlighted in Tab. 5.1 PVA 87-89% hydrolyzed (M_w 85,000-124,000) at a concentration of 20% w/w was found to show the best performances for the preparation of a film forming solution and was thus selected as the main component, with water, of the formulations.

PVA HD, M_w	% w/w	Comments
99+%, 146,000-186,000	10	- Too long time for solubilization (over 16 hours at 90 °C)
99+%, 89,000-98,000	10	- Too liquid, excess of water content in respect to the polymer
	15	- Too liquid, excess of water content in respect to the polymer
	20	- Polymer excess in respect to water content
98-99%, 146,000-186,000	10	- Long time required for solubilization for both concentrations
	15	- Keeping the polymer in water during night helps the process
87-89%, 85,000-124,000	10	- Good solubilization but the final solution is too liquid and the final film presents poor mechanical properties
	20	- Good solubilization, good initial consistency and mechanical properties of the final film
87-89%, 31,000-50,000	20	- Polymer excess in respect to the water content
80%, 9,000-10,000	20	- Polymer excess in respect to the water content

Table 5.1 Polyvinyl alcohol characteristics (hydrolysis degree HD and molecular weight M_w) and concentration (% w/w) used to prepare different formulations; comments relative to each combination are also reported.

5.2.2 Additives

Once the polymer characteristics were chosen, different formulations were designed by varying the amounts of the additives (volatile fraction and plasticizers) in order to obtain the best performances in terms of ease of application and film formation properties.

5.2.2.1 Ethanol

As reported in Chapter 3 (section 3.5.2) the addition of a component with high vapor pressure influences the evaporation rate of the liquid content (water). In particu-

lar ethanol, commonly used in cosmetic formulations, was suitable for this purpose, acting as drying enhancer thanks to its high volatility [3].

Since the higher the ethanol content the faster the evaporation rate, its amount can be modulated in order to obtain the desired evaporation rate, depending also on the environmental condition: application in condition of low temperature and high relative humidity may require the addition of more ethanol to enhance the evaporation of the liquid fraction. On the other hand too much ethanol would increase the overall liquid content, thus hindering the spatial control or the applicability on non-horizontal surfaces. For these reasons, a compromise between the overall liquid fraction content and the ethanol amount should be achieved.

Concentrations of ethanol between 10% and 20% w/w were tested by keeping the same amount of polymer and plasticizers. A content less than 10% w/w would entail poor effect on the overall evaporation rate, while concentrations above 20% w/w would result in poor evaporation increase and too liquid fraction amount.

Moreover, the addition of ethanol entails also a general water structuring effect, thus improving the final consistency of the polymeric solution, by creating an increase in the order of the 3-D structure of the polymeric network [10].

5.2.2.2 Plasticizers

Different combinations of plasticizer molecules were tested to find the suitable typology and quantity able to satisfy both the initial consistency requirements and, especially, the final properties of the film. Most of these plasticizers are commonly used in the cosmetic field in association with PVA, as reported in [2,11]. In particular the molecules listed below, with structural formula reported in Fig. 5.2, were used in the combinations listed in Tab. 5.2:

- propylene glycol [PG], a non toxic diol which appear as a clear, colorless, viscous and odorless liquid. Widely used in cosmetic industry as humectant and to improve the texture of the product, it is generally used in concentra-

tions lower than 2% w/w [12]. It Is soluble in water, ethanol and glycerol and the boiling point is 188 °C [1];

- dipropylen glycol [DPG], a mixture of three isomeric compounds (2,2'-dihydroxydiisopropropylether, 2,2'-dihydroxydipropylether, 2-hydroxypropyl-2'-hydroxyisopropylether) typically 98% pure. It is a colorless, odorless, liquid, with a boiling point of 222-236 °C, soluble in water and ethanol with low toxicity. It is used in cosmetic industry as humectant, emollient and plasticizer [13];
- 2-methyl-1,3-propanediol [MPD], a non symmetric aliphatic diol with a methyl branch. It appears as a low viscous liquid miscible with alcohols and water. It is used as emulsifier and humectant in personal care products and the boiling point is 212 °C[1];
- glycerol [GLY], a simple polyol compound with three hydroxyl groups responsible for its solubility in water and its hygroscopic nature. It is a clear, colorless, odorless, viscous liquid, miscible with water and ethanol, widely used in cosmetic formulations as lubricant, humectant, plasticizer, solvent and preservative. It has a boiling point of 290 °C and it is non toxic [1];
- polyethylene glycol [PEG], a polyether compound which can present different chain length, from molecular weights of 300 g/mol up to 10,000,000 g/mol. For this reason PEG can be liquid (soluble in water and ethanol, non toxic) or solid depending on the M_w. In particular low-molecular weight PEGs (e.g. 300-400 g/mol) are clear, colorless, viscous, non toxic liquids, soluble in water and ethanol; higher molecular weight PEGs (3,500 and 10,000 g/mol) are white solids in powder form, rather soluble in water (67% and 53% w/w at 20 °C respectively). PEG is used often in combination with glycerin and xanthan gums, as lubricant, plasticizer and stabilizer in cosmetic products [14].

[1] www.chemicalland21.com, consulted on November 2015.

- xanthan gum (polysaccharide) [XAN], a high molecular weight polysaccharide, commonly used as stabilizer and viscosity modifier in cosmetic formulations. It appears in the form of a faint brown powder, easily soluble in water, generally used in the mount of 0.5-1 % w/w. It is also able to give tixotropic properties to the liquid where it is added, thus entailing a sol-gel transition induced by mechanical stress. It is very stable under a wide range of temperature and pH [15];
- polyacrylic acid sodium salt [NaPAA], is an high molecular weight polymer, already described in Chapter 2 (section 2.4). It is mainly used in cosmetic field as emulsifier [1].

The preparation, during the first year of this PhD, of the formulations reported in Tab. 5.2, led to the following considerations:

- the use of NaPAA as principal plasticizer, gave as result turbid and too liquid formulations (86PVA6, 79PVA9 and 71PVA16), also because of the low amount of PVA;
- the use of 6% w/w PG in 78PVA9, gave as result a too liquid formulation, while the other one, 76PVA6, was too viscous and opaque, with lumps diffused in the polymer matrix, probably because of the presence of high molecular weight PEG (10,000);
- the use of high molecular weight PEGs, such as 3,500 and 10,000, requires a further step to solubilize them in water before addition, so the liquid form of lower M_w (300-400) was preferred;
- formulations with PVA amount lower than 20% w/w were too liquid to attain good applicability properties, as already mentioned in section 5.2.1;
- the best performances in terms of both initial consistency (texture) and final film properties were achieved by the combination of four plasticizers (DPG, MPD, GLY and PEG 300-400), all belonging to the polyols class, commonly used to plasticize PVA, as reported in Chapter 3 (section 3.5.3.4) and in ref. [11,16].

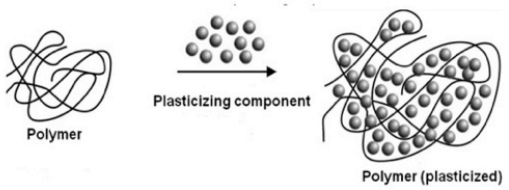

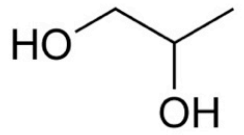

propylene glycol [PG]

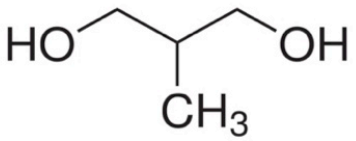

2-methyl-1,3-propanediol [MPD]

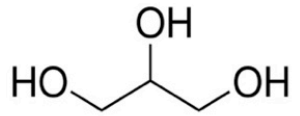

glycerol [GLY]

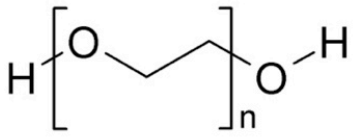

polyethylene glycol [PEG]

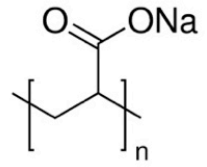

polyacrylic acid [NaPAA]

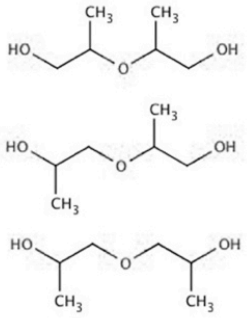

dipropylene glycol [DPG]

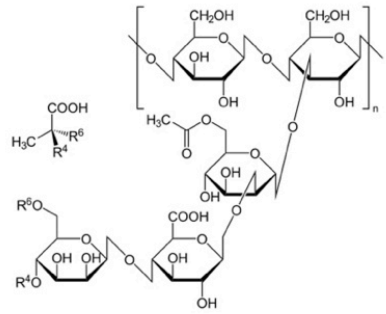

xanthan gum [XAN]

Figure 5.2 Chemical structures of the different plasticizer molecules tested for the preparation of the polymeric systems.

Formulation	**Water**	**Ethanol**	**PVA**	**Plasticizers**			
				DPG	MPD	GLY	PEG
76PVA4	58	18	20	1.5	1.5	0.6	0.4
73PVA7	57	16	20	3	3	0.6	0.4
74PVA6	57	17	20	1.5	1.5	0.6	2.4
72PVA8	56	16	20	3	3	1.2	0.8
70PVA10	55	15	20	3	3	2.5	1.5
72.5PVA7.5	56.5	16	20	1.5	1.5	1.5	3
71PVA9	55	16	20	1.5	1.5	3	3
70.5PVA9.5	55	15.5	20	3	3	2	1.5
68PVA12	54	14	20	3.5	3.5	3	2
80PVA8	70	10	12	1.4	0.6	/	6
80.5PVA4.5	67.5	13	15	1.5	1.5	0.8	0.8
86PVA4	63	23	10	1.5	1.5	0.6	[3,350] 0.4
80.5PVA4.5	67.5	13	15	1.5	1.5	0.8	[3,350] 0.8
72PVA8/bis	56	16	20	3	3	1	[400] 1
				DPG	NaPAA	GLY	PEG
86PVA6	76	10	8	/	3	3	/
79PVA9	67	12	12	/	6	3	/
71PVA16	41	30	13	3	12	0.6	0.4
				PG	XAN	GLY	PEG
78PVA9	58	20	13	6	/	3	/
76PVA6	57.5	18.5	18	3	1	0.6	[10,000] 1.5

Table 5.2 Compositions of different formulations (in % w/w) named as *X*PVA*Y*, where *X* represents the sum of the liquid content (water + ethanol) and *Y* the overall plasticizers amount; the polymer concentration can be obtained by subtraction. Several combinations, by varying the typology and the relative content of the different components (water, ethanol, PVA, plasticizer), are listed.

5.2.3 Application tests on non-horizontal surfaces

One of the principle requirements of these formulation concerns their ability to be applied also on non-horizontal surfaces, as for the majority of metallic surfaces *in situ*. For this reason application tests with selected formulations were carried out on glass slides placed on vertical or sloping stands.

If the selected formulation is applied as a thick layer, it will obviously start to flow towards the bottom, because of the gravity force, as showed in Fig. 5. 3.

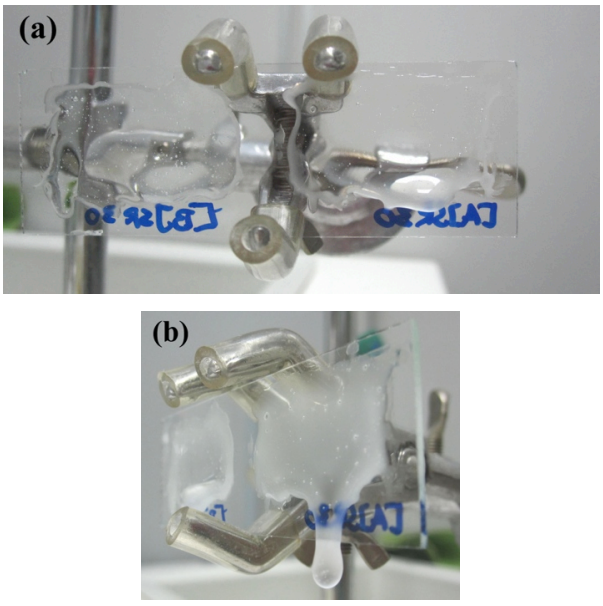

Figure 5.3 Application tests of two different formulations (a): if the layer is too thick (b) it will start to drip because of the gravity force.

The application testes were carried out by applying the same amount of each formulation (0.2 μL) with a syringe, without the needle, followed by a light pressure with the flat part of a spatula; formulations were previously slightly heated in a warm water bath to favor the sample taking with the syringe.

By comparing different formulations with increasing amount of plasticizers, it has been observed that the higher is the plasticizer content, the higher is the initial viscosity and, thus, the resistance against gravity. For example by comparing the formulations 73PVA7, 72PVA8 and 70PVA10, corresponding to [B], [D] and [E] respectively, the application properties of [D] and [E] were very similar, while [B], with lower plasticizer content and higher amount of liquid fraction, presented minor resistance over gravity force, thus tending to agglomerate to the bottom, as showed in Fig. 5.4.

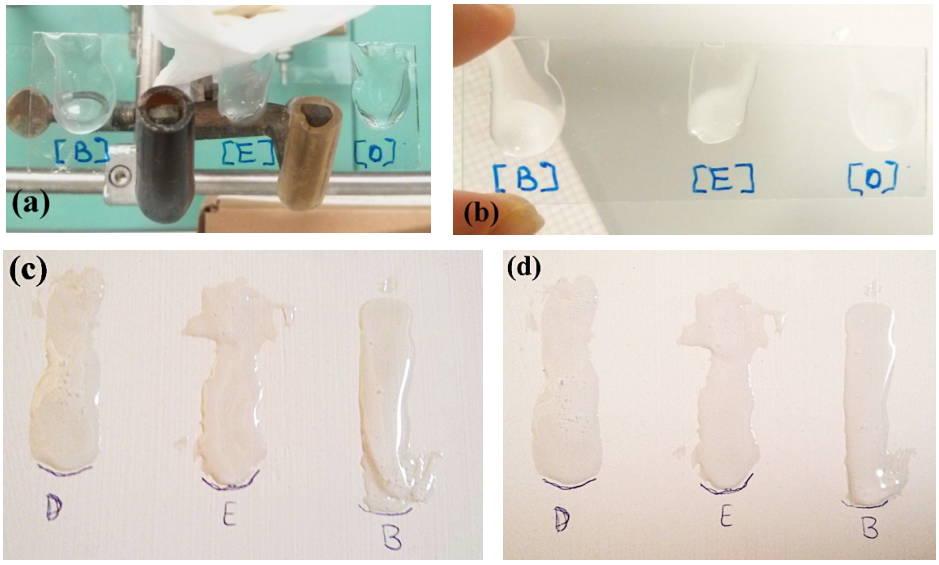

Figure 5.4 Applicative tests on a glass slide (a) and a wall (c) of three different formulations: [B] has the higher liquid content, thus tending to flow downwards under gravity force, while [D] and [E] have lower liquid and higher plasticizer content, thus showing similar resistance under gravity force (b),(d).

Then further application tests were carried out with the selected formulations [D] and [E], in order to find the maximum quantity, for each formulation, applicable without dripping. Increasing amounts of the formulations were applied on the different sections of the glass slice with a syringe, without any pressure, as showed in Fig. 5.5 (a) (b) for [D] and (c) (d) for [E]. The maximum quantity applicable is between 75-100 µL for both formulations, while above these limits the sample start to drip.

Finally the application of 75 µL of both [D] and [E] were carried out (on an approximate surface of 6.7 x 13.5 mm^2), after a light pressure of the spatula, to better simulate the application modality. This test confirmed the good adherence properties of both formulations, as showed in Fig. 5.6, and gave an idea about the suitable amount of the system to take for real applications, for a given area.

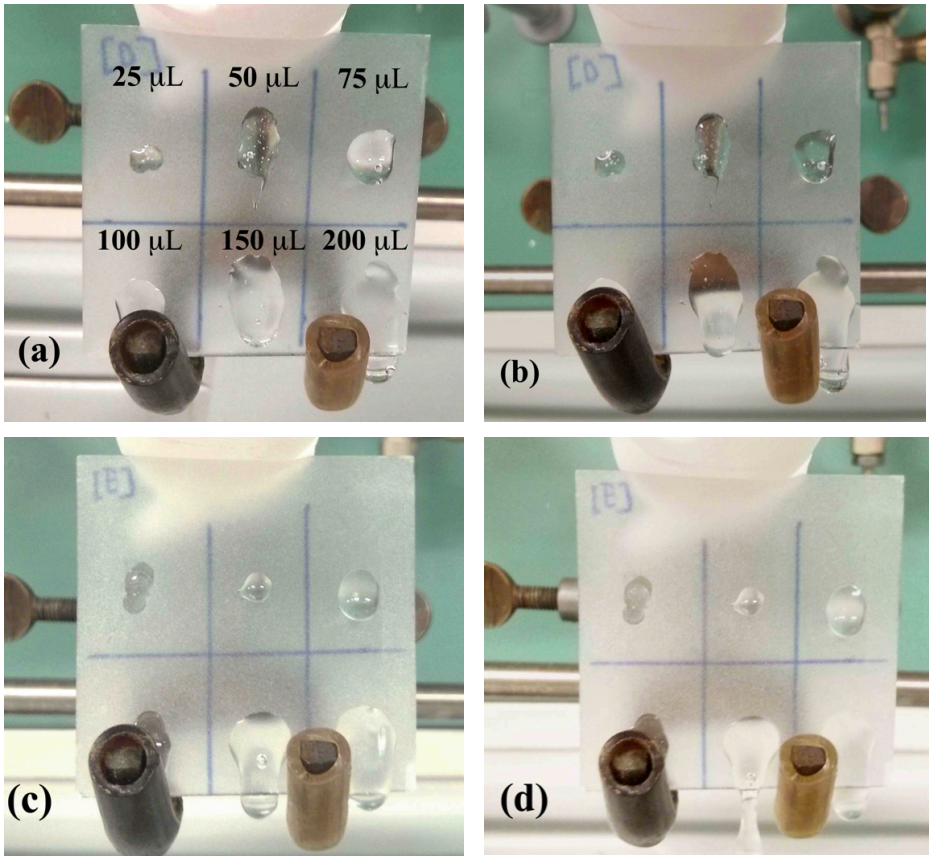

Figure 5.5 Progressively increasing amount of formulations [D] (a) (b) and [E] (c) (d) applied on a glass slide: 25, 50, 75, 100, 150 and 200 µL. Quantities above 75-100 µL will start to drip.

Figure 5.6 Application of 75 µL of the most suitable formulation for applicative tests on non-horizontal surfaces, [D] and [E]: after a gentle pressure with a spatula they maintain their position without dripping.

5.2.4 Selected formulations

As revealed by experimental tests, polyols resulted as the most suitable plasticizers to be tested, since among the additives commonly used in similar formulations [17–19], they present desirable properties, such as good solubility in both water and ethanol, low-toxicity, low-cost and chemical affinity to the polymer. Further tests were thus executed using the four plasticizers DPG, MPD, GLY and PEG (300 and 400). Three formulations were designed by varying the relative content of water, ethanol and plasticizers, to obtain the compositions listed in Tab. 5.3:

Formulation	**Water**	**Ethanol**	**PVA**	**Plasticizers**			
				DPG	MPD	GLY	PEG*
PVA74	57	17	20	2.5	2.5	0.6	0.4
PVA70	55	15	20	3	3	2.5	1.5
PVA68	54	14	20	3.5	3.5	3	2

Table 5.3 Compositions (% w/w) of the selected formulations named as PVA*XX*, where the suffix *XX* refers to the total volatiles content (water + ethanol); since the PVA amount is fixed at 20% w/w, the plasticizer content can be obtained by subtraction. *Both PEG 300 or 400 can be used.

The macroscopic characteristics of these selected systems depend mainly on their i) liquid fraction and ii) plasticizer content: PVA74 is the most liquid formulation, suitable for applications on horizontal surfaces, with high ethanol (17% w/w) and low plasticizer content (6% w/w), thus entailing fast evaporation rate; PVA68 presents the higher amount of plasticizers (12% w/w), thus being suitable for applications on non-horizontal surfaces, although the high plasticizer content contributes to hinder the evaporation process because of the hygroscopic nature and humectant action of plasticizers; PVA70 presents intermediate properties between these two systems, being applicable onto oblique surfaces thanks to its high plasticizer content (10% w/w), with high evaporation rate assured by the intermediate ethanol content (15% w/w), and good spatial control thanks to the intermediate liquid fraction ($68 < 70 < 74$).

The composition of such polymeric systems can be adjusted by varying the amount of each component, to satisfy the final desired properties. For example if the application has to be done on an outdoor object, the main requirement would be good adhesion on non-horizontal surface, while the evaporation rate can be a negligible parameter, being influenced by the environmental conditions (ventilation, temperature and relative humidity). On the other hand, if the application has to be done indoor, with very high relative humidity and low temperature, without ventilation, a formulation with higher ethanol content, thus more fluid, may be recommended. The extreme versatility and ease of adjustability to specific requirements make these systems very useful in the field of cleaning of metallic artifacts. In Fig. 5.7 an example of the initial fluidity of the system is reported along with a final film removed from an artificially aged sample: the application of this evolution in the physical state for cleaning purposes represent the main innovative element of these cleaning tools.

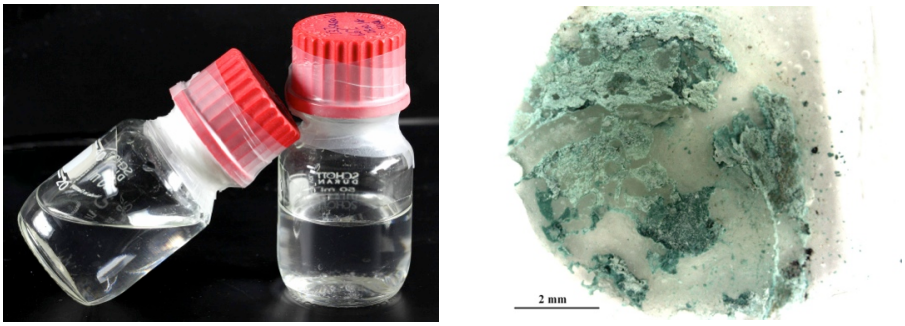

Figure 5.7 Example of the initial fluid consistency of the polymeric systems (left), and the final dry film removed from a corroded surface along with Cu(II) corrosion products (right).

5.3 Preparation of the formulations

5.3.1 Materials

Polyvinyl alcohol [PVA] (87-89% hydrolyzed, M_w 85,000-124,000, DP ≈ 2000, cps 23.0-27.0, Aldrich), dipropylen glycol [DPG] (purity 99% mixture of isomers, Aldrich), 2-methyl-1,3-propanediol [MPD] (purity 99%, Aldrich), glycerol [GLY] (for

analysis, Merck), polyethylene glycol [PEG] (average M_n 300 and 400, Aldrich and Fluka respectively), ethanol (purity ≥ 98%, Fluka), ethylenediaminetetraacetic acid disodium salt dihydrate [Na_2EDTA] (purity 99.9-101.0%, Aldrich), potassium sodium tartrate tetrahydrate [RS] (purity 99%, Sigma-Aldrich), triethylenetetramine [TETA] (purity 60%, Aldrich), tetraethylenepentamine [TEPA] (technical grade, Aldrich), pentaethylenehexamine [PEHA] (technical grade, Aldrich), NH_4OH solution (30-33% NH_3, Sigma-Aldrich) were used as received. Water was purified by a Millipore MilliRO-6 Milli-Q gradient system (resistivity > 18 MΩ·cm).

5.3.2 Preparation procedure

A 20% (w/w) aqueous polymeric solution is obtained by dissolving the weighted quantity of PVA powder into purified water. Complete solubilization is achieved by heating the system at 90 °C for 5h and by mechanically mixing it with a Vortex stirrer every hour. After PVA solubilization, the plasticizers (DPG, MPD, PEG, GLY) and, eventually, the complexing agent are added, then keeping the resulting solution at 75 °C for further 2 hours until complete homogenization. Ethanol is added as the last step, under mechanical stirring to avoid lumps formation. To eliminate the formed air bubbles, the obtained system is then sonicated in pulsed mode for 2 hours until a transparent polymeric dispersion is obtained.

The resulted formulations must be kept in well-sealed containers in order to prevent undesired evaporation that can induce the beginning of the film forming process. The so-stored formulations are stable for months (up to six), although a certain increase in viscosity and thickening was observed after two-three weeks, thus making the sample withdraw difficult. The problem, mainly due to aging processes, can be easily solved by immersing the sealed vials in hot water (about 50 °C) to restore the viscoelastic properties of the system (above the glass transition temperature); after cooling to room temperature the system is again easy to handle and to apply.

5.4 Complexing agents

As described in the previous section, the complexing agent has to be loaded in the polymer matrix during the preparation procedure, after PVA solubilization and addition of plasticizers, but before the addition of ethanol. Often the chelating agent is used as aqueous solutions, so the amount of solution added must be taken into account in respect to the overall water content, to avoid the consequent formation of a too liquid system. For this reason the amount of water added with the solution is subtracted from the overall water content of the system and the concentration of the complexing agent is calculated as weight fraction in % w/w over the entire weight (g) of the formulation.

5.4.1 Rochelle salt

Potassium sodium tartrate tetrahydrate, or Rochelle salt [RS], has very good solubility in water (630 g/L at 20°C[2]), therefore aqueous stock solutions at 30% (pH 7), 35 % (pH 11) and 60% (pH 8) w/w were easily prepared and stored for several months (then a flocculate starts to form). The range of concentrations used was between 1-7% w/w, although in restoration practice concentrations up to 35% w/w are commonly used (see the case of the 'Porta del Paradiso'[20,21]), because of the bland action of RS. However amounts over 7% w/w RS significantly modified the structural characteristics of the system. In fact, RS hydroxyl groups interact strongly with the PVA chains, resulting in an excessively entangled polymeric network. As a result the aliquot of RS loaded into the polymeric matrix and taken form the stock solutions at 35% w/w (pH 11) and 60 % w/w (pH 8), gave rise to phases separation and precipitation phenomena, because of the excess of –OH groups. Phase separation processes could be avoided by using the more diluted 30% w/w (pH 7) stock

[2] http://tartaric.com/rochelle-salt/, consulted on November 2015

solution. Moreover RS presents poor solubility in ethanol, thus forming acicular crystals that precipitate on the bottom, after few days (see Fig. 5.8).

5.4.2 EDTA

Ethylenediaminetetraacetic acid disodium salt dihydrate [Na_2EDTA] is slightly soluble in water (100 g/L at 20 °C and pH 7), thus a stock solution at 0.5 M and pH 8 was prepared and stored in fridge for several months [22]. The maximum amount of loadable EDTA is around 3-4% w/w, while the concentrations commonly used in restoration practice are around 3-12% (or more) in aqueous solutions [23]. This limit derives from the insolubility in ethanol, which causes phase separation phenomena, resulting in the precipitation (anyhow negligible if compared to the total amount) of white agglomerate crystals, as showed in Fig. 5.8. Moreover, the presence of EDTA increases the polymer chain entanglements and vicinity, thus modifying the 3-D polymer network structure, as will be reported in the Chapter 6 [24] In fact, an excess of EDTA causes undesired interactions between the polymer chains that excessively modify the characteristic of the system. Some initial attempts to load higher amounts of EDTA were carried out by using its solution instead of the sole water to solubilize PVA in the preparation procedure, with the formation of a compact and unprocessable agglomerate as result.

EDTA has a formation constant of 18.8 (see Tab. 4.3), higher than the one of RS (5.7), thus exerting a more effective action toward the Cu^{2+} ions. Moreover the efficacy of this chelating agent can be further enhanced by varying the pH, as reported in Chapter 4 (section 4.2.2). The pH of the EDTA loaded polymeric system was adjusted to 9-10 ± 0.2 (as indicated by Whatman Indicator Paper, pH 8.0-10.0 narrow range), through the drop wise addition of an aqueous solution of NH_3 after the addition of ethanol in the preparation procedure. In this way meaningful amounts of both the trianionic HY^{3-} and tetranionic Y^{4-} species of EDTA are present, thus enhancing its complexing efficacy.

The research of more effective complexing agents, different from those commonly used in restoration practice, was carried out mainly to overcame the limits related to the loadable amount of both RS and EDTA in the polymer matrix (increasing for example the efficacy, *i.e*. higher formation constants) and to solve the problem of insolubility in ethanol.

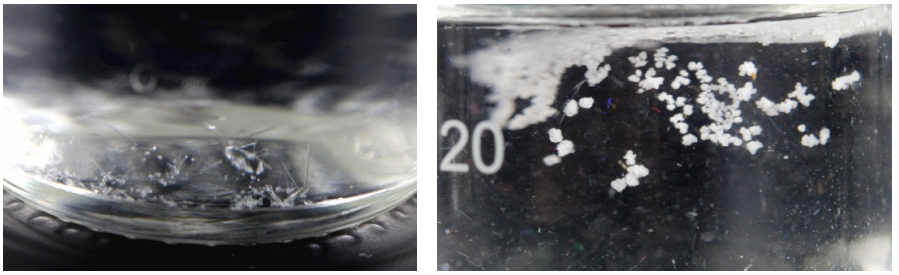

Figure 5.8 Phase separation and precipitation of acicular crystals for Rochelle salt (left) and white agglomerates for EDTA (right), after some days (3-4), due to low insolubility in ethanol.

5.4.3 Glycine

Glycine presents water solubility of 225 g/L at 20 °C [25], thus a 2.5 M (about 18% w/w) stock solution was prepared. This complexing agent in not commonly used in the restoration field, so starting formulations were prepared with concentrations of 3% w/w. The formation of the light blue complex glycine-Cu(II) over the metallic substrate after the application resulted in a significant alteration of the surface color and in a difficult removal of the complexed residues.

5.4.4 Macrocycles

Three different macrocycle molecules, characterized by high complexing efficacy, were tested as possible substitutes of EDTA and RS. In particular 1,4,7,10-tetraazacyclodecane-1,4,7,10-tetraacetic acid [DOTA], 4,10-dimethyl-1,4,7,10-tetraazacyclo-dodecane-1,7-diacetic acid [AMCC] and 2,5,8-triaza[9]-[9](2,9)[1,10]-phenanthrolino-phane [NEODEN] were supplied by the research

group of Prof. A. Bianchi, A. Bencini and V. Valtancoli (Department of Chemistry, University of Florence), who extensively study coordination chemistry of macrocycle ligands [26–35].

These macrocycle compounds present high stability constant towards Cu(II) ions: DOTA $K_\beta = 22.2$ [36], AMCC $K_\beta = 20.85$ [27] and NEODEN $K_\beta = 16.17$ [28]; their molecular structures are reported in Fig. 5.9 and Fig. 4.9 for DOTA, along with their distribution diagrams in function of pH.

Since very small amounts (about 20 mg) of these systems were supplied, they were loaded into 500 mg of polymeric systems each with a final concentration of 2% w/w.

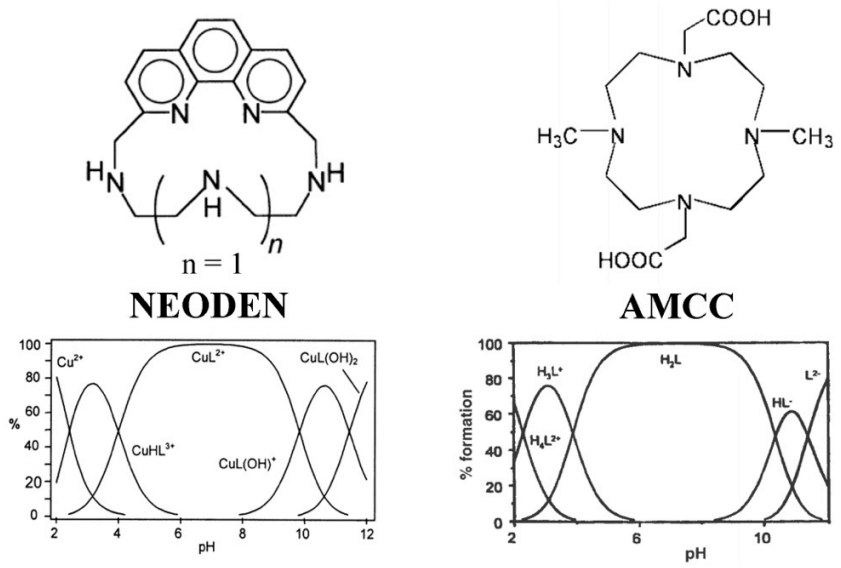

Figure 5.9 Molecular structures of NEODEN and AMCC macrocycles and their relative distribution diagrams in function of pH [27,28].

Although their ability to form strong complexes with Cu(II), some drawbacks are related to these macrocycle molecules, preventing their practical use for the purpose of this thesis. In particular: i) they have very high costs (e.g. 340 € for 250 mg

DOTA[3]); ii) they are not commercially available (AMCC, NEODEN) but they should be appositively synthetized; iii) their toxicity and dangerousness (e.g. hazard statements for DOTA, H315, H319 and H335) [37]; iv) poor solubility in ethanol [38].

5.4.5 Polyethyleneamines

Polyethyleneamines represent a good alternative to macrocyclic molecules, thanks to their lower cost and comparable complexation efficacy. In particular three molecules were selected: triethylenetetramine [TETA], tetraethylenepentamine [TEPA] and pentaethylenehexamine [PEHA]. Their stability constants toward cupric ions, reported in Tab. 4.3, are $K_\beta = 20.1$ for TETA, $K_\beta = 22.8$ for TEPA and $K_\beta = 26.2$ for PEHA, while their structural formula is showed in Fig. 4.10. Moreover these polyethyleneamines present i) good solubility properties both in water and ethanol; ii) liquid state, so they can be easier loaded into the polymeric system; iii) low cost. However they still present some issues related to toxicity and environmental safety: according to EU Directives 67/548/EEC or 1999/45/ECas, they are classified as very harmful for skin contact (R21, R22, R34, R43) and for aquatic environment (R50, R53).

Concentrations between 3% and 10% w/w were tested and PEHA was selected as the more effective agent, thanks to its higher complex formation constant. These polyamines form complexes with Cu(II) of an intense blue color and they can be loaded in a considerable amount inside the polymeric system. However, despite their high complexing efficacy in respect to all previously tested chelating agents, they establish extra-bonds within the polymeric network, acting as cross-linkers and causing undesired additional gelification of the system. After 3-4 days this process is still reversible by heating the sample, but after 5-6 days an irreversible and unusable gelled system is obtained.

[3] http://www.sigmaaldrich.com, consulted on November 2015

All the complexing agents presented in this chapter have both, advantages and drawbacks, thus making the research of and effective, non toxic and compatible agent still open. However the selection of a suitable chelating agent has to be done depending on the cleaning case study: for example for a gilded surface a bland action with Rochelle salt is advisable, while EDTA is the most safe agent, in terms of both toxicity and compatibility with the polymeric system, so it is suitable for almost every situation. The use of glycine and macrocycle molecules was rejected, because their drawbacks overcome the advantages. Polyamines-loaded systems seemed the most promising solution for improved complexation efficacy, thanks to polyamines high formation constants with Cu(II) and good solubility properties, even though they compromise the stability of the polymeric system and are toxic.

5.5 Bibliography

[1] BAREL, A.O., PAYE, M., AND MAIBACH, H.I., EDS. *Cosmetic Science and Technology.* Informa Healthcare, **2009**.

[2] LANGE, W.E. *Aqueous Topical Adhesives I. Film Forming Base.* J. Soc. Cosmetic Chemistry *16*, (**1965**), 563–570.

[3] O'REILLY BERINGHS, A., ROSA, J.M., STULZER, H.K., AND BUDAL, R.M. *Green clay and aloe vera peel-off facial masks: response surface methodology applied to the formulation design.* AAPS PharmSciTech *14*, 1 (**2013**), 445–455.

[4] NISHIKAWA, D.O. AND ZAGUE, V. *Avaliação da estabilidade de máscaras faciais peel-off contendo rutina.* Journal of Basic and Applied Pharmaceutical Science *28*, 2 (**2007**), 227–232.

[5] SHISEIDO. *Emulsified cosmetic face pack EP 0 978 270 B1.* **2006**, 1–7.

[6] SLAVTCHEFF, C.S. *Cosmetic mask 5 747 022.* **1998**, 5–10.

[7] SPERANDIO, J. AND WARD, J.B. *Cosmetic Application of PVA.* Journal of the Society of Cosmetic Chemists *15*, (**1964**), 327–335.

[8] VIEIRA, R.P., FERNANDES, A.R., AND KANEKO, T.M. *Physical and physicochemical stability evaluation of cosmetic formulations containing soybean extract fermented by Bifidobacterium animalis.* Brazilian Journal of Pharmaceutical Science *45*, 3 (**2009**), 515–525.

[9] VIEIRA, R.P., FIALHO-PEREIRA, F., AND VELASCO, M.V. *Short-term clinical of peel-off facial mask moisturizers.* Department of Pharmacy, Sao Paulo, Brazil, .

[10] LAMANNA, R. AND CANNISTRARO, S. *Effect of ethanol addition upon the structure and the cooperativity of the water H bond network.* Chemical Physics *213*, 1–3 (**1996**), 95–110.

[11] WYPYCH, G., ED. *Handbook of plasticizers.* William Andrew Publishing, Toronto, New York, **2004**.

[12] FOWLES, J.R., BANTON, M.I., AND POTTENGER, L.H. *A toxicological review of the propylene glycols.* Critical Reviews in Toxicology *43*, 4 (**2013**), 363–390.

[13] OECD SIDS. *Dipropylene glycol.* Unep Publications, **2001**.

[14] *Polyethylene glycol.* In *The MAK-Collection for Occupational Health and Safety*. Wiley-VCH Verlag GmbH & Co. KGaA, **1998**.

[15] DAVIDSON, R.L. *Handbook of water-soluble gums and resins.* New York : McGraw-Hill, **1980**.

[16] WU, W., TIAN, H., AND XIANG, A. *Influence of Polyol Plasticizers on the Properties of Polyvinyl Alcohol Films Fabricated by Melt Processing.* Journal of Polymers and the Environment *20*, 1 (**2012**), 63–69.

[17] SAKELLARIOU, P., HASSAN, A., AND ROWE, R.C. *Interactions and partitioning of diluents/plasticizers in hydroxypropyl methylcellulose and polyvinyl alcohol homopolymers and blends . Part I : Diethylene glycol. 1090*, (**1993**), 1083–1090.

[18] SAKELLARIOUL, P., HASSAN, A., AND ROWE, R.C. *Interactions and partitioning of diluents/plasticizers in hydroxypropyl methylcellulose and polyvinyl alcohol homopolymers and blends . Part II : Glycerol. 56*, (**1994**), 48–56.

[19] SAKELLARIOUL, P., HASSAN, A., AND ROWE, R.C. *Interactions and partitioning of diluents/plasticizers in hydroxypropyl methylcellulose and polyvinyl alcohol homopolymers and blends . Part III : Polyethylene glycol 400. 227*, (**1994**), 220–227.

[20] FIORENTINO, P., MARABELLI, M., MATTEINI, M., AND MOLES, A. *The condition of the 'Door of Paradise' by L. Ghiberti. Tests and proposals for cleaning.* Studies in Conservation *27*, (**1982**), 145–153.

[21] FERRETTI, M. AND SIANO, S. *The gilded bronze panels of the Porta del Paradiso by Lorenzo Ghiberti: non-destructive analyses using X-ray fluorescence.* Applied Physics A *90*, 1 (**2007**), 97–100.

[22] *EDTA Product Information.* SIGMA, (**2003**).

[23] SCOTT, D.A. *Copper and bronze in art.* The Getty Conservation Institute, Malibu, **2002**.

[24] CA, V., RUIZ, J., AND MANTECO, A. *Synthesis and properties of hydrogels from poly (vinyl alcohol) and ethylenediaminetetraacetic dianhydride. 42*, (**2001**), 6347–6354.

[25] *Glycine Product Information.* SIGMA, (**2013**).

[26] BAZZICALUPI, C., BENCINI, A., FUSI, V., GIORGI, C., PAOLETTI, P., AND VALTANCOLI, B. *Lead complexation by novel phenanthroline-containing macrocycles.* Journal of the Chemical Society, Dalton Transactions, (**1999**), 393–400.

[27] BARBARO, P., BIANCHINI, C., CAPANNESI, G., ET AL. *Synthesis and characterization of the tetraazamacrocycle 4,10-dimethyl-1,4,7,10-tetraaz-acyclododecane-1,7-diacetic acid ($H_2Me_2DO_2A$) and of its neutral copper(II) complex [Cu(Me2DO2A)].* Journal of the Chemical Society, Dalton Transactions, 14 (**2000**), 2393–2401.

[28] CHAND, D.K., SCHNEIDER, H.J., BENCINI, A., ET AL. *Affinity and nuclease activity of macrocyclic polyamines and their Cu(II) complexes.* Chemistry - A European Journal, (**2000**), 4001–4008.

[29] BIANCHI, A., MICHELONI, M., AND PAOLETTI, P. *Large polyazacycloalkanes: ligational properties and anion coordination chemistry. 60*, 4 (**1988**), 525–532.

[30] BAZZICALUPI, C., BENCINI, A., BERNI, E., ET AL. *New terpyridine-containing macrocycle for the assembly of dimeric Zn(II) and Cu(II) complexes coupled by bridging hydroxide anions and π-stacking interactions.* Inorganic Chemistry *43*, 16 (**2004**), 5134–5146.

[31] ANDA, C., BAZZICALUPI, C., BENCINI, A., ET AL. *Cu (II) and Ni (II) complexes with dipyridine-containing macrocyclic polyamines with different binding units.* (**2003**), 1299–1307.

[32] BAZZICALUPI, C., BELLUSCI, A., BENCINI, A., ET AL. *A new dipyridine-containing cryptand for both proton and Cu(II) encapsulation. A solution and solid state study.* Journal of the Chemical Society, Dalton Transactions, 10 (**2002**), 2151–2157.

[33] BENCINI, A., BIANCHI, A., GARCIA-ESPANA, E., AND MICHELONI, M. *Synthesis and ligational properties of the two very large Polyazacycloalkanes [33]aneN11 and [36]aneN12 forming trinuclear copper (II) complexes.* Inorganic Chemistry *27*, (**1988**), 176–180.

[34] HAZLE, A. *Synthesis and complexing properties of the large polyazacycloalkane 1,4,7,10,13,16,19,22,25,28-Decaazacyclotriacontane (L). Crystal structure of the monoprotonated dicopper(II) complex $[CU_2(L)HCI_2](ClO_4)_34H2O$.* Inorganic Chemistry *26*, (**1987**), 1243–1247.

[35] BIANCHI, A., GARCIA-ESPANA, E., GIUSTI, M., AND MICHELONI, M. *Solution*

Chemistry of Macrocycles. 5. Synthesis and ligational behavior toward hydrogen and copper(II) Ions of the large polyazacycloalkane 1,4,7,10,13,16,19,22,25-nonaazacycloheptacosane ([27]aneN9). 26, (**1987**), 681–684.

[36] MARTELL, A.E. AND SMITH, R.M. *Critical stability constants. Second supplement.* Springer Science + Business Media, New York, **1989**.

[37] SIGMA-ALDRICH. *1,4,7,10-Tetraazacyclododecane-1,4,7,10- tetraacetic acid.* Safety Data Sheet, .

[38] *Process for producing 1,4,7,10-tetraazacyclododecane-1,4,7,10-tetraacetic acid and complexes thereof WO 2014114664 A1.* **2014**.

Chapter 6

Characterization of the polymeric systems

6.1 Introduction

Preliminary investigations over the physico-chemical characteristics of polymeric formulations are described in this chapter. The analysis of appositely prepared formulations, with polyvinyl alcohol as the constituent polymer, different additives (ethanol, plasticizers), loaded with complexing agents (EDTA, Rochelle salt) were carried out through different methodologies. In particular two main aspects were studied over both, complexing agent-loaded and not loaded systems: i) the kinetics of film formation, by investigating the evolution of the systems from polymeric dispersions towards the formation of elastic films and ii) the evaluation of the formed films properties, through the crystallinity degree parameter. The techniques used to obtain information over the evolution of the system through time, involved the use of gravimetry, thermogravimetry (both scanning and isothermal), and rheology (both dynamic and rotational experiments). On the other hand the evaluation of the mechanical properties and of the degree of crystallinity of the dried films was carried out through differential scanning calorimetry (DSC) and ATR-FTIR spectroscopy experiments. Instrumental conditions and sample preparation are also reported.

The discussion over the obtained results will be divided by taking into account the influence of each component that can be added and adjusted to vary the system properties, *i.e.* the influence of: i) the volatile fraction (water and ethanol); ii) the plasticizers (different polyols); iii) the complexing agent (different amounts of

EDTA and RS). Finally the evaluation of the variations in the viscoelastic behavior over time of a selected formulation (PVA70) before and after the addition of a complexing agent solution was carried out through rheology.

6.2 Preparation of the polymeric systems and of the dry films

Different formulations were expressely prepared for the physico-chemical characterization, with compositions reported in Tab. 6.1, according to the preparation procedure already described in Chapter 5. Relative amounts of each component were opportunely varied in order to reveal their respective influence over the final system properties. The comparisons between the formulations was carried out with the aim of highlighting the influence of:

- ethanol in respect to the sole aqueous polymer solution (PVA/H_2O and PVA/H_2O/EtOH);
- plasticizers single or in combination between them (PVA/DPG, MPD, GLY, PEG and PVA68, 70 and 74 respectively);
- ethanol and its amount in respect to formulations with the same plasticizer and polymer content (PVA70 against PVA_{noEtOH} and between PVA 70:30, 80:20, 85:15 respectively);
- different complexing agents (EDTA and Rochelle salt);
- increasing amount of a complexing agent (EDTA), also at different pH values (7 and 9).

The resulting polymeric systems were firstly analyzed alone, without the addition of a chelator, in order to define their evolution though time and to study the influence of the single components. Then, in order to study the complete system to be used for cleaning purposes, also systems loaded with selected complexing agents and working conditions (pH) were analyzed. In particular EDTA seemed the most versatile complexing agent to be tested, as mentioned in Chapter 5 (section 5.4), if compared to Rochelle salt-loaded systems. Finally, since from experimental evaluations PVA70 resulted the best formulation in terms of applicability performances,

thanks to its intermediate properties among the other designed formulations, it was characterized as confining system for the complexing agents. The typology, amount, and pH of the PVA70-loaded formulations are reported in Tab. 6.2.

Some characterization experiments were carried out on the fluid systems, to evaluate their behavior over time. Other methods were used to study the mechanical properties of dry films. In this latter case, samples were prepared as follows: dry films were obtained by applying 1 g of the selected polymeric dispersion on a 5 x 2.5 cm^2 glass slide, dried at 60 °C for 17 hours, then equilibrated at 55% RH for at least one week.

Formulation	Water	Ethanol	PVA	Plasticizers			
				DPG	MPD	GLY	PEG
PVA/H_2O	80	-	20	-	-	-	-
PVA/H_2O/EtOH	65	15	20	-	-	-	-
PVA68	54	14	20	3.5	3.5	3	2
PVA74	57	17	20	2.5	2.5	0.6	0.4
PVA70	55	15	20	3	3	2.5	1.5
$PVA70_{noEtOH}$	70	-	20	3	3	2.5	1.5
PVA70/DPG	55	15	20	10	-	-	-
PVA70/MPD	55	15	20	-	10	-	-
PVA70/GLY	55	15	20	-	-	10	-
PVA70/PEG	55	15	20	-	-	-	10
PVA70 70/30	50	20	20	3	3	2.5	1.5
PVA70 80/20	55	15	20	3	3	2.5	1.5
PVA70 85/15	60	10	20	3	3	2.5	1.5

Table 6.1 List of the compositions, expressed in % w/w, of the formulations used for the physico-chemical characterization.

Formulation PVA70		
Complexing agent	**Amount % w/w**	**pH**
EDTA	1	7
	2	7
	3	7
	3	9
Rochelle salt	6	7

Table 6.2 Formulation PVA70 loaded with EDTA and Rochelle salt, as complexing agents, at different amounts and pH, for the physico-chemical characterization.

6.3 Methods and instrumental conditions

Different methodologies were used to investigate the behavior of the system though time (*i.e.* kinetics of film formation), evolving from a fluid polymeric solution toward a solid elastic film. In particular gravimetric, thermogravimetric (TG) and rheological measurements were carried out in order to study the behavior of the fluid selected fluid formulations until the formation of the final film is formed. Parameters affecting the mechanical properties of the dry film, in particular the degree of crystallinity, were studied by differential scanning calorimetry (DSC) and by attenuated total reflection FTIR spectroscopy (ATR-FTIR) techniques.

6.3.1 Kinetics of film formation

6.3.1.1 Gravimetric measurements

The evaporation of the volatile fraction from different polymeric systems was evaluated by means of gravimetric measurements, which allow to simulate the process of film formation in real thermo-hygrometric and applicative conditions. With this aim, same amounts of different formulations (0.5 g) were applied on a fixed area of a microscope slide (2.6 x 2.5 cm^2), as shown in Fig. 6.1 (a). To evaluate the evaporation of the volatile fraction, the systems were weighed on a Sartorius CP225D analytical balance at regular time intervals, until the film could be easily removed with tweezers from the glass without breaking or leaving residues, Fig. 6.1(b).

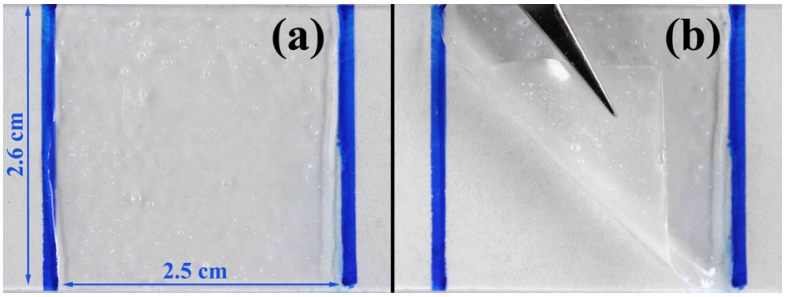

Figure 6.1 Application of the selected formulation on the microscope slide (a) and removal after film formation (b).

The evaporation kinetics are expressed as volatile fraction loss (water and ethanol) over time and the weight decrease was calculated as reported in Eq. (6.1) [1]:

$$W_{vf} = \frac{(W_i - W_d)}{(W_w - W_d)} \times 100 \qquad \text{Eq. 6.1}$$

where W_{vf} is the volatile fraction loss in function of time, W_i is the weight of the sample at the specific time i, W_d the dry weight and W_w the sample weight at its maximum content of volatile fraction.

6.3.1.2 Thermogravimetric analysis

Data from gravimetric experiments were compared to those obtained in a controlled environment through isothermal thermogravimetric analysis (TGA), performed using a TA Instruments (SDT-Q600) apparatus. To simulate conditions as close as possible to the typical application environment of these systems, the volatile fraction loss during drying of the fluid samples, was monitored at the lowest instrumental temperature (40°C) under nitrogen flow at 100 mL/min in open Al pans (empty pan used as reference) with 10-20 mg of each sample. The evaporation of the volatile fraction was considered concluded when a constant weight was reached.

The influence of the different components over the volatile fraction loss rate was evaluated also by scanning TG measurements, by heating the fluid samples from room temperature to 220°C (scan rate 10°C/min) under nitrogen flow in open Al pans. Results are reported using DTG values and the relative DSC thermograms.

6.3.1.3 Rheological measurements

The investigations on changes in viscoelastic behavior as a function of time during drying was performed by means of rotational and oscillatory shear measurements, performed both on a PVA70 formulation before and after loading with 3% w/w EDTA (pH 7). Measurements were carried out on a Paar Physica (UDS200) rheometer at 25.0 ± 0.1°C (Peltier temperature control system) using a plate-plate geometry (25 mm diameter); the gap was adjusted in order to obtain a maximum normal

force of 0.9 N. Measurements were performed at fixed time intervals to monitor the rheological changes during the drying process. Fluid samples were continuously kept under manual stirring in order to maintain the homogeneity of the systems. Film samples were prepared by pouring 11 g of the polymeric dispersion into a Petri dish, then equilibrated for two days at 25°C and 55% RH. Flow curves were collected over a torque range between 10^{-4} and 50 mN·m; zero shear viscosity values (η_0) were obtained from the plateau of the flow curves in the low-Newtonian region. Frequency sweep measurements were carried out within the linear viscoelastic range (5% strain) determined by previous amplitude sweep tests. The storage (*G'*) and loss (*G''*) moduli were measured over the frequency range 0.01 to 100 Hz and *G'* values, at a fixed frequency (5 Hz), reported in function of different times.

6.3.2 Films characterization and evaluation of crystallinity degree

6.3.2.1 Thermoanalysis by DSC

The thermal properties of dried film samples were determined by differential scanning calorimetry (DSC) on a TA Instruments (Q1000) apparatus. The film samples were cut in small disks with the same diameter of the hermetical steel pan used for the measurements. Sets of non-plasticized, one-plasticized and four-plasticized polymer dispersions were used for the preparation of the dried films (compositions are listed in Tab. 6.1).

To erase the thermal history of the samples a first heating cycle was performed from room temperature to 250 °C, at a scanning rate of 10 °C/min. After 3 min at 250 °C the sample was cooled until 25 °C (10 °C/min), kept at this temperature for 3 min then reheated (second cycle) from 25 °C to 250 °C (10°C/min) always under nitrogen flow (50 mL/min) [2].

Glass transition temperature (T_g) values were obtained from the thermograms of the first heating cycle, while melting temperatures (T_m) values from the second one, which display a single endothermic melting peak, whose integrated area gives the enthalpy of fusion (ΔH_m). The crystallization temperature (T_c) was evaluated from

the maximum of the crystallization exothermic peak showed by the cooling thermogram and the relative enthalpy of crystallization (ΔH_c) from its integrated area. Each measurement was performed twice.

The final degree of cristallinity (*DC*%) of the films was determined by the ratio between the experimental enthalpy of fusion (see Eq. 6.2) and the enthalpy of fusion of completely crystalline PVA [3–8] (ΔH_{100} = 138.6 J/g, from [5]):

$$DC\% = (\Delta H_m / \Delta H_{100}) \times 100 \qquad \text{Eq. 6.2}$$

6.3.2.2 ATR-FTIR spectroscopy

Attenuated total reflectance Fourier transform infrared spectroscopy (ATR-FTIR) measurements were performed on the same film samples, with a Thermo Nicolet (Nexus 870) spectrometer in order to confirm DSC values. Data were collected with a MCT detector cooled with liquid nitrogen and a sampling area of 150 μm^2. The spectra were obtained from 128 scan and 4 cm^{-1} of optical resolution in the range 4000-650 cm^{-1}.

It is well-known that the intensity of absorption band at 1141 cm^{-1} of PVA is related to crystalline C-O stretching vibration and depends on the crystallinity degree of the sample [4,9–12]. To evaluate the crystallinity degree, the intensity at 1141 cm^{-1} can be related to the intensity of another peak, not affected by the crystallization process, which can be used as internal standard. The 1089 cm^{-1} band was preferred to that commonly used at 850 cm^{-1}, as suggested by Tretinnikov et al. [13,14], because of its major vicinity to the crystalline dependent peak that seems to reduce the error due to the non-ideal contact of the reflecting element of ATR-FTIR with the sample. Thus cristallinity of the dry films was evaluated by the ratio I_{1141}/I_{1089} between the crystallinity-sensitive intensity of the band at 1141 cm^{-1} *(a*, in Eq. 6.3*)* and the independent peak at 1089 cm^{-1} (*b*, in Eq. 6.3) [6,13].

The ratio I_{1141}/I_{1089} can be used as a relative index of the degree of crystallinity thanks to the existence of a direct proportionality between them even thought the lack of the constants values (*A* and *B*) to complete the equation, from [4]:

$$DC\% = A(a/b) + B \qquad \text{Eq. 6.3}$$

Measurements were repeated twice and peak intensities were obtained after linear baseline subtraction, within the range 1300-800 cm^{-1}, with MagicPlotPro® application.

6.4 Results and discussion

The discussion over the results obtained from the above-mentioned methodologies of analysis, will be divided in relation to the contribution of each additive to the properties of the cleaning systems, *i.e.* volatile fraction, plasticizers, complexing agent, to finally describe the evolution through time of both the loaded and not loaded systems.

6.4.1 Effect of the volatile fraction

Thanks to its high vapor pressure, the addition of ethanol (EtOH) into the polymer dispersions contributes to increase the evaporation rate, thus reducing the time needed for film formation. Furthermore, the ethanol acts upon the water hydrogen-bond network as a structuring agent, by inducing an increment in the H-bond formation probability [15]. This feature contributes to reinforce the overall 3-D network structure by inducing an ordering effect on the liquid fraction of the polymeric system as already discussed in Chapter 3 (section 3.5.2). In fact, as soon as ethanol is added into the formulation, a noticeably improvement of the homogeneity and consistency of the polymeric system is immediately observed. This behavior has an effect also on the final applicability of the polymeric dispersion that becomes, for example, easier to handle (e.g. to be taken with a spatula).

The effect of the H_2O/EtOH ratios on the formulations properties was studied by means of gravimetric measurements and scanning thermogravimetric analysis. Fig. 6.2 (a) reports the gravimetric evaporation curves for three different formulations (PVA70 70/30, 80/20, 85/15, composition listed in Tab. 6.1), characterized by the same polymer and plasticizer content but increasing H_2O/EtOH ratios. Evaporation

curves are obtained by using Eq. 6.1. The presence of ethanol promotes an increase in the evaporation rate, as showed by the initial slope of the three curves (see inset of Fig. 6.2 (a)) in the first 10 minutes: the more the ethanol, the faster the evaporation process. This obviously influence also the time of film formation, represented by solid symbols in Fig. 6.2 (a): from 240 minutes required by the formulation PVA70 70/30, up to 360 minutes for the formulation PVA70 85/15. It is worth noting that film formation generally occurs before complete evaporation of the liquid fraction, when water content reaches about 10 % w/w or lower inside the polymer network. This feature allows maintaining suitable mechanical properties for the peeling-off removal, by assuring a certain flexibility of the final film.

The same trend is confirmed by the thermogravimetric curves (DTG) obtained in scanning temperature mode, reported in Fig. 6.2 (b). The derivative weight loss of different formulations is reported as a function of the increasing temperature (see 6.3.1.2), thus evidencing the evaporation process by a sharp peak, at which maximum, the volatile fraction loss occurs. The formulations with an increasing ethanol content are compared with the same formulation, prepared without the addition of ethanol ($PVA70_{noEtOH}$). By decreasing the ethanol content, a progressive shift of the peak maxima towards higher temperatures is observed. In particular, the major shift is observed for the PVA70 formulation without ethanol, for which the evaporation of the liquid fraction occurs at 111 ºC, while the others are around 100 ºC (95 ºC, 97 ºC, 99 ºC for 70/30, 80/20 and 85/15 respectively).

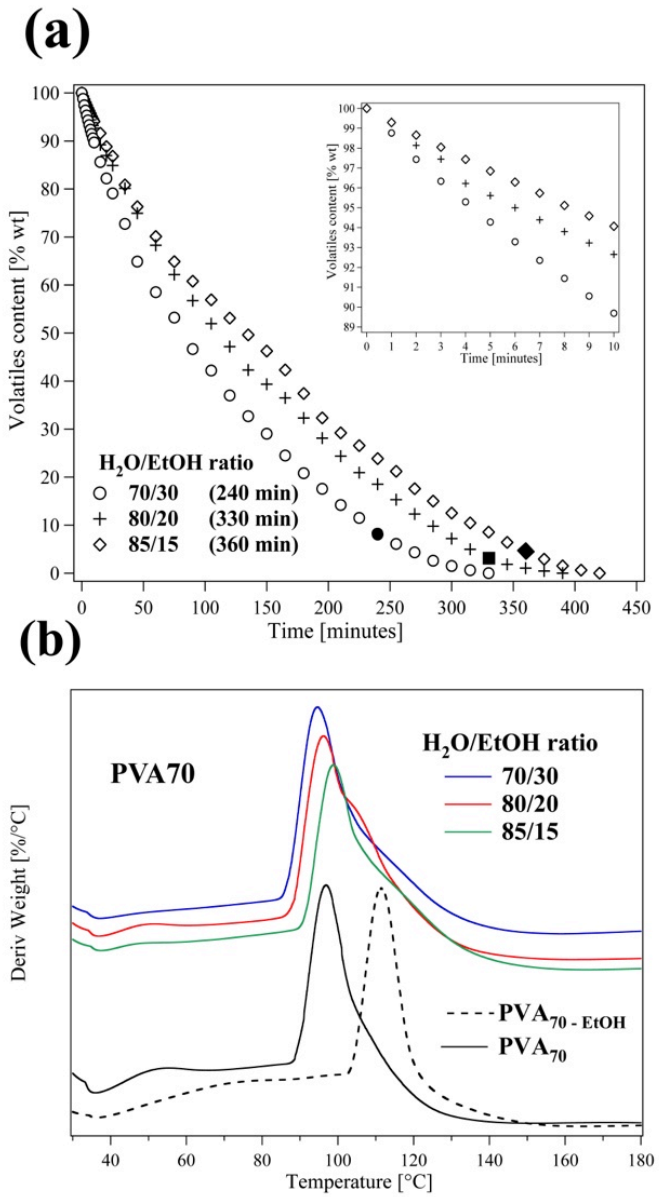

Figure 6.2 (a): gravimetric evaporation curves of PVA70 formulations with different H_2O/EtOH ratios; solid symbols represent the time of film formation, when they can be easily removed from the glass slide; inset: initial slope of the curves. (b): DTG thermograms of PVA70 formulations with decreasing ethanol content; the displayed maxima of the derivatives weight loss represent the evaporation temperatures of the volatile fraction.

6.4.2 Effect of the plasticizers

The addition of plasticizers in the PVA polymeric dispersion allows the modulation of the initial consistency and of the mechanical and adhesive properties of the final dry film, as reported in Chapter 3 (section 3.5.3). In fact, plasticizers act as lubricants between the polymer chains by weakening their inter-molecular secondary forces and by increasing the overall free volumes. This process causes a decrease in the thermal transition temperatures (see Chapter 3, section 3.2.3) and in the overall crystallinity degree of the final films (*DC*%, section 3.2.2). As a consequence, the addition of plasticizers producs a reduction in adhesion, hardness and brittleness, and an increase in flexibility, toughness and tensile strength of the final films.

Polyols (DPG, MPD, GLY and PEG) were chosen as the most suitable plasticizers, as reported in Chapter 5 (section 5.2.4), thanks to their compatibility with the polymer, low-price, low-toxicity and good solubility properties. The analyzed films were prepared from unplasticized (PVA/H_2O and PVA/H_2O/EtOH), one-plasticized (PVA70 /DPG, MPD, PEG, GLY) and four-plasticized formulations (PVA70 and $PVA70_{noEtOH}$), with starting composition listed in Tab. 6.1.

Differential scanning calorimetric experiments (DSC) carried out on dried films, allowed to evaluate the trend of thermal parameters (glass transition T_g, melting T_m and crystallization T_c temperatures) after the addition of plasticizers in the polymer matrix. The decrease, on different extent, in the glass transition temperature of one-plasticized samples [16–18] in respect to PVA_{dry} (the sole polymer powder) or its aqueous solution (PVA/H_2O), is reported in Tab. 6.3. The relationship between plasticizers and T_g can be explained by the Free-Volume Theory [19] (see Chapter 3, section 3.5.3.2), *i.e.* the addition of molecules with lower T_g and the introduction of many free volumes contribute to reduce the overall polymer T_g value; the extent of this reduction can be estimated by the Kelly-Bueche equation for a two-components system [20] (see Eq. 3.20). The typical glass transition temperature, for the amorphous part, of partially hydrolyzed PVA is around 58 °C (see Tab. 3.1 in

Chapter 3), while the obtained values for dry PVA though DSC experiments is around 50-52 °C, with little differences between the samples. However, a slight decrease in the T_g values between one-plasticized and unplasticized samples can be observed; T_g values are obtained from the first heating cycle, that is before erasing the thermal history of the samples. As reported in Tab 6.3, PVA_{dry} presents the higher value of T_g, reduced by the plasticizer effect of water in PVA aqueous solutions with and without ethanol [2]; the values of plasticized samples are very similar with each other, with the lowest values for the PVA/GLY film sample.

Formulation	**DSC**					
	T_m (°C)	**ΔH_m (J/g)**	**T_g (°C)**	**T_c (°C)**	**ΔH_c (J/g)**	**DC %**
PVA_{dry}	157.7 ± 0.4	19.8 ± 0.7	52.2 ± 0.2	100.5 ± 1.2	12.3 ± 0.6	14.3
PVA/H_2O	161.3 ± 0.1	17.7 ± 0.1	51.5 ± 0.3	107.2 ± 1.8	12.4 ± 0.2	12.8
PVA/H_2O/EtOH	146.6 ± 0.8	16.1 ± 0.6	51.1 ± 0.2	89.1 ± 0.7	8.4 ± 1.0	11.6
PVA70	139.3 ± 0.2	10.9 ± 0.7	/	85.3 ± 0.5	9.4 ± 1.3	7.9
$PVA70_{noEtOH}$	137.3 ± 0.1	11.4 ± 1.1	/	85.2 ± 0.8	9.5 ± 0.5	8.2
PVA70/PEG	157.7 ± 1.0	11.5 ± 0.9	50.9 ± 0.3	109.9 ± 3.5	11.8 ± 0.4	8.3
PVA70/DPG	150.0 ± 0.3	12.1 ± 1.5	51.3 ± 0.1	100.2 ± 0.6	9.1 ± 1.4	8.7
PVA70/MPD	138.8 ± 0.5	11.7 ± 0.5	51.1 ± 0.4	85.3 ± 0.6	8.8 ± 0.3	8.4
PVA70/GLY	121.0 ± 0.6	7.9 ± 0.1	50.0 ± 0.4	54.3 ± 1.3	2.8 ± 0.1	5.7

Table 6.3 Thermal parameters obtained through DSC experiments (second heating cycle) on dry film samples to evaluate the influence of the different additives (e.g. plasticizers). Degree of crystallinity, *DC*% values were determined by using Eq. 6.2, while T_g values are obtained from the first heating cycle.

As for T_g, there is a relationship between the variation of melting temperature T_m and the presence of plasticizers. Fig. 6.3 shows the DSC heating thermograms (second cycle) with the endothermic melting peak, according to the plasticized or unplasticized formulations. A general shift towards lower temperatures is observed for

plasticized samples in respect to the dry PVA or its aqueous solutions, along with the reduction of the enthalpies of fusion values (ΔH_m), obtained from the integrated area of the heating melting peak (see section 6.3.2.1). This behavior is directly connected to the reduction of the crystallinity degree, because plasticizers molecules introduce defects into the crystal lattice by inserting between the polymer chains and favoring their mobility [16]. This behavior prevents chain alignment and thus the formation fo crystalline domains.

Moreover, between the glass transition and the melting temperature, a very slight transition can be observed between 80 °C and 125 °C in the second heating cycle, probably related to residual bounded water.

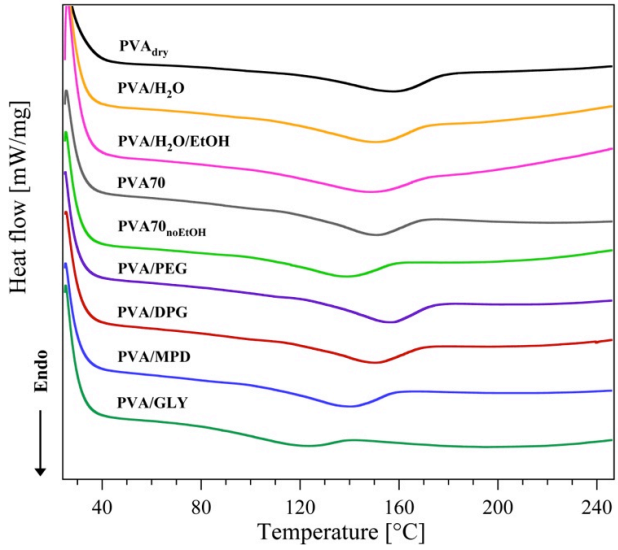

Figure 6.3 DSC thermograms of different film samples (second heating cycle), showing the endothermic melting peak, shifting towards lower temperature with the addition of plasticizers.

A compromise between the formation of crystalline domains and the amorphous regions within the polymer network is of paramount importance to obtain suitable mechanical properties of the final film for an easy and safe removal. In particular low *DC*% values are preferable for our purposes: crystalline domains confer hard-

ness and rigidity to the final film, while the amorphous regions enhance mainly its flexibility, as for plasticizers, thus favoring an easy peeling-off action. Moreover, experimental tests performed by comparing the final properties of films formed from a neat PVA aqueous solution with those from different plasticized formulations, revealed an excessive adhesiveness, which results in a too aggressive peeling action and poor mechanical properties of the sole PVA film (too rigid and brittle, 12.8 *DC*%) in respect to the plasticized samples (for whom the *DC*% values range between 5.7 and 8%). Thus, the presence of both plasticizers and of amorphous regions into the polymeric system, assures a major control over the final adhesiveness, flexibility and tensile resistance of the resulting films. It has to be noticed also that the initial *DC*% values of PVA_{dry} and its aqueous solution (11-14%), are considerably lower than those reported for completely hydrolyzed PVA (40-50%) [21], because of the presence of residual acetate groups on the PVA chains and it is further decreased by the plasticizers effect.

As reported in Tab. 6.3 also the molecular structure of the plasticizers plays a primary role in determining the *DC*% values. In fact small plasticizer molecules, like glycerol, show an enhanced effect in lowering this parameter (up to 5.7%) while for DPG, MPD and PEG higher values have been observed (around 8%). This behavior may be related to their higher molecular size that results in a more difficult insertion between the polymeric chains [17,22–24].

The formulation PVA70, prepared with the addition of four different plasticizers, displays a *DC* value of 7.9%, almost the half in respect to the dry PVA powder (14.3%), due to the combined action of the mixed molecules.

Also the presence of ethanol influences the crystallinity degree, by inhibiting the formation of ordered domains: the high evaporation rates of the liquid phase result in a faster development of the glassy region during film formation, as explained in Chapter 3 (section 3.4), thus preventing further crystallinity formation. In fact, as indicted in Tab. 6.3, the formulations PVA/H_2O/EtOH and PVA70, are characterized by lower *DC*% values than the same formulations without ethanol (PVA/H_2O and $PVA70_{noEtOH}$ respectively).

ATR-FTIR experiments, on the same film samples, were carried out to confirm data obtained through DSC measurements. In fact the values of the ratio I_{1141}/I_{1089} are proportional to the degree of crystallinity, as previously described in section 6.3.2.2. Peak intensities were obtained from the ATR-FTIR spectra of dried films as reported in Fig. 6.4, after baseline subtraction.

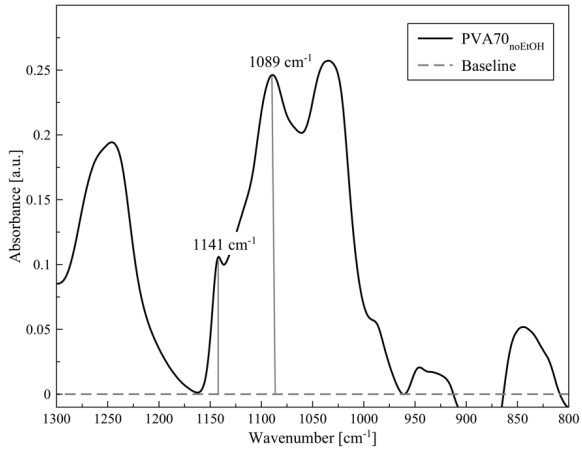

Figure 6.4 ATR-FTIR spectrum of sample $PVA70_{noEtOH}$ after baseline subtraction (dotted line), obtained with MagicPlotPro®. Intensities of the crystalline peak at 1141 cm^{-1} and of the amorphous peak at 1089 cm^{-1} are showed.

Formulation	**ATR-FTIR [cm^{-1}]**		
	I_{1141} [$\times 10^{-3}$]	**I_{1089} [$\times 10^{-3}$]**	**I_{1141}/I_{1089} [$\times 10^{3}$]**
PVA_{dry}	64.8 ± 0.8	130.1 ± 0.5	498.1 ± 16
PVA/H_2O	167.1 ± 1.2	343.6 ± 0.9	490.3 ± 9.7
PVA/H_2O/EtOH	162.7 ± 0.3	339.1 ± 0.3	479.5 ± 2.6
PVA70	98.5 ± 0.9	242.7 ± 4.0	405.8 ± 25
$PVA70_{noEtOH}$	105.3 ± 0.2	246.5 ± 0.4	427.2 ± 3.5
PVA70/PEG	164.3 ± 1.1	345.4 ± 6.0	475.6 ± 24
PVA70/DPG	128.8 ± 0.4	269.7 ± 0.6	477.6 ± 5.3
PVA70/MPD	115.7 ± 1.2	243.4 ± 0.4	475.3 ± 12
PVA70/GLY	61.3 ± 1.1	196.9 ± 1.2	311.3 ± 24

Table 6.4 Crystalline (1141 cm^{-1}) and amorphous (1089 cm^{-1}) peak intensities for the analyzed dry film samples. I_{1141}/I_{1089} represents a qualitative index, proportional to the crystallinity of the samples.

The results displayed in Tab. 6.4 are in accordance with the trend observed for DSC *DC*%, although complete percent values were not calculated. Moreover the error associated to some ratios values are, in some cases, very high because the intensity related to the crystalline-dependent peak at 1141 cm^{-1}, was often not very simple to identify. In fact, due to the low crystallinity of the film samples, the peak at 1141 cm^{-1} is often not well defined. However the general trend of the calculated values perfectly reflects that from DSC measurements, where the unplasticized samples show higher crystallinity values in respect to one- or four-plasticized formulations. The one plasticized with glycerin shows also in this case the lowest crystallinity value, while the combination of four plasticizers results in a further decrease of *DC*%, in respect to one-plasticized formulations.

The time required, for the different formulations, to attain the complete evaporation of the volatile fraction (and indirectly the film formation) was evaluated by means of isothermal thermogravimetric measurements at 40°C (TGA), as described in section 6.3.1.2. Data reported in Tab. 6.5 indicate that the volatile fraction loss occurs earlier for aqueous PVA solutions without the addition of plasticizers (formulations PVA/H_2O, 66 min, and PVA/H_2O/EtOH, 68 min). Longer times (102-213 min) are required for formulations containing plasticizers, which hinder the evaporation process on different extent, depending on their retentive power and molecular sizes.

Formulations PVA74, PVA70 and PVA68, characterized by the same polymer content but different volatiles and plasticizers amounts (see Tab. 6.1), require less time for the complete loss of the volatile fraction than the one-plasticized formulations, thus representing the most suitable candidates for the applicative tests (see Fig. 6.5). In fact reduced times for film formation are preferable to attain more control over the cleaning procedure, because:

- too hours required for the formation of the film would result in scarce advantage in terms of time in respect to traditional cleaning methods;

- fast formation of the film assures the possibility of frequently controlling the evolution of the cleaning process, carried out through complexing reactions;
- the cleaning system can be applied for numbers of times required to obtain the desired level of cleaning during a single working day.

Formulation	TGA [min]
PVA/H_2O	66
PVA/H_2O/EtOH	68
PVA74	109
PVA70	102
PVA68	133
$PVA70_{noEtOH}$	135
PVA70/PEG	164
PVA70/DPG	200
PVA70/MPD	213
PVA70/GLY	205

Table 6.5 Time (min) required for the complete evaporation of the volatile fraction obtained through isothermal TGA experiments (40°C) for different formulations.

In particular PVA70 formulation presents the best properties for applicative purposes, because of its rapid film formation (see Fig. 6.5, 102 min), intermediate amount of liquid fraction and plasticizers content (which confer an initial consistency suitable for application on different surfaces) and very good mechanical properties of the final peelable film (7.9 DC%). The relative DSC thermograms (see inset Fig. 6.5) show an endothermic peak before the complete evaporation of the volatile fraction is completed, ascribable to a change in the evaporation rate. This probably represents the formation of an entirely glassy system, where the residual volatile fraction is almost completely evaporated and the process of film formation is completed. Gravimetric curves (see Fig. 6.2 (a) and Fig. 6.6 (a)) confirm that the formation of the film generally occurs before the complete evaporation of the volatile fraction.

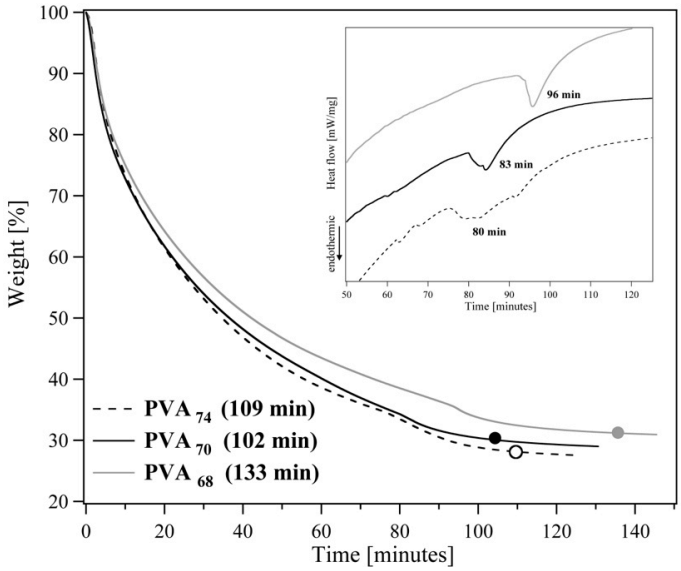

Figure 6.5 Isothermal TG thermograms (40°C) of three formulations with different volatiles and plasticizers content; complete evaporation of the volatile fraction is achieved in correspondence of the highlighted dots; inset: relative DSC curves showing an endothermic peak ascribable to the completion of the film formation process.

6.4.3 Effect of the complexing agent

The effect of the complexing agent on the overall polymeric system properties (PVA70) was studied by adding increasing quantities of EDTA (1-3% w/w) at two different pH values (7 and 9), as reported in Tab. 6.2. The presence of a complexing agent, in fact, should not negatively affect the initial consistency of the system, the evaporation rate and the final film mechanical properties.

The maximum amount of loaded EDTA was around 3-4% w/w, since ethanol acts as insolubilizing agent for this chelator, causing phase separation processes over this threshold (see Fig. 5.8).

Gravimetric data (Fig. 6.6 (a)) show that upon raising the EDTA amount, an increase in the evaporation rate of the volatile fraction occurs, allowing further applicative advantages thanks to the reduced times needed for film formation. This behavior is also confirmed by DTG experiments: the position of the peak attributed

to the evaporation process (Fig. 6.6 (b)), shifts towards lower temperatures as the content of the complexing agent increases (from 100 °C for the formulation without EDTA up to 90 °C for the formulation containing 3% w/w EDTA).

This trend can be ascribed to the increase in polymer chain entanglements and vicinity, induced by EDTA, acting as a sort of cross-linker [25]. The modification of the 3-D polymer network structure results in higher entanglements and crystalline domains formation, with a consequent reduction of the number of sites available for hydrogen bonds formation with H_2O and ethanol molecules. This results in less volatile fraction molecules linked to the PVA chains, that are thus free to evaporate. The higher *DC*% values, of about 9% for formulations containing EDTA (8.9 for 1% EDTA, 9.0 for 2% EDTA, 9.3 for 3% EDTA pH 7 and 9.2 for 3% EDTA pH 9), in respect to the same formulation without added EDTA (PVA70, 7.9 *DC*%), confirm the theory of an increase in the overall cristallinity, due to EDTA-induced cross-links that favor chains vicinity.

Finally, also the pH value, regulated by the addition of NH_3 solution, has a further influence on the evaporation rate, as reported in Fig. 6.6 (b) (maximum at 96 ºC for pH 7 and at 90 ºC for pH 9 with the same EDTA content).

The comparison between PVA70 formulations loaded with different complexing agents (EDTA and Rochelle salt) in different concentrations (3% and 6% w/w respectively), was carried out by means of isothermal thermogravimetric experiments (see Fig. 6.7). The presence of tartrate molecules considerably hinders the evaporation process of the volatile fraction in respect to the EDTA-loaded or not loaded PVA70 formulations. The higher amount of loadable Rochelle salt and its higher hygroscopy, in respect to EDTA, causes a major retentive power towards the water molecules, thus extending the times required for film formation. On the other hand, the presence of EDTA slightly lowers the evaporation rate and film formation, in respect to the sole PVA70 formulation, thus confirming gravimetric and thermogravimetric data obtained in scanning mode, reported above.

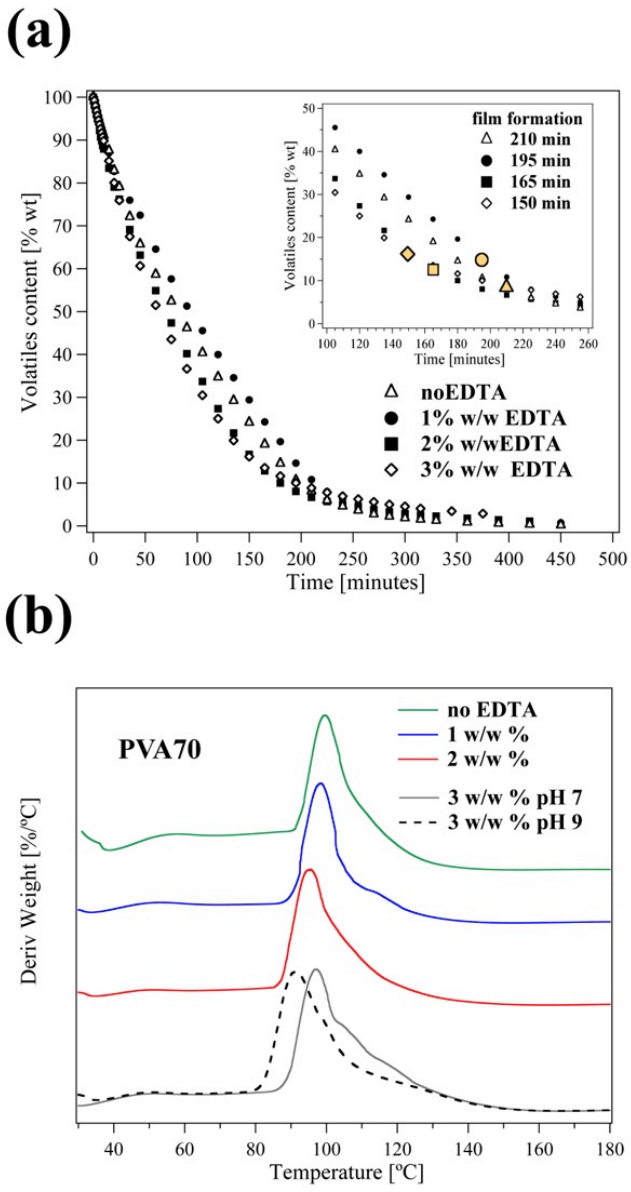

Figure 6.6 (a): gravimetric evaporation curves of PVA70 formulations with increasing EDTA content; inset: complete film formation occurred in correspondence of the solid symbols. (b): DTG thermograms of PVA70 formulations with increasing EDTA content and different pH; the displayed maxima of the derivatives weight loss represent the evaporation temperatures of the volatile fraction.

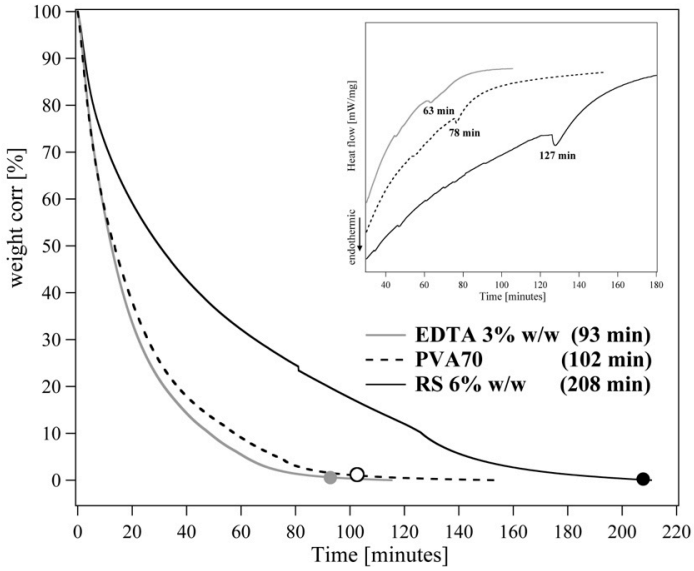

Figure 6.7 Isothermal TG thermograms (40°C) of PVA70 formulations with different amounts (3% and 6% w/w) of complexing agents (respectively EDTA and Rochelle salt); complete evaporation of the volatile fraction is achieved in correspondence of the solid symbols; inset: relative DSC curves showing an endothermic peak ascribable to the completion of the film formation process at different times.

6.4.4 The evolution of the viscoelastic behavior through time

In order to follow the evolution of the mechanical properties of PVA70 during the evaporation of the liquid phase, a rheological characterization of the not loaded (*NL*) and 3% w/w EDTA pH 7 loaded (*EL*) system has been carried out at room temperature, as a function of time.

Frequency sweep tests show a prevalent viscous behavior with $G' < G''$ over almost the entire range of explored frequencies. A cross-over between G' and G'' moduli is observed at high frequencies (see Fig. 6.8), as typical for entangled networks (see Chapter 2, section 2.2.1) [26,27]. As the volatile fraction evaporates, the increase of the G' values indicates a progressive enhancement of entanglement density between polymer chains, due to the formation of inter- and intra-molecular H-bonds. Furthermore, the increase of both the apparent relaxation time τ_c, (defined as

ω_c^{-1}, where ω_c is the crossover frequency between *G'* and *G''* curves) and of the cross-over modulus (G_c) indicates an enhancement of the solid-like character of the system, as reported in Fig. 6.8.

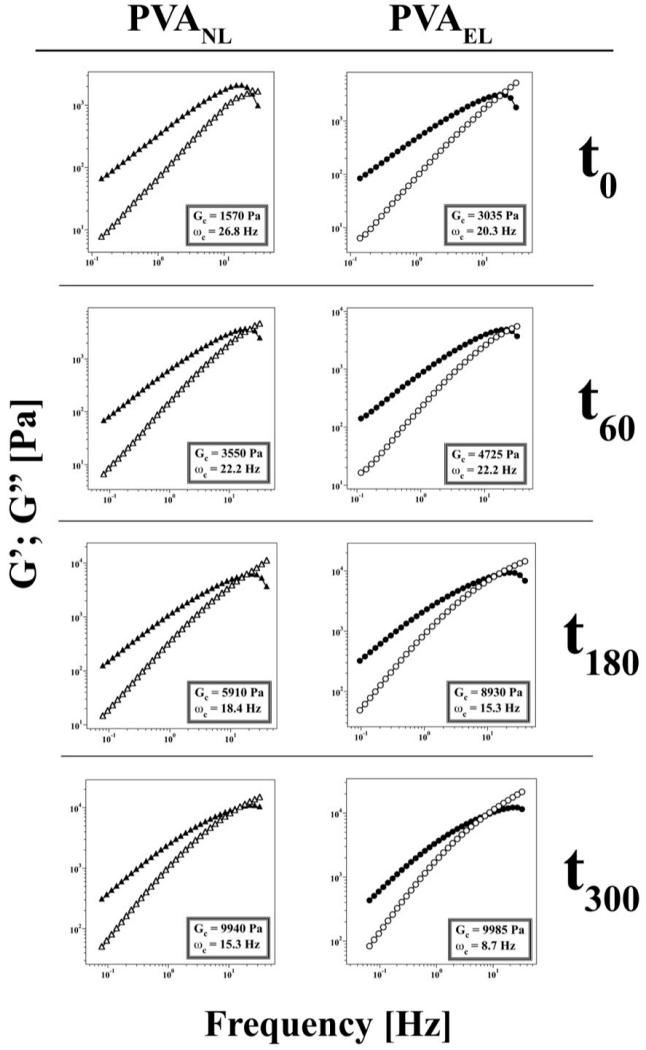

Figure 6.8 Frequency sweep curves reported in function of four different times for both the *NL* and *EL* system. Solid symbols (▲and ●) represent the loss modulus (*G''*) while empty symbols (△ and ○) the storage modulus (*G'*). Each image shows an inset with the cross-over parameters, showing the progressive shift towards higher frequencies for the cross-over modulus G_c, and towards lower frequencies for the cross-over frequency ω_c, with time (expressed in minutes).

The variations in the viscoelastic behavior through time indicate that the system evolves from an initial high viscous polymeric dispersion, towards a final solid-like film. In fact, frequency sweep curves concerning the final films (see section 6.3.1.3 for film sample preparation) are characterized by the absence of a crossover between *G'* and *G''* curves: the *G'* values always higher than *G''* all over the investigated frequency range, indicate that the system is characterized by a solid-like behavior (as reported for the *EL* system in Fig. 6.9 and in Chapter 2, section 2.2.1).

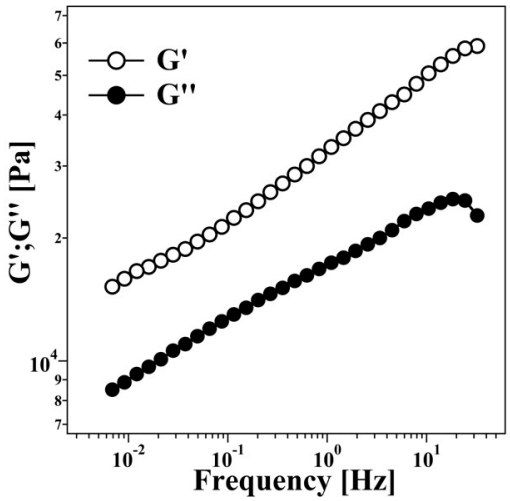

Figure 6.9 EDTA-loaded system frequency sweep curves of the dry film, where the storage modulus *G'* is always higher than the loss modulus *G''* and no cross-over occurs between them, thus indicating a solid-like behavior of the final film.

In Fig. 6.10 the trend of the storage modulus *G'* at a fixed frequency (5 Hz) is reported for $PVA70_{NL}$ and $PVA70_{EL}$ as a function of time (between 0 min and 300 min). Upon the evaporation of the liquid phase, for both samples, a progressive increase of the *G'* values occurs indicating the formation of an increasingly stronger 3-D network. In particular, the additional EDTA-induced entanglements between the PVA chains make the G'_{EL} values always higher than the G'_{NL} ones. Once the films are obtained, the value of the G'_{EL} modulus is almost the double (7000 Pa) in respect to that of the *NL* system (4500 Pa). From the applicative point of view, the

magnitude of the *G'* modulus, in particular for the *EL* system, guarantees an ease and safe (without residues) removal of the final film, in one piece simply by means of a peeling-off action.

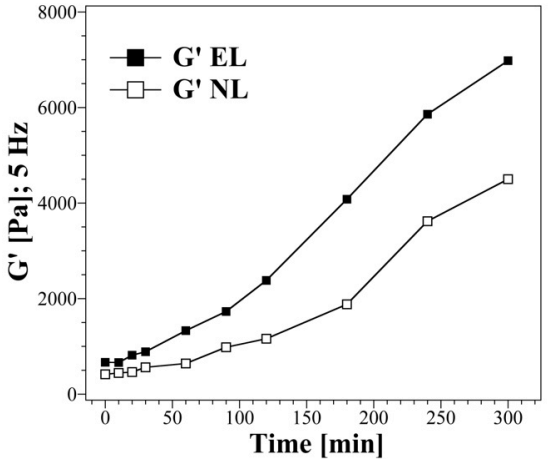

Figure 6.10 Storage modulus (*G'*) values at 5 Hz reported in function of time for the *NL* and *EL* systems. Both the increase of the elastic modulus with the evaporation of the volatile fraction, and the *EL* values always higher than the *NL* formulation, indicate the progressive formation of a stronger 3-D network (5% calculate error).

Flow curves obtained by rotational experiments show shear thinning viscosity (η) behavior (see Chapter 2, section 2.3.1), particularly evident at high shear values (see Fig. 6.11). The zero shear viscosity (η_0) values of both the *NL* and *EL* formulation are reported in Fig. 6.12 and Tab. 6.6.

	η_0	
	PVA_{NL}	**PVA_{EL}**
t_0	80	97
t_{120}	202	406

Table 6.6 η_0 values for two different times acquired in the low-Newtonian region and reported for the *NL* and *EL* PVA70 formulations.

In particular a linear growth of zero shear viscosity is observed until 240 min, after which, an abrupt increase of η_0 suggests a further enhancement of the 3-D network

structure. The observed values of η_0 for the *EL* system are always higher than the *NL* ones, thus confirming the EDTA-induced extra-bonds formation, with a η_0 value starting from ca. 100 Pa·s, for both systems, towards one order of magnitude for the *NL* and of two orders higher values for the *EL* system.

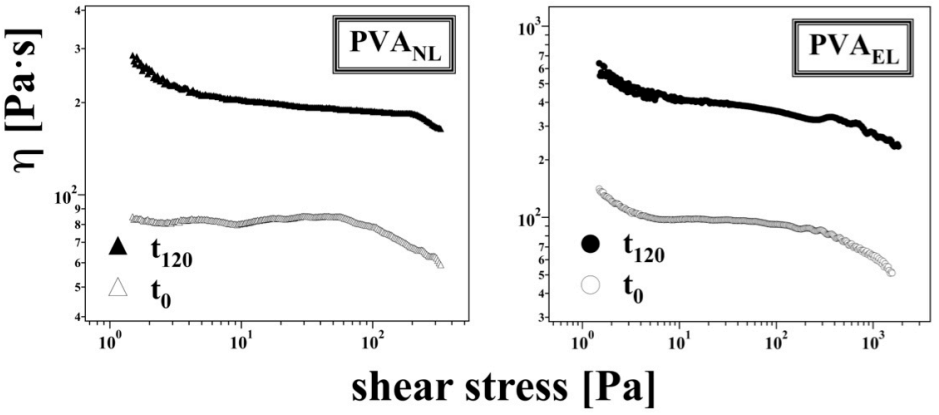

Figure 6.11 Flow curves of both the *NL* and *EL* system at two different times (t_0 and t_{120}) showing a shear thinning behavior. Viscosity increases with time and the values of the *EL* systems are always higher than the *NL* ones.

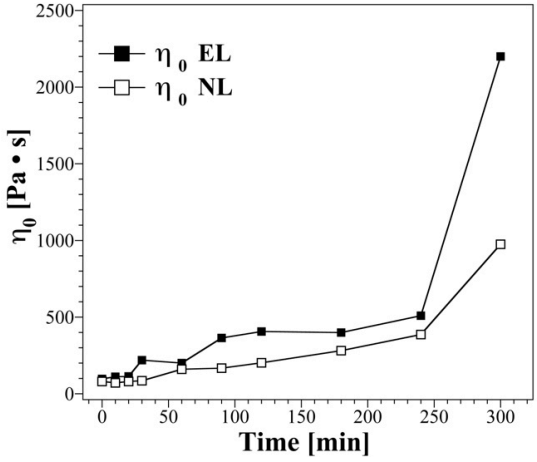

Figure 6.12 Zero shear viscosity (η_0) values acquired in the low-Newtonian region (at 10 Pa), reported in function of time for both *NL* and *EL* formulations.

6.5 Bibliography

[1] DOMINGUES, J.A.L., BONELLI, N., GIORGI, R., FRATINI, E., GOREL, F., AND BAGLIONI, P. *Innovative Hydrogels Based on Semi-Interpenetrating p(HEMA)/PVP Networks for the Cleaning of Water-Sensitive Cultural Heritage Artifacts.* Langmuir *29*, (**2013**), 2746–2755.

[2] JELINSKA, N. AND KALNINS, M. *Poly(vinyl alcohol)/poly(vinyl acetate) blend films.* Scientific Journal of Riga Technical University *21*, (**2010**), 55–61.

[3] NGUI, M.O. AND MALLAPRAGADA, S.K. *Understanding isothermal semicrystalline polymer drying: mathematical models and experimental characterization.* Journal of Polymer Science *36*, (**1998**), 2771–2780.

[4] MALLAPRAGADA, S.K. AND PEPPAS, N.A. *Dissolution mechanism of semicrystalline Poly(vinyl alcohol) in water.* Journal of Polymer Science *34*, (**1996**), 1339–1346.

[5] PEPPAS, N.A. AND MERRILL, E.W. *Differential scanning calorimetry of crystallized PVA hydrogels.* Journal of Applied Polymer Science *20*, (**1976**), 1457–1465.

[6] TRETINNIKOV, O.N. AND ZAGORSKAYA, S.A. *Determination of the degree of crystallinity of poly(vinyl alcohol) by FTIR spectroscopy.* Journal of applied Spectroscopy *79*, 4 (**2012**), 538–543.

[7] WONG, S., ALTINKAYA, S.A., AND MALLAPRAGADA, S.K. *Understanding the effect of skin formation on the removal of solvents from semicrystalline polymers.* Journal of Polymer Science Part B: Polymer Physics *43*, (**2005**), 3191–3204.

[8] WONG, S., ALTINKAYA, S.A., AND MALLAPRAGADA, S.K. *Crystallization of Poly(vinyl alcohol) during solvent removal: infrared characterization and mathematical modeling.* Journal of Polymer Science *45*, (**2007**), 930–935.

[9] KENNEY, J.F. AND WILLCOCKSON, G.W. *Structure–property relationships of poly(vinyl alcohol). III. Relationships between stereo-regularity, crystallinity, and water resistance in poly(vinyl alcohol).* Journal of Polymer Science Part A-1: Polymer Chemistry *4*, 3 (**1966**), 679–698.

[10] LEE, J., JIN LEE, K., AND JANG, J. *Effect of silica nanofillers on isothermal crystallization of poly(vinyl alcohol): In-situ ATR-FTIR study.* Polymer Testing *27*, 3 (**2008**), 360–367.

[11] MANSUR, H.S., SADAHIRA, C.M., SOUZA, A.N., AND MANSUR, A.P. *FTIR spectroscopy characterization of poly(vinyl alcohol) hydrogel with different hydrolysis degree and chemically crosslinked with glutaraldehyde.* Materials Science and Engineering C *28*, 4 (**2008**), 539–548.

[12] PEPPAS, N.A. *Infrared spectroscopy of semicrystalline poly(vinyl alcohol)*

networks. Die Makromolekulare Chemie *178*, 2 (**1977**), 595–601.

[13] SUSHKO, N.I., ZAGORSKAYA, S.A., AND TRETINNIKOV, O.N. *Infrared spectra and structure of poly(vinyl alcohol) film obtained from aqueous solutions with potassium iodide additive.* Journal of applied Spectroscopy *80*, 5 (**2013**), 677–680.

[14] BUSLOV, D.K., SUSHKO, N.I., AND TRETINNIKOV, O.N. *IR investigation of hydrogen bonds in weakly hydrated films of poly(vinyl alcohol).* Polymer Science Series A *53*, 12 (**2011**), 1121–1127.

[15] LAMANNA, R. AND CANNISTRARO, S. *Effect of ethanol addition upon the structure and the cooperativity of the water H bond network.* Chemical Physics *213*, 1–3 (**1996**), 95–110.

[16] JANG, J. AND LEE, D.K. *Plasticizer effect on the melting and crystallization behavior of polyvinyl alcohol.* Polymer *44*, (**2003**), 8139–8146.

[17] LIM, L.Y. AND WAN, L.S.C. *The effect of plasticizers on the properties of polyvinyl alcohol films.* Drug Development and Industrial Pharmacy *20*, 6 (**1994**), 1007–1020.

[18] PU-YOU, J., CAI-YING, B., LI-HONG, H., AND YONG-HONG, Z. *Properties of poly(vinyl alcohol) plasticized by glycerin.* Journal of Forest products and Industries *3*, 3 (**2014**), 151–153.

[19] FOX, T.G. AND FLORY, P.J. *Second-order transition temperatures and related properties of polystyrene.* Journal of Applied Physics *21*, 6 (**1950**).

[20] KELLEY, F.N. AND BUECHE, F. *Viscosity and glass temperature relations for polymer-diluent systems.* Journal of Polymer Science *50*, 154 (**1961**), 549–556.

[21] HASSAN, C.M. AND PEPPAS, N.A. *Structure and Applications of Poly (vinyl alcohol) Hydrogels Produced by Conventional Crosslinking or by Freezing / Thawing Methods.* Advances in polymer science *153*, (**2000**).

[22] FELDSTEIN, M.M., KUPTSOV, S.A., SHANDRYUK, G.A., AND PLATE, N.. A. *Relation of glass transition temperature to the hydrogen-bonding degree and energy in poly(N-vinyl pyrrolidone) blends with hydroxyl-containing plasticizers. Part 2. Effects of poly(ethylene glycol) chain length.* Polymer *42*, (**2001**), 981–990.

[23] FELDSTEIN, M.., SHANDRYUK, G.., AND PLATÉ, N.. *Relation of glass transition temperature to the hydrogen-bonding degree and energy in poly(N-vinyl pyrrolidone) blends with hydroxyl-containing plasticizers. Part 1. Effects of hydroxyl group number in plasticizer molecule.* Polymer *42*, 3 (**2001**), 971–979.

[24] FELDSTEIN, M.M., ROOS, A., CHEVALLIER, C., CRETON, C., AND DORMIDONTOVA, E.E. *Relation of glass transition temperature to the hydrogen bonding degree and energy in poly(N-vinyl pyrrolidone) blends with hydroxyl-containing plasticizers: 3. Analysis of two glass transition temperatures featured for PVP solutions in liquid poly(ethyle.* Polymer *44*, 6 (**2003**), 1819–1834.

[25] CA, V., RUIZ, J., AND MANTECO, A. *Synthesis and properties of hydrogels from poly (vinyl alcohol) and ethylenediaminetetraacetic dianhydride. 42*, (**2001**), 6347–6354.

[26] ANGELOVA, L.V., TERECH, P., NATALI, I., DEI, L., CARRETTI, E., AND WEISS, R. G. *Cosolvent gel-like materials from partially hydrolized poly(vinyl acetate)s and borax.* Langmuir *27*, 18 (**2011**), 11671–11682.

[27] E., C. *Physicochemical characterization of partially hydrolized poly(vinyl acetate)-borate aqueous dispersions.* Soft Matter, (**2014**).

Chapter 7

Applicative tests on artificially aged samples

7.1 Introduction

Cleaning of Cultural Heritage artifacts represents one of the most delicate operations within the restoration process, because it is potentially invasive and aggressive for the original materials as well as completely irreversible. As discussed in Chapter 1 (section 1.4), an adequate cleaning procedure of a copper-based alloy should aim at the complete removal of the esthetically defacing and harmful corrosion products and also at the preservation of the protective cuprite layer.

Traditional cleaning involves the use of both mechanical and chemical methods, depending on the morphology and typology of the *patina*, both characterized by advantages and drawbacks (see Chapter 1, sections 1.4.1 and 1.4.2). During this PhD project an alternative polymer-based cleaning tool was developed, which combines both a mechanical action, thanks to the peeling-off removal of the final film, with a chemical action, thanks to the presence of a complexing agent.

In order to find the best combination between polymeric formulations and complexing agents, able to ensure a controlled and selective cleaning action, several tests were performed over artificially aged Cu-based samples, provided by the ISMN-CNR of Rome (Monterotondo).

These samples reproduced typical ancient bronze alloys and archaeological *patina*, thanks to a procedure developed at ISMN-CNR laboratories. The metallic samples were first characterized by means of a set of instruments and methodologies commonly used for the study of ancient metallic artifacts, in order to have a com-

plete knowledge of the products to remove with the cleaning tests. After the identification of the corrosion products, cleaning tests were performed through a wide range of polymeric systems, loaded with different complexing agents, to select suitable and effective combinations applicable on real cases studies.

7.2 Artificially aged samples production

The availability of reference artificial samples that can be sacrificed, instead of more precious archaeological artifacts, is of paramount importance for testing new materials for cleaning and procedures for the inhibition of corrosion. Ingo et al. [1] developed a procedure aimed to the production of Cu-based alloys with chemical and metallurgical features similar to ancient alloys, for carrying out accelerated degradation processes to reproduce *patina* and corrosion products as similar as possible to the archaeological ones [2–4]. The study of the most common corrosion products grown on archaeological Cu-based artifacts and of the metallurgical features of the alloys revealed the quite ubiquitous and nearly constant presence of chlorine as the main corroding agent, as well as the typical structures of the alloys [1].

The artificially-induced degradation methods were based on soil, chemical and combined chemical+soil degradation, where the last one produced the most similar *patina*, from a chemical, structural and micro-morphological point of view, to those grown on archaeological artifacts. The sole chemical-induced degradation method gave, as result, the fast growth of a *patina* with composition similar to the ancient one, but not very cohesive and adherent to the substrat. Cleaning tests were performed on both chemically aged and buried samples.

7.2.1 Production of the reference bronze alloys

Ingots of Cu-Sn alloy were produced in an electrically heated furnace at 1100 °C by using graphite crucibles purposely designed in order to tailor the solidification and cooling behavior of the alloys and, therefore, their metallurgical features. Cop-

per-iron sulphides and zinc, which are commonly found in ancient Cu-based alloys as inclusions or alloying element respectively, were added to the melt before casting, in order to produce samples with micro-chemical structure and metallurgical features similar to those of ancient alloys. Two representative compositions, listed in Tab. 7.1, were chosen for the production of reference bronze alloys (CNR128 and CNR 143).

CNR 128	**Cu**	**Sn**	**Pb**	**$CuFeS_2$**
	92.3	7.5	0.2	0.2
CNR143	**Cu**	**Sn**	**Pb**	**Zn**
	91.6	7.5	0.2	0.5

Table 7.1 Composition in % w/w of the two reference alloys used for the artificial degradation process.

Disks of reference alloys with diameter of about 20-30 mm and thickness of 2-3 mm (see Fig. 7.2) were used for carrying out the accelerated degradation experiments, with the procedure reported in the following section.

7.2.2 Production of the artificial patina

In order to simulate the *patina* of real archaeological bronze artifacts, the reference alloys substrates were degraded by an accelerated corrosion procedure that involves a chemically induced degradation and a subsequent period of aging (artificial weathering). The chemical treatment entails the selective formation of a cuprite (Cu_2O) layer and of copper-chloride compounds, by using a 0.1 M $CuCl_2$ solution and 0.5 M NaCl solution. Micro-drops of these solutions were sprayed onto the surface of the reference bronze alloys and the samples were exposed to moisture and air in a sealed glass container, where distilled water ensured a high humidity level (100% RH) or an HCl solution further enhanced the corrosion process, as reported in Fig. 7.1. The glass container was then placed in an electrically heated stove at a selected temperature (30 °C or 60 °C) for days (from 3 up to 15), depending on the desired progress of the reaction. After this procedure, the artificially corroded alloys

already present a preliminary *patina*: some samples were kept in this intermediate state, while other samples were further buried in an archaeological soil, thus inducing the formation of more complex corrosion products (see Fig. 7.2) [5–8]. Since the nature of the soil is of primary importance for the formation of a *patina* as similar as possible to the real archaeological buried metals [1], the chemically corroded bronzes were embedded in some soil samples from the archaeological site of Tharros (western Sardinia, Italy), typical of a marine environment, for a minimum of 6 months up to years.

The alloys and the accelerated aging treatments used for the production of the artificial samples are summarized in Tab. 7.2.

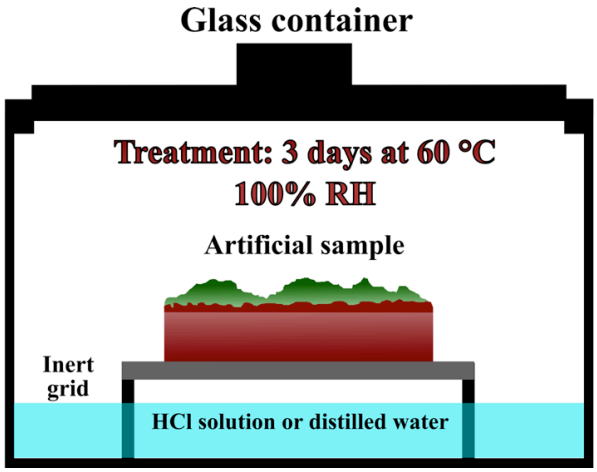

Figure 7.1 Sealed glass container used for the accelerated degradation methodology of Cu-base alloy samples: the alloy sample is placed over an inert grid and kept at controlled temperature and high relative humidity level; distilled water can be substituted by HCl solution, thus further accelerating the corrosion process.

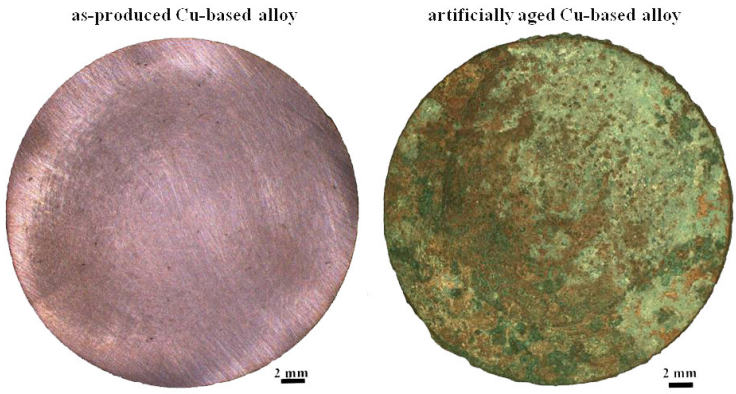

Figure 7.2 The as-produced bronze alloy (left) and its appearance (right) after the artificial aging (chemical treatment+burial of several months) [9].

Alloy	chemically aged samples (CAS)		burial natural age (BNA)
	water	HCl	(two sides)
CNR128	CAS1	CAS5	**BNA1**
	CAS2	**CAS6**	**BNA2**
	CAS3	**CAS7**	
	CAS4	CAS8	
	CUP1	/	**CUP2**
CNR143	**CAS10**	/	**BNA3**
	CAS11		**BNA4**

Table 7.2 The artificially aged samples for the cleaning tests were prepared starting from two different alloys, aged with a sole chemical treatment (CAS samples) or further buried in archaeological soil for several months or years (BNA samples) in order to produce a *patina* more similar to the ancient one. Also samples with only a cuprite layer (CUP) were prepared. Only the characterization of bold samples is reported in section 7.3.2.

Samples with only a cuprite layer were also prepared, by exposing the metallic sample to oxygen and moisture at a given temperature (CUP1) and by embedding the sample in archaeological soil, without any previous chemical treatment (CUP2).

The obtained samples were then subject to surface characterization through a set of techniques commonly used in the study of ancient metals [10–13]: optical microscopy (OM), scanning electron microscopy with energy dispersive X-ray analy-

sis (SEM/EDS), X-ray diffraction (XRD) and μ-FTIR spectroscopy, already described in Chapter 1 (section 1.3.4). Each sample were characterized by the above-mentioned techniques, but only the most relevant, considering the cleaning tests results, will be reported.

7.3 Artificial samples characterization

7.3.1 Instrumental conditions

The artificial patina of the chemically aged samples (CAS) was characterized by means of FTIR spectroscopy in micro-reflectance mode using a Thermo Nicolet (Nexus 80) spectrometer equipped with a microscope and a MCT detector to collect the signal in the 4000-650 cm^{-1} range. A gilded surface was used to collect the background and the spectra were acquired at 128 scans and 4 cm^{-1} of resolution with Kubelka-Munk conversion.

Raman measurements for the residues analysis were performed with a Renishaw spectrometer equipped with a cooled CCD detector in conjunction with a Leica microscope. A 100X objective was used to focus the laser light on the samples and to collect the Raman signal. The excitation light was the 514.5 nm line of an argon ion laser. The spectra were processed by the Fityk 0.9.8 software.

X-ray diffraction and SEM-EDS investigations were performed to obtain information on the composition of the buried artificial sample. The structural identification of crystalline phases was determined by a Siemens 5000 X-ray powder diffractometer using a Ni-filtered Cu K_α radiation (λ = 1. 5418 Å). Angular values in the range between 10° and 80° in additive mode, a step size of 0.05° and a sampling time of 2 s were the experimental parameters used for data acquisition. In order to identify the crystalline species, X-ray diffraction patterns analysis was carried out by using electronic databases.

Metallic samples surface were studied firstly through optical microscopy with a stereomicroscope LEICA (Multifocus). Then SEM-EDS characterization was carried out through a Cambridge 360 scanning electron microscope equipped with a

LaB_6 filament, an energy-dispersive X-ray spectrometer (EDS) INCA 250 and a four-sector backscattered electron detector (BSE).

7.3.2 Characterization data sheets

The results of the surface analysis for selected samples will be presented as data sheets. Samples aged through only a chemical treatment (CAS) can be used for cleaning tests only by one side, while buried samples (BNA) have two sides available for the tests. Moreover, CAS samples present a *patina* less adherent and cohesive in respect to the BNA samples, but their production require less time (hours) instead of months or years. For this reason CAS samples were used for 'pre-preliminary' cleaning tests, before the preliminary tests over the more complex and similar to ancient *patina* BNA samples.

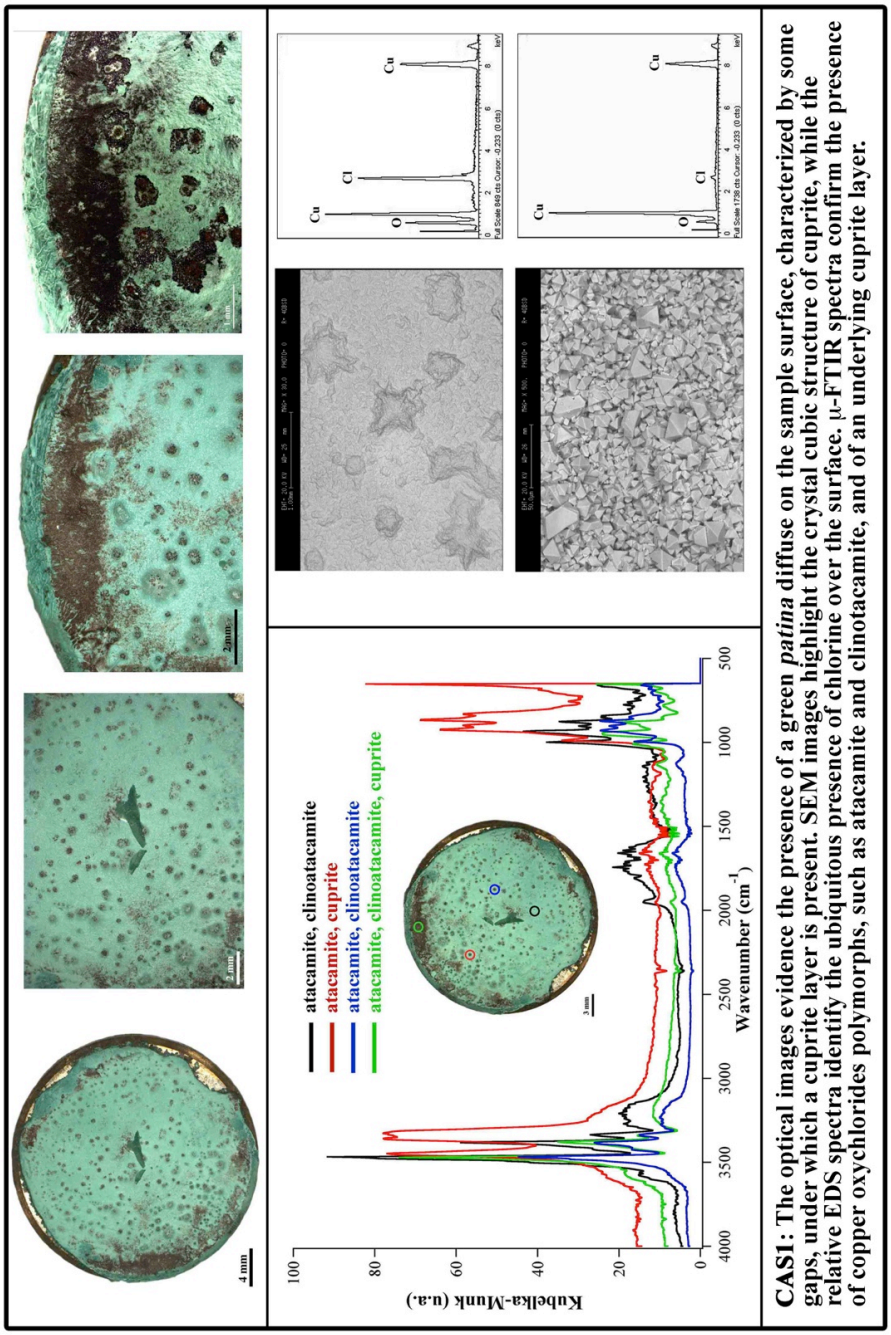

CAS1: The optical images evidence the presence of a green *patina* diffuse on the sample surface, characterized by some gaps, under which a cuprite layer is present. SEM images highlight the crystal cubic structure of cuprite, while the relative EDS spectra identify the ubiquitous presence of chlorine over the surface. μ-FTIR spectra confirm the presence of copper oxychlorides polymorphs, such as atacamite and clinotacamite, and of an underlying cuprite layer.

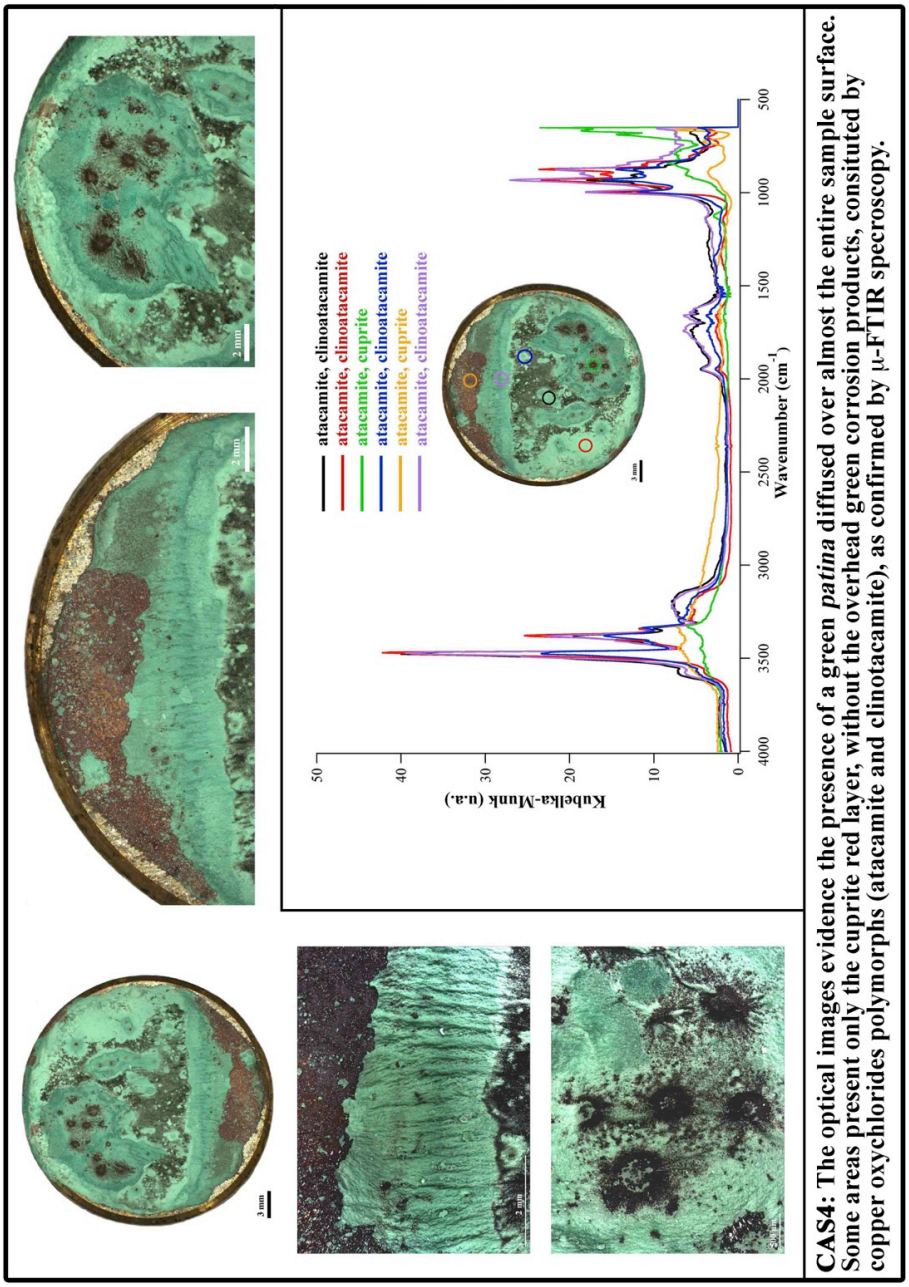

CAS4: The optical images evidence the presence of a green *patina* diffused over almost the entire sample surface. Some areas present only the cuprite red layer, without the overhead green corrosion products, consituted by copper oxychlorides polymorphs (atacamite and clinotacamite), as confirmed by μ-FTIR specroscopy.

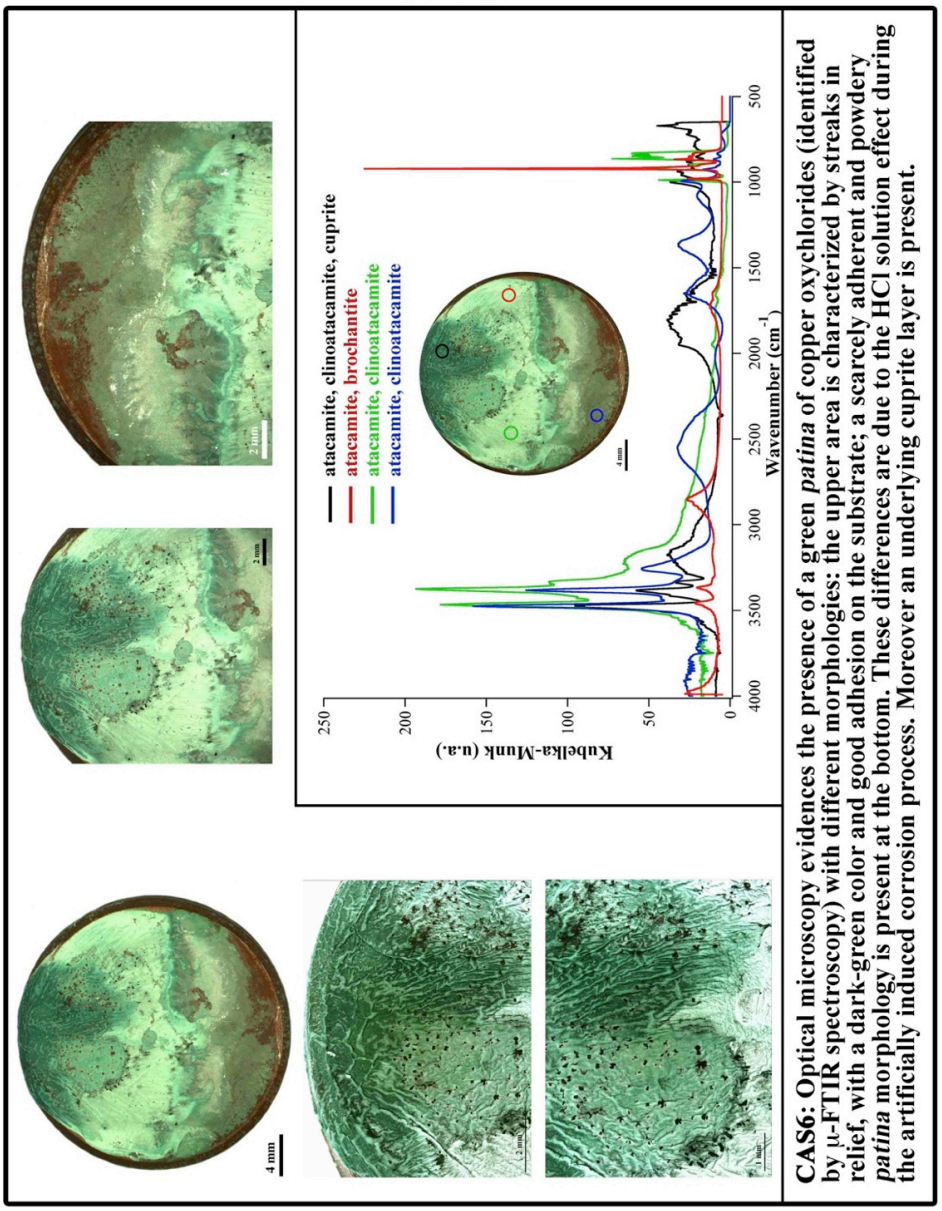

CAS6: Optical microscopy evidences the presence of a green *patina* of copper oxychlorides (identified by μ-FTIR spectroscopy) with different morphologies: the upper area is characterized by streaks in relief, with a dark-green color and good adhesion on the substrate; a scarcely adherent and powdery *patina* morphology is present at the bottom. These differences are due to the HCl solution effect during the artificially induced corrosion process. Moreover an underlying cuprite layer is present.

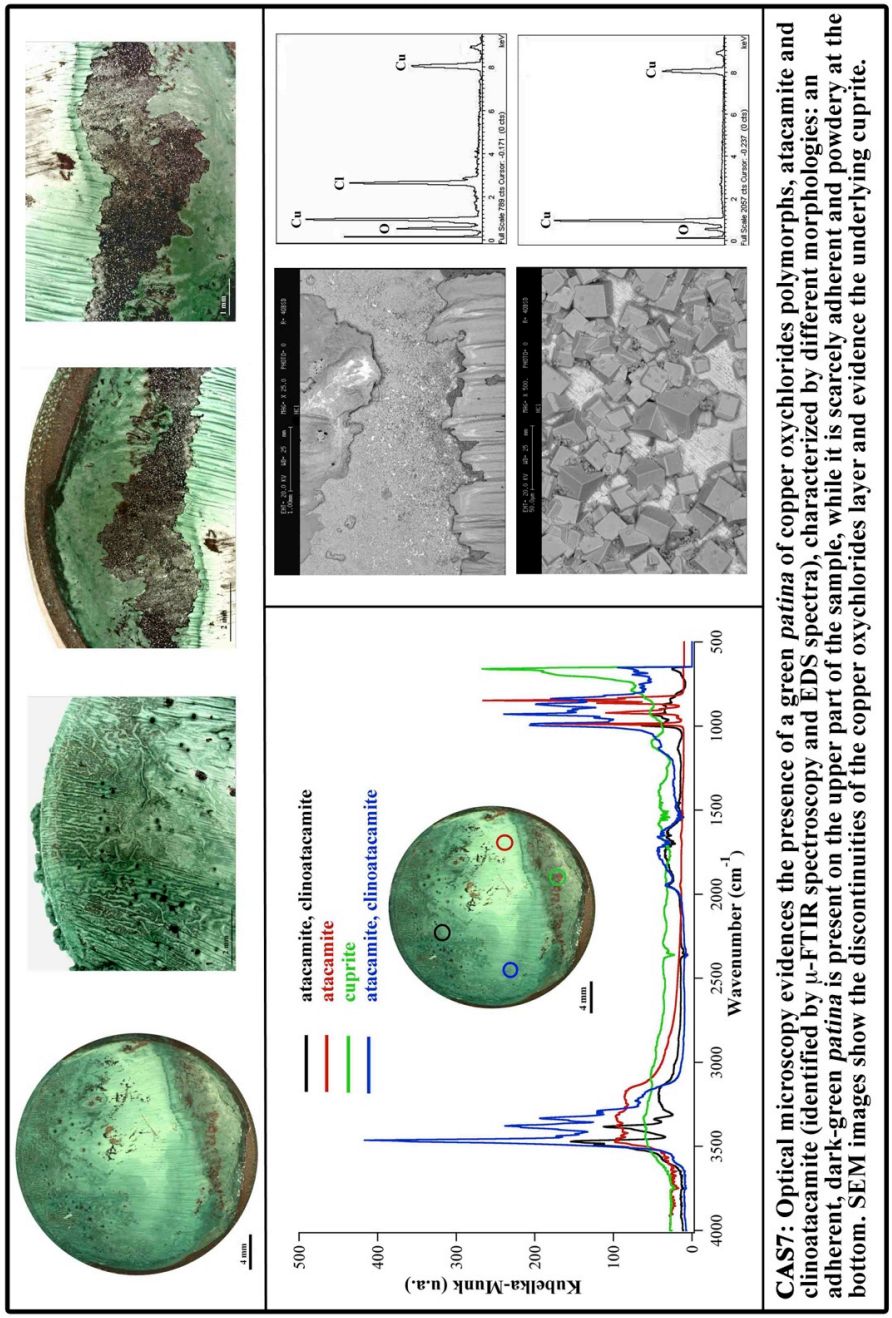

CAS7: Optical microscopy evidences the presence of a green *patina* of copper oxychlorides polymorphs, atacamite and clinoatacamite (identified by μ-FTIR spectroscopy and EDS spectra), characterized by different morphologies: an adherent, dark-green *patina* is present on the upper part of the sample, while it is scarcely adherent and powdery at the bottom. SEM images show the discontinuities of the copper oxychlorides layer and evidence the underlying cuprite.

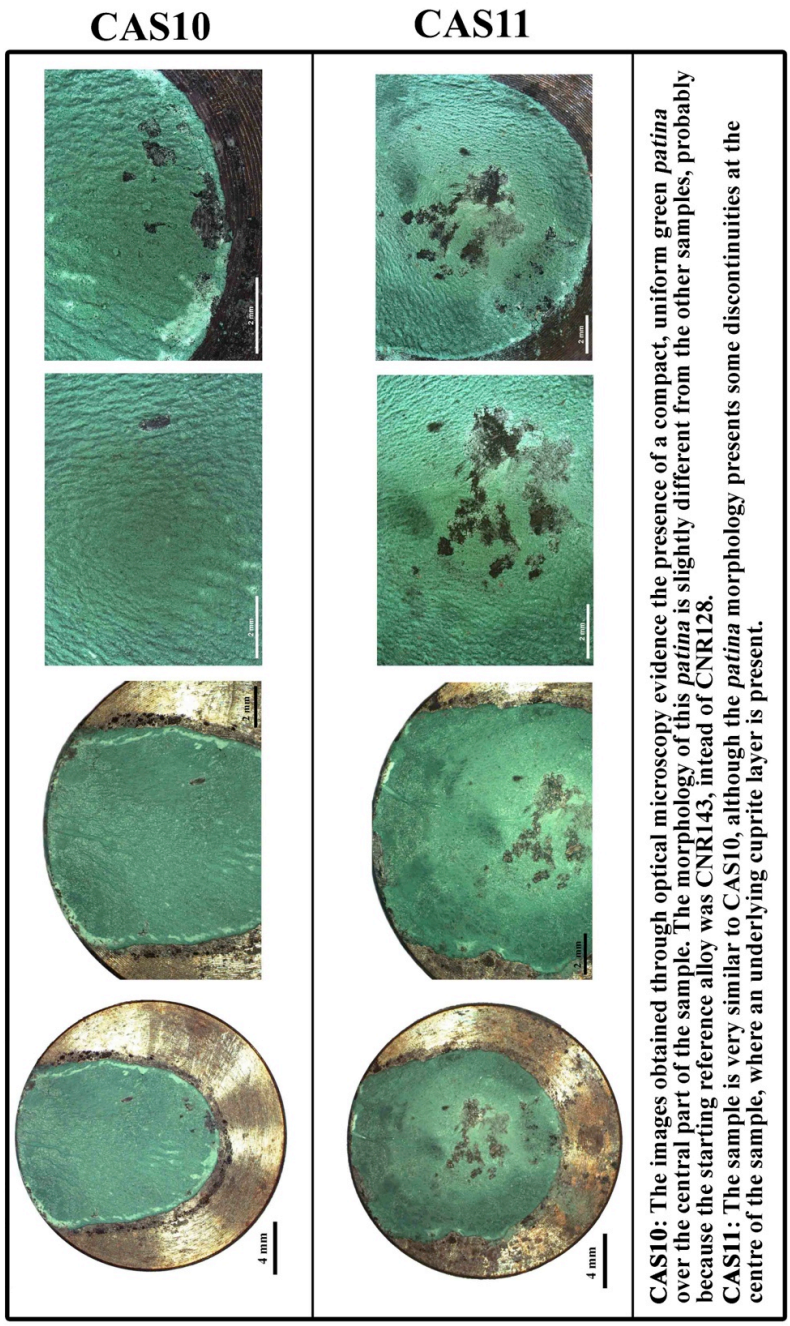

CAS10: The images obtained through optical microscopy evidence the presence of a compact, uniform green *patina* over the central part of the sample. The morphology of this *patina* is slightly different from the other samples, probably because the starting reference alloy was CNR143, intead of CNR128.
CAS11: The sample is very similar to CAS10, although the *patina* morphology presents some discontinuities at the centre of the sample, where an underlying cuprite layer is present.

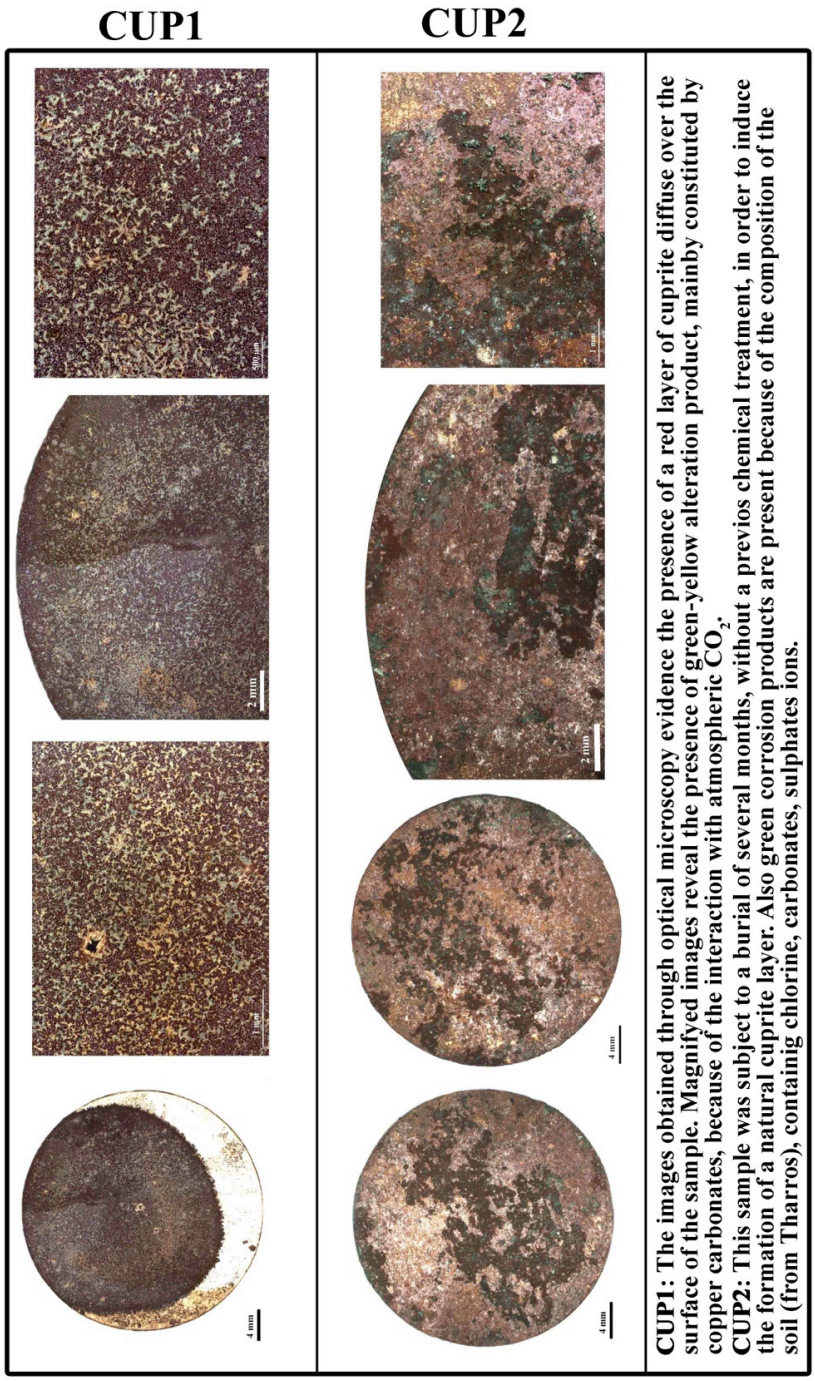

CUP1: The images obtained through optical microscopy evidence the presence of a red layer of cuprite diffuse over the surface of the sample. Magnifyed images reveal the presence of green-yellow alteration product, mainby constituted by copper carbonates, because of the interaction with atmospheric CO_2.
CUP2: This sample was subject to a burial of several months, without a previos chemical treatment, in order to induce the formation of a natural cuprite layer. Also green corrosion products are present because of the composition of the soil (from Tharros), containig chlorine, carbonates, sulphates ions.

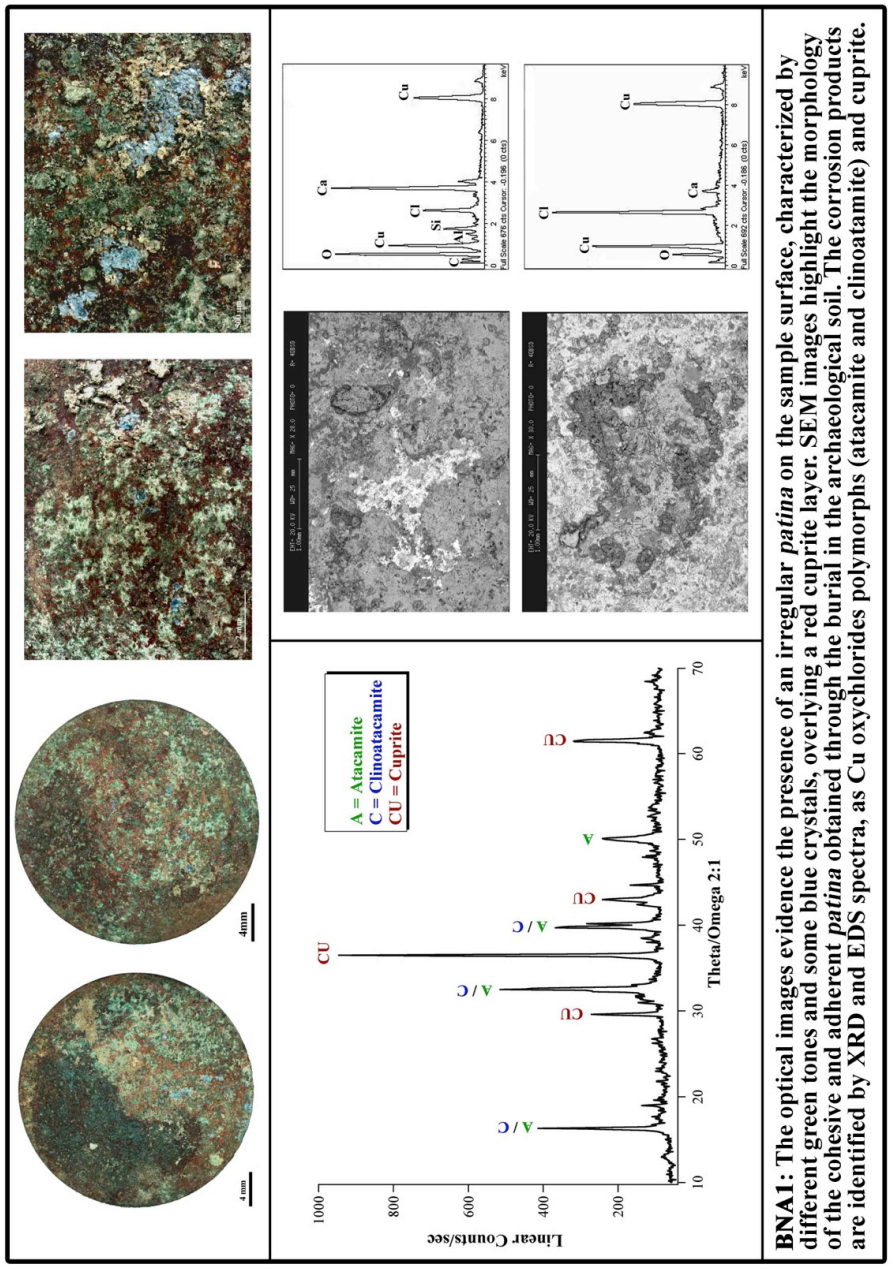

BNA1: The optical images evidence the presence of an irregular *patina* on the sample surface, characterized by different green tones and some blue crystals, overlying a red cuprite layer. SEM images highlight the morphology of the cohesive and adherent *patina* obtained through the burial in the archaeological soil. The corrosion products are identified by XRD and EDS spectra, as Cu oxychlorides polymorphs (atacamite and clinoatamite) and cuprite.

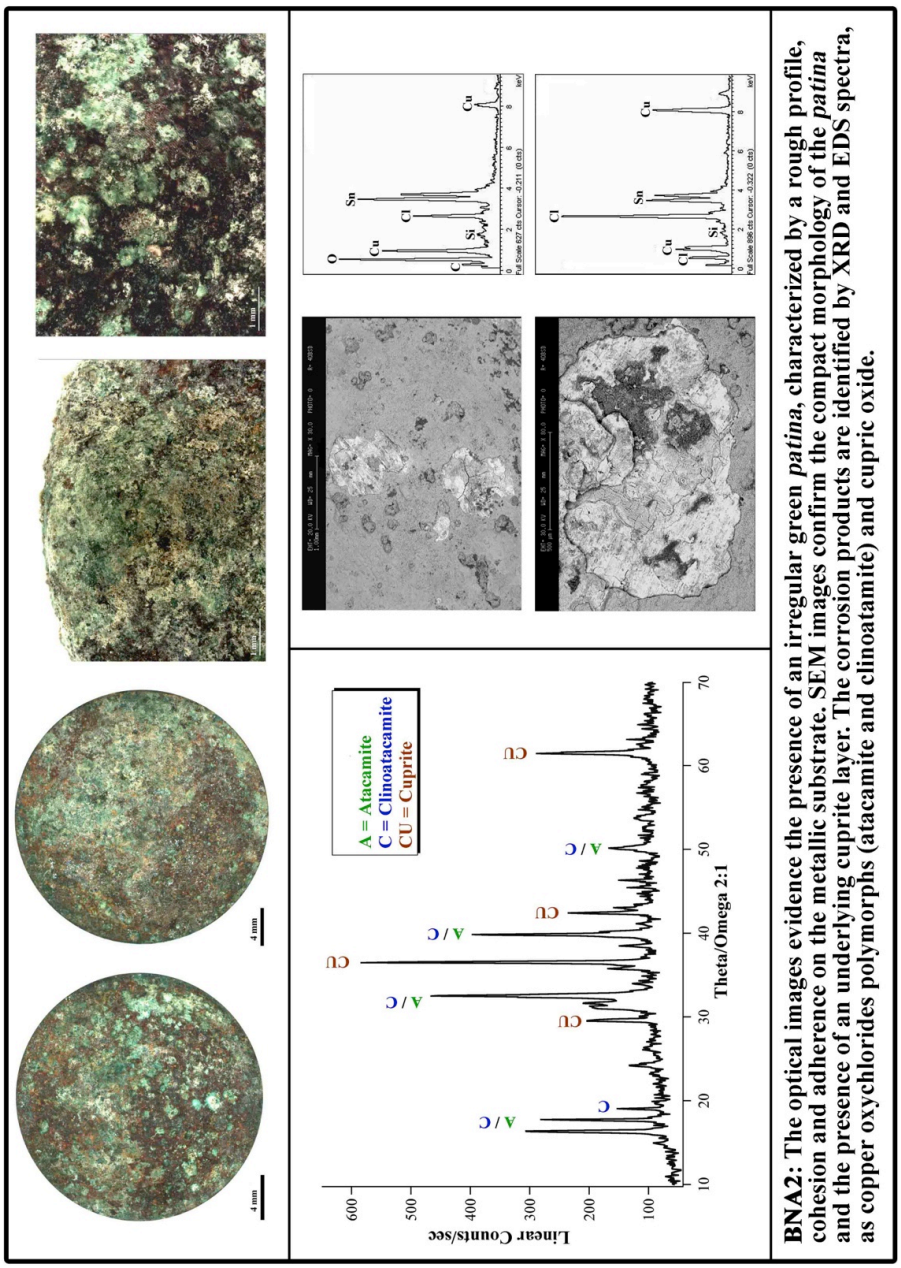

BNA2: The optical images evidence the presence of an irregular green *patina*, characterized by a rough profile, cohesion and adherence on the metallic substrate. SEM images confirm the compact morphology of the *patina* and the presence of an underlying cuprite layer. The corrosion products are identified by XRD and EDS spectra, as copper oxychlorides polymorphs (atacamite and clinoatamite) and cupric oxide.

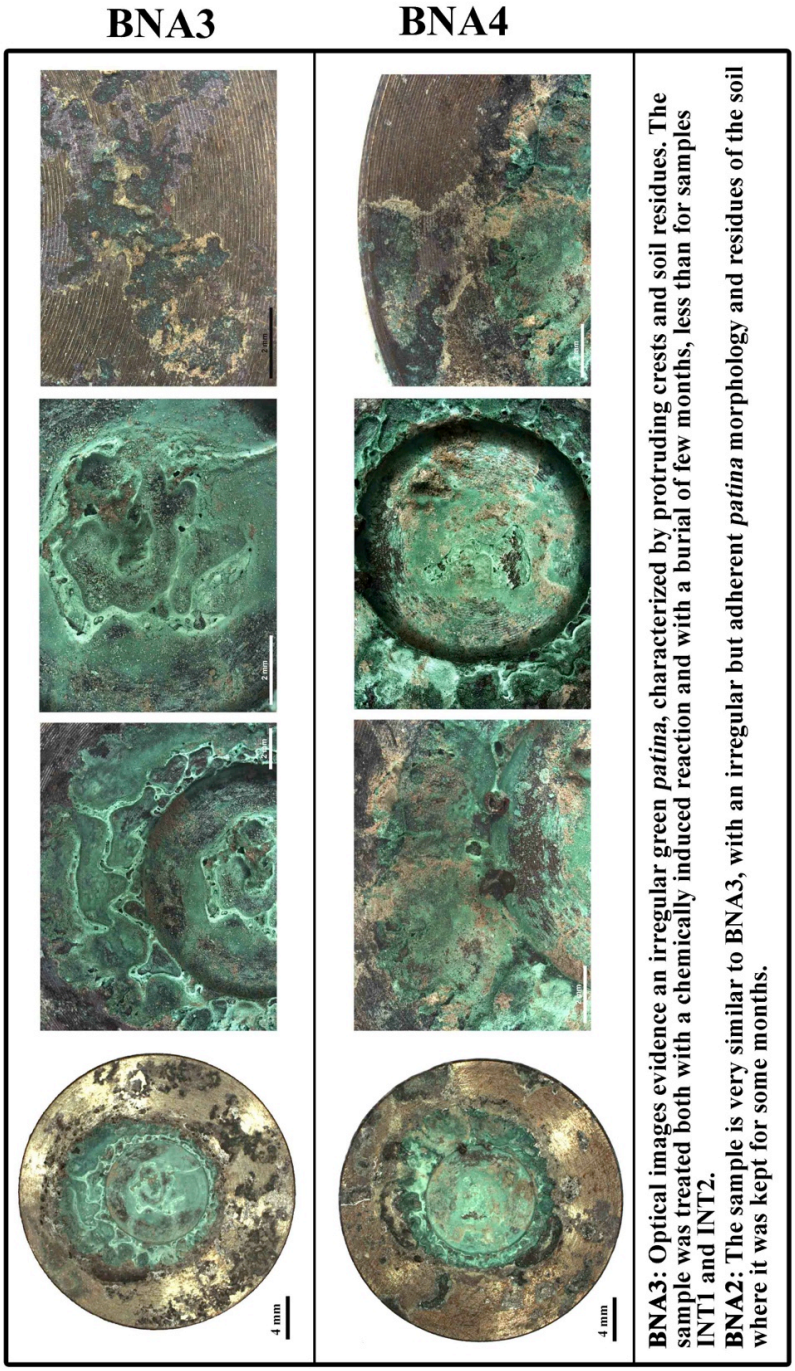

BNA3: Optical images evidence an irregular green *patina*, characterized by protruding crests and soil residues. The sample was treated both with a chemically induced reaction and with a burial of few months, less than for samples INT1 and INT2.
BNA2: The sample is very similar to BNA3, with an irregular but adherent *patina* morphology and residues of the soil where it was kept for some months.

7.4 Cleaning tests

The results of the preliminary cleaning tests will be presented in this section. Different complexing agents (described in Chapter 5, section 5.4) were used, loaded in different polymeric systems (see Chapter 5.2). The selection of the most performing cleaning systems was finally carried out for applications on real cases study.

7.4.1 Tests on chemically aged samples

7.4.1.1 Rochelle salt

One of the fundamental requirement for these innovative cleaning systems, concerns the respect of the protective cuprite layer, during the complexing reaction and the removal by peeling of the final film [7]. For this reason two formulations (73PVA7 and 74PVA6), loaded with 3.5% and 1.4% w/w of Rochelle salt respectively, were tested on a cuprite layer (sample CUP1). The final result, showed in Fig. 7.3, confirms the selectivity of the complexing reaction of RS towards the cuprous ions of cuprite: the layer remains intact and no residues are visible on the removed films. The slight change of the color can be ascribed to the presence of residual humidity, due to the prolonged contact with the cleaning system, and to the removal of powdery deposits, due to the artificial aging process.

The evaluation of the possible presence of polymeric residues after the test was carried out through Raman spectroscopy. In Fig. 7.4 the spectrum collected right after the removal of the film, reveals some residues of PVA (between 1600-1400 cm^{-1}), easily removed by a gentle mechanical action with a cotton swab soaked with water. Anyway the presence of polymeric residues doesn't represent a serious problem for what concerns metallic substrates, thanks to the inorganic nature of metals. However, in order to avoid the undesired growth of biological organisms, a final washing step is always advisable.

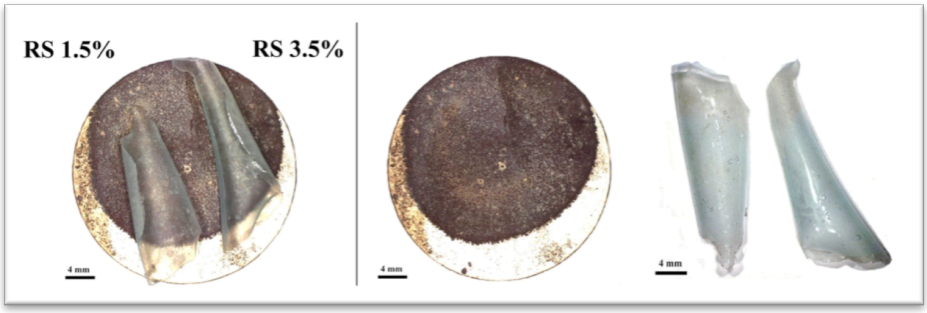

Figure 7.3 CUP1 sample after the treatment with a 73PVA7 formulation loaded with 3.5% w/w RS (for 3.5 hours) and with a 74PVA6 formulation loaded with 1.4% w/w RS (for one night).

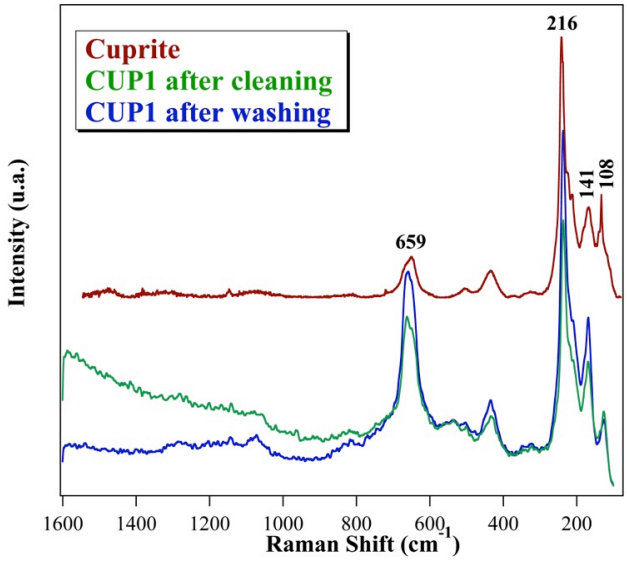

Figure 7.4 Raman spectra of CUP1 sample after the removal of the polymeric film (green) and after a gentle mechanical washing with water (blue): this final step assures the removal of any polymeric residues.

The same formulation (76PVA4) loaded with different amounts of the same complexing agent (RS, 3% and 6% w/w) was tested on the CAS6 sample. The result of the cleaning tests is showed in Fig. 7.5. The central pale green area on the sample

surface corresponds to a more powdery *patina* formed during the artificial aging process, while the upper dark green part consists of a strongly adherent *patina*. The application of both the cleaning systems allowed to easily remove the powdery corrosion products, mainly because of the mechanical peeling action of the film; the different concentration of RS slightly affected the removal of the coherent *patina*, which was only partially removed.

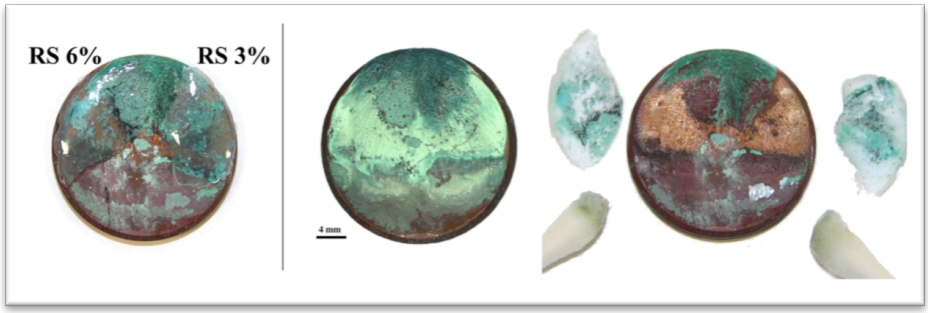

Figure 7.5 Cleaning tests performed with the same formulation (76PVA4) loaded with different amount of RS (3% and 6% w/w) on the CAS6 sample for one night.

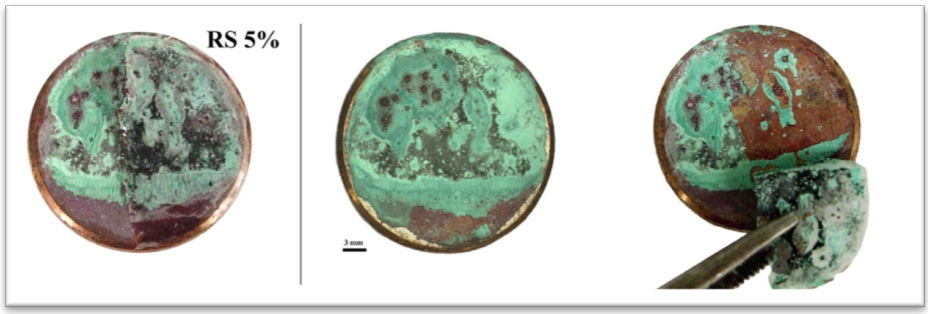

Figure 7.6 Cleaning test over the CAS4 sample with the formulation 70PVA10 loaded with 5% w/w RS, after heating the sample at 60 °C for two hours to accelerate the film formation.

Another test was performed on the CAS4 sample, to confirm the selectivity of RS towards the cuprite layer. The formulation 70PVA10 loaded with 5% w/w RS was

applied on the half part of the sample and the result of the cleaning test is showed in Fig. 7.6. The removal of the green *patina* of copper oxychlorides is almost complete without affecting the underlying cuprite layer. To accelerate the evaporation process, the sample was heated in a stove at 60 °C for two hours.

7.4.1.2 EDTA

The comparison between two different chelating agents (EDTA and SR), at their maximum amount loadable (3.7% and 6% w/w respectively) in the same formulation (76PVA4), was executed on the CAS1 sample. The results of the cleaning tests are visible in Fig. 7.7: the RS loaded formulation was efficient in removing the green corrosion layer by respecting the underlying cuprite layer, while the EDTA loaded formulation entailed a little removal of the red protective layer, maybe because of the high concentration of complexing agent used for cleaning the fragile *patina.*

A further application was then carried out with two cellulose pulp compresses, loaded with a 30% w/w RS solution and 15% w/w EDTA solution. The test gave as result the excessive removal of the cuprite layer, for both the applied systems, as showed in Fig. 7.8. Furthermore an additional mechanical step is required after the removal of the dry compresses to remove the complexed corrosion products left on the surface that entailed further mechanical stress for the fragile *patina*. The concentrations of the solutions used for this test were taken from literature [7,14,15], although lower concentrations are generally used [16]. However the aim was to test here the maximum effect of the complexing reactions over the metallic substrate, compared with the better control over the cleaning action and over the cuprite layer assured by the confined systems.

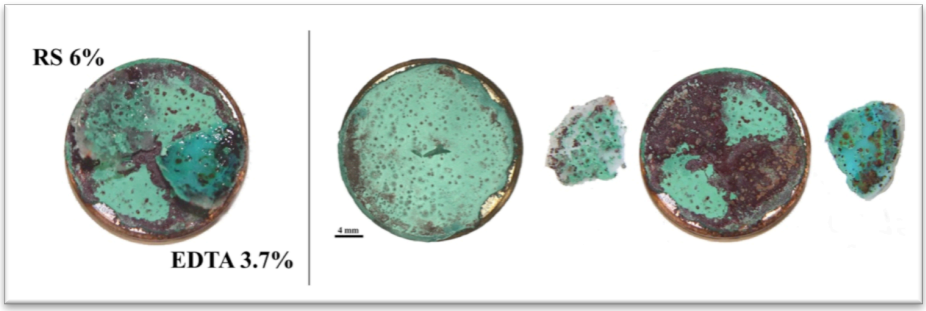

Figure 7.7 Cleaning tests executed with the same formulation (76PVA4) loaded with different complexing agents, 6% w/w RS and 3.7% w/w EDTA, left drying for one night.

Figure 7.8 Application of EDTA (18% w/w) and RS (35% w/w) solutions, supported by cellulose poultice, on the CAS1 sample, for one night.

As reported in Chapter 4 (section 4.2.2), the pH plays a fundamental role in the effectiveness of the complexing agent. In particular the enhanced amount of the deprotonated trianionic HY^{3-} and tetranionic Y^{4-} species, thanks to the increased pH values, results in better efficacy for the chelating action of EDTA (see Chapter 4, section 4.3.1). In fact, as showed in Fig. 7.9, the application of 70PVA10 loaded with 3% w/w EDTA at pH 10 on the CAS10 sample, resulted in a considerable removal of the corrosion products after a single application. The complete removal of the residual compact oxychlorides layer was achieved by a gentle mechanical action with a cotton swab soaked with distilled water.

Figure 7.9 Application of 70PVA10 formulation loaded with 3% w/w EDTA at pH 10 on the sample CAS10, for 4 hours.

The analysis carried out on the CAS10 sample (see the highlighted points in Fig. 7.9) by μ-FTIR spectroscopy, before and after the cleaning test, confirmed the complete removal of the two oxychlorides polymorphs (atacamite and clinoatacamite), by preserving the integrity of the cuprite layer (see Fig. 7.10).

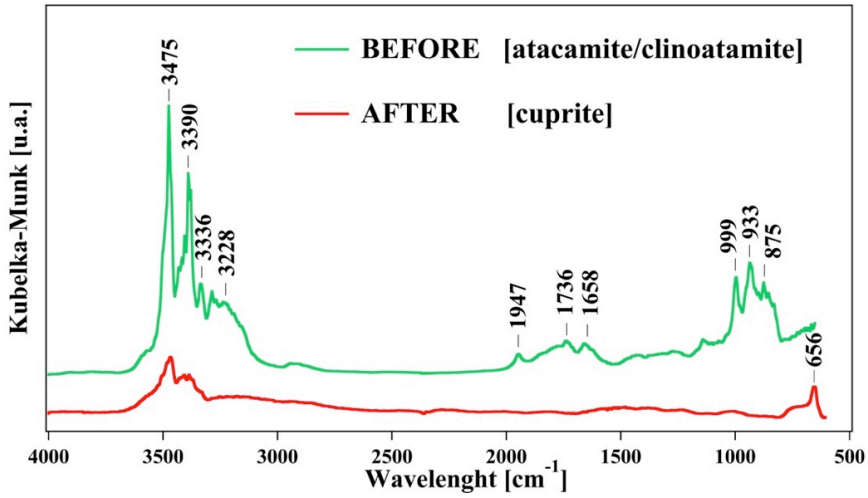

Figure 7.10 μ-FTIR spectra obtained from the same point of sample CAS10, before and after the cleaning action.

7.4.1.3 Glycine

An alternative complexing agent to the commonly used EDTA and RS in restoration practice, the amino acid glycine, was tested on the sample CAS6. A dry film was obtained from the formulation 72PVA8, and then re-hydrated by immersion in a solution of 18% w/w glycine. The loaded film was put in contact with the metallic surface and left until complete drying. The reaction between glycine and Cu(II) changed the surface color, because of the formation of a light blue complex, very adherent to the substrate and difficult to remove also through a mechanical action. This result, visible in Fig. 7.11, discouraged the possible substitution of the previous tested chelators with this amino acid. Moreover, the re-hydration method of the polymeric film, was rejected because the re-hydrated EDTA and SR films dissolved in the aqueous solution after few hours.

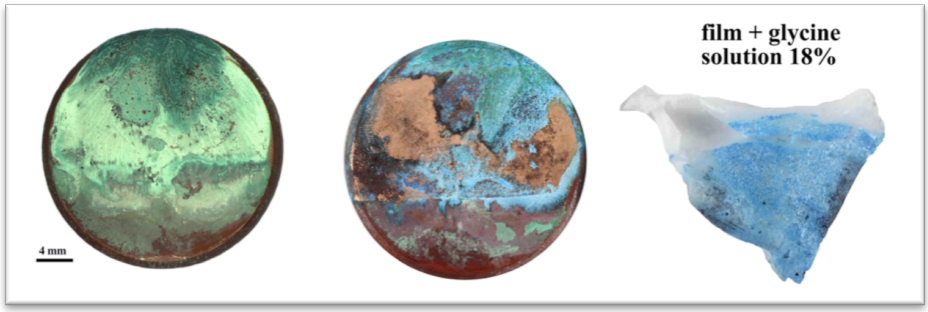

Figure 7.11 Application of a re-hydrated film (with a 18% w/w glycine solution), obtained from a 72PVA8 polymeric system, on the CAS6 sample, until complete drying.

7.4.1.4 Polyethyleneamines

Three different polyethyleneamines were tested: TETA (triethylenetetramine), TEPA (tetraethylenepentamine) and PEHA (pentaethylenehexamine). In Fig. 7.12 the results after two consecutive applications of polyamine loaded polymeric systems (with pH 9) on the CAS7 sample, are shown. The first test was carried out by applying a 3% v/v TEPA loaded 70PVA10 formulation that resulted in little removal

of the corrosion products (see Fig. 7.12, center) and in the formation of a dark blue complex. The second test was executed by applying the same formulation, loaded with 10% v/v PEHA, which resulted in a considerable removal of the corrosion layer, without the necessity of any further mechanical or chemical action (see Fig. 7.12, right). The higher stability constant of PEHA towards Cu(II) in respect to TEPA, made this complexing agent more effective for the removal of the corrosion products, event though also the related skin corrosive effect increases. Moreover, lower selectivity towards the cuprite layer, in respect to RS and EDTA, was observed after film removal, as well as poor mechanical properties of the 10% v/v loaded formulation.

Figure 7.12 Two consecutive applications of polyamine-loaded 70PVA10 formulations (3% v/v TEPA and 10% v/v PEHA) on the CAS7 sample.

7.4.2 Tests on buried samples

7.4.2.1 Rochelle salt

A comparison between the selectivity towards the cuprite layer of the same polymeric system (76PVA4), loaded with two different complexing agents (3.7% w/w EDTA and 6% w/w RS), was carried out through application on the buried sample CUP2. Rochelle salt loaded formulation revealed better selectivity over the cuprite layer, in respect to EDTA, as reported in Fig. 7.13. Moreover, some corrosion prod-

ucts grown over the cuprite layer during the burial in archaeological soil, were easily removed.

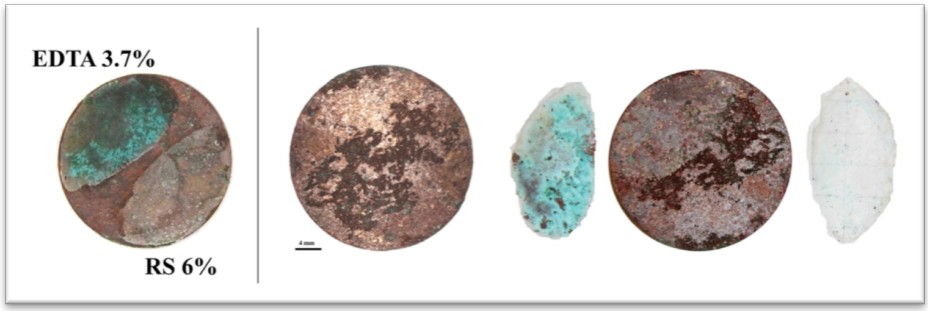

Figure 7.13 Cleaning tests performed over the CUP2 sample with the same formulation (76PVA4) loaded with 3.7% w/w EDTA and 6% w/w RS, in order to compare their selectivity.

A solution at a concentration of 35% w/w of Rochelle salt (pH 10) was applied on the sample BNA4 by cellulose poultice, as showed in Fig. 7.14, and compared with a 76PVA4 formulation loaded with 4% w/w EDTA. The confined chelating agent exerted a controlled and gradual reaction, while the Rochelle salt solution resulted too aggressive, by removing the entire *patina* present on the metal surface.

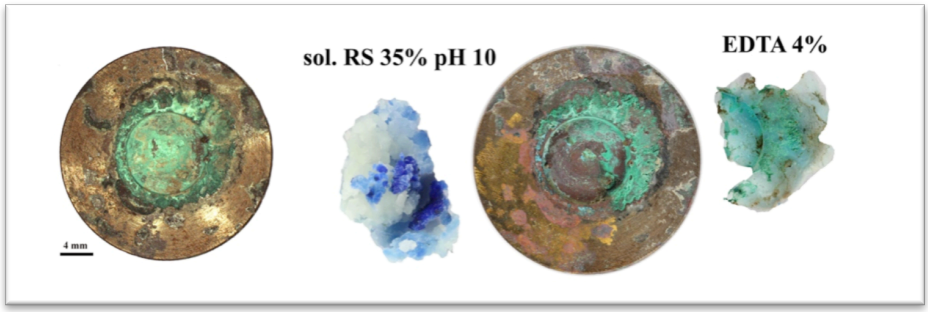

Figure 7.14 Comparison tests on BNA 4 sample, between a confined chelating solution (76PVA4 loaded with 4% w/w EDTA) and a 'free' RS solution, which resulted too aggressive towards the metal surface.

7.4.2.2 Glycine

A simultaneous cleaning test was carried out on the BNA1 sample, with different formulations and complexing agents, at the same concentration (3% w/w): EDTA loaded 76PVA4, RS loaded 74PVA6, glycine loaded 76PVA4 and not loaded 68PVA12 formulations. The results are visible in Fig. 7.15, where i) the formation of a light blue copper-glycine complex, strongly adherent to the metallic substrate, confirms the result obtained for sample CAS6; ii) the EDTA loaded formulation achieved a good removal of the corrosion products without affecting the underlying cuprite layer; iii) the polymeric system with Rochelle salt exerted a milder cleaning action, insufficient in this case, because of the different nature of the corrosion products formed under burial conditions; iv) finally, the not loaded formulation was used to test the sole mechanical action of the film removal by peeling, that was in this case, very gentle thus making the chemical cleaning action predominant.

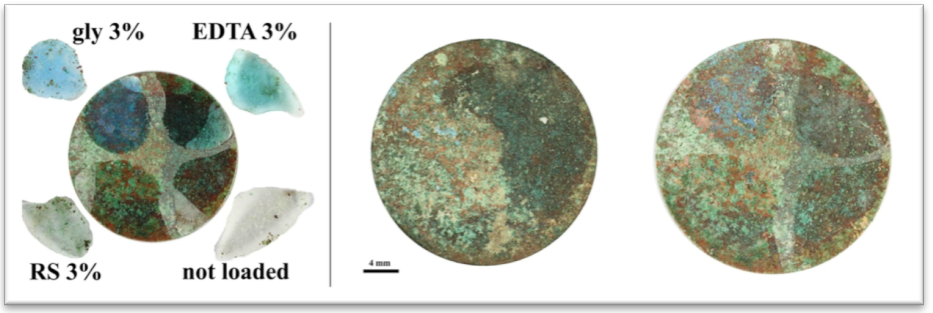

Figure 7.15 Applicative tests on the BNA1 sample with four different cleaning systems, through 3% w/w EDTA loaded 76PVA4, 3% w/w RS loaded 74PVA6, 3% w/w glycine loaded 76PVA4 and not loaded 68PVA12 formulations.

7.4.2.3 EDTA

A PVA aqueous solution (20% PVA, 50% H_2O and 30% EtOH w/w) was applied on the upper part of the BNA2 sample, in order to test the sole mechanical removal of the polymeric system, without plasticizers. The results, showed in Fig. 7.16, evi-

denced extremely aggressive adhesive properties, with the removal of the entire *patina* of the buried sample. On the other hand, a 3% w/w EDTA (pH 9) loaded 72PVA8 formulation was applied twice on the other half of the sample, showing a partial and controllable removal of the adherent and cohesive corrosion products.

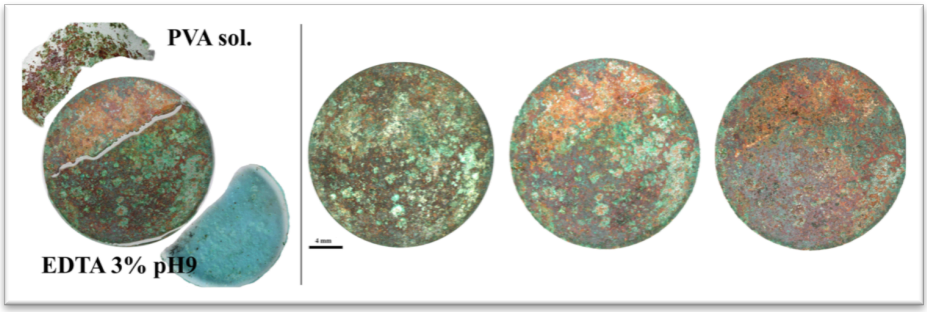

Figure 7.16 BNA2 sample treated with a polymeric solution, without addition of plasticizers and with a 3% w/w EDTA loaded (pH 9) 72PVA8 formulation.

7.4.2.4 Macrocycles

Cleaning tests on the sample BNA3 with polymeric systems loaded with 2% w/w macrocycles (Neoden and AMCC), are showed in Fig. 7.17. Probably, the low concentration of the complexing agent and the low amount of the polymeric formulation prepared (about 500 mg of 72PVA8), can explain the scarce cleaning performances obtained and the poor mechanical properties of the films observed for the applied systems. In fact, due to their cost, only few mg of these macrocycles molecules were provided to load the polymeric systems, thus making the preparation procedure very difficult.

Figure 7.17 Cleaning tests with two polymeric systems (72PVA8) loaded with 2% w/w of Neoden and AMCC macrocycles, performed on the BNA3 sample.

7.4.2.5 Polyethyleneamines

Preliminary tests were performed by applying 'free' complexing agents aqueous solutions, through cellulose poultice compresses, on the metallic surfaces of buried sample (BNA1 and BNA2). In particular EDTA and TETA solutions were firstly compared at the same concentration (3% w/v) on the sample BNA1, by observing higher cleaning performances for the polyethyleneamine-copper complex. Further tests were performed by comparing the cleaning action of 3% v/v TEPA and PEHA solutions on the BNA2 sample, where a moderate cleaning action, with very similar results for both the solutions applied by compress were observed.

A polymeric 70PVA10 system was loaded with 3% v/v TETA and applied on the BNA2 sample. The application evidenced the instant formation of a strong dark blue color, as showed in Fig. 7.18, which didn't affect the aspect of the metallic substrate as for glycine, but remained confined to the film. The film presented good mechanical properties and the test resulted in good cleaning performances, with a consistent removal of the corrosion product after a single application.

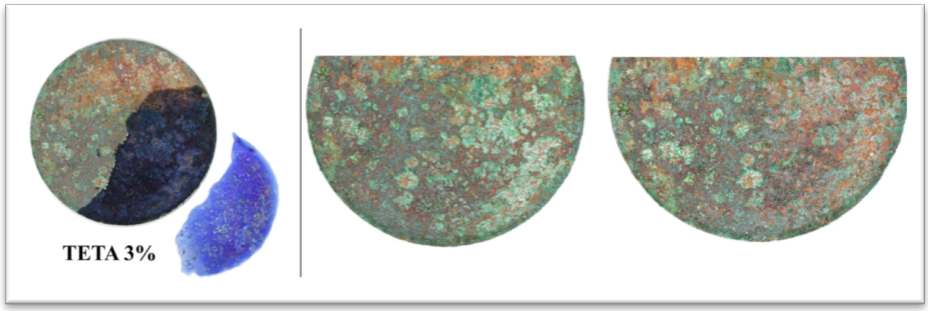

Figure 7.18 Cleaning tests performed with a 70PVA10 formulation loaded with 3% v/v TETA polyamine, for two hours, on the BNA2 sample.

The most effective polyethyleneamine, PEHA, was tested on the BNA1 sample, by applying two consecutive polymeric loaded systems. The formulations were prepared by opportunely decreasing the plasticizer content, because of the possible cross-linking effect of polyamine molecules over the polymeric network. Thus, formulations 70PVA4 loaded with 6% v/v PEHA and 66PVA4 loaded with 10% v/v PEHA were tested. The results, reported in Fig. 7.19, reveal the high sequestering efficacy of this complexing agent towards cupric ions. In fact, the removal of the corrosion products is complete after two applications, without any further mechanical action, with medium removal of the cuprite layer. Moreover, the mechanical properties of the films removed by peeling were scarce, thus entailing breakages and possible residues lefts.

After two days from the preparation of the polymeric dispersions loaded with the polyamine complexing agent, the formulation needed to be heated in warm water to restore its viscoelastic properties, before application. This process became irreversible after few days and the system cannot be used anymore, because a solid gel forms.

Figure 7.19 Cleaning tests performed by two consequent application of a 70PVA4 formulation loaded with 6% v/v of PEHA and a 66PVA4 formulation loaded with 10% v/v of PEHA, on the BNA1 sample.

7.5 Final remarks

Cleaning test results evidenced that the action of the complexing agent loaded in the polymeric dispersion is fully controllable, thus permitting a gradual layer-by-layer removal of the corrosion products. Moreover, the initial consistency of the system allows a perfect contact with the rough surface of the sample, so the complexing reaction can take place also in areas where no removal through a sole mechanical action could be achieved. Finally, the mechanical action due to the removal by peeling favors the cleaning process by assisting the chemical action of the chelator

The preliminary applicative tests performed on the artificially aged samples, revealed both the advantages and drawbacks of each chelating agent, as well as the complexity of the cleaning procedure depending on the surface characteristics. The main observations on the complexing agents performances are summarized in Tab. 7.3. The prevalence of negative aspects related to the use of macrocycles and glycine as complexing agents for Cu(II) determined their exclusion.

Depending on the characteristics of the sample to clean, the suitable sequestering agent should be carefully chosen: Rochelle salt guarantees a delicate and gentle chemical action, by respecting the cuprite or gold layer present; EDTA is versatile and can perform a very controllable cleaning action, by tuning also the pH values;

polyamines can be used for a more effective cleaning action, thanks to their high formation constant for the complex with Cu(II).

Moreover, different polymeric formulations were tested as confining systems for the complexing agents. The best performances in terms of both applicability and properties of the final film, were obtained by the selected formulations already described in Chapter 5 (section 5.2.4): 74PVA6, 70PVA10 and 68PVA12, thus used for cleaning tests on real cases study.

Complexing agent	Performances
Rochelle salt	– Poor efficacy on cohesive and adherent *patina*, such as BNA samples + Excellent preservation of the cuprite layer
Glycine	– Change of the surface color by formation of a light blue complex with Cu(II)
EDTA	– Limited amount loadable into the polymeric system (about 4% max) + Controlled and effective cleaning action over all the tested substrates + Complexing power controllable by the pH value + Good preservation of the cuprite layer
Macrocycles	– High costs and toxicity – Poor cleaning results on the treated sample
Polyamines	+ Highest complexing efficacy over all the treated samples – Corrosives for skin – Instability of the loaded systems and poor mechanical properties of the films – Medium preservation of the cuprite layer

Table 7.3 Positive (+) and negative (–) aspects of the complexing agents used for the preliminary tests on the artificially aged samples.

7.6 Bibliography

[1] CASALETTO, M.P., DE CARO, T., INGO, G.M., AND RICCUCCI, C. *Production of reference "ancient" Cu-based alloys and their accelerated degradation methods.* Applied Physics A: Materials Science and Processing *83*, (**2006**), 617–622.

[2] CRADDOCK, P.T. *The composition of the copper alloys used by the Greek, Etruscan and Roman civilizations 1. The Greeks before the archaic period.* Journal of Archaeological Science *3*, 2 (**1976**), 93–113.

[3] CRADDOCK, P.T. *The composition of the copper alloys used by the Greek, etruscan and Roman civilisations.* Journal of Archaeological Science *4*, 2 (**1977**), 103–123.

[4] CRADDOCK, P.T. *The composition of the copper alloys used by the Greek,*

Etruscan and Roman civilizations: 3. The Origins and Early Use of Brass. Journal of Archaeological Science *5*, 1 (**1978**), 1–16.

[5] INGO, G.M., ANGELINI, E., BULTRINI, G., CALLIARI, I., DABALA, M., AND DE CARO, T. *Study of long-term corrosion layers grown on high-tin leaded bronzes by means of the combined use of GDOES and SEM + EDS.* Surface and Interface Analysis *34*, 1 (**2002**), 337–342.

[6] ROBBIOLA, L., BLENGINO, J.M., AND FIAUD, C. *Morphology and mechanisms of formation of natural patinas on archaeological Cu–Sn alloys.* Corrosion Science *40*, 12 (**1998**), 2083–2111.

[7] SCOTT, D.A. *Copper and bronze in art.* The Getty Conservation Institute, Malibu, **2002**.

[8] SCOTT, D.A. *Metallography and Microstructure of Ancient and Historic Metals.* The Getty Conservation Institute, Malibu, **1991**.

[9] FARALDI, F. *Environmentally friendly plasma treatments for surface nano-functionalisation and protection of metals.* **2014**.

[10] INGO, G.M., ANGELINI, E., DE CARO, T., AND BULTRINI, G. *Combined use of surface and micro-analytical techniques for the study of ancient coins.* Applied Physics A *79*, 2 (**2004**), 171–176.

[11] INGO, G.M., ANGELINI, E., BULTRINI, G., DE CARO, T., PANDOLFI, L., AND MEZZI, A. *Contribution of surface analytical techniques for the microchemical study of archaeological artefacts.* Surface and Interface Analysis *34*, 1 (**2002**), 328–336.

[12] INGO, G.M. AND PARISI, E.I. ET AL. *Gold coated copper artifacts from the Royal Tombs of Sipán (Huaca Rajada, Perù): manufacturing techniques and corrosion phenomena.* Applied Physics A *113*, 4 (**2013**), 877–887.

[13] INGO, G.M., ÇILINGIROĞLU, A., FARALDI, F., ET AL. *The bronze shields found at the Ayanis fortress (Van region, Turkey): manufacturing techniques and corrosion phenomena.* Applied Physics A *100*, 3 (**2010**), 793–800.

[14] FERRETTI, M. AND SIANO, S. *The gilded bronze panels of the Porta del Paradiso by Lorenzo Ghiberti: non-destructive analyses using X-ray fluorescence.* Applied Physics A *90*, 1 (**2007**), 97–100.

[15] FIORENTINO, P., MARABELLI, M., MATTEINI, M., AND MOLES, A. *The condition of the 'Door of Paradise' by L. Ghiberti. Tests and proposals for cleaning.* Studies in Conservation *27*, (**1982**), 145–153.

[16] MARABELLI, M. *The Monument of Marcus Aurelius: facts and comments.* In D. Scott, ed., *Ancient & Historic Metals.* The Getty Conservation Institute, Malibu, **1993**, 1–20.

Chapter 8

Applicative tests on real cases study

8.1 Introduction

Testing the developed new materials in real case studies is extremely important to check the impact that these materials might have in the conservation and restoration field. This is due to the fact that each artistic object has its own degradation history, which is very far from what can be reproduced by mock-ups or artificial samples produced in laboratory. During this research project, there was the opportunity to test the film forming polymeric systems loaded with different complexing agents, on two important cases study, the 'Fontane dei Mostri Marini" by P. Tacca placed in Ss. Annunziata square, Florence, along with several artifacts coming from archaeological contexts. These case studies were ideal to test the applicability and efficacy properties of the developed system, for the removal of copper corrosion products with different compositions and morphologies.

Furthermore, the diagnostic campaign previously carried out on the eastern fountain, allowed to better understand the conservative problems, to identify the alteration products and to study the metallurgical features of the alloy, by means of optical microscopy, SEM/EDS, FTIR spectroscopy and X-ray diffraction.

The applicative tests performed also on very different substrates from copper-based alloys, such as parchment, gypsum, and leather, allowed to demonstrate the extreme versatility of these cleaning systems, although they were specifically designed for metals.

8.2 The cases study of the 'Fontane dei Mostri Marini' by P. Tacca

The two fountains are placed in Ss. Annunziata Square, in Florence, at the symmetrical sides of the equestrian monument of Ferdinando I de' Medici. The fountains were firstly thought by their creator, Pietro Tacca, to enrich the monument of the 'Quattro Mori', placed in Livorno, although the gran duke of Ferdinando II de' Medici, astonished by the rare beautiful of the two sculptures, decided to move them in their current position. P. Tacca and its apprentices completed the two fountains in 1962.

The two bronze sculpture elements were inspired by the marine world, in fact, they represent imaginary figures, with zoomorphic and anthropomorphic characteristics. They are positioned on a marble circular base, enclosed by bronze decorative elements (fishes, shells and shellfishes garlands) and by the two bronze basins.

In 2014 the eastern fountain was subject to a conservative intervention supervised by the 'Comune di Firenze' and executed by 'Nike Restauro Opere d'Arte'. A diagnostic campaign was carried out at CSGI and ISMN-CNR laboratories, after the design of a diagnostic project, in order to understand the conservative problems, identify the alteration products and analyze the metallurgical feature of the alloy.

The western fountain has been restored in 2015 and the diagnostic analysis is still in progress.

8.2.1 The diagnostic project

The eastern fountain of the 'Mostri Marini' presented the typical alteration forms of an outdoor exposed bronze. In fact a *patina* with different colors, depending on the alteration products, was present all over the surface, thus defacing the original aspect of the artifact.

The archaeometric problems investigated during the diagnostic campaign, concerned the following aspects [1–3]:

- determination of the chemical composition and of the metallurgical characteristics of the Cu-based alloy, in order to identify the manufacturing and working techniques;
- identification of the degradation agents and mechanisms in order to propose useful advises for the definition of tailored strategies for the conservative intervention.

The two principal factors that contribute to the general degradation processes of metallic artifacts are mainly due to:

- *internal factors*: related to the intrinsic properties of the artifact, such as chemical composition, structure, metallurgical features, and the subjected working processes;
- *external factors*: related to the conservation environment and to the possible improper conservative treatments.

In the particular case of outdoor exposed bronzes, the environmental factors play a preponderant role, mainly related to the atmospheric parameters (pollutants, climate, etc.), in respect to the internal factors that mainly influence the alteration processes of archaeological objects [4].

The principal degradation phenomena, *i.e.* the corrosion processes that can affect metallic objects, in particular bronze alloys, has been extensively discussed in Chapter 1 (section 1.3), as well as the main factors influencing the alteration processes in outdoor environment, for which we can refer to section 1.3.1.3. In the specific case of this sculptural group, the prolonged exposition to the atmospheric agents and pollutants, along with the internal losses of the hydric system, entailed the continuous exposition to aggressive conditions, which resulted in the formation of aesthetically defacing products. In order to understand these mechanisms of alteration and to identify the alteration products, a statistically representative number of samples were taken from the artifact surface, by trying not to affect the same. Very low amount of samples was sufficient, by considering the experimental characterization techniques available for the analysis.

The surface alteration products were sampled by taking few milligrams from areas that seemed meaningful and sacrificable, after a visual inspection, for the micro-destructive analysis, as reported in Fig. 8.1. The obtained samples were in the powdery form or as micro-fragments. The alloy metallic samples were taken from hidden areas of the sculpture (see Fig. 8.2) and analyzed at the ISMN-CNR laboratories of Rome.

The investigations techniques used for the characterization of both the alteration products and the metallurgical features of the alloy were: optical microscopy (OM), FTIR spectroscopy in KBr, scanning electron microscopy with microanalysis (SEM/EDS) and X-ray diffraction [5].

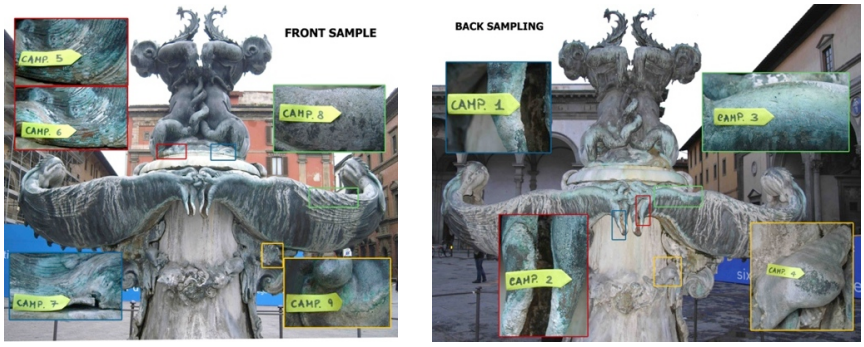

Figure 8.1 Maps of the front and back sampling of the alteration products on the surface of the eastern fountain.

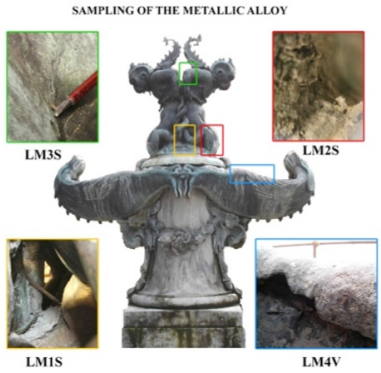

Figure 8.2 Map of the metallic alloy sampling from hidden areas of the eastern fountain.

8.2.2 Results and discussion

The execution of a diagnostic campaign allowed to identify the compositional and metallurgical characteristics of the alloy, as well as the manufacturing techniques, the type and the structure of the corrosion products. The results obtained by optical microscopy, FTIR spectroscopy, X-ray diffraction and SEM-EDS analysis are reported in Fig. 8.3.

The obtained data revealed the presence of corrosion products typical of copper-based alloys exposed to external environment and water. In particular, copper carbonates (malachite $CuCO_3(OH)_2$), sulphates (antlerite $Cu_3(SO_4)(OH)_4$, brochantite $Cu_4(SO_4)(OH)_6$), nitrates and chlorides (atacamite $Cu_2Cl(OH)_3$ and its polymorph clinoatacamite), confer a green colored aspect to the surface (Fig. 8.3 (a,b,c)). The presence of these corrosion species can be ascribable to the direct exposition to the atmospheric agents in presence of pollutants, which induced simultaneous mechanisms of attack, extremely aggressive for the object. Moreover, despite of the suspension since years of the distribution of water because of malfunctions of the hydric system, a lot of alteration phenomena may be attributed to the constant and ubiquitous presence of water both inside and outside the object. A further contribution of the species responsible for the degradation processes also came from the aqueduct water, very rich in nitrates, sulphates, chlorides, calcium and magnesium ions[1]. The presence of striations of different colors that affect very seriously the aesthetical legibility of the surface, may be attributed to the different solubility of the alteration products, which can be washed away by the flowing water, depending also on the exposition areas [6].

Furthermore, calcium carbonate (calcite) and sulphate (gypsum), in the form of white to dark-grey concretions, are widely diffused all over the investigated surfaces. Their presence is mainly correlated to the high Ca^{2+} ion content coming from the rain and aqueduct water as well as from atmospheric particulate.

[1] www.publiacqua.it consulted on December 2015.

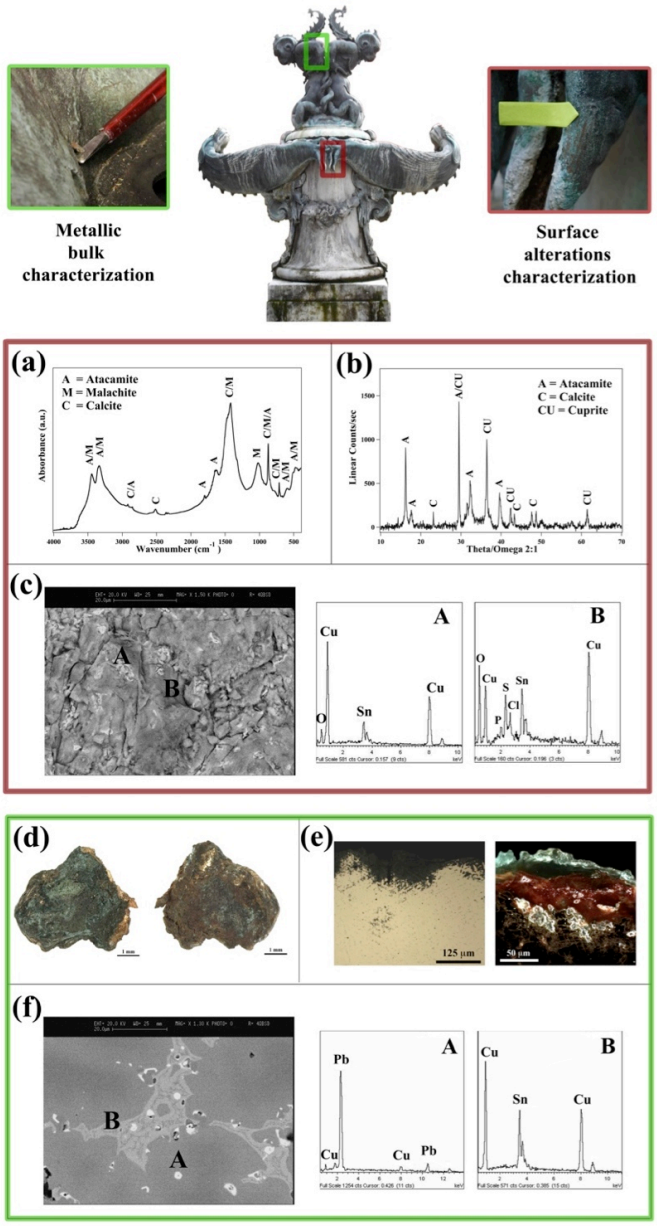

Figure 8.3 Characterization of the surface alteration products (upper panel) and of the alloy (lower panel). (a) FTIR spectrum of the green corrosion product; (b) XRD diffractogram confirming FTIR analysis; (c) SEM image and relative EDS spectra of sample surface; (d) optical microscopy images of an alloy sample; (e) metallographic images in bright and dark field of a sample section; (f) SEM image and relative EDS spectra of the sectioned alloy.

Stratigraphic analysis confirmed the composition and the morphology of the typical bronze corrosion products, described in Chapter 1 (section 1.3.4.1). The dark field images obtained by the metallographic microscope (Fig. 8.3 (e)), in fact, permitted to identify stratified layers constituted by red cuprite, nantokite and green copper oxychlorides and sulphates. The presence of copper oxychlorides (Fig. 8.3 (a,b)) was considered as a symptom of an active 'bronze disease' phenomenon [6,7], extensively explained in Chapter 1 (section 1.3.3). The bronze alloy is characterized by a medium tin content of 9-10% w/w, and a very low lead amount (< 1% w/w), as revealed by EDS microanalysis. The microstructure morphology is typically dendritic with rare eutectoid α+δ phases diffused in the metallic bulk, as showed by SEM image (Fig. 8.3 (f)) and described in Chapter 1 (section 1.2). The production technique was identified as the lost-wax casting method (see Chapter 1, section 1.2.2).

8.2.2.1 Instrumental conditions

The diagnostic investigations of the eastern "Fontana dei Mostri Marini" corrosion products were carried out on powder samples analyzed through FTIR spectroscopy by incorporating 4-5 mg into KBr pellets. Spectra were collected in transmission mode with a BioRad (FTS-40) equipped with a DTGS Mid-IR detector in the 4000-400 cm^{-1} range, at 64 scans and 4 cm^{-1} resolution.

X-ray diffractometry was used to confirm FTIR measurement on the same samples with a Bruker (D8 Advance) powder diffractometer. Angular values in the 10° and 70° range in additive mode, a step size of 0.05° and a sampling time of 2s were the experimental parameters used.

Metallic samples surfaces and sections were studied firstly through optical microscopy with a stereomicroscope LEICA (Multifocus) and a metallographic microscope LEICA (MEF 4M) equipped with a digital camera to collect images.

SEM-EDS characterization was carried out on a Cambridge 360 scanning electron microscope equipped with a LaB_6 filament, an energy-dispersive X-ray spectrome-

ter (EDS) INCA 250 and a four-sector backscattered electron detector (BSE). In order to prepare cross sections, samples were embedded in epoxy resin for 24 h and sectioned using a diamond saw, then polished with silicon carbide papers and diamond pastes and finally coated with a thin layer of carbon to avoid charging effects.

8.2.3 Applicative cleaning tests

Cleaning tests on the eastern "Fontana dei Mostri Marini" of P. Tacca were performed during its conservative intervention, occurred in 2014. The cleaning intervention was entirely performed by traditional mechanical methods, by using vibrating and abrasive tools, micro-peening with vegetal granulates, etc., thus entailing the implications reported in Chapter 1 (section 1.4.1). An alternative cleaning procedure was proposed and preliminary tested, by performing applicative tests with selected film forming polymeric systems, loaded with complexing agents, listed in Tab. 8.1.

The applicability of these formulations was tested over non-horizontal surfaces, with the addition of two different complexing agents (EDTA and Rochelle salt) at different concentrations (2.5%, 3% and 3.5% w/w for EDTA and 6.6% w/w for RS). The effectiveness of the loaded formulations was also compared with a not-loaded system, to observe the mechanical contribute of the peeling action.

Formulation	Complexing agent	Concentration % w/w
76PVA4	EDTA	3.5
72PVA8	EDTA	2.5
70PVA10	EDTA	3
	RS	6.6
	not loaded	/

Table 8.1 Typology of polymeric formulations loaded with two different complexing agents at different concentrations (pH 7).

The cleaning tests were performed on the selected areas reported in Fig. 8.4, but only the most relevant will be reported.

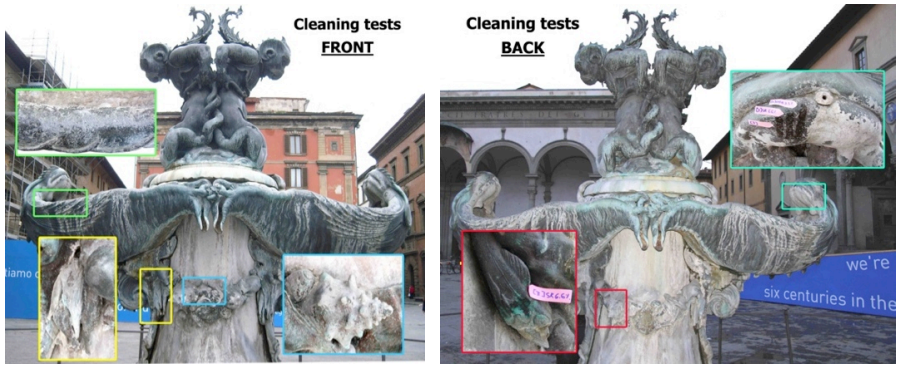

Figure 8.4 Maps of the application areas for the cleaning tests, performed both on the front and on the back side.

A first applicative test was performed on the decorative group of five fishes, placed around the marble base on the front side, in an undercut area. A thick white concretion of calcium carbonate and sulphates covered the entire decoration (Fig. 8.6 (a)), under which green corrosion products (copper carbonates and sulphates) were visible. Three different formulations (76PVA4, 72PVA8 and 70PVA10), loaded with EDTA (3.5%, 3%, 3.5% w/w respectively) were applied over the areas evidenced in Fig. 8.5 and Fig. 8.6.

After the removal of the dried film by peeling (see Fig. 8.7), a consistent reduction of the white layer of calcite and gypsum was achieved as well as the partial removal of the underlying corrosion products (see details in Fig. 8.6 (b) and Fig. 8.6 (c) respectively). In fact, EDTA is an effective complexing agent also for Ca^{2+} ions, thus performing a double cleaning action in a single application. The cuprite layer was not visible affected by the complexing reaction and the differences between the used concentrations of EDTA were negligible.

The applied polymeric formulations showed different performances, depending on their compositions: i) the 76PVA4 and 72PVA8 were too liquid and some drops fall down after the application, while the 70PVA10 formulation assured a good adhesion also on a non-horizontal surface; ii) the mechanical properties of the final films removed by peeling were good for all the formulations tested, as well as the

initial consistencies of the systems, which allowed to perfectly follow the shaping of the surface (see Fig. 8.7); iii) the 76PVA4 formulation presented the strongest adhesion to the substrate, while 70PVA10 the least one, because of its higher plasticizer content.

Figure 8.5 Applicative tests of different formulation over a decoration of the fountain: 76PVA4 with 3.5% w/w EDTA (yellow), 72PVA8 with 3% w/w EDTA (green) and 70PVA10 with 2.5% w/w EDTA (red). The times of application varied from two hours up to the entire night; the pH was maintained at 7.

Finally, high control over the cleaning process was ensured, since the complexing reaction cannot further occur after volatile fraction loss and the formation of the polymeric film. In fact some applications were performed by allowing the formulations drying during night.

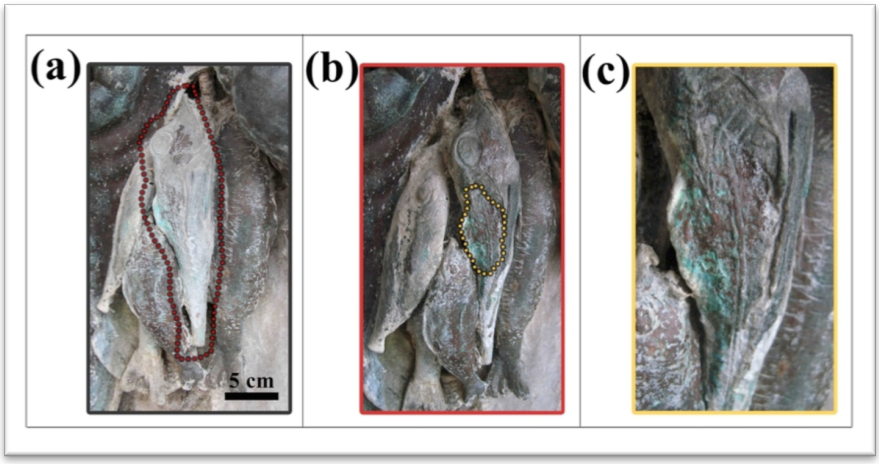

Figure 8.6 (a): the area chosen for the cleaning test with a white layer of calcium carbonate/sulphates and an underlying layer of copper corrosion products; (b): partial removal of the calcium carbonate/sulphates layer after one application of the 3.5% w/w EDTA (pH 7) loaded 72PVA8 formulation; (c) enlargement showing the partial removal of the copper-based corrosion products after a single application.

Figure 8.7 Optical image of the film removed from the fish decoration, showing the shape of the eye, thus confirming the perfect adhesion, thanks to the initial consistency, of the polymeric system to the substrate.

Another applicative test was performed on a decorative fish placed at the same position of the previous group, but on the back side. The formulation applied was loaded with 6.6% Rochelle salt, and the result of the test is showed in Fig. 8.8. As remarked by the applicative tests on the artificially aged samples (see Chapter 7, sections 7.4.1.1, 7.4.2.1), Rochelle salt, has a milder action in complexing Cu(II) ions, compared to EDTA. In fact, a scarce removal was achieved after a single application, although the following mechanical removal by scalpel resulted easier. The formulation 70PVA10, assured good applicability on the non-horizontal surface, but the mechanical properties of the final film was not satisfying, maybe because of the insufficient amount of polymeric system applied that resulted in a thin film.

Figure 8.8 Application of a RS loaded 70PVA10 formulation (6.6% w/w) on the fish decoration placed at the back side, for two hours.

A decoration with the form of a shell, placed at the base of the fountain in an undercut area, presented extended white calcium carbonate and sulfate deposits on the surface with the presence of underlying green corrosion products. High amount of the formulation 70PVA10, loaded with 3% w/w EDTA, was applied and allowed to drying over night. The result, reported in Fig. 8.9, evidences a consistent removal of the white alteration layer and also some corrosion products (copper carbonates, sulphates and chlorides) were partially removed (see the detail in Fig. 8.10). The lack-

ing of a direct contact between the applied system and the corrosion products, because of the presence of the intermediate carbonate layer, affected the efficiency of the complexing reaction that partially occurred. The high thickness of the applied formulation entailed some dripping of the cleaning system, visible after the final removal (see Fig. 8.9, right).

Figure 8.9 The shell decoration, placed at the base of the front side, where the formulation 70PVA10 loaded with 3% w/w EDTA was applied and allowed drying over night.

Figure 8.10 Enlargement of a detail of some green corrosion products removed from the shell decoration, along with a the white calcite and gypsum layers.

Applicative tests with film forming polymeric system was performed also on the sculpture group of the western fountain, with a specifically prepared formulation (77PVA2 with 15% w/w of PVA), loaded with 6% v/v of PEHA. In Fig. 8.11 the results of the cleaning test evidence a partial removal of the corrosion products after a single application of an hour. A certain variation of the surface color, toward the blue of the complexed system, was noticed.

Figure 8.11 Applicative test on the sculpture body of the western fountain, with the formulation 77PVA2 loaded with 6% v/v PEHA, for one hour.

8.3 Applicative tests on gilded surfaces

The artifact, visible in Fig. 8.12 was removed from its original position and moved to the laboratories of V. Castoldi (Studio Restauri Formica srl) in Milan, for a conservative intervention. The object is constituted by a star with multiple tips starting from a central sphere and presented the typical alteration products of an outdoor bronze (mainly copper sulphates, brochantite and antlerite), localized in correspondence of the corners and of the tips faces. Moreover, the central sphere and some tips presented gilding, obtained by a firing process, where an amalgam of gold and mercury is applied to the metallic surfaces, the mercury being subsequently volatilized, leaving a film of gold. Some tips were disassembled from the structure to simplify the cleaning process, performed through traditional methods (mechanical cleaning by scalpel and complexing solutions of EDTA at 3-5% w/w applied by soaking in cotton balls).

Cleaning tests with a selected formulation was performed on the 21st tip (see Fig. 8.12), which presented a gilded surface. Black deposits and corrosion products were concentrated at the base of the tip, which corresponded to the part attached to the sphere, less exposed to the washing of rainwater, thus causing an accumulation of deposits.

Figure 8.12 The artefact at its original position (left) and the 21st tip (right).

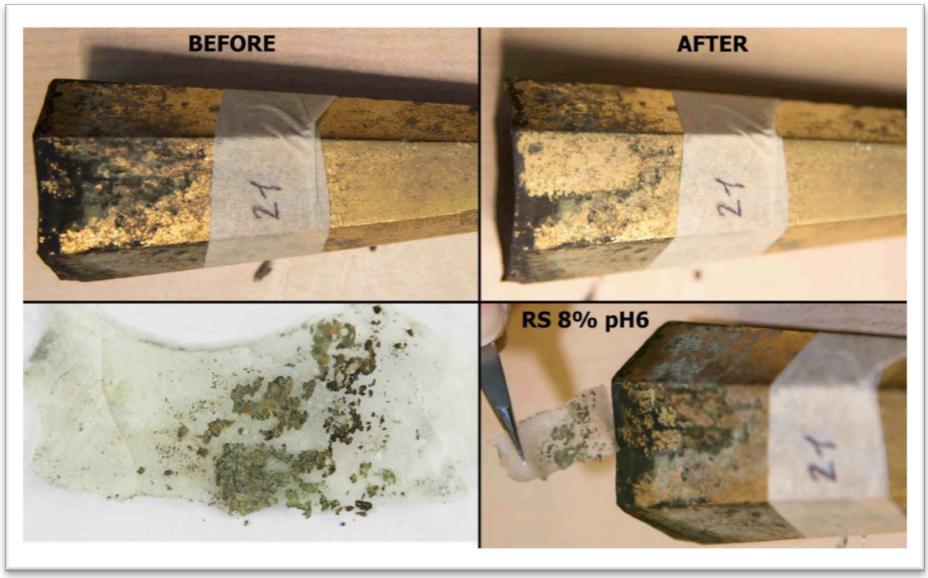

Figure 8.13 Cleaning test performed with the formulation 70PVA10 loaded with 8% w/w of Rochelle salt, on the gilded surface of the 21st tip for three hours.

The formulation 70PVA10 loaded with 8% w/w of Rochelle salt (pH 6) was applied in correspondence of the upper part of the tip, as showed in Fig. 8.13. After three hours the formed film was removed, with good cleaning performances and by respecting the gold layer. In fact, Rochelle salt was chosen instead of EDTA, thanks to its milder action toward gilded surfaces [8,9]. A subsequent mechanical treatment, by means of a scalpel, allowed the complete removal of the alteration layer, which resulted considerably softened, with a significant saving of time.

8.4 Applicative tests on archaeological objects

Applicative tests were executed on several archaeological objects, with a negligible historical value, at the ISMN-CNR laboratories in Rome. This allowed to test the cleaning systems on real *patina* formed during a long burial. The objects were preliminary characterized by the above-mentioned techniques, in particular with electron microscopy with microanalysis (SEM/EDS), Raman spectroscopy and optical microscopy, by using the same instrumental conditions reported in section 8.2.2.1 of this chapter and in Chapter 7 (section 7.3.1).

Several object were selected for the cleaning tests and previously characterized, but only the most representative will be reported. The characterization results are reported as data sheets.

COIN 5£: The bronze coin of the king Vittorio Emanuele III presented residues of the soil on the surface, as cpnfirmed by EDS elemental analysis, which evidenced Al, Si, P, Ca, etc., typical soil components. SEM images show the morphology of the surface and of the corrosion products, while EDS spectra evidence the presence of chlorine (atacamite, paratacamite) and of tin enrichments (cassiterite). Raman analysis of the surface, confirmed the presence of cuprite.

NAIL

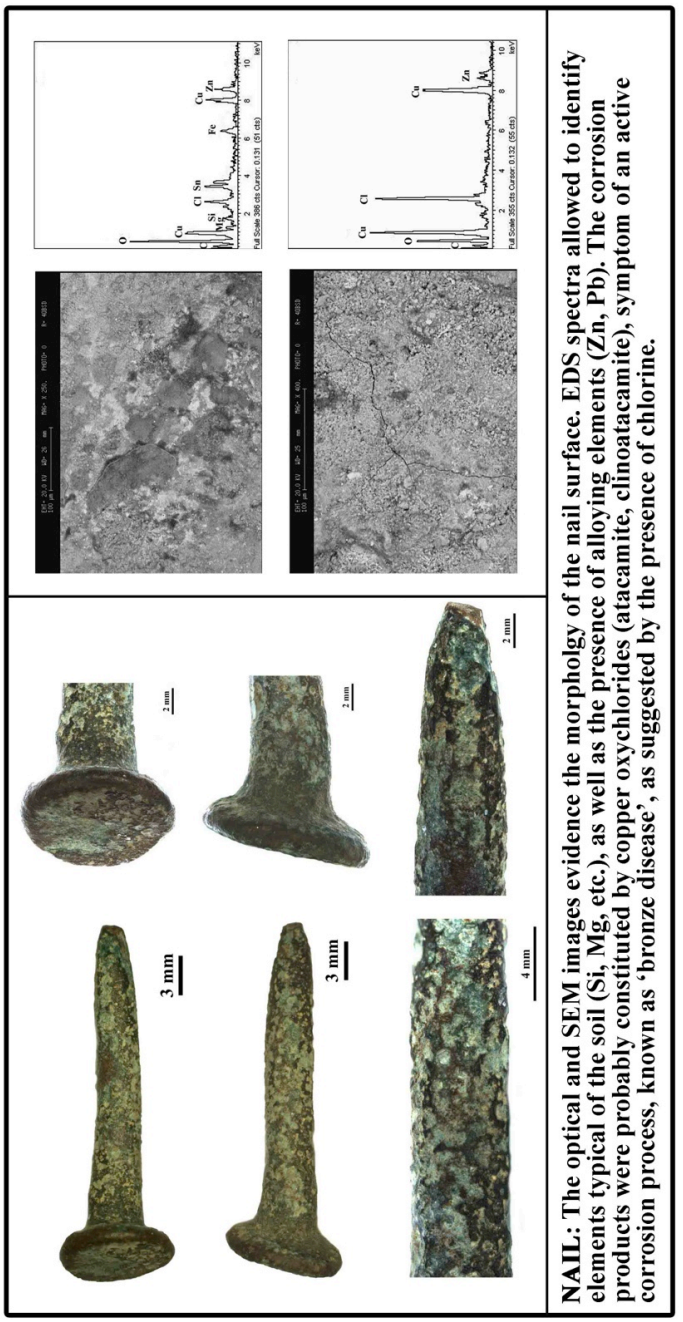

NAIL: The optical and SEM images evidence the morpholgy of the nail surface. EDS spectra allowed to identify elements typical of the soil (Si, Mg, etc.), as well as the presence of alloying elements (Zn, Pb). The corrosion products were probably constituted by copper oxychlorides (atacamite, clinoatacamite), symptom of an active corrosion process, known as 'bronze disease', as suggested by the presence of chlorine.

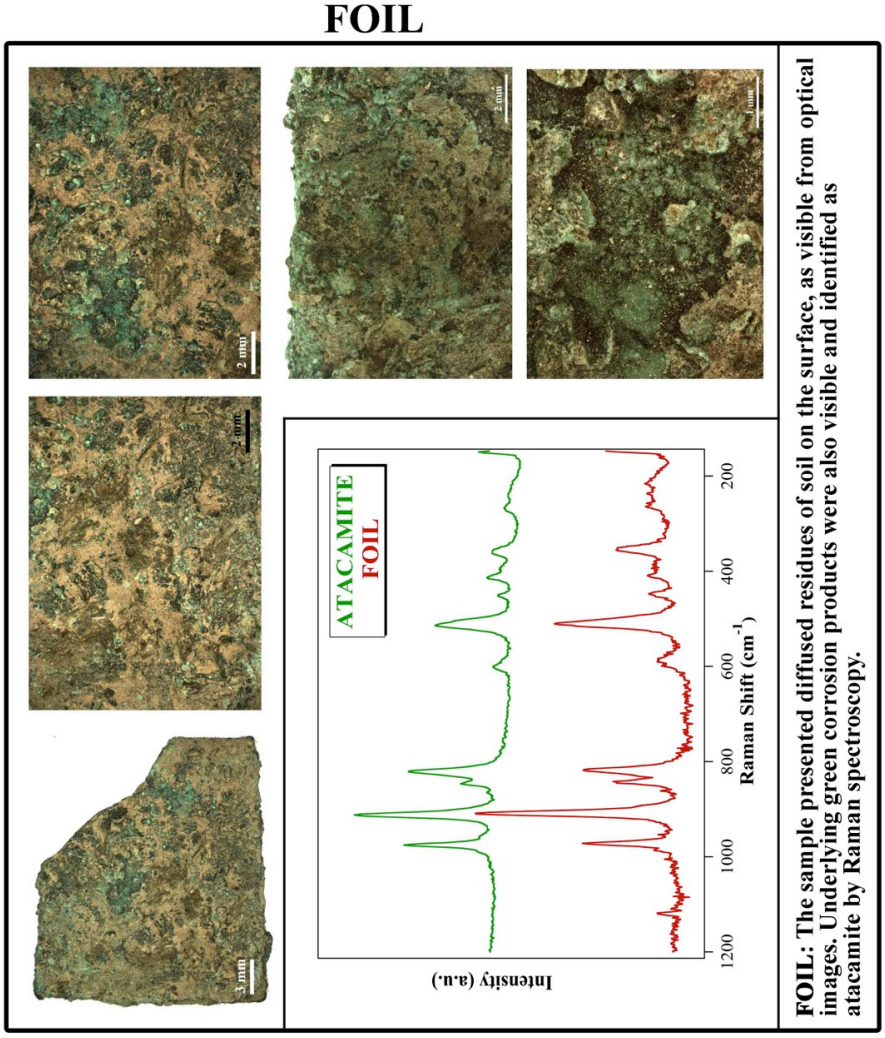

FOIL: The sample presented diffused residues of soil on the surface, as visible from optical images. Underlying green corrosion products were also visible and identified as atacamite by Raman spectroscopy.

A 5 £ copper coin of 1931 was cleaned, after characterization, with different steps on the heads side: i) formulation 70PVA10 loaded with 4.5% w/w EDTA (pH 9) applied on the entire surface; ii) 70PVA4 loaded with PEHA 6% v/v applied on the entire surface; iii) PEHA loaded formulation applied only at the borders. The progressive results are reported in Fig. 8.14, where the removal of the soil residues and of the corrosion products is visible. Moreover, it has to be noticed that the viscoelastic properties of the fluid system allowed the application over a circumscribed zone (see Fig. 8.15), with an excellent spatial control thanks to the initial consistency.

Figure 8.14 Cleaning of a 5 £ copper coin by progressives steps: application of 70PVA10 formulation loaded with 4.5% w/w EDTA and of the 70PVA4 formulation loaded with 6% v/v PEHA twice.

Figure 8.15 The remove films of the EDTA loaded formulation (left) and of the PEHA loaded formulation (right), which ensured an excellent spatial control.

Other tests were performed with differently loaded formulations on a nail coming from an archaeological site: a comparison between i) a not loaded 70PVA10 formulation and ii) a 70PVA10 loaded with 3% w/w EDTA formulation, was carried out, although it resulted in poor removal of the corrosion products. Further application with macrocycles loaded formulations 72PVA8 was applied: iii) 2% w/w Neoden on the upper part of the nail and iv) 2% w/w AMCC on the point. The results are reported in Fig. 8.16, where the action of the macrocycles complexing reaction resulted in a consistent removal of the corrosion products from the treated areas, although the mechanical properties of the films formed were not satisfying.

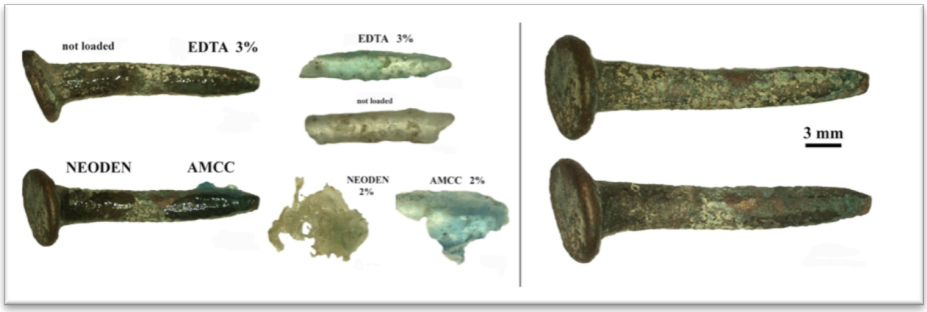

Figure 8.16 Application tests in two steps on a nail, with a not loaded 70PVA10 formulation compared to the same loaded with 3% w/w of EDTA; 72PVA8 formulations, loaded with Neoden and AMCC macrocycles, was further applied.

A foil bronze fragment coming from an archaeological site, was subjected to applicative tests, through different steps on three areas of the surface: i) application of the same formulation (70PVA10), loaded with different complexing agents (EDTA 3% w/w, Rochelle salt 6.6% w/w) compared with a not loaded formulation; ii) the second application was performed by applying different formulations (76PVA4, 74PVA6 and 70PVA10), loaded with different amount of the same complexing agent, EDTA (3.5%, 3%, 3% w/w respectively); iii) the last application was performed with the macrocycles loaded formulations (2% w/w of DOTA, Neoden and AMCC). The results, reported in Fig. 8.17, highlight the progressive removal of the soil residues from the surface, thanks also to the mechanical action of the peeling,

thus making easier the contact with the corrosion products layer. The *patina* is well cohesive and adherent to the substrate, but the initial fluidity of the polymeric formulations allowed to perfectly follow the surface discontinuities, thus favoring the chemical removal of the copper oxychlorides (see Fig. 8.18).

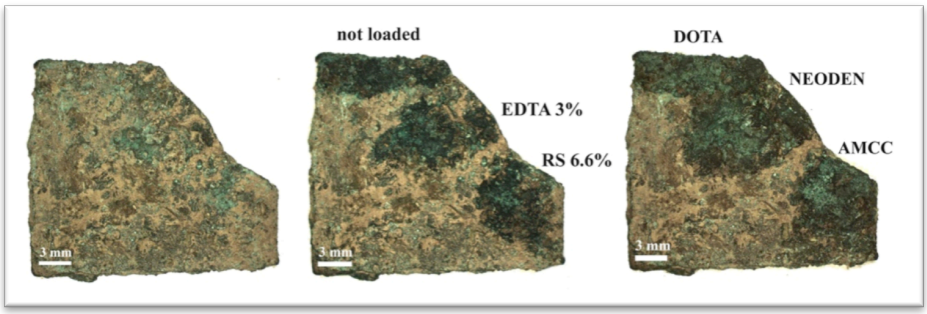

Figure 8.17 Cleaning tests were performed through subsequent tests, with different formulation and complexing agents (see text).

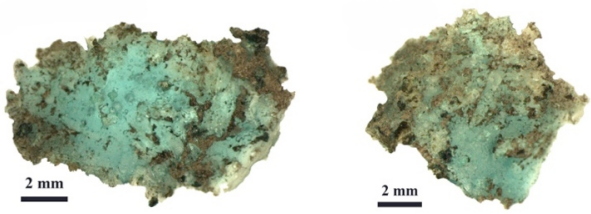

Figure 8.18 Some examples of the removed film, which perfectly followed the sample surface and removed the first layer of soil residues.

8.5 Other applicative tests

The polymeric formulation loaded with complexing agents presented in this PhD thesis, were devised for the specific purpose of cleaning metallic objects. However, they were tested also over other supports, such as gypsum, parchment and painted leather.

The polymeric formulations, in fact, can be used without the addition of a complexing agent and by modulating their mechanical properties, for the removal of

grime and water sensible deposits from gypsum substrates and parchment. The simple mechanical action provided by the removal of the film and the confined presence of low water amounts, assures a controllable and safe removal. The presence of paintings layers and of fragile surfaces (e.g. gold leaf), instead, discourages the use of such these cleaning systems, in favor of other systems appositively designed for these purposes [10–13] (see Chapter 2, section 2.4).

An extremely particular case of application was an altar 'paliotto' (see Fig. 8.19), made of painted leather with a complex stratification: a silver foil was in contact with the leather, covered by a yellowish 'meccatura' of organic resins and gums (which conferred the gilded aspect), over which an azurite layer was identified by the preliminary diagnostic analysis. A final layer of white lead was used to cover the azurite and it had to be removed from the surface, in order to restore the original aspect. Thus, some tests with the polymeric film forming systems was performed, by using the EDTA ability of complexing also lead ions. In Fig. 8.20 the controlled removal of the white lead layer, to unearth the azurite layer, is showed. The applied formulations was 74PVA6 and 70PVA10, loaded with 3% w/w EDTA (pH8) and 2.5% w/w EDTA (pH 9) respectively. A satisfying removal after a single application was achieved, without any removal of the azurite pigment. The procedure was then adjusted by using traditional solvents (DMSO) and cleaning methods (ethyl lactate in Carbopol®), in order to obtain a complete removal of the white lead layer (see Fig. 8.21).

Figure 8.19 The aspect of the altar 'palio', made of a complex stratifications: the removal of the white lead layer was carried out with EDTA loaded film forming system, to restore the original layer of azurite.

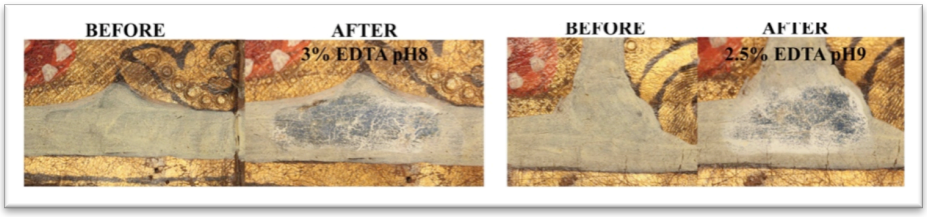

Figure 8.20 Cleaning tests with 76PVA4 loaded with 3% w/w EDTA (pH 8) and 70PVA10 loaded with 2.5% w/w EDTA (pH 9), performed by complexing Pb ions thanks to EDTA.

Figure 8.21 Final results of the cleaning tests performed with the film forming systems, assisted by traditional methods.

8.6 Final remarks

Cleaning tests, performed over various typologies of metallic and nonmetallic substrates, allowed to evaluate the real possibilities of the film forming systems.

The initial fluid consistency allows to perfectly follow any kind of surface morphology, thus guaranteeing a good contact between the products to be removed and the complexing agent confined in the polymeric system, on the contrary respect to 'rigid' confining systems. Moreover, this feature assures also to penetrate in each roughness of the surface, which is impossible for the traditional mechanical methods.

The removal of the final films assures a mechanical action, thanks to the peeling, that further enhances the cleaning performances of these systems. In fact, the not loaded systems can be used to remove water sensitive deposits from different substrates (gypsum, parchment, etc.), by considering that a certain cohesiveness is required.

The addition of different complexing agents assures a chemical cleaning action that can be tuned depending on the *patina* composition and morphology. The possibility of loading other and more effective chelating agents for metallic substrates or adapt these cleaning systems to other conservative purposes would be an interesting development of this research for the future.

8.7 Bibliography

[1] INGO, G.M. AND PARISI, E.I. ET AL. *Gold coated copper artifacts from the Royal Tombs of Sipán (Huaca Rajada, Perù): manufacturing techniques and corrosion phenomena.* Applied Physics A *113*, 4 (**2013**), 877–887.

[2] FARALDI, F. ET AL. *Micro-chemical and micro-structural investigation of archaeological bronze weapons from the Ayanis fortress (lake Van, Eastern Anatolia, Turkey).* Applied Physics A: Materials Science and Processing *113*, (**2013**), 911–921.

[3] INGO, G.M., ÇILINGIROĞLU, A., FARALDI, F., ET AL. *The bronze shields found at the Ayanis fortress (Van region, Turkey): manufacturing techniques and corrosion phenomena.* Applied Physics A *100*, 3 (**2010**), 793–800.

[4] ROBBIOLA, L., FIAUD, C., AND PENNEC, S. *New model of outdoor bronze corrosion and its implications for conservation.* ICOM Committee for Conservation 10th triennial meeting: Washington, DC, 22-27 August 1993: preprints, (**1993**), 796–802.

[5] INGO, G.M., ANGELINI, E., BULTRINI, G., DE CARO, T., PANDOLFI, L., AND MEZZI, A. *Contribution of surface analytical techniques for the microchemical study of archaeological artefacts.* Surface and Interface Analysis *34*, 1 (**2002**), 328–336.

[6] SCOTT, D.A. *Copper and bronze in art.* The Getty Conservation Institute, Los Angeles, **2002**.

[7] SCOTT, D.A. *Bronze disease: a review of some chemical problems and the role of relative humidity.* JAIC *29*, (**1990**), 193–206.

[8] MATTEINI, M., LALLI, C., TOSINI, I., GIUSTI, A., AND SIANO, S. *Laser and chemical cleaning tests for the conservation of the Porta del Paradiso by Lorenzo Ghiberti.* Journal of Cultural Heritage *4*, (**2003**), 147–151.

[9] FIORENTINO, P., MARABELLI, M., MATTEINI, M., AND MOLES, A. *The condition of the 'Door of Paradise' by L. Ghiberti. Tests and proposals for cleaning.* Studies in Conservation *27*, (**1982**), 145–153.

[10] DOMINGUES, J.A.L., BONELLI, N., GIORGI, R., FRATINI, E., GOREL, F., AND BAGLIONI, P. *Innovative Hydrogels Based on Semi-Interpenetrating p(HEMA)/PVP Networks for the Cleaning of Water-Sensitive Cultural Heritage Artifacts.* Langmuir *29*, (**2013**), 2746–2755.

[11] DOMINGUES, J., BONELLI, N., GIORGI, R., AND BAGLIONI, P. *Chemical semi-IPN hydrogels for the removal of adhesives from canvas paintings.* Applied Physics A *114*, 3 (**2014**), 705–710.

[12] CARRETTI, E., NATALI, I., MATARRESE, C., ET AL. *A new family of high viscosity polymeric dispersions for cleaning easel paintings.* Journal of Cultural Heritage *11*, 4 (**2010**), 373–380.

[13] NATALI, I., CARRETTI, E., ANGELOVA, L., BAGLIONI, P., WEISS, R.G., AND DEI, L. *Structural and Mechanical Properties of " Peelable " Organoaqueous Dispersions with Partially Hydrolyzed Poly (vinyl acetate) -Borate Networks : Applications to Cleaning Painted Surfaces.* (**2011**), 13226–13235.

CONCLUSIONS

Conclusions

During this PhD project a system able to perform both a chemical and a mechanical action, specifically tailored for the cleaning of Cu-based artifacts, has been developed. In particular the 'peeling' of a polymeric film from the surface assures a certain mechanical action, while the presence of a chelating agent specific for Cu(II), carries out the chemical action.

The development of such a system required primarily the selection of a suitable film forming polymer (PVA), then of opportune additives able to modify the polymeric dispersion depending on the desired final properties (as reported in Chapter 5). Thus different formulations were prepared to find the best composition that fulfills the desired requirements in terms of applicability and mechanical properties. The design of this innovative confining system was completed by the selection of suitable complexing agents to load into the polymer matrix. They had to be specific for Cu(II), the main species of the corrosion products related to Cu-based artifacts, and able to entrap these cupric ions as effectively as possible, thus removing them from the surface. The research of such chelating agents started from commonly used products in the restoration field (e.g. EDTA and Rochelle salt), and was then carried on with the selection of more effective complexing agents, belonging to the class of macrocycles or polyethyleneamines, by using as selective criterion their stability constant with Cu(II). Several formulations were prepared by varying the relative amount and the typology of each component, in order to find the best equilibrium between them. Finally three different polymeric formulations were selected as the most suitable to be loaded with the complexing agent and to be used for applicative tests.

Preliminary investigations over the physico-chemical characteristics were carried out over selected polymeric formulations and reported in Chapter 6. In particular two main aspects were studied over both, complexing agent-loaded and not loaded systems: i) the kinetics of film formation, by investigating the evolution of the systems from polymeric dispersions towards the formation of elastic films and ii) the evaluation of the formed films properties, through the crystallinity degree parameter. The techniques used to obtain information over the evolution of the system through time, involved the use of gravimetry, thermogravimetry (both scanning and isothermal), and rheology (both dynamic and rotational experiments). On the other hand the evaluation of the mechanical properties and of the degree of crystallinity of the dried films was carried out through differential scanning calorimetry (DSC) and ATR-FTIR spectroscopy experiments. The obtained results allowed to evaluate the influence of each component on the system properties.

The volatile fraction, in particular the content of the high volatile ethanol, influences the evaporation rate of the systems, thus the time of film formation. Gravimetric methods and thermogravimetry in scanning mode, allowed to evaluate the influence of increasing quantities of ethanol on the overall evaporation rate of the system, with the same plasticizer content.

The addition of plasticizers allows the modulation of the initial consistency and of the mechanical and adhesive properties of the final dry film. In fact, plasticizers act as lubricants between the polymer chains by weakening their inter-molecular secondary forces and by increasing the overall free volumes. As a consequence, the addition of plasticizers produces a reduction in adhesion, hardness and brittleness, and an increase in flexibility, toughness and tensile strength of the final films. Differential scanning calorimetric experiments (DSC) carried out on dried films, allowed to evaluate the trend of thermal parameters (glass transition, melting and crystallization temperatures) after the addition of plasticizers in the polymer matrix. The decrease, on different extent, of the overall transition temperatures and of the crystallinity degree in plasticized samples, confirmed that the presence of both plasticizers and amorphous regions into the polymeric system, assures a major control

over the final adhesiveness, flexibility and tensile resistance of the resulting films. Also the molecular structure of the plasticizers plays a primary role in determining the crystallinity values. In fact small plasticizer molecules, like glycerol, show an enhanced effect in lowering the crystallinity value in respect to molecules with higher sizes. ATR-FTIR experiments also confirmed the plasticizers influence over the final mechanical properties of the films.

Moreover, the time required, for the different formulations, to attain the complete evaporation of the volatile fraction (and indirectly the film formation) was evaluated by means of isothermal thermogravimetric measurements at 40°C (TGA). The obtained data indicate that the volatile fraction loss occurs earlier for aqueous PVA solutions without the addition of plasticizers, while longer times are required for formulations containing plasticizers, which hinder the evaporation process on different extent, depending on their retentive power and molecular sizes. In particular one formulation, 70PVA10, showed the best properties for applicative purposes, because of its rapid film formation, intermediate amount of liquid fraction and plasticizers content (which confer an initial consistency suitable for application on different surfaces) and very good mechanical properties of the final peelable film.

The effect of the complexing agent on the overall polymeric system properties was evaluated by adding increasing quantities of EDTA (1-3% w/w) at two different pH values (7 and 9), to selected formulations. The presence of a complexing agent, in fact, should not negatively affect the initial consistency of the system, the evaporation rate and the final film mechanical properties. Gravimetric data showed that upon raising the EDTA amount, an increase in the evaporation rate of the volatile fraction occurs, allowing further applicative advantages thanks to the reduced times needed for film formation. This behavior is also confirmed by DTG experiments and it can be ascribed to the increase in polymer chain entanglements and vicinity, induced by EDTA, acting as a sort of cross-linker. The modification of the 3-D polymer network structure results in higher entanglements and crystalline domains formation, with a consequent reduction of the number of sites available for hydrogen bonds formation with H_2O and ethanol molecules. This results in less vol-

atile fraction molecules linked to the PVA chains, that are thus free to evaporate. Finally, also the pH value, regulated by the addition of NH_3 solution, had a further influence on the evaporation rate.

In order to follow the evolution of the mechanical properties of a selected formulation during the evaporation of the liquid phase, a rheological characterization of the not loaded and EDTA loaded system was carried out at room temperature, as a function of time. Frequency sweep tests showed a prevalent viscous behavior over almost the entire range of explored frequencies. A progressive enhancement of entanglement density between polymer chains, due to the formation of inter- and intra-molecular H-bonds, was observed with time, due to an enhancement of the solid-like character of the system. The variations in the viscoelastic behavior through time indicate that the system evolves from an initial high viscous polymeric dispersion, towards a final solid-like film. Flow curves obtained by rotational experiments show shear thinning viscosity behavior. The zero shear viscosity trend values of both the loaded and not loaded formulations confirm the progressive enhancement of the 3-D network structure.

Cleaning tests was performed on artificially aged sample, prepared by following a procedure developed by ISMN-CNR laboratories of Rome, as described in Chapter 7. This step was relevant to qualitatively evaluate the benefits and assets, as well as the limits of the application procedure. Cleaning test results evidenced that the action of the complexing agent loaded in the polymeric dispersion is fully controllable, thus permitting a gradual layer-by-layer removal of the corrosion products. Moreover, the initial consistency of the system allows a perfect contact with the rough surface of the sample, so the complexing reaction can take place also in areas where no removal through a sole mechanical action could be achieved. Finally, the mechanical action due to the removal by peeling favors the cleaning process by assisting the chemical action of the chelator The preliminary applicative tests performed on the artificially aged samples, revealed both the advantages and drawbacks of each chelating agent, as well as the complexity of the cleaning procedure depending on the surface characteristics. The prevalence of negative aspects related

to the use of macrocycles and glycine as complexing agents for Cu(II) determined their exclusion. Depending on the characteristics of the sample to clean, the suitable sequestering agent should be carefully chosen: Rochelle salt guarantees a delicate and gentle chemical action, by respecting the cuprite or gold layer present; EDTA is versatile and can perform a very controllable cleaning action, by tuning also the pH values; polyamines can be used for a more effective cleaning action, thanks to their high formation constant for the complex with Cu(II).

Moreover, different polymeric formulations were tested as confining systems for the complexing agents. The best performances in terms of both applicability and properties of the final film, were obtained by the selected formulations: 74PVA6, 70PVA10 and 68PVA12, thus used for cleaning tests on real cases study.

Cleaning tests, performed over various typologies of metallic and non-metallic substrates, allowed to evaluate the real performances of the film forming systems. The initial fluid consistency allows to perfectly follow any kind of surface morphology, thus guaranteeing a good contact of the products to be removed with the complexing agent confined in the polymeric system, on the contrary respect to 'rigid' confining systems. At the same time, spatial control and applicability also on non-horizontal surfaces is obtained, by tuning the formulations composition. The removal of the final films assures a mechanical action, thanks to the peeling-off, which further enhances the cleaning performances of these systems. In fact, this property makes these systems suitable also for the removal of water sensitive deposits from different substrates (gypsum, parchment, etc.), by considering that a certain cohesiveness is required. The addition of different complexing agents assures a further chemical cleaning action that can be tuned depending on the *patina* composition and morphology. The possibility of loading other and more effective chelating agents for metallic substrates or adapt these cleaning systems to other conservative purposes would be an interesting development of this research for the future.

Acknowledgements

I would like to start expressing my gratitude to my supervisor and tutor, Prof. Piero Baglioni, who assisted and supported me throughout this pathway over these three years. At the same time my special gratitude goes to my co-tutor, Prof. Gabriel M. Ingo, without whom I would not had the chance of doing this experience. I would additionally like to thank Prof. Rodorico Giorgi for his constant support during the course of this research project.

I wish to thank Dr. Emiliano Carretti for the help with the rheological analysis experiments and for the useful discussions over polymers stuff.

Furthermore, I would like to acknowledge the professionals that made the cleaning tests on real case studies possible: Archt. Maria Bonelli, who gave me the possibility of carrying out applicative tests on the 'Fontane dei Mostri Marini' with extreme willingness, the restorers Gabriella Ton and Louis, D. Pierelli from Nike Restauro s.n.c., for the useful discussion over conservation methodologies for metallic objects.

Vittoria Castoldi, from the Studio Restauri Formica s.r.l. and her assistants, who demonstrate very interest towards this innovative approach for cleaning and made available different case studies for applicative tests.

Claudius Schettino, from Philobiblion Laboratorio di Restauro, who provided an interesting case study to test the versatility of the cleaning systems on non-metalic surfaces.

Part of this PhD project was executed at ISMN-CNR laboratories of Rome (Monterotondo), where it all started. I would like to gratefully thank my friends and former colleagues Cristina Riccucci and Federica Faraldi, who saved me from the hovel.

Almost the entire work presented in this dissertation was carried out at the laboratories of the Chemistry Department, University of Florence. The everyday interaction with my colleagues of the CSGI group, gave me the possibility of increase my professional experience, but especially of establishing good relationships with everyone. In particular I would like to thank people of the Cultural Heritage Team, who patiently supported me during these three years, by making it an enjoyable experience: Michele, former office roommate, who was the first who made me feel accepted in the new workplace; Giovanna, for the conversations in 181 and the goat; Nicole, for being my first mentor through the gel world and for the constant practical and moral support, especially during this last year; Joana, for being my constant reference person for professional issues but, above all, a good friend. A special thanks also goes to my actual office roommates, trustworthy confidants and pushers of junk food, Costanza and Arianna.

Finally, I would like to express my personal gratitude to my parents, whose love and sacrifices gave me the possibility of reach this goal and of being the person who I am. My brother and sisters, who can distract me from everyday problems with a single photo or video of our sole and unique fat Divinity.

To my friends, Valeria and Ilary, who supported, comforted and helped me over these years, despite the distance.

To Simone, who took care of me with endless love and patience during the final and most difficult part of this pathway.

Erica I. Parisi

December 2015